Dissertation

submitted to the

Combined Faculties of the Natural Sciences and Mathematics

of the Ruperto-Carola-University of Heidelberg, Germany

for the degree of

Doctor of Natural Sciences

Put forward by

Dipl.-Phys. Mischa Gerstenlauer

born in: Göppingen

Oral examination: 6$^{\text{th}}$ December 2011

An Analysis of Inflationary Correlation Functions

Referees : Prof. Dr. Arthur Hebecker
Prof. Dr. Christof Wetterich

Eine Analyse inflationärer Korrelationsfunktionen — Zusammenfassung

Kosmologische Inflation, eine Phase beschleunigter Ausdehnung des frühen Universum, hat sich in den vergangenen Jahrzehnten zu einem wesentlichen Bestandteil der modernen Kosmologie entwickelt. In dieser Doktorarbeit präsentieren wir eine Analyse der in dieser Phase auftretenden Quantenfluktuationen, aus welchen im Laufe der Zeit die heutigen großräumigen Strukturen wie Galaxien und Galaxienhaufen entstanden sind. Im ersten Teil der Arbeit diskutieren wir die seit langem bestehene Frage inwiefern Korrelationsfunktionen dieser Quantenfluktuationen von Infrarot-Divergenzen beeinflusst sind. Wir identifizieren den Ursprung dieser Infrarot-Divergenzen und definieren infrarot-sichere Korrelationsfunktionen, die von solchen Divergenzen unbetroffen sind. Herkömmliche Korrelationsfunktionen können leicht durch unsere infrarot-sicheren Korrelationsfunktion ausgedrückt werden. Die zu den herkömmlichen Korrelationsfunktionen gehörigen Infrarot-Divergenzen treten hierbei automatisch in einer kompakten und zu allen Ordnungen gültigen Form auf. Darüber hinaus diskutieren wir Abweichungen der Quantenfluktuationen von der Gaußschen Statistik. Namentlich untersuchen wir die Skalenabhängigkeit dieser nicht-Gaußianitäten für Modelle mit (quasi) lokalen, nicht-Gaußschen Fluktuationen und charakterisieren diese durch neue Observablen. Zusätzlich analysieren wir die Möglichkeit diese nicht-Gaußianitäten durch Messungen des schwachen Linseneffektes zu messen.

An Analysis of Inflationary Correlation Functions — Abstract

Cosmological inflation, which postulates a period of accelerated expansion in the very early universe, has become a major ingredient to modern cosmology over the past decades. In this thesis, we present an analysis of quantum fluctuations which occur during this process and which form the seeds for the growth of structure in our universe. We start by discussing the long-standing question how correlation functions of these fluctuations are affected by infrared divergences. We clarify the origin of these infrared effects and define infrared-safe correlation functions which are not plagued by this issue. Conventional correlation functions are easily recovered from our infrared-safe definition and the corresponding infrared corrections automatically emerge in a resummed, all-orders form. We then continue to discuss deviations of inflationary fluctuations from Gaussian statistics. In particular, we calculate the scale-dependence of this non-Gaussianity for (quasi) local models of non-Gaussian fluctuations and characterize this scale-dependence in terms of new observable parameters. Furthermore, we analyse the possibility of detecting non-Gaussianity by weak lensing measurements.

Contents

Chapter 1

Preface

> "... the universe itself acts on us as a random, inefficient, and yet in the long run effective, teaching machine. ... our way of looking at the universe has gradually evolved through a natural selection of ideas." ([1], p. 158)

Since ages and ages ago humans were attracted and fascinated by the view on a clear nighttime sky, evident by the ancient findings of images showing star constellations and star signs in any known culture back to 15000 to 17000 BC (caves of Lascaux). Hence, it is no surprise that, at a relatively early stage in human history, people were seeking for explanations of the celestial mechanics and the origin of the world embedding the earth. The first known attempts to provide these explanations date back to Babylonian cosmology (Enuma Elish) around the 16^{th} century BC. Even though of mythical origin the Babylonian cosmology very likely had influence on the Greek cosmology which formed the basis of western cosmology untill the 16^{th} century.

Clearly, observational progress has always come hand in hand with technical progress. For instance, celestial maps had been continuously improved by the ability of determining the positions of stars more and more accurate with new or improved measuring instruments. However, even though knowing their orbit and positions at the sky to a for the time impressive accuracy, any progress was made by observations of celestial objects visible for the naked eye and painted already by the people in the caves of Lascaux thousands of years ago. Thus, the beginning of the the 17^{th} century, with the invention of the telescope in the Netherlands, marks a real turning point in the history of cosmology. For the first time in human history, people were able to make observations of objects far out in the deep sky that are invisible to the naked eye.

Naturally, this incredible increase of new observational data, gained by the invention of the telescope, lead to an ongoing understanding of celestial mechanics and the corresponding underlying physics. Already in 1676 the Danish astronomer O. Rømer was able to demonstrate the finiteness of the speed of light by studying eclipses of Jupiter's moon Io. These eclipses get shorter as the earth orbiting around the sun approaches Jupiter and longer as the earth moves further away, ruling out an infinite speed of light. The general acceptance of this finding took until 1729 when the aberration of light was discovered, confirming a finite speed of light. Nevertheless, it's been known since several centuries that, due to the finiteness of the speed of light, light from very distant objects was emitted in the far past. Therefore, a look at distant objects is always a look into the past itself. This logic, leading to the possibility of observing the past of our universe, which we still apply today is surprisingly old. Still, technical limitations and the lack of a deeper theoretical understanding prolonged the beginning of modern cosmology until the

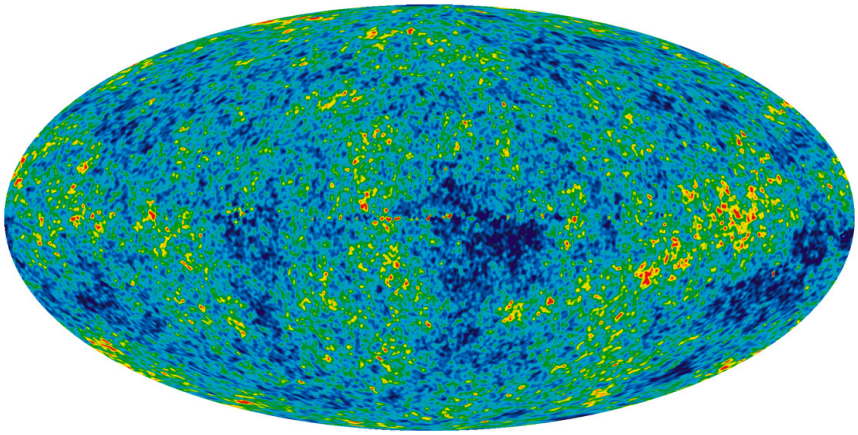

Figure 1.1: The detailed, all-sky picture of the infant universe created from seven years of WMAP data. The image reveals 13.7 billion year old temperature fluctuations (shown as color differences) that correspond to the seeds that grew to become the galaxies. The signal from our Galaxy was subtracted using the multi-frequency data. This image shows a temperature range of $\pm 200 \mu$Kelvin.[1]

20^{th} century.

Today, we are able to observe stars whose light was emitted up to 13 billion years ago. However, the radiation which allows us to dip deepest into the universe's history is invisible for the human eye. The *Cosmic Microwave Background (CMB)*, which is strongest in the microwave region of the radio spectrum, was emitted around 13.7 billion years ago. The discovery of the CMB and its measurement is a cornerstone of modern cosmology and major test for the cosmological standard model. According to the latter, the universe has been expanding from an initially very hot and dense state. In this state matter, e.g. protons and electrons and radiation, interacted heavily with each other. Due to the expansion, the content of the universe cooled down. At some point (around 13.7 billion years ago) it became cold enough for electrons and protons to form hydrogen atoms. These atoms could no longer absorb radiation and, hence, the universe turned from an opaque fog into being transparent. This moment is known as *decoupling* since radiation, which beforehand interacted heavily with matter, could now travel freely as a remnant of this initially hot and dense state. On its journey the radiation cooled further down, due to the ongoing expansion of the universe, until we see it today as what we call CMB radiation with a temperature of 2.725Kelvin. The discovery of the CMB is a strong support for the assumption of the universe being initially in a hot and dense state and, therefore, a cornerstone of modern cosmology.

Another cornerstone is the CMB's angular variation. In Fig. 1.1 we show the all-sky map of the 7-year data from the WMAP satellite. It shows the angular deviation from the average temperature of the CMB. The strongest of these temperature fluctuations deviate by about 0.1% and, hence, the CMB radiation is isotropic to a very high accuracy. This supports the cosmological principle of an almost homogeneous and isotropic early universe, setting the initial conditions for its later evolution. It is important to note that this initial state cannot be perfectly homogeneous and isotropic, but has to have fluctuations. These fluctuations, which we observe today as the aforementioned temperature fluctuations in the CMB, correspond to the seeds that grew to become today's galaxies.

[1]Fig. 1.1 and 1.2 are taken from the WMAP webpage http://map.gsfc.nasa.gov/ .

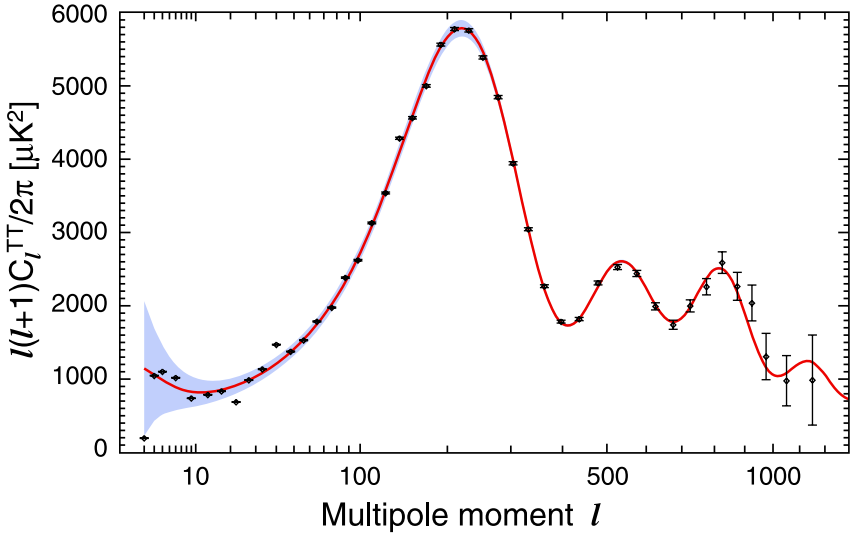

Figure 1.2: The 7-year temperature (TT) power spectrum from WMAP. The curve is the ΛCDM model best fit to the 7-year WMAP data: $\Omega_b h^2 = 0.02270$, $\Omega_c h^2 = 0.1107$, $\Omega_\Lambda = 0.738$, $\tau = 0.086$, $n_\zeta = 0.969$, $\mathcal{P}_\zeta = 2.38 \times 10^{-9}$ and $A_{\rm SZ} = 0.52$. The plotted errors include instrument noise, but not the small, correlated contribution due to beam and point source subtraction uncertainty. The gray band represents cosmic variance.[1]

Even though we cannot look further back than to the time of decoupling, we have precious indications of what might have happened. Again we have gotten this information from the CMB. A theory describing the universe before decoupling has to explain the origin of the special shape and characteristics of the CMB radiation. Among other things, this theory must explain the origin of homogeneity and isotropy of this initial hot and dense state. Obviously, very widely separated regions had causal contact with each other, an observation which is difficult to explain. Furthermore, this theory must explain the origin of the aforementioned deviations from homogeneity and isotropy, observed today as temperature fluctuations. These temperature fluctuations (Fig. 1.1) follow a very significant angular distribution which is shown in Fig. 1.2. Clearly, the correct theory must reproduce this very significant spectrum. Together with other open issues like the flatness or the relic problem whose details are not mentioned here, this sets very stringent conditions for any pre-decoupling theory.

In the past decades cosmologists have found one and so far only one mechanism resolving all these issues simultaneously. This mechanism is called *inflation* [2–6]. It postulates a period in the very early universe in which it underwent a phase of exponential or almost exponential expansion. As a direct consequence the whole observable universe today originates from a small and causally connected region. The (quasi-) exponential expansion made this region very rapidly almost perfectly homogeneous, isotropic and spatially flat. Deviations occurred due to tiny quantum fluctuations present during this process. The characteristics of the fluctuations produced in this way are precisely those to explain the spectrum shown in Fig. 1.2 (taking also into account physical processes between the end of inflation and decoupling). The fluctuations' amplitude is almost scale-invariant and their statistical distribution is at least to leading order Gaussian. Thus, the inflationary mechanism resolves all the aforementioned ambiguities. Of course, the prize one has to pay is to explain the physical origin of this (quasi-) exponential expansion. Consequently, there is not a single theory of inflation. Any physical process yielding such a period of (sufficiently long) exponential expansion may be such a theory. Therefore, a unique

theory of inflation is far from being determined, neither from a theoretical nor from an observational point of view.

Nevertheless, not any theory of inflation is as good as others, e.g. due to problems associated with the end of the inflationary process or with fine-tuning. The most prominent class of inflationary theories is the category of *slow-roll inflation* [5, 6]. In these inflationary models at least one scalar field, dominating the energy density during inflation, slowly rolls down its potential. This process leads to a quasi-exponential expansion of the universe continuing until the slow-roll ends, typically when the scalar field approaches its potential minimum. The scalar field then starts to oscillate around this minimum and decays.

The generation of fluctuations during inflation at linear order has been analysed and investigated to a wide extend [7–13]. However, there are various reasons why it is important to extend the analysis of these fluctuations to non-linear order. First of all, it is natural to try to obtain a deeper understanding of inflation and the underlying theory. This clearly requires to learn about the non-linear processes during the inflationary phase. Furthermore, the ability of making reliable statements on inflationary quantities strongly relies on having control also over non-linear processes. Last but not least, non-linear effects in inflationary fluctuations lead to deviations from the leading order Gaussian statistics. Particularly in light of forthcoming observational data, e.g. from the Planck satellite, these non-Gaussiantities are expected to be of great value by narrowing down the number of inflation models which are in agreement with observational data.

In this thesis, we present an analysis of inflationary fluctuations and their correlation functions with a focus on non-linear effects. After an introductive chapter we start by discussing the long-standing question how inflationary correlation functions are affected by infrared divergences. Such divergences explicitly arise in loop corrections to inflationary observables or through the non-linear dependence of the curvature perturbation on fluctuations of an underlying scalar field. We clarify the physical origin of these infrared divergences. Furthermore, we define correlation functions that are independent of these infrared effects. The conventional correlation functions can be easily related to our infrared-safe definition. In this relation the corresponding infrared divergences automatically emerge in a resummed, all-orders form. We then continue to discuss the scale-dependence of non-Gaussianity for a wide range of inflationary models. We characterise this scale-dependence in terms of new observable parameters which can help to discriminate between models of inflation since they are sensitive to properties of the inflationary physics that are not probed by the standard observables. In the last part of this thesis, we discuss the possibility of detecting primordial non-Gaussianity by weak lensing measurements, especially with a view on the planned Euclid space telescope. Although not as sensitive to primordial non-Gaussianity as CMB measurements or galaxy surveys, weak lensing can place useful independent constraints.

This thesis is based on the following publications:

I *Inflationary Infrared Divergences: Geometry of the Reheating Surface vs. δN Formalism.*
C.T. Byrnes, M. Gerstenlauer, A. Hebecker, S. Nurmi and G. Tasinato.
JCAP, 1008:006, 2010.

II *Inflationary Correlation Functions without Infrared Divergences.*
M. Gerstenlauer, A. Hebecker and G. Tasinato.
JCAP, 1106:021, 2011.

III *Scale-dependent non-Gaussianity probes inflationary physics.*
C.T. Byrnes, M. Gerstenlauer, S. Nurmi, G. Tasinato and D. Wands.
JCAP, 1010:004, 2010.

IV *A weak lensing view on primordial non-Gaussianities.*
B.M. Schäfer, A. Grassi, M. Gerstenlauer and C.T. Byrnes
arXiv:1107.1656 [*astro-ph.CO*]

Today, we are able to observe radiation emitted at the time of decoupling 13.7 billion years ago. It may be that in the future we will observationally be able to look back even further in time, for instance via gravitational waves. Definitely, upcoming and already ongoing observations like the Planck satellite will improve and refine the available data from the time of decoupling. In either case, observational and theoretical progress will improve our knowledge and understanding of primordial fluctuations in the early universe. We hope that this thesis and the underlying publications may make a contribution to this process.

Chapter 2

Introduction

In this chapter, we give a summary of the theory of inflation, the theory of cosmological perturbations and the δN-formalism. By no means, this is meant to be an introductive review on these topics, but a collection of elements which will be important for the following chapters. For an introductive review on the theories of inflation, cosmological perturbations and δN-formalism, we refer the reader to the available reviews on these subjects (e.g [14–17]). We conclude this chapter presenting an overview of the body of this thesis in sec. 2.5.

2.1 Inflation

The simplest model of slow-roll inflation is given by

$$S = \frac{m_p^2}{2}\int d^4x\sqrt{-g}\,R + \int d^4x\sqrt{-g}\left[\frac{1}{2}\nabla^\mu\varphi\nabla_\mu\varphi - V(\varphi)\right] \quad , \tag{2.1}$$

where the two integrals represent the Einstein-Hilbert action and the action of a canonical scalar field, the inflaton, which couples to gravity via the metric $g_{\mu\nu}$. At background-level, the system is homogeneous and isotropic and the background metric is given by

$$ds^2 = g^{(0)}_{\mu\nu}\,dx^\mu dx^\nu = -dt^2 + a^2(t)\,d\vec{x}^2 \quad , \tag{2.2}$$

where $a(t)$ is the scale factor and $\vec{x}$ are the comoving spatial coordinates. Homogeneity and isotropy require the background scalar field φ_0 to depend only on time such that the equations of motion are given by

$$H^2 \equiv \left(\frac{\dot{a}}{a}\right)^2 = \frac{1}{3m_p^2}\left[\frac{\dot{\varphi}_0^2}{2} + V(\varphi_0)\right] \quad , \tag{2.3}$$

$$\dot{H} = -\frac{\dot{\varphi}_0^2}{2m_p^2} \qquad \text{and} \tag{2.4}$$

$$0 = \ddot{\varphi}_0 + 3H\dot{\varphi}_0 + V_\varphi \quad . \tag{2.5}$$

Note that, here and henceforth, a subscript φ denotes a differentiation along the scalar field φ, i.e. $V_\varphi = \partial V/\partial\varphi$, and dots denote derivatives with respect to cosmic time t. Eqs. (2.3) and (2.4) are Friedman's equations, written in terms of the Hubble parameter H, and eq. (2.5) describes the evolution of the scalar inflaton field. Only two out of the eqs. (2.3)-(2.5) are independent.

Current observations require the inflationary process to provide for at least $\mathcal{O}(60)$ e-foldings of expansion during the inflationary era. This requires the Hubble parameter to be sufficiently constant over a sufficiently long period, leading to the two conditions

$$\epsilon \equiv -\frac{\dot{H}}{H^2} \ll \mathcal{O}(1) \qquad\qquad \frac{\dot{\epsilon}}{\epsilon H} \ll \mathcal{O}(1) \quad . \tag{2.6}$$

The minus sign in the definition of the first slow-roll parameter ϵ is introduced for convenience resulting in a non-negative value (according to eq. (2.4) $\dot{H} \leq 0$ during inflation). The two conditions in eq. (2.6) are called the *slow-roll conditions*. The first condition implies that the scalar field φ_0 is rolling sufficiently slowly, $\dot{\varphi}_0^2 \ll H^2 m_p^2$. Hence, the energy driving inflation is dominated by the potential energy of the scalar field. The second condition further implies $\ddot{\varphi}_0 \ll \dot{\varphi}_0 H$. Therefore, the slow-roll conditions set restrictions on the system of evolution equations (2.3)-(2.5) such that the first Friedman equation and the evolution equation of the scalar field simplify to

$$H^2 = \frac{V}{2m_p^2} \qquad \text{and} \tag{2.7}$$

$$0 = 3H\dot{\varphi}_0 + V_\varphi \quad , \tag{2.8}$$

respectively. With eq. (2.7) and (2.8), it is straightforward to show that the slow-roll conditions are fulfilled if

$$\epsilon \equiv \frac{m_p^2}{2}\left(\frac{V_\varphi}{V}\right)^2 \ll \mathcal{O}(1) \qquad\qquad \eta \equiv m_p^2 \frac{V_{\varphi\varphi}}{V} \ll \mathcal{O}(1) \quad . \tag{2.9}$$

The two definitions of ϵ in eq. (2.6) and (2.9) agree in the slow-roll limit and we have introduced the second slow-roll parameter[1] η. Consequently, the inflaton potential has to be relatively flat compared to its height.

2.2 Cosmological perturbations

Cosmological perturbations describe small deviations of the universe away from some perfectly homogeneous and isotropic universe given by the line-element in eq. (2.2). For instance, at decoupling these perturbations were of order 10^{-5} [18]. Therefore, a natural strategy is to split all quantities $Q(t, \vec{x})$ into a homogeneous background $Q_0(t)$ depending only on cosmic time and a space dependent perturbation $\delta Q(t, \vec{x})$. For instance, scalar field and metric perturbations are given by

$$\varphi(t, \vec{x}) = \varphi_0(t) + \delta\varphi(t, \vec{x}) \qquad\qquad g_{\mu\nu} = g^{(0)}_{\mu\nu}(t) + \delta g_{\mu\nu}(t, \vec{x}) \quad , \tag{2.10}$$

respectively. The various perturbations (scalar field, metric, energy density, ...) are coupled to each other via Einstein's equations and the Klein-Gordon equation and, hence, it is not possible to treat them separately. An additional subtlety for the study of cosmological

[1] Another definition of the second slow-roll parameter is $\eta_H \equiv \dot{\epsilon}/(\epsilon H)$ originating from the second slow-roll condition in eq. (2.6). Contrary to ϵ, the two definitions for η do not agree in the slow-roll limit, but $\eta_H = 4\epsilon - 2\eta$. Defining slow-roll parameters via H and its time derivatives is more general and applies also to other non-slow-roll mechanisms resulting in inflation and a scale-invariant power spectrum. In this work, we mainly consider slow-roll inflation and, hence, use the definitions in eq. (2.9).

perturbations is the fact that the split in eq. (2.10) into background and perturbations is not unique, but depends on the choice of coordinates also called a *gauge choice*. To be more precise, a perturbations δQ is defined as the difference between the value Q defined on the inhomogeneous, physical spacetime and the value Q_0 defined on the homogeneous background spacetime. In order to make this comparison meaningful, one must identify points of these two different spacetimes. Specifying this identification of points (a map) between background and physical spacetime is precisely the choice of a gauge.

It is common to decompose the metric perturbations according to their helicity with respect to local rotations of the spatial coordinate on hypersurfaces of constant time into scalars, divergence-free vectors and transverse, trace-free, symmetric tensors[2]. Vector perturbations are not created by the simplest models of inflation where, due to the absence of rotational velocity fields, the only degrees of freedom are scalar field and metric fluctuations. But even if they were created they would decay due to the subsequent expansion of the universe after inflation[3].

Neglecting vector perturbations and focusing on single-field inflation, we are left with 5 scalar degrees of freedom (4 metric perturbations + $\delta\varphi$) and the symmetric, transverse, trace-free tensor perturbations (denoted by γ from here on) whose degrees of freedom are the two polarisations. The choice of a gauge allows for removing two scalars by time reparametrisations and spatial reparametrisations of the form $x^i \to x^i + \partial^j\alpha$. Other reparametrisations would act on vector modes. At leading order, the tensor perturbation γ is not affected by such reparametrisations and, hence, gauge invariant. This is no longer true at subleading order due to combinations of reparametrisation parameters, like $\partial_i\alpha\,\partial_j\alpha$, affecting γ_{ij} (see e.g. [15]). For the following, this (higher order) gauge-dependence of γ will not be of interested and, hence, neglected. Returning to scalars, it is possible to define 3 scalar perturbations that do not change under reparametrisations of coordinates and, hence, are gauge-invariant. At linear order in the perturbations, this has been introduced first by Bardeen [12, 20] defining the two Bardeen potentials and a gauge-invariant scalar perturbation. A generalisation to higher order is possible and reviewed in [15].

Even though possibly gauge-invariant, the remaining 3 scalar perturbations are not independent. There are two additional constraints from Einstein's equation relating the metric perturbations to matter perturbations, i.e. $\delta\varphi$ in our case. Again, the tensor γ remains unaffected and we are left with 1 scalar and two tensor degrees of freedom. The choice which scalar degree to maintain depends on the desired calculation. Some governing equations are simpler in one gauge than in others. For the purpose of this paper, it is sufficient to consider two choices: the *spatially-flat gauge* and the *uniform-density gauge.*

We start with the *spatially-flat gauge*. In this gauge one selects spatial hypersurfaces on which the induced 3-metric is left unperturbed by scalar perturbations. All the scalar fluctuations on constant-time hypersurfaces are then in the scalar field(s) [14, 15]

$$\varphi(t,\vec{x}) = \varphi_0(t) + \delta\varphi(t,\vec{x}) \qquad\qquad g_{ij} = a^2(t)\,(e^{\gamma})_{ij} \quad , \tag{2.11}$$

where the symmetric tensor fulfils $\gamma_{ii} = 0 = \partial^i\gamma_{ij}$. Note that, here and henceforth, we have chosen to parametrise metric perturbations using the exponential function following [21–24] and subsequent papers. It is very convenient to calculate the evolution equation

[2]See particularly [16], 9.1.3 and A.2 explaining the decomposition according to helicity.

[3]This is true if non-linearities in the matter are absent, but not for e.g. cosmological defects (see e.g. [19] and references therein).

of scalar field perturbations in this gauge. At linear order and for the case of single field inflation, it reads [25–28] (for a generalisation to second order and multiple fields see [29])

$$\ddot{\delta\varphi} + 3H\dot{\delta\varphi} + \left[-\frac{\nabla^2}{a^2} + V_{\varphi\varphi} + 2\frac{\dot{H}}{H}\left(3H - \frac{\dot{H}}{H} + 2\frac{\ddot{\varphi}_0}{\dot{\varphi}_0}\right)\right]\delta\varphi = 0 \quad . \tag{2.12}$$

Note the term $2\dot{H}/H\,(\ldots)$ which is the coupling of the scalar field to gravity. It is evidently absent in pure deSitter space. We return to eq. (2.12) in a moment in order to calculate the mode functions of scalar field perturbations in inflationary spacetime.

Beforehand let us introduce the *uniform-density gauge* which is the second gauge we apply in this thesis. Obviously, it is defined by requiring that constant-time hypersurfaces are surfaces of constant energy-density. For the case of single-field inflation, uniform-density hypersurfaces trivially coincide with hypersurfaces of constant inflaton, i.e. $\delta\varphi = 0$. Note that this is generally not true for multi-field models[4]. The importance of this gauge for the forthcoming is that the gauge-invariant *scalar curvature perturbation* ζ can be non-perturbatively identified via the spatial metric parametrisation

$$g_{ij} = a^2(t)\; e^{2\zeta}\; (e^{\gamma})_{ij} \quad , \tag{2.13}$$

where again $\gamma_{ii} = 0 = \partial^i\gamma_{ij}$. It has been shown [23] that this is sufficient to uniquely define the comoving curvature perturbation ζ . For single field, slow-roll inflation ζ and γ are conserved quantities on superhorizon scales [22, 23, 31]. For multi-fields this is generally not true.

We note that there are several definitions of the comoving curvature perturbation ζ in the literature (see particularly the discussion in [32]). In eq. (2.13), we use the exponential function to parametrise the spatial part in the uniform-density gauge. Other authors prefer to work with the parametrisation

$$g_{ij} = a^2(t)\; \delta_{ij}\,(1 + 2\tilde{\zeta}) \tag{2.14}$$

(setting $\gamma_{ij} = 0$ for the moment). These two definitions are related by

$$\tilde{\zeta} = \zeta + \zeta^2 + 2\zeta^3/3 + \ldots \quad . \tag{2.15}$$

Thus, they coincide at linear order. Furthermore, also $\tilde{\zeta}$ is gauge-invariant and conserved on superhorizon scales due to its exclusive dependence on ζ. However, contrary to $\tilde{\zeta}$, the variable ζ is a an almost Gaussian variable in single field slow-roll inflation. This can be seen as follows: In this scenario, the leading order expression of the 3-point correlator $\langle\,\zeta^3\,\rangle = \mathcal{O}(\epsilon,\eta) \times \langle\,\zeta^4\,\rangle$ is suppressed by slow-roll parameters [22]. By contrast, the corresponding expression $\langle\,\tilde{\zeta}^3\,\rangle = \langle\,\zeta^4\,\rangle \gg \langle\,\zeta^3\,\rangle$ is much larger. Similar arguments also apply to higher n-point functions that are related to deviations from Gaussian statistics[5].

Though it is possible and common to define ζ non-perturbatively via the spatial metric in the uniform-density gauge, it leaves out the aspect that ζ is a gauge-invariant variable.

[4]In the simplest multi-field models, one field, the inflaton φ, is dominant during inflation. Hence, the uniform-density gauge corresponds to $\delta\varphi = 0$ also in these models. However, during or after inflation other scalar fields may become dominant as for instance in the curvaton scenario (see e.g. [30])

[5]For a discussion why it is the variable ζ being almost Gaussian and not $\tilde{\zeta}$ or any other expression $f(\zeta)$ see [32], sec. VI,A.

Thus, there should be a third definition of ζ applicable in a generic slicing. Such a gauge-invariant definition of ζ exists at first and second order in cosmological perturbation theory [15, 32] (and thus at every known order). To be more precise, for a generic slicing

$$g_{ij} = a^2(t)\, e^{2\psi}\ (e^{\gamma})_{ij} \tag{2.16}$$

there exists a gauge-invariant definition for ζ of the form

$$\zeta = \psi + F(\delta\rho, \rho_0, \ldots) \qquad \text{with} \qquad F(\delta\rho = 0, \rho_0, \ldots) = 0 \quad . \tag{2.17}$$

Recall that $\rho_0(t)$ denotes the homogeneous background energy density. Whether this applies non-perturbatively on all scales is still an open question. However, a non-perturbative gauge-invariant expression for the comoving curvature perturbation ζ on superhorizon scales was found in [23]. It reads

$$\zeta(t, \vec{x}) = \psi(t, \vec{x}) + \frac{1}{3} \int_{\rho_0(t)}^{\rho(t,\vec{x})} \frac{d\tilde{\rho}}{\tilde{\rho} + P} \quad , \tag{2.18}$$

where $\rho(t, \vec{x}) = \rho_0(t) + \delta\rho(t, \vec{x})$ and P denotes the pressure. Obviously, the integral is zero on slices of uniform energy density and, thus, coincides with eq. (2.13) in the uniform density gauge.

The quantity ζ (to much weaker extend in slow-roll inflation also γ) is of great interest since it specifies the geometry of the reheating surface (or any other surface after the end of inflation). As such the curvature perturbation ζ is directly related to observables, e.g. the temperature fluctuations of the CMB (Sachs-Wolfe effect [33]) or the distribution of matter in the early universe. Hence, at least indirectly ζ and γ are observable quantities. To calculate ζ we will make strong usage of its presence in the spatial part of the metric in the uniform-density gauge. The technicalities of this calculation will be discussed in sect. 2.3.

Let us now turn to the quantisation of the scalar field perturbations according to

$$\delta\varphi(t, \vec{x}) = \int \frac{d^3k}{(2\pi)^3} \left(f_{\vec{k}}(t, \vec{x})\, a_{\vec{k}} + f^*_{\vec{k}}(t, \vec{x})\, a^\dagger_{\vec{k}} \right) \quad , \tag{2.19}$$

where $a_{\vec{k}}$ and $a^\dagger_{\vec{k}}$ are respectively annihilation and creation operators satisfying the usual commutation relations. This requires to have knowledge on the mode functions $f_{\vec{k}}(t, \vec{x})$. For this purpose, we return to the evolution equation of the scalar field, eq. (2.12). In Fourier space

$$\delta\varphi(t, \vec{x}) = \int \frac{d^3k}{(2\pi)^3}\ e^{i\vec{k}\vec{x}}\, \delta\varphi_{\vec{k}}(t) \tag{2.20}$$

eq. (2.12) can be brought into the form of the Mukhanov-Sasaki equation, which can be solved analytically in the quasi-deSitter approximation. The general solution of this differential equation is a linear combination of Hankel's functions of the first and second kind, each of them solving the Mukhanov-Sasaki equation separately. To determine the mode functions completely, we need two conditions fixing the two linearity coefficients of the general solution.

The first condition to the mode functions is that they are orthonormal with respect to the invariant Klein-Gordon inner product, i.e.

$$\left(f_{\vec{k}}, f_{\vec{p}}\right) = -i \int d\Sigma^{\mu} \left(f_{\vec{k}} \overset{\leftrightarrow}{\partial}_{\mu} f^{*}_{\vec{p}}\right) = (2\pi)^3 \delta^{(3)}(\vec{k} - \vec{p}) \quad , \tag{2.21}$$

where $d\Sigma^{\mu}$ represents volume element and unit normal vector of the spatial hypersurface (see e.g. [34,35]). It is precisely this normalisation that ensures the commutator of annihilation and creation operator to be[6] $[a_{\vec{k}}, a^{\dagger}_{\vec{p}}] = (2\pi)^3 \delta^{(3)}(\vec{k} - \vec{p})$. For instance, in Minkowski space this fixes the mode function of a massless scalar field to

$$f_{\vec{k}} = \frac{1}{\sqrt{2k}} \, e^{-ikt + i\vec{k}\vec{x}} \quad , \tag{2.22}$$

where $k \equiv |\vec{k}|$.

The second condition that fixes the mode functions completely is more involved and comes from *vacuum selection*. Due to the absence of a globally time-like Killing vector in the inflationary spacetime, there is no canonical choice of a time variable to which one classifies modes as being positive or negative frequency and, hence, to associate them with creation or annihilation operators in the quantisation process. Therefore, contrary to Minkowski space there is not a single vacuum state in the inflationary spacetime, but a one parameter family of vacua. The standard choice is the Minkowski vacuum of a comoving observer in the infinite past $t \to -\infty$ (when all scales are well inside the horizon $\sim 1/H$). Due to the overall expansion, the identification of mode functions with their counterparts in Minkowski space can only be made in a comoving frame and with comoving time $\tau \equiv \int dt/a \approx -1/[aH(1-\epsilon)]$. This imposes[7]

$$\lim_{\tau \to -\infty} f_{\vec{k}}(\tau, \vec{x}) = \frac{1}{a(\tau)} \, \frac{e^{-ik\tau + i\vec{k}\vec{x}}}{\sqrt{2k}} \tag{2.23}$$

which fixes both conditions and uniquely determines the mode equations. The vacuum chosen this way is called the Bunch-Davies vacuum.

For the complete expression of the mode functions $f_{\vec{k}}$, we refer the reader again to the already mentioned reviews, e.g. [14, 16, 17]. Here, we are only interested in their limiting behaviour on superhorizon scales. Outside the horizon, i.e. for $|k\tau| \ll 1$, the expression of the quantum perturbations simplifies to

$$\delta\varphi(\vec{x}) \approx \int \frac{d^3k}{(2\pi)^3} \; e^{i\vec{k}\vec{x}} \, \frac{H(k)}{\sqrt{2k^3}} \, \hat{a}_{\vec{k}} \quad . \tag{2.24}$$

It turns out that the factor $\exp(i\vec{k}\vec{x})$ is the only imaginary part of the mode functions $f_{\vec{k}}$ on superhorizon scales. Hence, annihilation and creation operators always appear in the combination $\hat{a}_{\vec{k}} \equiv i(a^{\dagger}_{\vec{k}} - a_{-\vec{k}})$ in this limit. It is common to continue the calculation with the operator $\hat{a}_{\vec{k}}$ which has zero mean and variance $\langle \hat{a}_{\vec{k}} \; \hat{a}_{\vec{p}} \rangle = (2\pi)^3 \delta^{(3)}(\vec{k} + \vec{p})$. Higher correlation functions of $\hat{a}_{\vec{k}}$ follow by Wick's theorem. The argument of the Hubble

[6] For QFT in Minkowski space it is convenient to normalise modes such that the integration measure is Lorentz invariant, leading to the slightly different commutator relation $[a_{\vec{k}}, a^{\dagger}_{\vec{p}}] = (2\pi)^3 \; 2k \; \delta^{(3)}(\vec{k} - \vec{p})$.

[7] In case of a small mass $m \ll H$, k should be replaced by $\sqrt{k^2 + m^2}$. However, this does not affect the superhorizon regime which we are interested in.

function $H(k)$ denotes that it should be evaluated at horizon exit of the mode k (when $k = aH$). From this point on the mode remains frozen in[8].

When crossing the horizon, cosmological perturbations make a transition from a quantum to a classical regime. Pragmatically, this can be seen as follows: Inside the horizon, cosmological perturbations oscillate similar to quantum scalar fluctuations in flat spacetime. The quantum field operator of such a perturbation is expressed by annihilation and creation operators (and their corresponding mode functions $f_{\vec{k}}$ and $f^*_{\vec{k}}$). By contrast, on superhorizon scales $\delta\varphi$ can be expressed in a classical way including only a single operator $\hat{a}_{\vec{k}}$ with Gaussian statistics. It can be shown that The quantum fluctuation $\delta\varphi$ is effectively equivalent to a classical fluctuation consisting of a Fourier amplitude and a *Gaussian random variable* $\hat{a}_{\vec{k}}$. An extensive discussion on this issue is given in [36].

At leading order, eq. (2.24) is the expression of quantum scalar field fluctuations on superhorizon scales in the spatially flat gauge. From this expression one can deduce the curvature perturbation ζ via the δN-formalism (see sec. 2.3). In many cases, it is sufficient to consider this leading order analysis of scalar field perturbations and we will do so in the following. In slow-roll inflation, corrections to leading order results are suppressed by the slow-roll parameters and the Hubble scale $H/m_{\rm pl}$. We note that there are cases where leading-order results originate partially from higher-order calculations of $\delta\varphi$, the most prominent example being the non-Gaussianity parameter $f_{\rm NL}$ [22]. In these cases, the scalar field perturbations should be calculated to more accurate order. For this purpose, it is very convenient to apply the In-In formalism to cosmology [22, 24].

The last point to mention in this section is the analogous expression for tensor perturbations γ. They are calculated in a very similar way as scalar perturbations and, hence, we only give the result. At leading order tensor perturbations are given by

$$\gamma_{ij}(\vec{k}) = \sum_{s=+,\times} \frac{H(k)}{\sqrt{k^3}}\, \epsilon^s_{ij}(\vec{k})\, b^s_{\vec{k}} \quad , \tag{2.25}$$

where the polarisation tensors ϵ^s_{ij} are chosen to satisfy the transversality and tracelessness conditions, as well as an orthogonality relation[9].

2.3 The δN-formalism

In this section, we give a pedagogical introduction to the δN-formalism [23, 25, 37–39] which is a powerful tool to calculate the primordial curvature perturbation ζ from many inflaton models. The main observation of this formalism is that ζ can be identified as the perturbation in the local expansion.

In Friedmann-Robertson-Walker spacetimes there exists a preferred foliation of spatial hypersurfaces which is maximally symmetric. On these hypersurfaces, the matter density and pressure are homogeneous and isotropic. As we have seen before in sec. 2.2, this is different for inhomogeneous space-times, for which we perturb around the homogeneous part and the identification of points on homogeneous and inhomogeneous spacetime yields some

[8] Contrary to ζ and γ in single-field, slow-roll inflation $\delta\varphi$ is not conserved on superhorizon scales, but its evolution is strongly suppressed. In the following, correlation functions of $\delta\varphi$ will always be evaluated around the time of horizon exit. Hence, the evolution of $\delta\varphi$ outside the horizon is indeed negligible.

[9] Similar to $\hat{a}_{\vec{k}}$, the operator $b^s_{\vec{k}}$ has zero mean and variance $\langle\, b^s_{\vec{k}}\; b^{s'}_{\vec{p}}\,\rangle = (2\pi)^3\; \delta^{(3)}(\vec{k}+\vec{p})\;\; \delta^{ss'}$. The polarisation tensor for gravitational waves satisfies $\epsilon^s_{ii}(\vec{k}) = 0 = k_i \epsilon^s_{ij}(\vec{k})$ and the orthogonality relation $\sum_{ij} \epsilon^s_{ij}(\vec{k})\; \epsilon^{s'}_{ij}(-\vec{k}) = 2\delta_{ss'}$.

additional gauge freedom which does not destroy any symmetry. Therefore, it is desirable to have quantities that are invariant under the corresponding gauge transformations. An example is the comoving curvature perturbation ζ. Its non-perturbative gauge-invariant definition on superhorizon scales is already given in eq. (2.18) and reads [23]

$$\zeta(t,\vec{x}) = \psi(t,\vec{x}) + \frac{1}{3}\int_{\rho_0(t)}^{\rho(t,\vec{x})} \frac{d\tilde{\rho}}{\tilde{\rho}+P} \quad . \tag{2.26}$$

Furthermore, on superhorizon scales it can be shown [23] that the change in ψ, going from one slice at time t_i to another at t_f, is equal to the difference of the actual number of e-folds N and the background value $N_0 = \ln(\, a(t_f)/a(t_i)\,)$, i.e.

$$\psi(t_f,\vec{x}) - \psi(t_i,\vec{x}) = N(t_f,t_i,\vec{x}) - N_0(t_f,t_i) \quad . \tag{2.27}$$

As expected the actual number of e-folds N is equal to the background value N_0 if we choose the spatially-flat slicing where $\psi = 0$ at t_i and t_f. Another consequence of eq. (2.27) is that for two different slicings 1 and 2 which coincide for a spatial point $\vec{x}$ at time t_i, i.e. $\psi_1(t_i,\vec{x}) = \psi_2(t_i,\vec{x})$, the difference of slicing 1 and 2 at the final time t_f can be expressed by the difference in the actual number of e-folds

$$\psi_2(t_f,\vec{x}) - \psi_1(t_f,\vec{x}) = N_2(t_f,t_i,\vec{x}) - N_1(t_f,t_i,\vec{x}) \quad . \tag{2.28}$$

Here, the indices 1 and 2 refer to the respective slicing.

Due to gauge invariance, there is no preferred way to evaluate eq. (2.26). However, it is technically simplest to evaluate ζ by considering two different slicings. Slicing 1 starts and ends on spatially flat slices, i.e. $\psi_1(t_i,\vec{x}) = 0 = \psi_1(t_f,\vec{x})$ and $N_1(t_f,t_i,\vec{x}) = N_0(t_f,t_i)$. Slicing 2 also starts on a flat slice, but ends on a for the moment arbitrary slicing $\psi_2(t_f,\vec{x})$. Eq. (2.28) then yields

$$\psi_2(t_f,\vec{x}) = N_2(t_f,t_i,\vec{x}) - N_0(t_f,t_i) \quad . \tag{2.29}$$

Since slicing 1 only yields the background value N_0 in this equation, we will drop the index 2 and keep in mind that the quantities $\psi(t_f,\vec{x})$ and $N(t_f,t_i,\vec{x})$ refer to slicing 2. The expression $\psi(t_f,\vec{x})$ can now be combined with eq. (2.26) to calculate $\zeta(t_f,\vec{x})$. This can be further simplified if slicing 2 ends on a uniform-density slice. In this case, the integral in eq. (2.26) does not contribute yielding the main result of the δN-formalism [23, 25, 37–39]

$$\zeta(t_f,\vec{x}) = N(t_f,t_i,\vec{x}) - N_0(t_f,t_i) \equiv \delta N(t_f,\vec{x}) \quad . \tag{2.30}$$

We recall that $N(t_f,t_i,\vec{x})$ is the actual number of e-folds at the spatial point $\vec{x}$ from an initial spatially-flat slice to a final slice of uniform energy density and $N_0(t_f,t_i) = \ln(\, a(t_f)/a(t_i)\,)$ is the corresponding background value. By construction this expression for the curvature perturbation $\zeta(t_f)$ is independent of the choice of the initial spatially flat slice at time t_i as long as one stays in the superhorizon regime where eq. (2.26) is applicable. This property follows from the gauge-invariant definition in eq. (2.26) and was demonstrated in [40].

Eq. (2.30) can be physically motivated by considering comoving superhorizon patches, i.e. scales where spatial gradients and anisotropies can be safely neglected. Since they are causally disconnected, these patches or scales evolve independently from each other and

their evolution is well described by the Friedmann equations for a homogeneous universe with local (homogeneous) density and pressure. This picture is known as the "separate universe approach" [39] and may be derived from the full inhomogeneous dynamics by a gradient expansion to first order [21, 41, 42], i.e. in the long-wavelength limit. The only difference among different positions is a space-dependent scale factor. The curvature perturbation then arises as the difference in the number of e-foldings, δN.

We note that the initial time t_i should be chosen such that the scale of interest is well outside the horizon. Otherwise, quantum interactions would require a more complete treatment like the In-In formalism (first applied to cosmology in [22, 24]). By contrast, superhorizon modes behave as c-number, possibly time-dependent background for horizon-size, comoving patches in the In-In formalism. Hence, these can be evolved independently and classically. It is precisely this quantum to classical transition of modes crossing the horizon that allows for the use of the simpler and (semi-)classical calculation of the δN-formalism instead of performing the technically by far more involved complete quantum mechanical treatment (e.g. In-In formalism).

Nevertheless, we require knowledge of the statistics of the scalar field perturbation(s) $\delta\varphi$ on the initial spatially-flat hypersurface and, hence, we need to have knowledge of near and subhorizon fluctuations of the field(s). This requires a full quantum mechanical treatment and in this sense δN-formalism is not completely classical. To lowest order, all relevant scales are Gaussian on the initial surface with an amplitude given by the amplitude at horizon crossing of the corresponding mode. In many cases it is sufficient to restrict the calculation to this order in the scalar field fluctuations and, in most parts of this thesis, we will make this restriction. However, this is not true in general as for instance demonstrated by Maldacena [22] for the non-squeezed bispectrum in single-field inflation.

As already mentioned before, the "separate universe approach" [39] models the inhomogeneous universe by a patchwork of locally homogeneous region and, due to causality, these regions evolve independently from each other. Furthermore, via Friedmann equations applied locally to each region, one can determine the local expansion N in terms of the initial scalar field value(s) $\varphi(t_i) + \delta\varphi(t_i, \vec{x})$ in each patch. For instance in single-field, slow-roll inflation this relation is given to leading order by

$$N(\varphi) = \int_{\varphi_{\rm end}}^{\varphi} \frac{V}{V_\varphi}\, d\varphi \quad , \tag{2.31}$$

where we have assumed that t_f is some time after the end of inflation (e.g. reheating) and $\varphi_{\rm end}$ denotes the field configuration at which inflation ends. Otherwise, $\varphi_{\rm end}$ should be replaced by $\varphi(t_f)$. Clearly, $\varphi_{\rm end}$ is a model dependent parameter and, for the case of slow-roll inflation, is given by the field configuration along the trajectory in field space beginning to violate the slow-roll conditions. A Taylor expansion of eq. (2.30) yields

$$\zeta = N(\varphi + \delta\varphi(\vec{x})\,) - N(\varphi) \tag{2.32}$$

$$= N_\varphi\, \delta\varphi(\vec{x}) + \frac{1}{2} N_{\varphi\varphi}\, \delta\varphi^2(\vec{x}) + \frac{1}{6} N_{\varphi\varphi\varphi}\, \delta\varphi^3(\vec{x}) + \dots \quad . \tag{2.33}$$

We recall that a subscript φ denotes a derivative with respect to φ, i.e. $N_\varphi = \partial N/\partial\varphi$. Note that we have evolved classically the unperturbed $\varphi(t_i)$ on the initial hypersurface to the unperturbed final hypersurface, and denoted the unperturbed number of e-foldings by $N(\varphi)$. Contrary to the perturbed number of e-foldings $N(\varphi + \delta\varphi(x)\,)$, $N(\varphi)$ is a

constant that can be shifted (for instance in order to make $\langle\, \zeta \,\rangle = 0$). Such a constant shift in ζ can always be compensated by a redefinition of spatial coordinates or the scale factor. We stress again that the set of parameters $N_\varphi, N_{\varphi\varphi}, \ldots$ are model dependent quantities. Moreover, in slow-roll inflation $N_\varphi, N_{\varphi\varphi}, \ldots$ may be expressed by the set of slow-roll parameters $\epsilon, \eta, \xi, \ldots$ and vice versa. The first two relations are

$$N_\varphi^2 = \frac{1}{2m_p^2\,\epsilon} \qquad\qquad \frac{N_{\varphi\varphi}}{N_\varphi^2} = 2\epsilon - \eta \quad . \tag{2.34}$$

Working in δN-formalism it is common to express results in terms of derivatives of N instead of slow-roll parameters to keep equations simple.

With eq. (2.33) it is then easy to express any correlator of comoving curvature perturbations by a series of scalar field correlators. Typically, this is done in terms of Fourier components $\zeta_{\vec{k}}$ and $\delta\varphi_{\vec{k}}$. As usual, powers of $\delta\varphi(\vec{x})$ yield convolutions in Fourier space, e.g.

$$\left(\delta\varphi^2\right)_{\vec{k}} = \int \frac{d^3q}{(2\pi)^3}\; \delta\varphi_{\vec{q}}\, \delta\varphi_{\vec{k}-\vec{q}} \quad , \tag{2.35}$$

which introduces also an integration over long-wavelength modes. The first terms in the series for n-point correlators are

$$\langle\, \zeta_{\vec{k}_1}\, \zeta_{\vec{k}_2} \,\rangle = N_\varphi^2\, \langle\, \delta\varphi_{\vec{k}_1}\, \delta\varphi_{\vec{k}_2} \,\rangle \tag{2.36}$$

$$\langle\, \zeta_{\vec{k}_1}\, \zeta_{\vec{k}_2}\, \zeta_{\vec{k}_3} \,\rangle = \frac{1}{2} N_{\varphi\varphi} N_\varphi^2\, \langle\, \left(\delta\varphi^2\right)_{\vec{k}_1}\, \delta\varphi_{\vec{k}_2}\, \delta\varphi_{\vec{k}_3} \,\rangle + 2 \text{ perm.} \tag{2.37}$$

$$\vdots$$

They can be further evaluated by knowing the statistics of the scalar field fluctuations $\delta\varphi$. Strictly speaking, this is not part of the δN-formalism, but the result of an extra quantum mechanical calculation. As already mentioned above, we will consider only linear field perturbations on spatially flat hypersurfaces in canonical, slow-roll inflation (see sec. 2.2), where $\delta\varphi_{\vec{k}} = (H/\sqrt{2k^3})\, \hat{a}_{\vec{k}}$. Recall that H is evaluated at horizon exit of the mode k and $\hat{a}_{\vec{k}}$ is again a Gaussian random variable. The fact that the value of H at horizon exit is locally dependent on long-wavelength modes will be a central point in chapter 3. With this statistics, the spectra of the comoving curvature perturbation ζ in single-field, slow-roll inflation read[10]

$$\mathcal{P}_\zeta^{(0)}(k) = \left(\frac{N_\varphi H}{2\pi}\right)^2 \tag{2.38}$$

$$B_\zeta^{(0)}(k_1, k_2, k_3) = N_{\varphi\varphi} N_\varphi^2 \left[P_{\delta\varphi}^{(0)}(k_1)\; P_{\delta\varphi}^{(0)}(k_2) + 2 \text{ perm.} \right] \tag{2.39}$$

$$\vdots$$

where we attached the superscript $^{(0)}$ to indicate that these are leading order results. Note that we used the standard notation for the bispectrum including the uncurly power spectrum $P(k) = (2\pi^2/k^3)\, \mathcal{P}(k)$ which takes into account volume factors and the naive scaling in k-space. Recall that ζ is conserved on superhorizon scales in single-field, slow-roll inflation. Hence, quantities in the expression of $\zeta_{\vec{k}}$ should be evaluated at horizon exit

[10] The power and bispectrum are defined in the usual way, i.e. $\langle\, \zeta_{\vec{k}} \zeta_{\vec{p}} \,\rangle = (2\pi)^3\, \delta^{(3)}(\vec{k}+\vec{p})\; (2\pi^2/k^3)\, \mathcal{P}_\zeta(k)$ and $\langle\, \zeta_{\vec{k}}\, \zeta_{\vec{p}}\, \zeta_{\vec{q}} \,\rangle = (2\pi)^3\, \delta^{(3)}(\vec{k}+\vec{p}+\vec{q})\; B_\zeta(k,p,q)$, respectively.

of the mode $\vec{k}$ making them explicitly $\vec{k}$-dependent. Thus, for instance the expression of the power spectrum in eq. (2.38) has a scale-dependence

$$n_\zeta - 1 \equiv \frac{d \ln \mathcal{P}_\zeta}{d \ln k} = 2\eta - 6\epsilon \quad , \tag{2.40}$$

defining the spectral index n_ζ.

When reviewing the δN-formalism, one should also mention its critical aspects. Due to the quantum to classical transition of modes crossing the horizon, it seems rather natural to split the much more involved full quantum mechanical calculation into a subhorizon part, which still has to be tackled with quantum mechanical methods, and a classical superhorizon part. However, the technical implementation of this split is very prone to errors. For instance, one has to carefully check which order of the subhorizon calculation will be relevant for the final superhorizon result. The standard assumption of modes being Gaussian at horizon exit is not sufficient in many cases and, hence, higher-order corrections of the subhorizon part need to be included (see chapter 3).

Furthermore, one has to keep in mind that the δN-formalism is only valid on superhorizon scales when $k \ll aH$ for all scales k. This statement is to be understood as follows: The results of the δN-formalism are in fact leading order results of an expansion in $k/(aH)$. Due to the exponential expansion, these leading order results quickly become extremely accurate after horizon crossing of the scale k. However, directly at horizon crossing (when $k = aH$) the δN-formalism may not be a good approximation. Thus, the initial time t_i cannot be taken to be the time of horizon crossing but slightly later when the condition $k \ll aH$ is well fulfilled. The subhorizon calculation only yields the results at horizon exit. A solution would be to extend the quantum mechanical subhorizon calculation to the (superhorizon) time t_i. However, such an extension would destroy the simplification gained from the split and, hence, a complete quantum mechanical treatment for all scales would be more appropriate. Consequently, applying the δN-formalism implies assuming that the change of modes from horizon exit to the time t_i is negligible.

An example for the aforementioned criticisms is the expression of the bispectrum in single-field slow-roll inflation whose correct expression was not known until the In-In formalism was applied to cosmology [22]. Nevertheless, the δN-formalism is in many cases a simple and powerful technique to calculate the primordial curvature perturbation ζ. One has merely to be careful in which cases it is reliable and in which cases the δN-formalism only gives an order of magnitude estimate and the correct result has to be calculated using a complete quantum mechanical formalism.

As a last point of this section, let us briefly discuss how the above generalises to the case of multi-field inflation, where we have a set of scalar fields $\{\varphi^a\}$ during inflation. The inflaton is one of them, but can also be a linear combination of φ^a which varies as a function of time. The other fields, which are orthogonal to the inflaton in field space, are called isocurvatons. Again, we pick an initial spatially flat hypersurface and a final uniform-density surface for the same reason as described above. Initially all fluctuations are in the scalar fields $\varphi^a + \delta\varphi^a(\vec{x})$ and, again, we evolve all the fields from the initial to the final slice in order to get

$$\zeta(\vec{x}) = \delta N(\vec{x}) = N_a \, \delta\varphi^a(\vec{x}) + \frac{1}{2} N_{ab} \, \delta\varphi^a(\vec{x}) \, \delta\varphi^b(\vec{x}) + \ldots \quad . \tag{2.41}$$

In multi-field inflation, it is common to denote a derivative along the scalar field labelled by a with a subscript a, i.e. $N_a = \partial N / \partial \varphi^a$. We will also adapt the standard notation in

this work, i.e. N_φ for single-field and N_a for multi-field inflation, and sincerely apologise to the reader for the possible confusion. Furthermore, a summation over repeated indices is understood in eq. (2.41). One can then proceed in a similar fashion as in single-field inflation and express ζ-correlators in terms of correlators of field fluctuations and apply the statistics of the fluctuations $\{\delta\varphi^a\}$. Contrary to single-field inflation, the curvature perturbation ζ is generally not conserved if more than one field is present. In this case, the evolution of ζ has to be taken into account, resulting in slightly more complicated expression for N_φ, $N_{\varphi\varphi}$, ... (see e.g. [15, 17, 43]).

2.4 Non-Gaussianity and Infrared effects

In the previous section we gave a pedagogical introduction to the δN-formalism, yielding the expression

$$\zeta_{\vec{k}} = N_\varphi \, \delta\varphi_{\vec{k}} + \frac{1}{2} N_{\varphi\varphi} \, \left(\delta\varphi^2\right)_{\vec{k}} + \frac{1}{6} N_{\varphi\varphi\varphi} \, \left(\delta\varphi^3\right)_{\vec{k}} + \dots \tag{2.42}$$

for the curvature perturbation ζ. In order to explain current observations, it is sufficient to consider only the leading term on the right hand-side of this equation (assuming $\delta\varphi$ to be Gaussian at horizon exit). However, theoretically and in light of forthcoming observations, it is worthwhile to additionally consider effects originating from higher order terms. In this work, we will particularly focus on two of these effects.

The first is the generation of *non-Gaussianity*. Considering only the leading expression for ζ corresponds to considering a curvature perturbation ζ which is subject to Gaussian statistics. In this limit any n-point function of odd n obviously vanishes exactly and higher n-point functions of even n follow the usual Gaussian expressions determined by the two-point function. The higher order terms in the expression of ζ, eq. (2.42), cause deviations from these Gaussian expressions and, hence, introduce non-Gaussianity. For instance, the leading, non-zero expression of the three-point function, given in eq. (2.39), is originating from the first and second term on the right hand-side in eq. (2.42) (plus possible non-Gaussian parts in $\delta\varphi$). It is now widely accepted that non-Gaussianity is a powerful probe to discriminate between the many currently viable inflationary models [17, 44–49].

The deviation from Gaussian statistics is commonly parametrised by dimensionless non-Gaussianity parameters like $f_{\rm NL}$ or $g_{\rm NL}$. Their precise definitions depend on the particular form of non-Gaussianity and is based on the leading, non-zero expression of the corresponding correlation function. For instance for non-Gaussianity of the local form [21, 50], the parameter $f_{\rm NL}$ is defined by

$$B_\zeta(k_1, k_2, k_3) = \frac{6}{5} \, f_{\rm NL} \, \left[P_\zeta(k_1) \, P_\zeta(k_2) + 2 \text{ perm.}\right] \quad . \tag{2.43}$$

In single-field slow-roll inflation the correct expression of $f_{\rm NL}$ was calculated first in [22]. We note that the non-Gaussianity parameters are defined such that they are scale-independent at leading order. In general, they acquire scale-dependencies from higher order terms [40, 51–54]. This behaviour will be analysed for local non-Gaussianity in chapter 5. Other forms of non-Gaussianity are considered in chapter 6 where we also give the corresponding definitions of $f_{\rm NL}$ and summarise from which models the various non-Gaussianity forms typically arise (see sec. 6.3.1).

Furthermore, higher-order corrections introduce a dependence on long-wavelength background modes. Such infrared effects explicitly arise in loop corrections to inflationary observables (using e.g. the In-In formalism) or through the nonlinear dependence of

the curvature perturbation on fluctuations of an underlying scalar field (e.g. in the δN approach). For instance, in the latter case the next-to-leading order result includes an expression of the form

$$N_{\varphi\varphi}^2 \langle\, (\delta\varphi^2)_{\vec{k}} (\delta\varphi^2)_{\vec{p}} \,\rangle = N_{\varphi\varphi}^2 \int \frac{d^3q}{(2\pi)^3} \frac{d^3l}{(2\pi)^3} \,\langle\, \delta\varphi_{\vec{q}}\, \delta\varphi_{\vec{k}-\vec{q}}\, \delta\varphi_{\vec{l}}\, \delta\varphi_{\vec{p}-\vec{l}} \,\rangle \tag{2.44}$$

$$\sim N_{\varphi\varphi}^2 H^4 \int \frac{d^3q}{q^3} \sim N_{\varphi\varphi}^2 H^4 \ln(kL) \quad . \tag{2.45}$$

Here, we have introduced an IR cut-off $1/L$ and we have assumed (in the second line) that the power spectrum of $\delta\varphi$ is sufficiently scale-invariant. We have dropped the UV-part of the integral since we are interested exclusively on the dependence on long-wavelength, background (IR) modes. Furthermore, the UV-part can be handled by standard field theoretical methods. Infrared divergences associated with the inflationary power spectrum are a long-standing issue [8, 9, 55–58] which has more recently received a lot of attention following [24, 59]. It has been argued [60] that the cut-off L should be taken as the side-length of the region in which the measurement has been performed. As a subresult of our findings in chapter 4 (see also [61]), we will later confirm this size of the cut-off.

The physical origin of this IR divergences/IR effects is closely related to the well-known divergence in deSitter space [62, 63]. DeSitter space is effectively compact. Thus, the zero mode is dynamical and diffuses similar to a quantum mechanical particle without a potential. However, assuming that fluctuations on the reheating surface are (at least indirectly) observable quantities, we perform a measurement and the divergence becomes irrelevant. Nevertheless, it returns through higher order corrections.

According to the construction of the δN-formalism, the complete calculation is split into a sub- and a superhorizon regime. The subhorizon calculation enters the curvature perturbation ζ via the expression of $\delta\varphi$ at horizon exit while the superhorizon calculation is essentially given by eq. (2.42). Thus, it is important to note that each of the aforementioned effects may enter in the sub- and in the superhorizon regime. The fact that corrections may enter already in the subhorizon regime will play a central role in chapter 3.

2.5 Overview

This thesis is organised as follows: Each of the main chapters 3-6 is based on a publication. The corresponding reference is given at the very beginning of the chapter, followed by short overview of discussion in the chapter. There is only a mild dependence among the chapters and the reader who is particularly interested in a certain subject may directly jump to the relevant chapter.

The content of chapter 3 "Inflationary Infrared Divergences: Geometry of the Reheating Surface vs. δN-Formalism" is published in [64]. In this chapter, we describe a simple way of incorporating fluctuations of the Hubble scale H during the horizon exit of scalar perturbations into the δN-formalism. As discussed in sec. 2.4, curvature perturbations during inflation are affected by infrared divergences. We approach these IR effects starting from δN-formalism. It turns out that the problem can be rather easily resolved by a modification of the δN-formalism taking into account the aforementioned fluctuations of the Hubble scale H. The Hubble scale is appearing in the expression of the scalar

field perturbation $\delta\varphi_{\vec{k}} \sim H$ and, therefore, is an "external" input to the δN-formalism in the sense that the correct expression around horizon exit has to be known by different methods, e.g. the In-In formalism. The non-linear dependence of the scalar field perturbation on the number of e-folds and its derivatives $N_\varphi, N_{\varphi\varphi}, \ldots$ is taken into account by higher-order terms in the δN expansion. As an "external" input the backreaction of modes $\delta\varphi_{\vec{q}}$ with $\vec{q} \neq \vec{k}$ on $\delta\varphi_{\vec{k}}$ itself and, hence, on H is clearly not incorporated in the δN-formalism. This incorporation has been neglected in any δN calculation so far.

Since we are interested in IR effects, we only include fluctuations of the Hubble scale due to long-wavelength modes $\delta\varphi_{\vec{q}}$ ($q \ll k$). We note that locally the sum of long-wavelength modes (long-wavelength compared to the mode $\vec{k}$)

$$\delta\bar{\varphi}(\vec{x}) = \int\limits_{q\ll k} \frac{d^3q}{(2\pi)^3}\, e^{i\vec{q}\vec{x}}\, \delta\varphi_{\vec{q}} \tag{2.46}$$

introduces a shift on top of the homogeneous and isotropic background φ_0. We incorporate this shift by writing the scalar field perturbation in a quasi-deSitter background as

$$\delta\varphi(\vec{x}) = \int \frac{d^3k}{(2\pi)^3} \frac{e^{i\vec{k}\vec{x}}}{\sqrt{2k^3}}\, H(\,\varphi_0 + \delta\bar{\varphi}(\vec{x})\,)\;\hat{a}_{\vec{k}} \quad . \tag{2.47}$$

The calculation of ζ-correlators can then be done in the familiar way by evaluating correlators of $\hat{a}_{\vec{k}}$. Clearly, the incorporation of fluctuations of the Hubble scale according to eq. (2.47) leads to IR effects on top of the familiar 'c-loops' effects from the δN-formalism. Combining both these contributions the first log-enhanced correction to the power spectrum takes the very simple form

$$\mathcal{P}_\zeta(k) = \mathcal{P}_\zeta^{(0)}(k) + \frac{1}{2}\langle\, \delta\bar{\varphi}^2 \,\rangle\, \frac{d^2}{d\varphi^2}\mathcal{P}_\zeta^{(0)} \quad . \tag{2.48}$$

Here, the expression $\langle\, \delta\bar{\varphi}^2 \,\rangle \sim H^2 \ln(kL)$ corresponds to the expectation value of scalar field perturbations measured on a length scale $1/k$. Therefore, up to the order of the first log-enhanced correction, the complete power spectrum can be expressed as the tree-level result plus its derivatives times the variance of the background $\delta\bar{\varphi}$.

The physical significance of eq. (2.48) can be understood as follows: Disregarding tensor modes, the geometry of the reheating surface (or any other surface of uniform energy-density), parametrised by coordinates $\vec{y}$, can be characterised by a single scalar function $\zeta(\vec{y})$, the comoving curvature perturbation. The power spectrum $\mathcal{P}_\zeta$ may be defined as the logarithmic derivative of the correlation function $\langle\, \zeta(\vec{x})\;\zeta(\vec{x}+\vec{y})\,\rangle$ with respect to $y = |\vec{y}|$. Alternatively, a closely related spectrum $\tilde{\mathcal{P}}_\zeta$ based on the invariant distance z between the pair of points in the correlator can be defined in an analogous manner. The latter power spectrum is an entirely local quantity and its expectation value does not depend on the size of the region in which the measurement is performed. Defining $\bar{\zeta}$ as the average value of ζ characteristic for a small region containing a particular pair of points $\vec{x}$ and $\vec{x}+\vec{y}$, the relation between the euclidean coordinate distance y and the invariant distance z is given by

$$z = e^{\bar{\zeta}}\, y \quad . \tag{2.49}$$

The two power spectra, which we denoted by $\mathcal{P}_\zeta(y)$ and $\tilde{\mathcal{P}}_\zeta(z)$, are then related by

$$\mathcal{P}_\zeta(y) = \langle\, \tilde{\mathcal{P}}_\zeta(y\, e^{\bar{\zeta}})\,\rangle \quad , \tag{2.50}$$

where the averaging process is over the potentially large region in which the measurement of correlation functions is performed. Clearly, the averages $\langle\, \bar{\zeta}\,\rangle$ and variance $\langle\, \bar{\zeta}^2\,\rangle$ strongly depend on this region and lead precisely to the same log-enhancement of $\mathcal{P}_\zeta$ found earlier in (our implementation of) the δN-formalism.

This agreement provides support for the implementation of the δN-formalism that we advocate. Furthermore, it makes the 'physical reality' of large logs from IR divergences particularly clear: The log-enhancement arises due to the use of global coordinates in a very large region, where these deviate significantly from the invariant distance. It can be avoided if one measures the power spectrum $\tilde{\mathcal{P}}_\zeta(z)$, which is defined using a two-point correlation function based on the invariant distance between each pair of points appearing in the spatial average.

Chapter 4 "Inflationary Correlation Function without Infrared Divergences" is published in [61]. It is a continuation of the results presented in chapter 3. In chapter 4, we define infrared-safe correlation functions directly in Fourier space taking into account the effect from long-wavelength scalar and tensor modes. These infrared-safe correlation functions are purely local quantities and, hence, have no sensitivity to the size L of the box used for observations. The conventional correlators with their familiar log-enhanced corrections, both from scalar and tensor long-wavelength modes, are easily recovered from our IR-safe correlation functions.

The way to define IR-safe correlation functions is again by making use of the invariant distance z on the reheating surface. For instance the power spectrum of a mode $\vec{k}$ can be written by definition as the Fourier transform of the correlation function in real space:

$$\mathcal{P}_\zeta(k) = \frac{k^3}{2\pi^2}\int d^3y\, e^{-i\vec{k}\vec{y}}\,\langle\, \zeta(\vec{x})\,\zeta(\vec{x}+\vec{y})\,\rangle \quad . \tag{2.51}$$

Since, we want to interpret this formula as a practical prescription for the measurement of the power spectrum, we view $\langle \ldots \rangle$ as averaging process over pairs of points separated by the coordinate-vector $\vec{y}$, i.e. as average over the position $\vec{x}$ of the pairs. Due to the effect of scalar and tensor long-wavelength modes, summed up in $\bar{\zeta}$ and $\bar{\gamma}$ respectively, the physical separation of a particular pair in the averaging process in eq. (2.51) is strongly dependent on the position $\vec{x}$. To be more precise, the physical separation, given by the invariant distance $z = |\, e^{\bar{\zeta}}\, e^{\bar{\gamma}/2}\,\vec{y}\,|$, depends on the local quantities $\bar{\zeta}(\vec{x})$ and $\bar{\gamma}(\vec{x})$. Hence, since $\langle\, \bar{\zeta}^2\,\rangle$ and $\langle\, \bar{\gamma}^2\,\rangle$ are $\sim \ln(kL)$, the invariant distance z is varying strongly over the possible large region of box-size L in which the measurement of the correlation functions is performed. Clearly, this problem is originating from the averaging process selecting pairs of points separated by a coordinate-vector $\vec{y}$ whose corresponding physical distance is only defined globally (in the whole observable region).

Our proposal to solve this problem is to define the spectrum by an average over pairs of points all having the *same physical separation* z (now with varying coordinate-vector $\vec{y}(\vec{x})$). This is implemented by the definition

$$\mathcal{P}^{(0)}_\zeta(k) = \frac{k^3}{2\pi^2}\int d^3y\, e^{-i\vec{k}\vec{z}}\langle\, \zeta(\vec{x})\,\zeta(\vec{x}+e^{-\bar{\zeta}(\vec{x})}\,e^{-\bar{\gamma}(\vec{x})/2}\,\vec{z})\,\rangle \quad . \tag{2.52}$$

Obviously the relation between $\vec{y}$ and $\vec{z}$ is given by $\vec{z} = e^{\bar{\zeta}}\, e^{\bar{\gamma}/2}\,\vec{y}$. Therefore, the pairs of points in the correlator of eq. (2.52) are indeed all separated by the same physical (or invariant) distance $z = \sqrt{\delta_{ij}\, z^i z^j}$. The z-dependence of this correlator is then a background-independent object and the corresponding power spectrum $\mathcal{P}^{(0)}_\zeta$ is IR-safe.

The expression for the original IR-sensitive power spectrum $\mathcal{P}_\zeta$ follows from comparing eqs. (2.51) and (2.52) and yields

$$\mathcal{P}_\zeta(k) = \left\langle \left[\left(e^{-\bar{\gamma}(\vec{x})}\right)_{ij} \hat{k}_i \hat{k}_j \right]^{-3/2} \mathcal{P}_\zeta^{(0)} \left(e^{-\bar{\zeta}(\vec{x})} e^{-\bar{\gamma}(\vec{x})/2} \vec{k} \right) \right\rangle \quad . \tag{2.53}$$

Here, the vector $\hat{k}$ is a unit-vector in $\vec{k}$-direction and the average is performed over the background quantities $\bar{\zeta}(\vec{x})$ and $\bar{\gamma}_{ij}(\vec{x})$. A Taylor expansion of the right hand-side yields the familiar log-enhanced corrections of scalar and tensor perturbations to the leading-order expression of the power spectrum. However, in our formalism corrections automatically emerge in a resummed, all-orders form.

We generalise our findings for the power spectrum to higher n-point functions and apply our results to the two- and three-point function of the comoving curvature perturbation ζ in single-field, slow-roll inflation. We also present a generalisation of the δN-formalism allowing for the incorporation of corrections originating from tensor modes (corrections originating from scalar modes are already incorporated correctly by considering fluctuations of the Hubble scale H, see chapter 3). As expected, this generalised δN-formalism yields the same results in all cases were the formalism is applicable.

Furthermore, our resummed, all-orders expression of eq. (2.53) allows us to evaluate IR corrections in a non-perturbative way by using statistical properties of the integrated long-wavelength fluctuations $\bar{\zeta}$ and $\bar{\gamma}$. We apply this framework to specific inflationary set-ups, obtaining a complete expression of the power spectrum that includes all contributions of long-wavelength modes, and to perform a convergence analysis of the perturbation series of IR log-enhanced corrections.

Chapter 5 "Scale-dependent non-Gaussianity probes inflationary physics" is published in [65]. While chapter 3 and 4 discuss the issue of IR effects in inflationary correlation functions, chapter 5 discusses the scale-dependence of the bispectrum and trispectrum in (quasi) local models of non-Gaussian primordial density perturbations. The properties of these spectra are contained in the non-linearity parameters $f_{\rm NL}$, $g_{\rm NL}$, and $\tau_{\rm NL}$. It has been recently pointed out that, both from a theoretical and observational point of view, $f_{\rm NL}$ is not necessarily a constant[11]. We show that the same holds true also for $g_{\rm NL}$ and $\tau_{\rm NL}$. Similar to the power spectrum and the spectral index, we characterise the scale-dependence of these quantities in terms of new observable parameters $n_{f_{\rm NL}}$, $n_{g_{\rm NL}}$ and $n_{\tau_{\rm NL}}$, respectively.

In order to study these observables, we apply an approach based on the δN-formalism, which allows us to obtain an expression for the curvature perturbation ζ that generalises the local ansatz and contains the aforementioned scale-dependence parameters. Schematically, the curvature perturbation can be written as

$$\zeta_{\vec{k}} = \zeta^{\rm G}_{\vec{k}} + \frac{3}{5} f^{\rm p}_{\rm NL} \left(1 + n_{f_{\rm NL}} \ln k\right) \left(\zeta^{\rm G} \star \zeta^{\rm G}\right)_{\vec{k}} + \frac{9}{25} g^{\rm p}_{\rm NL} \left(1 + n_{g_{\rm NL}} \ln k\right) \left(\zeta^{\rm G} \star \zeta^{\rm G} \star \zeta^{\rm G}\right)_{\vec{k}} + \dots \quad , \tag{2.54}$$

where $\zeta^{\rm G}$ is a Gaussian variable and $f^{\rm p}_{\rm NL}$ and $g^{\rm p}_{\rm NL}$ are constants. This approach allows us to directly calculate $n_{f_{\rm NL}}$, $n_{g_{\rm NL}}$ and $n_{\tau_{\rm NL}}$ in models with arbitrary inflationary potential and number of fields, assuming slow-roll inflation.

The explicit expressions of these scale-dependence parameters depend on properties of the inflationary potential, namely its third and fourth derivative along the direction of

[11] See references in sec. 5.1.

field space generating non-Gaussianity. Generally (and in particular in all observationally interesting cases) these do not coincide with the adiabatic direction during inflation. Consequently, they are sensitive to properties of the inflationary physics that are not probed by standard observables like the spectral index and its running. Therefore, they provide additional powerful observables, able to offer novel information about the inflationary mechanism.

In the first part of the chapter, we present the calculation of the quantities $f_{\rm NL}$, $g_{\rm NL}$, and $\tau_{\rm NL}$ and the parameters representing their scale-dependence $n_{f_{\rm NL}}$, $n_{g_{\rm NL}}$ and $n_{\tau_{\rm NL}}$. At this point we focus on equilateral configurations, i.e. $k_1 = k_2 = k_3$ for $f_{\rm NL}$ and analogously for $g_{\rm NL}$ and $\tau_{\rm NL}$. We apply our findings to the general single field case and to several two field models of inflation showing that the scale-dependence can be significant. In certain classes of these model, we find consistency relations of the scale-dependence parameters helping to discriminate among inflationary models.

So far in chapter 5, we have concentrated our analysis on the scale dependence of equilateral configurations (triangles and quadrilaterals), varying only the overall scale. Since it may be of interest to consider more general variations in which one changes the shape of the figure under consideration, we also analyse these cases. Furthermore, we find the combination of shape and scale-dependence which maximises the scale-dependence, e.g. $n_{f_{\rm NL}}$.

While in most of chapter 5 we work in momentum space, in the last part we also discuss how the shape dependencies of the non-linearity parameters affect the analysis in real space. We provide an expression for the curvature perturbation ζ in real space, that generalises the simplest local ansatz, and that exhibits directly in coordinate space the effect of scale-dependence of non-Gaussianity parameters.

Chapter 6 "A weak lensing view on primordial non-Gaussianities" is published in [66]. In this chapter we forecast the constraints which the weak lensing bispectrum will be able to make on primordial non-Gaussianity, especially with a view to the Euclid space telescope planned to be launched in 2017. So far most of the constraints on primordial non-Gaussianities are reported using CMB observations. The latest and tightest bounds have been obtained from the WMAP 7-year data [18]. Although the constraints from weak lensing are not competitive with the ones from CMB or galaxy surveys, they are complementary since they probe smaller scales. Hence, they provide additional, independent constraints on primordial non-Gaussianity and its scale-dependence.

First, we predict the signal-to-noise ratio generated in the Euclid weak lensing survey. We find the 1σ errors for $f_{\rm NL}$ are 200, 575 and 1630 for local, orthogonal and equilateral non-Gaussianities, respectively. The configuration space integrations for these calculations can be carried out very efficiently by Monte-Carlo integration schemes at a fraction of the computational cost. For instance, the signal-to-noise ratio of the weak lensing bispectrum $B(l_1, l_2, l_3)$ can be done with accuracies below a percent with only a fraction of $\mathcal{O}(10^{-4})$ evaluations in comparison to evaluating the direct sum over l_1, l_2 and l_3.

We also consider misestimates of $f_{\rm NL}$ by fitting the wrong bispectrum type to data. We find that misestimates up to a factor of ± 3 are easily possible. We found that one would notice such a strong discrepancy between data and model from values of $f_{\rm NL}$ of a hundred on by looking at the χ^2-function.

As a last point, we analyse degeneracies of the primordial bispectrum with other cosmological parameters (though only the matter density Ω_m plays a significant role) and the subtraction of the much larger, structure-formation generated bispectrum. The latter

can be subtracted if the underlying cosmology during structure formation is known precisely enough. Propagating the uncertainty in the cosmological parameter set, assuming a wCDM universe, we find misestimations from this subtraction process which are much less than the statistical accuracy. Hence, any residual structure formation bispectrum would influence the estimation of f_{NL} to a minor degree.

Finally, in chapter 7 we draw our conclusions and describe possible continuations of the discussed research topics.

Chapter 3

Inflationary Infrared Divergences: Geometry of the Reheating Surface vs. δN-Formalism

The content of this chapter is published in [64].

In this chapter, we describe a simple way of incorporating fluctuations of the Hubble scale during the horizon exit of scalar perturbations into the δN-formalism. The dominant effect comes from the dependence of the Hubble scale on low-frequency modes of the inflaton. This modifies the coefficient of the log-enhanced term appearing in the curvature spectrum at second order in field fluctuations. With this modification, the relevant coefficient turns out to be proportional to the second derivative of the tree-level spectrum with respect to the inflaton φ at horizon exit. A logarithm with precisely the same coefficient appears in a calculation of the log-enhancement of the curvature spectrum based purely on the geometry of the reheating surface. We take this agreement as strong support for the proposed implementation of the δN-formalism. Moreover, our analysis makes it apparent that the log-enhancement of the inflationary power-spectrum is indeed physical if this quantity is defined using a global coordinate system on the reheating surface (or any other post-inflationary surface of constant energy density). However, it can be avoided by defining the spectrum using invariant distances on this surface.

3.1 Introduction

It is well known that curvature perturbations created during cosmological inflation [5, 6, 9–12] [14] are affected by infrared (IR) divergences [60, 67] (see [68–79] for some recent discussions). These divergences are closely related to the familiar divergence of the scalar-field correlator in de Sitter space [35, 62, 63]. While, at leading order, the divergence can be absorbed into the definition of the background and is hence unobservable, higher orders in the curvature perturbation lead to corresponding log-enhanced corrections to the power spectrum. Since the IR cutoff appearing in these logarithms is provided by the size of the observed universe (rather than by, for example, the size of the universe created by inflation), these logarithms are, however, not particularly large in practice [60]. Nevertheless, it is conceivable that the power spectrum is measured by a very late observer,

who has access to the entire region of the universe created in 'our' inflationary patch.[1] For such a 'late' observer, the infrared logarithms can be extremely large and it is an interesting question of principle how to achieve consistency between his and our (i.e. the 'early' observer's) measurement of the power spectrum.

We approach these issues starting from the δN-formalism [23, 25, 37–39].[2] It turns out that the problem can be resolved rather easily if a simple modification of the δN-formalism, which takes fluctuations of the Hubble scale during slow-roll inflation into account, is implemented. In essence, this modification consists of treating the Hubble scale, which defines the normalization of the scalar-field correlator, as a function of the perturbed background value of φ relevant at the time of horizon exit of a given mode. Since this background perturbation depends only on modes with a smaller wave number, our proposal can be implemented in an unambiguous and straightforward way.

The Hubble-scale fluctuations discussed above lead to slow-roll suppressed but log-enhanced contributions to the power-spectrum, similar to the familiar 'c-loop' effects of the δN-formalism. Combining both these contributions, the coefficient of the first log-enhanced correction to the power spectrum takes a very simple form. It is essentially given by the second derivative in φ of the leading order power spectrum, $N_\varphi(\varphi)^2 H(\varphi)^2/(2\pi)^2$. Here the argument φ is the value of the inflaton corresponding to the horizon exit of the wave number k under consideration.

The physical significance of this proposal can be understood as follows: Consider the reheating surface (or any other surface of constant energy density after the end of inflation). Disregarding vector and tensor modes, the geometry of this surface, parameterized by coordinates $\vec{y} = (y^1, y^2, y^3)$, can be characterized by a single scalar function $\zeta(\vec{y})$, known as the curvature perturbation. The power spectrum may be defined as the logarithmic derivative of the correlation function $\langle \zeta(\vec{x})\zeta(\vec{x}+\vec{y})\rangle$ with respect to $y = |y|$. Alternatively, a closely related spectrum based on a fixed invariant distance s between pairs of points in the correlator can be defined. This latter power spectrum is an entirely local quantity and its expectation value does not depend on the size of the region over which the correlator is measured (i.e. on the 'age' of the observer). The two spectra, which we denote by $\mathcal{P}_\zeta(y)$ and $\tilde{\mathcal{P}}_\zeta(s)$, are related by $\mathcal{P}_\zeta(y) = \langle \tilde{\mathcal{P}}_\zeta(ye^{\bar{\zeta}})\rangle$, where $\bar{\zeta}$ is a coarse-grained value of ζ relevant for the distance-measurement between a given pair of points. In the relation between the two spectra, the averaging is over the potentially large observed region, with large expectation values of $\bar{\zeta}$ and $\bar{\zeta}^2$ in the case of a late observer. This leads to a log-enhancement of $\mathcal{P}_\zeta(y)$ which is easily seen to be precisely the log-enhancement found earlier in (our implementation of) the δN-formalism.

On the one hand, this agreement provides support for the implementation of the δN-formalism that we advocate. On the other hand, it makes the 'physical reality' of large logs from IR divergences particularly clear: The log-enhancement arises due to the use of global coordinates in a very large region, where these deviate significantly from the invariant distance. It can be avoided if one measures the power spectrum $\tilde{\mathcal{P}}_\zeta(s)$, which is defined using a two-point correlation function based on the invariant distance between each pair of points appearing in the spatial average.

While our work was being finalized, Ref. [80] appeared, which overlaps with part of our analysis. We will comment on this in more detail at the end of Sec. 3.3.

[1] Of course, this possibility is in practice limited by the presently observed dark energy or cosmological constant.

[2] The physical importance of higher-order terms in the δN-formalism was first appreciated in [37].

3.2 Hubble scale fluctuations in the δN-formalism

During inflation, the amplitude of scalar field fluctuations is controlled by the Hubble parameter H. The latter is usually evaluated at the value $\varphi(t_k)$ of the classical homogenous solution φ, where t_k is the time of horizon exit of the mode k: $H = H(\varphi(t_k))$. However, this approach does not account for the fact that perturbations with wavelength larger than k^{-1} have already left the horizon. These perturbations modify the value of the scalar field relevant for the mode k and need to be taken into account.

We do so by writing the scalar field perturbation in a quasi-de-Sitter background as

$$\delta\varphi(\vec{x}) \;\; = \int \tfrac{d^3k}{(2\pi)^3}\, \tfrac{e^{-i\vec{k}\vec{x}}}{\sqrt{2k^3}} \;\; H\left(\varphi(t_k) + \delta\bar{\varphi}(\vec{x})\right) \;\; \hat{a}_{\vec{k}}\,, \tag{3.1}$$

where

$$\delta\bar{\varphi}(\vec{x}) \;\; = \int\limits_{l\ll k} \tfrac{d^3l}{(2\pi)^3}\, \tfrac{e^{-i\vec{l}\vec{x}}}{\sqrt{2l^3}}\; H(\varphi(t_l)) \;\; \hat{a}_{\vec{l}}, \tag{3.2}$$

where $\hat{a}_{\vec{k}}$ is a normalized Gaussian random variable [3]. In writing eq. (3.1) and in the rest of the paper, we only include the leading order contributions to the fluctuations and neglect slow-roll corrections that are not enhanced by potentially large logarithms. The $\delta\bar{\varphi}(\vec{x})$ contribution in the argument of the Hubble parameter accounts for the backreaction of long wavelength modes on the scalar fluctuations $\delta\varphi(\vec{x})$ generated inside the horizon.

In order to analyze their effect, we expand the Hubble parameter up to second order in $\delta\bar{\varphi}$,

$$\delta\varphi(x) = \int \frac{d^3k}{(2\pi)^3}\, e^{-i\vec{k}\vec{x}}\chi_{\vec{k}} \left[1 + A_1 \int\limits_{l\ll k} \frac{d^3l}{(2\pi)^3}\; e^{-i\vec{l}\vec{x}}\chi_{\vec{l}} + \; A_2 \int\limits_{l,m\ll k} \frac{d^3l}{(2\pi)^3}\,\frac{d^3m}{(2\pi)^3}\, e^{-i(\vec{l}+\vec{m})\vec{x}}\chi_{\vec{l}}\chi_{\vec{m}}\right] \tag{3.3}$$

where we have introduced the Gaussian field

$$\chi_{\vec{k}} = \frac{H(\varphi(t_k))}{\sqrt{2k^3}}\; \hat{a}_{\vec{k}}\,. \tag{3.4}$$

We use the abbreviations $A_1 = H_\varphi/H$ and $A_2 = H_{\varphi\varphi}/(2H)$ for coefficients involving the first and second derivative of H with respect to φ. Note that as a result of the corrections proportional to A_1 and A_2, the scalar fluctuation in Fourier space, $\delta\varphi_{\vec{k}}$, are not Gaussian at Hubble exit. A similar idea was considered to second order in the scalar field perturbations, in the context of the tree-level bispectrum in [81]. Note that we neglect the quantum mechanically generated non-Gaussianity of the fields which is present at horizon exit [22].

We now turn to the curvature fluctuation ζ evaluated on a surface of uniform energy density (for our purposes, the reheating surface). The δN-formalism calculates ζ starting from scalar fluctuations on a flat surface,

$$\zeta(\vec{x}) \;=\; N(\varphi+\delta\varphi(\vec{x})) - N(\varphi) \;=\; N_\varphi\delta\varphi(\vec{x}) + \frac{1}{2}\,N_{\varphi\varphi}\delta\varphi(\vec{x})^2 + \frac{1}{6}N_{\varphi\varphi\varphi}\delta\varphi(\vec{x})^3 + \cdots\,. \tag{3.5}$$

Here N_φ, $N_{\varphi\varphi}$ are derivatives of the number of e-folds N as a function of φ, evaluated on the classical background trajectory. The resulting two point function for curvature

[3] It satisfies the relation $\langle \hat{a}_{\vec{k}}\hat{a}_{\vec{p}}\rangle \;=\; (2\pi)^3\delta^{(3)}(\vec{k}+\vec{p})\,.$

perturbations in Fourier space is given by

$$\langle\, \zeta_{\vec{k}}\zeta_{\vec{p}}\,\rangle = N_\varphi^2\langle\, \delta\varphi_{\vec{k}}\delta\varphi_{\vec{p}}\,\rangle + N_\varphi N_{\varphi\varphi}\langle\, \delta\varphi_{\vec{k}}\big(\delta\varphi^2\big)_{\vec{p}}\,\rangle + \frac{N_{\varphi\varphi}^2}{4}\langle\, \big(\delta\varphi^2\big)_{\vec{k}}\,\big(\delta\varphi^2\big)_{\vec{p}}\,\rangle + \frac{N_\varphi N_{\varphi\varphi\varphi}}{3}\langle\, \delta\varphi_{\vec{k}}\,\big(\delta\varphi^3\big)_{\vec{p}}\,\rangle. \tag{3.6}$$

Note that correlators of odd powers of $\delta\varphi$ are in general non-zero since $\delta\varphi_{\vec{k}}$ is not Gaussian. However, one may check that nevertheless $\langle\, \delta\varphi_{\vec{k}}\,\rangle = 0$. We have not set $<\zeta>=0$, though making this choice would not change in an essential way our results (we will discuss this in more detail later).

We now define the spectrum $\mathcal{P}_\chi$ through $\langle\chi_{\vec{k}}\chi_{\vec{p}}\rangle = (2\pi)^3\,\delta^3(\vec{k}+\vec{p})\,2\pi^2\mathcal{P}_\chi(k)/k^3$. This implies that $\mathcal{P}_\chi(k) = (H/2\pi)^2$. The spectrum of curvature perturbations $\mathcal{P}_\zeta$ is defined in an analogous way. It follows from a straightforward evaluation of eq. (3.6) (see Appendix 3.5.1 for details) that

$$\mathcal{P}_\zeta(k) = \mathcal{P}_\chi\left\{N_\varphi^2 + \mathcal{P}_\chi\ln(kL)\left[\left(A_1^2+2A_2\right)N_\varphi^2 + 4A_1N_\varphi N_{\varphi\varphi} + N_{\varphi\varphi}^2 + N_\varphi N_{\varphi\varphi\varphi}\right]\right\} \tag{3.7}$$

$$= \mathcal{P}_\chi N_\varphi^2 + \mathcal{P}_\chi\ln(kL)\,\frac{1}{2}\frac{d^2}{d\varphi^2}\left(N_\varphi^2\mathcal{P}_\chi\right)\,. \tag{3.8}$$

Here it is crucial that the IR cutoff L is set by the size of the region in which the correlator is measured. As mentioned before, we take it for granted that perturbations on even larger scales can be absorbed in the background and are hence unobservable. In other words, the classical evolution starts with the horizon exit of modes of scale $k \sim 1/L$. Our main interest is the dependence of the spectrum on the size L of the observed region.

We can express the second derivative along the scalar field, appearing in equation (3.7), in terms of slow-roll parameters. We define as usual $\epsilon = V_\varphi^2/(2V^2)$, $\eta = V_{\varphi\varphi}/V$, $\xi^2 = V_\varphi V_{\varphi\varphi\varphi}/V^2$, and we set $M_P^2 = 8\pi$. Using the well known relations $n_\zeta - 1 = 2\eta - 6\epsilon$ for the spectral index, and $\alpha_\zeta = 16\epsilon\eta - 24\epsilon^2 - 2\xi^2$ for its running, i.e. $\alpha_\zeta \equiv dn_\zeta/d\ln k$ (all quantities evaluated at Hubble exit) we find

$$\frac{d^2}{d\varphi^2}\left(N_\varphi^2\mathcal{P}_\chi\right) = \frac{\mathcal{P}_\chi\,N_\varphi^4}{4}\left[(\eta-2\epsilon)\,(n_\zeta-1) + (n_\zeta-1)^2 + \alpha_\zeta\right] \tag{3.9}$$

This quantity vanishes in the case of scale invariance, i.e. when $n_\zeta = 1$ and $\alpha_\zeta = 0$. In this case logarithmic corrections to the power spectrum drop out, at leading order in the slow-roll expansion. We will discuss an interpretation of this result in the next section.

At our level of accuracy, we can rewrite eq. (3.7) as

$$\mathcal{P}_\zeta(k) = \mathcal{P}_\chi N_\varphi^2 + \langle\varphi^2\rangle_{1/k}\,\frac{1}{2}\frac{d^2}{d\varphi^2}\left(N_\varphi^2\mathcal{P}_\chi\right)\,, \tag{3.10}$$

where

$$\langle\delta\varphi^2\rangle_{1/k} = \int_{L^{-1}}^{k}\frac{d^3k'}{(2\pi)^3}\,\frac{H^2}{2k'^3} = \mathcal{P}_\chi\ln(kL) \tag{3.11}$$

is the expectation value of $\delta\varphi^2$ measured on a length scale $1/k$. We see that the log-enhanced correction takes the suggestive form of the second term in a Taylor expansion. The physical meaning of this structure will be clarified below.

We note that the integration in eq. (3.11) was performed assuming that φ has an exactly scale invariant spectrum. More generally, if the power spectrum of φ has a constant spectral index n_φ, the $\ln(kL)$ term above should be replaced by

$$\ln(kL) \to \frac{1}{n_\varphi - 1}\left(1 - (kL)^{-(n_\varphi - 1)}\right). \tag{3.12}$$

However, provided that we do not consider an exponentially large range of scales and the field fluctuations are reasonably close to scale invariant, then $|n_\varphi - 1|\ln(kL) \ll 1$, and the more general result above is well approximated by $\ln(kL)$. Since the running of the spectral index is expected to be of order $(n_\varphi - 1)^2$, further corrections associated with this running are suppressed by a similar argument.

3.3 Infrared divergences from the geometry of the reheating surface

We now provide a physical interpretation for the log-enhanced correction to the power spectrum given in eq. (3.7). An observer, in order to make a measurement, specifies a coordinate system on the reheating surface (or on any other surface of constant energy density after the end of inflation). This can be done as follows. Choose a coordinate system where slices of constant time t have uniform energy density. Neglecting vector and tensor modes, we write the metric as

$$ds_4^2 \,=\, -dt^2 + a^2(t)\, e^{2\zeta(x)}\, \delta_{ij}\, dx^i dx^j \,. \tag{3.13}$$

We use conventions where reheating occurs at time t_f, at which the homogeneous scale factor $a(t_f) = 1$. This leads to the following metric on the three-dimensional reheating surface:

$$ds_3^2 \,=\, e^{2\zeta(x)}\, \delta_{ij}\, dx^i dx^j \,. \tag{3.14}$$

Important consequences for the power spectrum of ζ can be derived just from the geometry of the reheating surface specified above. To see this, let us define the power spectrum as the logarithmic derivative of the two point function,

$$\mathcal{P}_\zeta(y) \,\equiv\, \frac{d}{d\ln y}\,\frac{1}{2}\left\langle \left(\zeta(\vec{x}) - \zeta(\vec{x}+\vec{y})\right)^2\right\rangle = -\frac{d}{d\ln y}\left\langle \zeta(\vec{x})\,\zeta(\vec{x}+\vec{y})\right\rangle, \tag{3.15}$$

where y is the length of a coordinate vector on the reheating surface, $y^2 = (y^1)^2 + (y^2)^2 + (y^3)^2$. It is not difficult to see that eq. (3.15) gives the correct value for the power spectrum associated with the fluctuations of a slowly-rolling scalar in quasi-de Sitter background (see Appendix 3.5.2).

Alternatively, we can define the power spectrum averaging over pairs of points separated by a fixed invariant distance s,

$$\tilde{\mathcal{P}}_\zeta(s) \,\equiv\, \frac{d}{d\ln s}\,\frac{1}{2}\left\langle \left(\zeta(\vec{x}) - \zeta(\vec{x}+\vec{y}(s)\right)^2\right\rangle . \tag{3.16}$$

Here $\vec{y}(s)$ denotes a coordinate vector with invariant length s. We have introduced a tilde to distinguish this spectrum from eq. (3.15). It is clear that long-wavelength background fluctuations of ζ, which affect only the parameterization but not the physics of any local

patch of the reheating surface, are irrelevant for this new spectrum. In other words, $\tilde{\mathcal{P}}_\zeta(s)$ is a purely local quantity which, by its very definition, cannot depend on the size L of the observed region.

Defining $\bar{\zeta}$ as the average value of ζ characteristic of a small region containing a particular pair of points $\vec{x}$ and $\vec{x}+\vec{y}(s)$, we can write

$$\tilde{\mathcal{P}}_\zeta(s) \equiv \frac{d}{d\ln s}\frac{1}{2}\left\langle\left(\zeta(\vec{x})-\zeta(\vec{x}+\vec{e}se^{-\bar{\zeta}}\right)^2\right\rangle . \tag{3.17}$$

Here $\vec{e}$ is a coordinate unit vector. We see that the two spectra differ only by the selection of pairs of points in the averaging procedure. In one case, pairs with fixed coordinate distance y, in the other case pairs with fixed invariant distance

$$s = e^{\bar{\zeta}}y \tag{3.18}$$

are chosen. Hence we can express $\mathcal{P}_\zeta$ in terms of the locally defined spectrum $\tilde{\mathcal{P}}_\zeta$ through

$$\mathcal{P}_\zeta(y) = -\frac{d}{d\ln y}\langle\zeta(\vec{x})\,\zeta(\vec{x}+\vec{y})\rangle = -\frac{d}{d\ln s}\langle\zeta(\vec{x})\,\zeta\left(\vec{x}+\vec{e}\big(ye^{\bar{\zeta}}\big)e^{-\bar{\zeta}}\right)\rangle = \langle\tilde{\mathcal{P}}_\zeta(ye^{\bar{\zeta}})\rangle\,. \tag{3.19}$$

Here the second equality holds because logarithmic derivatives in y and s agree. The third equality relies on the fact that $\tilde{\mathcal{P}}_\zeta$ is a local quantity, as explained before. The averaging in the last term remains non-trivial because of the variation of $\bar{\zeta}$ over the large patch of size L on which $\mathcal{P}_\zeta$ was originally defined.

Expanding to second order in $\bar{\zeta}$, we find

$$\mathcal{P}_\zeta(y) = \tilde{\mathcal{P}}_\zeta(y) + \langle\bar{\zeta}\rangle\frac{d}{d\ln y}\tilde{\mathcal{P}}_\zeta(y) + \frac{1}{2}\langle\bar{\zeta}^2\rangle\frac{d^2}{d(\ln y)^2}\tilde{\mathcal{P}}_\zeta(y)\,. \tag{3.20}$$

This quantifies the deviation of the observer-patch-dependent spectrum $\mathcal{P}_\zeta$ from the locally defined spectrum $\tilde{\mathcal{P}}_\zeta$ for large patches. It also clarifies the origin of the large logarithms of L found in the δN-formalism. They arise because the expectation values of $\bar{\zeta}$ and $\bar{\zeta}^2$ grow logarithmically with L. We note that, if the power spectrum $\tilde{\mathcal{P}}_\zeta$ is scale independent, the two last terms in eq. (3.20) vanish. This is compatible with eqs. (3.7), (3.9) and has a simple intuitive reason: The log-enhancement occurs because in regions with a large background value of $\bar{\zeta}$ the scale of a given mode is effectively misidentified. However, in the scale-invariant case, such a misidentification has no consequences.

We now compare eqs. (3.20) and (3.7) quantitatively. To achieve this, we can rewrite derivatives in $\ln y$ in terms of derivatives in φ using $d\ln(y)/d\varphi = N_\varphi$ (alternatively we can directly use the results of Appendix 3.5.2) and express expectation values of $\bar{\zeta}$ and $\bar{\zeta}^2$ in terms of φ-correlators using eq. (3.5). Equivalently, we can observe that eq. (3.20) is simply a second order Taylor expansion around the classical trajectory. Since there is an unambiguous functional relation between fluctuations in φ and in ζ (the latter being equivalent to $\ln y$), we immediately conclude that

$$\mathcal{P}_\zeta(y) = \tilde{\mathcal{P}}_\zeta(y) + \frac{1}{2}\frac{d^2\tilde{\mathcal{P}}_\zeta}{d\varphi^2}\langle\delta\varphi^2\rangle = \tilde{\mathcal{P}}_\zeta(y) + \frac{1}{2}\mathcal{P}_\chi\ln(L/y)\frac{d^2\tilde{\mathcal{P}}_\zeta}{d\varphi^2}\,. \tag{3.21}$$

Here $\langle\delta\varphi^2\rangle$ is the zero-momentum $\delta\varphi$ correlator with UV cutoff y and IR cutoff L, in analogy to $\langle\bar{\zeta}^2\rangle$ above. Furthermore, we used the fact that the expectation value of $\delta\varphi$ vanishes. Thus, we have achieved complete agreement with the IR divergences or, more precisely, with the log-enhanced corrections which arise in the δN-formalism.

To summarize, we have obtained a simple physical interpretation for the logarithmic contributions to the power spectrum that were determined in the previous section: The log-enhancement arises due to the use of global coordinates in a very large region, where these deviate significantly from the invariant distance. It can be completely avoided if the power spectrum $\tilde{\mathcal{P}}_\zeta$ is considered, which is based on the two-point correlation function defined in terms of the invariant distance between each pair of points appearing in the spatial average.

As mentioned in the Introduction 3.1, a discussion closely related to the present section appeared in [80] while our paper [64] was being finalized. In particular, using an argument slightly different from ours, a log-enhancement arising from the large-scale geometry of the reheating surface was derived. Our findings can be brought into agreement with [80] if we drop the term $\sim \langle\bar{\zeta}\rangle$ in eq. (3.20) and set $\alpha_\zeta = dn_\zeta/d\ln k$ to zero. This corresponds to keeping just the $(n_\zeta - 1)^2$ term in our eq. (3.9). Indeed, the term proportional to $\langle\bar{\zeta}\rangle$ disappears if we rescale our coordinates on the reheating surface according to $y \to ye^{-\bar{\zeta}}$. This can be directly checked from eq. (3.20) and corresponds to the fact that, in these new coordinates, the average of ζ vanishes. While this is certainly a rather natural coordinate choice, it does not serve our purpose of comparing with the δN-formalism: Indeed, in this new coordinate system the value $\zeta = 0$ does not any more correspond to the endpoint of the classical trajectory. Nevertheless, setting questions related to the δN-formalism aside, the term $\sim \langle\bar{\zeta}\rangle$ appears just to be matter of different conventions between [80] and our discussion. By contrast, we believe that our term $\sim \alpha_\zeta$ is real and, in general, no more slow-roll suppressed than the $(n_\zeta - 1)^2$ term.

The agreement of the findings of this section (and of [80], subject to the caveats mentioned above) with the previously discussed calculation in the δN-formalism is a non-trivial result. In particular, [80] argue that any attempt to understand the IR divergences using the δN-approach is incomplete due to certain divergences of the $\delta\varphi$ correlation function which are already present at horizon crossing. One way of interpreting our modification of the δN-formalism is by saying that, via Eq. (3.3), we include such divergences in the formalism.[4] It thus appears that our purely classical modification to the δN-formalism is sufficient to fully capture the leading logarithmic behaviour.

3.4 Discussion

We have studied IR divergences during inflation using both the δN-formalism and a simple, phenomenological approach based just on the geometry of the reheating surface. By implementing a simple modification of the δN-formalism, we took into account the effect of modes that left the horizon long before the scales we are observing on the Hubble scale. Including this effect provides new log-enhanced contributions to the power spectrum, at the same order in H and slow-roll as the standard classical loop corrections. We found that the combination of all contributions can be assembled in an elegant formula, in which the log-enhanced contributions are weighted by the second derivative of the tree level power spectrum, with respect to the inflaton field.

This result can be understood intuitively by considering two power spectra: One is defined locally on the surface of reheating, using invariant distances to define the correlator. The other is based on the coordinate distance on this surface and depends on global

[4] We would like to thank Martin Sloth for a conversation helping us to correct our comments on this issue, in the first version of the paper.

features of this surface, in particular on long-wavelength modes. When expressed in terms of the local spectrum, this latter, global spectrum exhibits an IR divergence associated to the size of the region on which it is measured. It is, in fact, this latter spectrum that is calculated in the δN-formalism and the log-divergence found in both approaches is precisely the same. This provides strong support for the modification of the δN-formalism we propose. In the case of an exactly scale invariant spectrum, the IR logarithms are absent. For an observer dealing with a scale-dependent spectrum and having a very large region available for his measurement, the use of the local spectrum, which is not affected by our IR effects, appears to be clearly favored.

In single-field, slow-roll inflation the coefficient multiplying the logarithm is heavily suppressed. While it is usually also suppressed in multi-field models, this statement does not hold any more in complete generality. In fact, in some special cases the coefficient could be large enough to compensate for the power spectrum suppression found in single-field models [52, 82]. It would therefore clearly be of interest to extend our results to multi-field inflation. In these models, which contain isocurvature perturbations during inflation, the Hubble scale will depend on several fields, even if the primordial curvature perturbation depends on only one field. In cases where the loop correction is not small, it has been argued they could give an observable contribution to ζ through non-Gaussianity [37, 46, 83–88], in particular through a special type of scale dependence of the bispectrum non-linearity parameter [52, 82]. For a discussion of the scale dependence of the tree level bispectrum see [40]. It would thus be interesting to study the effect of our loop corrections on the bispectrum (and higher order n-point correlators).

3.5 Appendices

3.5.1 Correlator of the curvature perturbation

In this appendix, we present the calculation relating the correlator of curvature perturbations ζ to correlators of the Gaussian random field χ. The terms which need to be calculated are

$$\begin{aligned}\langle\, \zeta_{\vec{k}}\zeta_{\vec{p}}\,\rangle &= N_\varphi^2\langle\, \delta\varphi_{\vec{k}}\delta\varphi_{\vec{p}}\,\rangle + N_\varphi N_{\varphi\varphi}\langle\, \delta\varphi_{\vec{k}}\ \left(\delta\varphi^2\right)_{\vec{p}}\,\rangle \\ &\quad + \frac{N_{\varphi\varphi}^2}{4}\langle\, \left(\delta\varphi^2\right)_{\vec{k}}\left(\delta\varphi^2\right)_{\vec{p}}\,\rangle + \frac{N_\varphi N_{\varphi\varphi\varphi}}{3}\langle\, \delta\varphi_{\vec{k}}\ \left(\delta\varphi^3\right)_{\vec{p}}\,\rangle\,. \end{aligned} \tag{3.22}$$

In the previous equations, expressions like $(\delta\varphi^2)_{\vec{k}}$ indicate convolutions. The terms in the last two lines contain correlators between convolutions, that provide (see [83] for more details)

$$\langle\, \left(\delta\varphi^2\right)_{\vec{k}}\left(\delta\varphi^2\right)_{\vec{p}}\,\rangle = 4\,\mathcal{P}_\chi \ln(kL)\,\langle\, \chi_{\vec{k}}\chi_{\vec{p}}\,\rangle \quad , \tag{3.23}$$

$$\langle\, \delta\varphi_{\vec{k}}\ \left(\delta\varphi^3\right)_{\vec{p}}\,\rangle = 3\,\mathcal{P}_\chi \ln(kL)\,\langle\, \chi_{\vec{k}}\chi_{\vec{p}}\,\rangle \quad . \tag{3.24}$$

Using the expansion of eq. (3.3), written in momentum space, the 2-point correlator of the scalar field $\delta\varphi$ is given by

$$\langle\, \delta\varphi_{\vec{k}}\delta\varphi_{\vec{p}}\,\rangle = \langle\, \chi_{\vec{k}}\chi_{\vec{p}}\,\rangle\left[1 + \left(A_1^2 + 2A_2\right)\int_{l,m\ll k}\frac{d^3l}{(2\pi)^3}\,\frac{d^3m}{(2\pi)^3}\,\langle\, \chi_{\vec{l}}\chi_{\vec{m}}\,\rangle\right] \tag{3.25}$$

$$= \langle\, \chi_{\vec{k}}\chi_{\vec{p}}\,\rangle\left[1 + \left(A_1^2 + 2A_2\right)\mathcal{P}_\chi \ln(kL)\right] \quad . \tag{3.26}$$

Note that, after applying Wick's theorem, only one term survives the conditions $l, m \ll k$. The remaining correlator $\langle\, \delta\varphi_{\vec{k}}\ (\delta\varphi^2)_{\vec{p}}\,\rangle$, appearing in the second term of eq. (3.22), is of order three in $\delta\varphi$. Therefore, only terms at next-to-leading order, in the expansion of eq. (3.3), contribute to it. One finds

$$\begin{aligned}\langle \delta\varphi_{\vec{k}}\,(\delta\varphi^2)_{\vec{p}}\rangle &= A_1 \int \frac{d^3q}{(2\pi)^3}\int_{l\ll k}\frac{d^3l}{(2\pi)^3}\,\langle \chi_{\vec{k}-\vec{l}}\chi_{\vec{l}}\chi_{\vec{p}-\vec{q}}\chi_{\vec{q}}\rangle \\ &\quad +2A_1\int \frac{d^3q}{(2\pi)^3}\int_{l\ll q}\frac{d^3l}{(2\pi)^3}\,\langle \chi_{\vec{k}}\chi_{\vec{l}}\chi_{\vec{q}-\vec{l}}\chi_{\vec{p}-\vec{q}}\rangle. \end{aligned} \tag{3.27}$$

Decomposing the four point functions appearing in the integrands by means of Wick's theorem, and taking care of the conditions on the size of l, one finds

$$\langle\, \delta\varphi_{\vec{k}}\ \left(\delta\varphi^2\right)_{\vec{p}}\rangle = 4A_1\mathcal{P}_\chi \ln(kL)\,\langle\, \chi_{\vec{k}}\chi_{\vec{p}}\,\rangle\,. \tag{3.28}$$

Putting all terms together, the final result for the spectrum of curvature perturbations reads

$$\mathcal{P}_\zeta(k) = \mathcal{P}_\chi\left\{N_\varphi^2 + \mathcal{P}_\chi\ln(kL)\left[\left(A_1^2+2A_2\right)N_\varphi^2 + 4A_1N_\varphi N_{\varphi\varphi} + N_{\varphi\varphi}^2 + N_\varphi N_{\varphi\varphi\varphi}\right]\right\} \tag{3.29}$$

$$= \mathcal{P}_\chi N_\varphi^2 + \mathcal{P}_\chi\ln(kL)\,\frac{1}{2}\frac{d^2}{d\varphi^2}\left(N_\varphi^2\mathcal{P}_\chi\right)\,. \tag{3.30}$$

3.5.2 Power spectrum in coordinate space

In this appendix, we discuss properties of the power spectrum in coordinate space, defined in eq. (3.15) as

$$\mathcal{P}_\zeta(y) \equiv -\frac{d}{d\ln y}\,\langle\,\zeta(\vec{x})\,\zeta(\vec{x}+\vec{y})\,\rangle \quad . \tag{3.31}$$

The power spectrum in coordinate space is no more difficult to handle than the usual power spectrum in momentum space. Moreover, as discussed in the main text, it allows for a simpler and more direct analysis of log-enhanced contributions associated with this quantity.

However, for the purpose of this appendix, we consider only observed regions which are not much larger than y (i.e. IR cutoffs not much smaller than the relevant momentum scale k). Under this assumption, $\mathcal{P}_\zeta$ and $\tilde{\mathcal{P}}_\zeta$ coincide and all that follows applies to both spectra.

We can compare the two definitions of the power spectra as follows. Fourier expanding the two-point function of curvature perturbations, we can write

$$\mathcal{P}_\zeta(y) = -\frac{d}{d\ln y}\int\frac{d^3p}{(2\pi)^3}\frac{d^3k}{(2\pi)^3}\,e^{-i\left[\vec{p}\vec{x}+\vec{k}(\vec{x}+\vec{y})\right]}\,\langle\zeta(\vec{p})\zeta(\vec{k})\rangle \tag{3.32}$$

$$= -\frac{d}{d\ln y}\int\frac{k^2\,dk}{2}\int_{-1}^{1}d(\cos\theta)\,e^{i\,k\,y\,\cos\theta}\,\mathcal{P}_\zeta^F(k) \tag{3.33}$$

$$= -\frac{d}{d\ln y}\int_{k_0}\frac{\sin(ky)}{ky}\,\mathcal{P}_\zeta^F(k)\,d\ln k \quad . \tag{3.34}$$

To pass from the first to the second line, we used the definition of the power spectrum in momentum space, given before eq. (3.7). It is labeled by an F, to distinguish it from

the analogous quantity in real space. In the third line, we made the IR cutoff explicit introducing a scale k_0. We can expand $\mathcal{P}_\zeta^F$ as

$$\mathcal{P}_\zeta^F(k) \;=\; \mathcal{P}_\zeta^F(k_p) + \ln\left(\frac{k}{k_p}\right)\frac{d\mathcal{P}_\zeta^F}{d\ln k}\,(k_p) \;+\; \cdots\,, \tag{3.35}$$

where k_p is some pivot scale, the inverse of which is of the order of y: we can set $y \simeq k_p^{-1}$. The second and higher terms are slow-roll suppressed with respect to the first term. Substituting this expansion in eq. (3.32), we find

$$\mathcal{P}_\zeta(y) \;=\; \mathcal{P}_\zeta^F(k_p)\,\frac{\sin k_0 y}{k_0 y} \quad + \quad \text{slow-roll suppressed terms} \tag{3.36}$$

where the slow-roll suppressed terms are weighted by logarithms of order $\ln(k_0 y)$. We choose k_0 such that $k_0 y \simeq k_0/k_p \ll 1$, but not as small as to lead to large logarithms in the slow-roll suppressed terms. This implies that the power spectra in coordinate and momentum space coincide, up to negligible slow-roll corrections:

$$\mathcal{P}_\zeta(y) \simeq \mathcal{P}_\zeta^F(1/y)\,. \tag{3.37}$$

Chapter 4

Inflationary Correlation Functions without Infrared Divergences

The content of this chapter is published in [61].

As already discussed in chapter 3, inflationary correlation functions are potentially affected by infrared divergences. For example, the two-point correlator of curvature perturbation at momentum k receives corrections $\sim \ln(kL)$, where L is the size of the region in which the measurement is performed. In this chapter, we define infrared-safe correlation functions which have no sensitivity to the size L of the box used for the observation. The conventional correlators with their familiar log-enhanced corrections (both from scalar and tensor long-wavelength modes) are easily recovered from our IR-safe correlation functions. Among other examples, we illustrate this by calculating the corrections to the non-Gaussianity parameter f_{NL} coming from long-wavelength tensor modes. In our approach, the IR corrections automatically emerge in a resummed, all-orders form. For the scalar corrections, the resulting all-orders expression can be evaluated explicitly.

4.1 Introduction

Infrared divergences associated with the inflationary power spectrum are a long-standing issue [8, 9, 55–58] which has more recently received a lot of attention following [24, 59]. Our focus is on divergences which directly affect the power spectrum. According to [60] such divergences are cut off by the size L of the observed patch of the late universe. We are going to develop and generalize the analyses of [64, 80] (see also [89]). This approach emphasizes the way in which long-wavelength perturbations do (or do not) influence locally measured inflationary spectra. It may be related to earlier proposals of [71, 72] and is clearly in line with at least part of the subsequent discussion in [90].

Infrared divergences explicitly arise in loop corrections to inflationary observables (using e.g. the in-in formalism) or through the nonlinear dependence of the curvature perturbation on fluctuations of an underlying scalar field (e.g. in the δN approach). The vast amount of literature on the subject (see e.g. [38,69,70,73–77,79,91–106]) has recently been reviewed in [78]. More or less by definition, IR divergences are due to modes which have a much longer wavelength than the characteristic scale of the problem under consideration. Focussing on correlation functions, it is then clear that such IR modes left the horizon earlier than the modes which are directly accessed via the correlation function at a given scale. Hence a generic effect of these IR modes is a modification of the background in

which other modes propagate and are eventually observed.

Much debate has been raised on how to interpret such IR divergences. At least in the case of single-field slow-roll inflation, it is now widely accepted that log-divergent integrals over soft modes have to be cut off at a $k_{min} \sim 1/L$, where L is the typical size of the 'box' in which the observer measures some correlator at momentum $k \gg 1/L$ [60] (see also [37, 68, 83, 107]). It is thus more appropriate to talk about a log-enhancement rather than a log-divergence. The suggestion that long-wavelength modes can be absorbed in the background and hence do not affect the correlator at momentum k has been put forward long ago [108–113]. In this sense, the absence of IR divergences in situations where L is not much larger than k may have been apparent to many authors even before Lyth's paper [60] of 2007.

We note that backreaction of long-wavelength modes in quasi-de Sitter space-times has been considered also in other contexts [108–111, 114–122], most notably in attempts to compensate the cosmological constant or to explain the current accelerated expansion of the Universe. We have nothing to say concerning these topics and refer the reader to [78] for a more extensive compilation of the relevant literature.

In this chapter, we analyse IR effects associated with the backreaction of long-wavelength scalar and tensor modes in inflationary backgrounds, in the spirit of [64, 80]. This approach is related to the consistency relations [22, 123, 124]. Developing and generalizing a suggestion made in [64] (see also [90]), we propose an IR-safe definition of correlation functions involving curvature fluctuations. In doing so, we remove any sensitivity to modes that have a much longer wavelength than the scale at which the correlator is probed. The essential idea is to make use of the proper invariant distance on the reheating surface, where the curvature perturbation is evaluated. Considering two points on this surface, the dependence of the (physical) invariant distance on the coordinate vector, corresponding to the separation of the two points, is affected by long-wavelength contributions from geometrical quantities, namely the curvature and tensor perturbations. The misidentification of the distance due to long-wavelength modes is precisely the origin of IR effects. Consequently, by using the proper invariant distance, it is possible to construct n-point functions for the curvature perturbation that are free from the effect of long-wavelength modes and, hence, free from IR divergences associated with these contributions.

We show how to relate n-point functions, calculated in terms of the invariant distance, to the conventionally defined n-point functions. This allows us to provide closed expressions for the latter that manifestly exhibit the dependence on long-wavelength modes. As a consequence, in our approach the IR corrections to n-point functions automatically emerge in a resummed, all-orders form. When expanded at leading order in terms of long-wavelength modes, we recover the familiar log-enhanced, IR sensitive contributions. We apply our approach to the analysis of the two- and three-point functions for the curvature perturbation in slow-roll, single field inflation. The leading IR corrections to the power spectrum appear as log-enhanced contributions, multiplied by the power spectrum and second order slow-roll parameters. Furthermore, our resummed, all-orders expression allows us to evaluate IR corrections in a non-perturbative way by using statistical properties of the integrated long-wavelength fluctuation. We apply this framework to specific inflationary set-ups, obtaining a complete expression that includes all contributions of scalar long-wavelength modes to the power spectrum. Regarding the bispectrum, we derive the complete expression for long-wavelength scalar and tensor contributions to $f_{\rm NL}$. We then expand the result at leading order in slow-roll, showing that tensor modes dominate the slow-roll expansion and provide the leading log-enhanced contribu-

tions to non-Gaussianity. Contrary to the power spectrum, we find that the leading order correction to $f_{\rm NL}$ is suppressed only by first order slow-roll parameters.

We also show that, in all cases where the δN-formalism is applicable, our results can be equivalently obtained in terms of a suitable generalization of the δN-formalism, extending the discussion of [64]. In the present work, we include the effects of graviton long-wavelength modes, and we explain how to calculate IR contributions to arbitrary n-point functions involving curvature perturbations.

Log-enhanced contributions to inflationary observables, both in the in-in formalism and in the δN-formalism, have received much attention over the past few years. In the case of the δN-formalism, they have been associated with infrared divergences of the so called C-loops, and have been calculated mostly in terms of a diagrammatic expansion [83, 85, 125, 126]. Although our approach is related, it is conceptually and technically different. We derive IR contributions directly from geometrical quantities. These corrections appear automatically in a resummed, all-orders form and do not need any diagrammatic expansion. Following arguments given in [80], the presented derivation of IR effects from the geometry of the reheating surface matches IR contributions due to quantum loop effects of long-wavelength modes calculated à la Weinberg [24,59], although a direct comparison is beyond the scope of this chapter.

The chapter is organized as follows: In sec. 4.2, we present the definition of IR-safe correlation functions and we show the emergence of IR corrections in a resummed, all-orders form by relating conventional correlation functions to their IR-safe equivalents. Furthermore, we show for scalars how this expression can be evaluated explicitly. In sec. 4.3, we give an alternative approach in single field, slow-roll inflation in the language of the δN-formalism. In sec. 4.4 and sec. 4.5, we apply our results to the power spectrum and to the non-Gaussianity parameter $f_{\rm NL}$, respectively. We discuss our results in sec. 4.6.

4.2 Geometry of the reheating surface

In this section we provide a physical interpretation for the appearance of log-enhanced correction to inflationary correlation functions, developing and generalizing [64, 80]. We start from the assumption that the reheating surface (or any other surface of constant energy density after the end of inflation), viewed as a metric manifold, represents in principle a physical observable. Neglecting vector modes, the metric of this surface can be written as

$$ds_3^2 = e^{2\zeta(\vec{x})} \left(e^{\gamma(\vec{x})}\right)_{ij} dx^i dx^j \qquad . \tag{4.1}$$

We choose a gauge where the symmetric matrix γ is traceless and $\partial_i \gamma_{ij} = 0$. Of course, ζ is accessible only indirectly, e.g. via $\delta T/T$ of the CMB radiation, but for the present paper we simply assume that this does not limit its observability. Considering, for example, single field slow-roll inflation, the expressions for ζ and γ_{ij} (in momentum space) read [14]

$$\zeta(\vec{q}) = \frac{N_\varphi(q)\, H(q)}{\sqrt{2q^3}}\, \hat{a}_{\vec{q}} \qquad\qquad \gamma_{ij}(\vec{q}) = \sum_{s=+,\times} \frac{H(q)}{\sqrt{q^3}}\, \epsilon_{ij}^s(\vec{q})\, b_{\vec{q}}^s \quad . \tag{4.2}$$

These quantities are conserved on superhorizon scales [21–23]. In the equations above, $\hat{a}_{\vec{q}}$ and $b_{\vec{q}}^s$ are normalized Gaussian random variables and s is the helicity index for gravitational waves. The polarization tensors ϵ_{ij}^s are chosen to satisfy the transver-

sality and tracelessness conditions, as well as an orthogonality relation[1]. Furthermore, $N_\varphi(q) = V/(dV/d\varphi)$ and $H(q) = \sqrt{V(\varphi)/3}$ with both quantities evaluated at the time of horizon exit of the mode q.

Although, for definiteness, we focus on slow-roll inflation, the particular expressions for ζ and γ_{ij} given above are not essential for the formalism presented in this section. Consequently, our arguments are largely independent of the specific inflationary set-up under consideration. Important consequences for the n-point functions can be derived just from the geometry of the reheating surface specified above. Focussing on corrections to the curvature perturbation ζ, we start by discussing the power spectrum and then generalize to spectra of n-point functions, for arbitrary n.

4.2.1 The power spectrum

Using its definition, $\langle\, \zeta_{\vec{k}} \zeta_{\vec{p}} \,\rangle = (2\pi)^3 \delta^{(3)}(\vec{k}+\vec{p})\, 2\pi^2\, \mathcal{P}_\zeta(k)/k^3$, the power spectrum can be written as the Fourier transform of the correlation function in real space:

$$\mathcal{P}_\zeta(k) = \frac{k^3}{2\pi^2} \int d^3y\; e^{-i\vec{k}\vec{y}}\, \langle\, \zeta(\vec{x})\; \zeta(\vec{x}+\vec{y})\,\rangle \qquad . \tag{4.3}$$

Since we want to interpret this formula as a practical prescription for the measurement of the power spectrum, we do not view $\langle \cdots \rangle$ as an abstract ensemble average. Instead, the averaging is over pairs of points separated by a coordinate-vector $\vec{y}$ within a certain part of the reheating surface. In other words, we are averaging over the location $\vec{x}$ of such pairs. This prescription clearly relies on a certain parameterization of the reheating surface and is hence gauge dependent. Nevertheless, given the gauge choice made earlier, the resulting $\mathcal{P}_\zeta(k)$ is a well-defined observable.

An observer is not able to probe the whole inflationary region. We assume that the observable patch is a box of volume L^3 to which the $\vec{x}$-averaging is restricted. While this may not be immediately apparent from (4.3), the power spectrum measured by a given observer depends on the box-size L. Qualitatively, this can be seen as follows:

Focus on a certain momentum k. Due to the Fourier transform, the power spectrum at this k is determined by the behavior of the $\langle\, \zeta(\vec{x})\; \zeta(\vec{x}+\vec{y})\,\rangle$ as a function of y in the region $y \sim 1/k$ (here $y = \sqrt{\delta_{ij}\, y^i y^j}$ is the length of $\vec{y}$). However, at different $\vec{x}$ the same value of y may correspond to different physical (invariant) distances between points $\vec{x}$ and $\vec{x}+\vec{y}$ at which $\zeta(\vec{x})$ and $\zeta(\vec{x}+\vec{y})$ are evaluated. The reason for this is the long-wavelength background

$$\bar{\zeta}(\vec{x}) = \int\limits_{L^{-1}<q\ll k} \frac{d^3q}{(2\pi)^3}\; e^{i\vec{q}\vec{x}}\; \zeta(\vec{q}) \qquad \bar{\gamma}_{ij}(\vec{x}) = \int\limits_{L^{-1}<q\ll k} \frac{d^3q}{(2\pi)^3}\; e^{i\vec{q}\vec{x}}\; \gamma_{ij}(\vec{q}) \quad , \tag{4.4}$$

which varies significantly as $\vec{x}$ varies over a box of (sufficiently large) size L. Indeed, the physical distance between the points $\vec{x}$ and $\vec{x}+\vec{y}$ appearing in the average is given by $z^2 = e^{2\bar{\zeta}}\, (e^{\bar{\gamma}})_{ij}\, y^i y^j$. Moreover, this mismatch between y and the true distance z grows with L. This effect is at least one of the origins of the familiar IR-problems of inflationary correlation functions. At leading order, IR-problems originate precisely from this effect.

[1] We use conventions such that the Fourier transform reads $\zeta(\vec{x}) = \int \frac{d^3k}{(2\pi)^3}\; e^{i\vec{k}\vec{x}} \zeta(\vec{k})$. The Gaussian random variables $\hat{a}_{\vec{k}}$ and $b^s_{\vec{k}}$ have zero mean and variance $\langle\, \hat{a}_{\vec{k}}\; \hat{a}_{\vec{p}}\,\rangle = (2\pi)^3\; \delta^{(3)}(\vec{k}+\vec{p})$ and $\langle\, b^s_{\vec{k}}\; b^{s'}_{\vec{p}}\,\rangle = (2\pi)^3\; \delta^{(3)}(\vec{k}+\vec{p})\; \delta^{ss'}$. The polarization tensor for gravitational waves satisfies $\epsilon^s_{ii}(\vec{k}) = 0 = k_i \epsilon^s_{ij}(\vec{k})$ and the orthogonality relation $\sum_{ij} \epsilon^s_{ij}(\vec{k})\; \epsilon^{s'}_{ij}(-\vec{k}) = 2\delta_{ss'}$.

To be more precise, we somewhat jump ahead and note that $\langle\bar{\zeta}^2\rangle \sim (N_\varphi H)^2 \ln(kL)$, with a similar formula holding for $\bar{\gamma}$. In other words, the expectation value of $\bar{\zeta}^2$ grows logarithmically with L because of the summation over modes between $1/L$ and k involved in its definition. Thus, the effect of these backgrounds on ζ-correlators at the scale k can become large if the logarithm overcomes the suppression by the tree-level power spectrum $(N_\varphi H)^2$. Such a potentially large effect can come only from the factors $e^{2\bar{\zeta}}$ and $e^{\bar{\gamma}}$ relating the coordinate distance y and the invariant distance z, as explained above. If we are able to remove this effect from the definition of the power spectrum, then we have removed all IR effects at the *leading-logarithmic* order. By this we mean all corrections involving as many powers of $\ln(kL)$ as of the suppression factor $(N_\varphi H)^2$, at leading order in slow-roll.

To avoid this (leading-logarithmic) L-dependence (or IR-sensitivity), we propose to use the *invariant* distance z for the definition of the curvature correlator [64, 90]. The background contains, by its very definition, only modes much longer than the relevant scales $y \sim 1/k$. Hence the background is smooth at the scale y. Its presence corresponds to a (constant) coordinate transformation $\vec{y} \to \vec{z}$:

$$z^i = e^{\bar{\zeta}} \left(e^{\bar{\gamma}/2}\right)^i_j \, y^j \qquad . \tag{4.5}$$

The invariant distance $z = \sqrt{\delta_{ij}\, z^i z^j}$ represents the *physical* separation of the points $\vec{x}$ and $\vec{x}+\vec{y}$, independently of the location $\vec{x}$ and the background in its surroundings.

Thus, the correlator $\langle\, \zeta(\vec{x})\; \zeta(\vec{x} + e^{-\bar{\zeta}(\vec{x})}\, e^{-\bar{\gamma}(\vec{x})/2}\, \vec{z})\,\rangle$ involves an average over pairs of points that are separated by a certain invariant distance z. The z-dependence of this correlator is then a background-independent object. To make this even more apparent, we spell out the exact prescription for obtaining this correlator: The basic step consists in picking a pair of points from the reheating surface which are separated by an invariant distance z and multiplying the corresponding values of ζ. This in itself is not background independent since the background can shift ζ by a constant. However, once we restrict our interest to the z-dependence of this product of ζ-values, any such constant drops out. Hence, the z-dependence of $\langle\, \zeta(\vec{x})\; \zeta(\vec{x} + e^{-\bar{\zeta}(\vec{x})}\, e^{-\bar{\gamma}(\vec{x})/2}\, \vec{z})\,\rangle$ is indeed an IR-safe quantity: While the average is in practice over a certain region of size L, the expectation value is independent of where we are in this region. It can therefore not depend on the size L of the underlying region. To say it yet in another way: Single-field inflation ends in the same way in every part of the universe and hence a correlator, defined in a purely local manner, can not depend on the size of the region from which the sample of pairs of points is chosen.

Consequently, we can define an IR-safe power spectrum, that we denote $\mathcal{P}^{(0)}_\zeta$, by

$$\mathcal{P}^{(0)}_\zeta(k) = \frac{k^3}{2\pi^2} \int d^3z\; e^{-i\vec{k}\vec{z}} \left\langle\; \zeta(\vec{x})\; \zeta(\vec{x} + e^{-\bar{\zeta}(\vec{x})}\, e^{-\bar{\gamma}(\vec{x})/2}\, \vec{z})\right\rangle \qquad . \tag{4.6}$$

This Fourier transform at scale k is only sensitive to the z-dependence of the correlator in the region $z \sim 1/k$. It is hence IR-safe by the arguments given above.

The expression for the original IR-sensitive power spectrum $\mathcal{P}_\zeta$ given in (4.3) follows from comparing eq. (4.3) and eq. (4.6). Starting from eq. (4.3), we express the vector $\vec{y}$ in terms of the vector $\vec{z}$. Notice that this also affects the argument of the exponential. Then, we perform a coordinate transformation $d^3y \to d^3z$ in order to bring the integral in a form similar to eq. (4.6). As a final step, we can express the result in terms of the IR-safe power spectrum evaluated at $e^{-\bar{\zeta}(\vec{x})}e^{-\bar{\gamma}(\vec{x})/2}\vec{k}$. A detailed calculation can be found

in Appendix 4.7.1. The result reads

$$\mathcal{P}_\zeta(k) = \left\langle \left[\left(e^{-\bar\gamma(\vec x)}\right)_{ij} \hat k_i \hat k_j \right]^{-3/2} \mathcal{P}_\zeta^{(0)}\left(e^{-\bar\zeta(\vec x)} e^{-\bar\gamma(\vec x)/2}\vec k\right) \right\rangle \quad . \tag{4.7}$$

The vector $\hat k$ is a unit-vector in $\vec k$-direction and the average is performed over the background quantities $\bar\zeta(\vec x)$ and $\bar\gamma_{ij}(\vec x)$. Neglecting tensor fluctuations in the equation above, we recover our result [64] for corrections to the power spectrum due to scalar fluctuations, i.e. $\mathcal{P}_\zeta(k) = \langle\, \mathcal{P}_\zeta^{(0)}(ke^{-\bar\zeta})\,\rangle$. Let us point out the presence of a prefactor, containing only tensor fluctuations, in eq. (4.7). It is originating from the coordinate transformation $d^3y \to d^3z$ in the comparison of the two spectra. While scalar fluctuations receive a contribution from this transformation, tensor fluctuations do not, due to the fact that $\det e^\gamma = 1$. Expanding to leading non-trivial order in the background yields

$$\mathcal{P}_\zeta(k) = \left(1 - \frac{1}{20}\langle\, \mathrm{tr}\,\bar\gamma^2\,\rangle \frac{d}{d\ln k} + \frac{1}{2}\langle\,\bar\zeta^2\,\rangle \frac{d^2}{d(\ln k)^2}\right) \mathcal{P}_\zeta^{(0)}(k) \quad , \tag{4.8}$$

in agreement with [80] (see also Section 4.4). Here, we used the zero mean condition $\langle\,\bar\zeta(x)\,\rangle = 0 = \langle\,\bar\gamma_{ij}(\vec x)\,\rangle$, which can always be realized by a rescaling of coordinates. In principle, one may choose coordinates where this is not the case. But it is rather natural to assume that an observer would specify coordinates in such a way that his observable patch is not affected by a constant background shift. In the particular case of slow-roll inflation, both corrections in eq. (4.8) are of the same order. While, according to the scalar-to-tensor ratio, $\mathrm{tr}\,\bar\gamma^2$ is more slow-roll suppressed than $\bar\zeta^2$, it appears with only one derivative in $\ln k$. Hence, tensor corrections are as important as scalar corrections in slow-roll inflation.

The remaining task is to average the background quantities, given in eq. (4.4). In principle, we have to average $\bar\zeta(\vec x)$ and $\bar\gamma(\vec x)$ over the large observed region of box-size L. However, this is equivalent to an ensemble average of $\bar\zeta(0)$ and $\bar\gamma(0)$ with IR cut-off L. Thus, in single-field, slow-roll inflation, we are dealing with sums of Gaussian random variables $\hat a_{\vec q}$, respectively $b^s_{\vec q}$,

$$\bar\zeta = \int_{1/L}^{k} \frac{d^3q}{(2\pi)^3}\ \zeta(\vec q) = \int_{1/L}^{k} \frac{d^3q}{(2\pi)^3}\ \frac{N_\varphi(\vec q)\, H(\vec q)}{\sqrt{2q^3}}\ \hat a_{\vec q} \tag{4.9}$$

$$\bar\gamma_{ij} = \int_{1/L}^{k} \frac{d^3q}{(2\pi)^3}\ \gamma_{ij}(\vec q) = \int_{1/L}^{k} \frac{d^3q}{(2\pi)^3}\ \sum_{s=+,\times} \frac{H(\vec q)}{\sqrt{q^3}}\ \epsilon^s_{ij}(\vec k)\ b^s_{\vec q} \quad . \tag{4.10}$$

While their averages are vanishing, $\langle\,\bar\zeta\,\rangle = 0 = \langle\,\bar\gamma_{ij}\,\rangle$, one finds a scale-dependent result for the two-point functions. For instance under the assumption of a scale-invariant power spectrum, they obey a logarithmic scale-dependence

$$\langle\,\bar\zeta^2\,\rangle = \left(\frac{N_\varphi H}{2\pi}\right)^2 \ln(kL) \qquad \langle\,\mathrm{tr}\,\bar\gamma^2\,\rangle = \langle\,\bar\gamma_{ij}\ \bar\gamma_{ij}\,\rangle = 8\left(\frac{H}{2\pi}\right)^2 \ln(kL) \quad . \tag{4.11}$$

Neglecting tensor fluctuations for the moment, the background $\bar\zeta$ is a sum of Gaussian random variables $\hat a_{\vec q}$. Therefore, $\bar\zeta$ itself is a Gaussian random variable, with distribution[2]

$$\mathbb{P}\left[\bar\zeta\right] d\bar\zeta \ = \ \frac{1}{\sqrt{2\pi\sigma_\zeta^2}}\ \exp\left(-\frac{\bar\zeta^2}{2\sigma_\zeta^2}\right) d\bar\zeta \tag{4.12}$$

[2]This is related to the stochastic approach [38] of Starobinsky.

where the width is

$$\sigma_\zeta^2 = \langle\, \bar{\zeta}^2 \,\rangle = \int_{1/L}^{k} \frac{d^3q}{(2\pi)^3}\ \frac{N_\varphi^2(\vec{q})\, H^2(\vec{q})}{2q^3} \qquad . \tag{4.13}$$

Note that we do not assume a scale-invariant behavior of the power spectrum in this expression. Typically, the n-point functions we are interested in can be expressed as $\langle\, f(\,\bar{\zeta}(\vec{x})\,)\,\rangle$, for some function f. As usual for Gaussian variables, this may be expressed in terms of an integral over a Gaussian probability distribution

$$\langle\, f(\bar{\zeta})\,\rangle = \frac{1}{\sqrt{2\pi\sigma_\zeta^2}} \int d\bar{\zeta}\ \exp\left(-\frac{\bar{\zeta}^2}{2\sigma_\zeta^2}\right)\ f(\bar{\zeta}) \qquad . \tag{4.14}$$

As an example, the power spectrum is given by

$$\mathcal{P}_\zeta(k) = \frac{1}{\sqrt{2\pi\sigma_\zeta^2}} \int d\bar{\zeta}\ \exp\left(-\frac{\bar{\zeta}^2}{2\sigma_\zeta^2}\right)\ \mathcal{P}_\zeta^{(0)}(ke^{-\bar{\zeta}}) \qquad . \tag{4.15}$$

Consequently, the question of convergence of fluctuations due to long-wavelength modes reduces to convergence properties of this single integral. The usual series expansion can be recovered by expanding the function $\mathcal{P}_\zeta^{(0)}$ in the logarithm of the scale k. This yields

$$\mathcal{P}_\zeta(k) = \sum_{n=0}^{\infty} \frac{\langle\, \bar{\zeta}^{2n}\,\rangle}{(2n)!}\ \frac{d^{2n}\,\mathcal{P}_\zeta^{(0)}(k)}{d(\ln k)^{2n}} \tag{4.16}$$

$$\langle\, \bar{\zeta}^{2n}\,\rangle = \frac{1}{\sqrt{2\pi\sigma_\zeta^2}} \int d\bar{\zeta}\ \bar{\zeta}^{2n}\ \exp\left(-\frac{\bar{\zeta}^2}{2\sigma_\zeta^2}\right) \;=\; (2n-1)!!\ \left(\sigma_\zeta^2\right)^n \quad , \tag{4.17}$$

where $n!!$ denotes the double factorial. This is in agreement with [80]. We emphasize, however, that a breakdown of convergence of the series does not necessarily mean a breakdown of convergence of the integral in eq. (4.15). We return to this point in sect. 4.4. Notice also that in eqs. (4.9) and (4.10) we have neglected the intrinsic non-Gaussianity of curvature and tensor perturbations. Such intrinsic non-Gaussianity is present at sub-leading order in slow-roll. However, at every log-order, there is a term consisting solely of Gaussian contributions. Relative to this term, contributions with intrinsic non-Gaussian parts are suppressed by slow-roll parameters and the Hubble scale with no additional log-enhancement. Therefore, neglecting the non-Gaussian contribution is justified in our leading-log analysis of IR-corrections.

Attention has to be paid to the fact that inflation has ended at some point. Hence, there exists a value $k_{\max}$ corresponding to modes that have never left the horizon. The observer measuring $\mathcal{P}_\zeta(k)$ for some fixed k will have to exclude regions where $ke^{-\bar{\zeta}} > k_{\max}$ from his averaging procedure. Technically, this implies a lower bound for the $\bar{\zeta}$-integral, given by $\bar{\zeta}_{\min} = -\ln(k_{\max}/k)$.

$$\mathcal{P}_\zeta(k) = \frac{1}{\sqrt{2\pi\sigma_\zeta^2}} \int_{\bar{\zeta}_{\min}}^{\infty} d\bar{\zeta}\ \exp\left(-\frac{\bar{\zeta}^2}{2\sigma_\zeta^2}\right)\ \mathcal{P}_\zeta^{(0)}(ke^{-\bar{\zeta}}) \qquad . \tag{4.18}$$

The Gaussian function in eq. (4.18) gives a non-negligible contribution only in a limited range around zero. This range is of the order of σ_ζ. For large L (implying large σ_ζ) and for k sufficiently close to $k_{\rm max}$, the lower bound $\bar{\zeta}_{\rm min}$ enters this range. Hence, in such cases, the lower bound implies the subtraction of a significant contribution from the integral. We finally note that the existence of $k_{\rm max}$ and $\bar{\zeta}_{\rm min}$ are related to potential convergence problems of the series expansion in eq. (4.16). This is apparent since the slow-roll conditions, which are responsible for the smallness of derivatives of $\mathcal{P}_\zeta(k)$, break down near $k_{\rm max}$.

Including tensor modes is in principle straightforward, but complicated by the matrix structure of $\bar{\gamma}$ and the different independent polarizations involved. In order not to overburden formulae, we set the scalar background $\bar{\zeta}$ to zero in what follows. The complete power spectrum can then be expressed as

$$\mathcal{P}_\zeta(k) = \left\langle \left[\left(e^{-\bar{\gamma}}\right)_{ij}\hat{k}_i\hat{k}_j\right]^{-3/2} \mathcal{P}_\zeta^{(0)}\left(\left[\left(e^{-\bar{\gamma}}\right)_{ij}\hat{k}_i\hat{k}_j\right]^{\frac{1}{2}} k\right)\right\rangle \quad , \tag{4.19}$$

where $\hat{k}$ is the unit vector parallel to $\vec{k}$. We also introduce the notation

$$n \equiv \left[\left(e^{-\bar{\gamma}}\right)_{lm}\hat{k}_l\hat{k}_m\right] \quad . \tag{4.20}$$

Note that each entry of the matrix $\bar{\gamma}_{ij}$, being a sum of Gaussian random variables, is a Gaussian random variable. However, the various entries in the matrix are not statistically independent: this implies that it is not obvious how to calculate the statistical distribution of the entries of the *exponential* of $(-\bar{\gamma})$, that enters in the definition of n. Having this distribution, that we denote with $\mathbb{P}[n]$, it is straightforward to provide an integral representation for the power spectrum subject to tensor background modes:

$$\mathcal{P}_\zeta(k) = \int dn\ \mathbb{P}[n]\ n^{-\frac{3}{2}}(\hat{k})\mathcal{P}_\zeta^{(0)}\left(n^{\frac{1}{2}}k\right) \quad . \tag{4.21}$$

It is clear that, at least numerically, $\mathbb{P}[n]$ can be determined and the integral can be calculated.

4.2.2 Higher correlation functions

To discuss n-point functions, we could try to generalize the 'almost scale-invariant' spectrum of eq. (4.3) by writing

$$\mathcal{P}_n(\vec{k}_1,\ldots,\vec{k}_n) = \left\langle \left(\frac{k^3}{2\pi^2}\right)^n \int d^3y_1\ldots d^3y_n\ e^{-i(\vec{k}_1\vec{y}_1+\ldots+\vec{k}_n\vec{y}_n)}\,\zeta(\vec{x})\,\zeta(\vec{x}+\vec{y}_1)\ldots\zeta(\vec{x}+\vec{y}_n)\right\rangle \quad . \tag{4.22}$$

However, it is not clear which particular combination of $k_1\ldots k_n$ one should use to define k in the prefactor k^{3n}. This is not irrelevant since factors $e^{\bar{\gamma}/2}$ will get tangled up in this prefactor. Hence, we choose to write the general formula for the higher-order analogue of the conventional spectrum $P_\zeta(k) = 2\pi^2\mathcal{P}_\zeta(k)/k^3$. In doing so, prefactors will arise from the scaling of the d^3y_a. Since the determinant of the tensor contribution is one, this scaling consist exclusively of $\bar{\zeta}$, which only depend on the overall scale. Given these preliminaries, the generalization of our formalism is completely straightforward and the IR-safe spectrum is defined as

$$P_n^{(0)}(\vec{k}_1,\ldots,\vec{k}_n) = \left\langle \int d^3z_1\ldots d^3z_n\ e^{-i(\vec{k}_1\vec{z}_1+\ldots+\vec{k}_n\vec{z}_n)}\,\zeta(\vec{x})\,\zeta(\vec{x}+\vec{y}_1)\ldots\zeta(\vec{x}+\vec{y}_n)\right\rangle \quad , \tag{4.23}$$

where

$$\vec{y}_a = \vec{y}_a(\vec{z}_a, \bar{\zeta}, \bar{\gamma}) = e^{-\bar{\zeta}} e^{-\bar{\gamma}/2} \vec{z}_a \qquad . \tag{4.24}$$

This means that we measure the correlation function in terms of n invariant distances, characterized by a set of vectors $\vec{z}_a$, $a \in [1, \ldots, n]$. Hence, the $\vec{z}_a$-dependence of the corresponding n-point function is independent of background quantities and, therefore, IR-safe. Consequently, its Fourier transform, i.e. the spectrum $P_n^{(0)}$, is the desired IR-safe spectrum. A straightforward generalization of the previous calculation for the power spectrum provides the following result

$$P_n(\vec{k}_1, \ldots, \vec{k}_n) = \left\langle e^{-3n\bar{\zeta}} \, P_n^{(0)}(e^{-\bar{\zeta}} e^{-\bar{\gamma}/2} \vec{k}_1, \ldots, e^{-\bar{\zeta}} e^{-\bar{\gamma}/2} \vec{k}_n) \right\rangle \qquad . \tag{4.25}$$

As already stressed above, the prefactor $e^{-3n\bar{\zeta}}$ originates from the naive scaling $P_n^{(0)} \sim k^{-3n}$.

The log-enhancement-effects of higher correlation functions specified by eq. (4.25) can be directly applied to observables measuring non-Gaussianity, like $f_{\rm NL}$, as we are going to discuss in section 4.5.

4.3 An alternative approach within slow-roll inflation

In the previous section we discussed a systematic way to define IR-safe n-point functions. We have explained how to straightforwardly obtain, from these IR-safe quantities, the corresponding IR-sensitive objects. In this section, we present an alternative point of view: working only in momentum space, we will directly calculate the all-orders IR-enhancement of the conventional power spectrum. To be more specific, we will compute the curvature perturbation ζ, by implementing a suitable extension of the δN-formalism, in such a way as to include the effects of long-wavelength modes. The results coincide with what we obtained in the previous section, in all cases in which δN-formalism is applicable. So, in these cases, the two methods are equivalent.

We focus on a single, slowly rolling scalar field φ (the extension to multiple fields is outlined in Appendix 4.7.2). We assume the underlying metric to be of the form

$$ds^2 = -dt^2 + a^2(t) \, \bar{g}_{ij} dx^i dx^j \qquad . \tag{4.26}$$

Throughout this section, we are interested in quantities evaluated at some wave vector $\vec{k}$. To analyze contributions from the background to these quantities, we find it technically convenient to separate the fluctuations into modes characterized by momenta larger, and smaller, than k. For modes $\vec{q}$ with $q = |\vec{q}| \ll k$, we will work in a gauge with $\delta_{\vec{q}}\varphi = 0$. While for q around k and larger, we adopt a gauge with vanishing scalar metric fluctuations. The advantage of this splitting, and of these different gauge choices, is that the contribution from long-wavelength modes is contained in geometrical quantities and, therefore, contained in the 3-metric

$$\bar{g}_{ij} = e^{2\bar{\zeta}} \, (e^{\bar{\gamma}})_{ij} \quad . \tag{4.27}$$

Here, the scalar and tensor background, $\bar{\zeta}$ and $\bar{\gamma}_{ij}$, are defined as before. It would be interesting to understand whether the above construction can be done in a gauge invariant manner. On the other hand, let us stress that we proceed in this way only for technical convenience. One could also work with a gauge characterized by vanishing scalar

metric fluctuations for all $\vec{q}$. With this choice, however, the scalar background from long-wavelength $\delta_{\vec{q}}\varphi$ would affect the scalar field value at the time of horizon exit (see [64] for a treatment of background modes of the scalar field φ in this latter gauge choice). In contrast, the tensor background would still enter via the 3-metric. Therefore, the inclusion of tensor background modes within the δN-formalism requires a treatment as outlined in this section, contrary to the scalar background which might be calculated by different techniques.

The appearance of background contributions in the 3-metric eq. (4.27) has important consequences for the physical length scale associated with the wave vector $\vec{k}$, i.e. on the physical wavelength. Due to the deviation of $\bar{g}_{ij}$ from flatness, this scale is not the inverse of $k = \sqrt{k_i k_j \delta_{ij}}$, but is instead given by $1/k'$ with

$$k'^2 \;=\; e^{-2\bar{\zeta}} \left(e^{-\bar{\gamma}}\right)_{ij} k_i k_j \qquad . \tag{4.28}$$

Hence, the physical scale depends on the original vector $\vec{k}$ and on the background quantities $\bar{\zeta}$ and $\bar{\gamma}_{ij}$. This dependence on background quantities leads to a shift in the time of horizon exit for a given scalar mode of momentum $\vec{k}$, from t_k to $t_{k'}$. That is, since the time of horizon exit is defined by the relation $k = a(t_k)H(t_k)$ (a being the scale factor), at first order in slow-roll we have the relation

$$dt_k \;=\; \frac{1}{H}\, d\ln k \qquad . \tag{4.29}$$

For small time variations, and at leading order in slow-roll, we can integrate the previous equation and find

$$H\,(t_{k'} - t_k) = \ln\frac{k'}{k} \;=\; -\bar{\zeta} - \Delta \qquad \text{with} \tag{4.30}$$

$$\Delta \equiv \left(\frac{1}{2}\bar{\gamma}_{ij} - \frac{1}{4}\bar{\gamma}_{il}\bar{\gamma}_{lj}\right)\hat{k}_i\hat{k}_j + \left(\frac{1}{2}\bar{\gamma}_{ij}\;\hat{k}_i\hat{k}_j\right)^2 + \mathcal{O}(\bar{\gamma}^3) \qquad . \tag{4.31}$$

Here, $\hat{k}$ represents a unit vector in $\vec{k}$-direction. The quantity Δ collects the leading order contributions from the long-wavelength tensor modes, obtained from expanding the exponential in eq. (4.28).

The form of the background metric affects the dynamics of first order, massless scalar fluctuations. In momentum space, the equation of motion for the scalar perturbations reads

$$\left(\delta_{\vec{k}}\varphi\right)^{\cdot\cdot} + 3H\left(\delta_{\vec{k}}\varphi\right)^{\cdot} + \frac{k'^2}{a^2}\,\delta_{\vec{k}}\varphi \;=\; 0 \qquad , \tag{4.32}$$

where dots denote derivatives with respect to time. Note that the effect of background quantities enters via the Laplacian which leads to the k'^2 instead of k^2 in the third term on the left-hand side. The solution for the fluctuation $\delta_{\vec{k}}\varphi$ results in

$$\delta_{\vec{k}}\varphi = \delta_{\vec{k}}\varphi(k', \bar{g}_{ij}) = \frac{H(k')}{\left(\det{}^{\frac{1}{4}}\,\bar{g}_{ij}\right)\,(2k'^3)^{\frac{1}{2}}}\;\hat{a}_{\vec{k}} \tag{4.33}$$

in a superhorizon regime. In our notation $H(k')$ indicates that this quantity is evaluated at time of horizon exit of the scale k', instead of k, in order to take into account the shift due to long-wavelength contributions. The normalization of $\delta_{\vec{k}}\varphi$, $\det^{1/4}\bar{g}_{ij}$ in the

denominator, is obtained when imposing the usual commutation relations between the quantized scalar fluctuation and its momentum conjugate (see, for example, [34]). Another way to understand it is the following: the normalization of $\delta_{\vec{k}}\varphi$ is set by requiring that in the limit of short distances y, we recover the singularity of the scalar field in Minkowski space for $\langle\, \delta\varphi(\vec{x})\ \delta\varphi(\vec{x}+\vec{y})\,\rangle$. On these distances, the background quantities $\bar{\zeta}$ and $\bar{\gamma}_{ij}$ are constant and, hence, need to be absorbed in a redefinition of space variables in order to bring the metric in Minkowski-form. This redefinition is responsible for the factor $\det{}^{1/4}\,\bar{g}_{ij}$, appearing in the normalization of $\delta_{\vec{k}}\varphi$.

Since $\bar{\gamma}_{ij}$ is traceless, $\det \bar{g}_{ij} = \exp(6\bar{\zeta})$ and eq. (4.33) can be rewritten as

$$\begin{aligned}\delta_{\vec{k}}\varphi(k', \bar{g}_{ij}) = & \frac{H(k')}{\sqrt{2}\left[k_i k_j \left(e^{-\bar{\gamma}}\right)_{ij}\right]^{\frac{3}{4}}}\ \hat{a}_{\vec{k}} \\ = & \, m^{\frac{1}{2}}(\hat{k})\,\frac{H(k')}{(2k^3)^{\frac{1}{2}}}\ \hat{a}_{\vec{k}} \quad ,\end{aligned} \tag{4.34}$$

where we define the function $m(\hat{k})$ that depends on a unit vector $\hat{k}$ along the direction of $\vec{k}$:

$$m(\hat{k}) \ \equiv\ \left[\left(e^{-\bar{\gamma}}\right)_{ij}\hat{k}_i\hat{k}_j\right]^{-\frac{3}{2}} \qquad . \tag{4.35}$$

In equation (4.34), the dependence on background quantities is limited to the overall function $m(\hat{k})$ (that depends only on the tensor background, see eq. (4.35)) and to the 'time' argument k' of the Hubble parameter.

Starting from scalar fluctuations and by using δN-formalism [23, 25, 37–39], we can express the curvature fluctuation ζ at superhorizon scales on a constant energy density slice, that we take to be the reheating surface, in terms of $\delta\varphi$. The curvature perturbation $\zeta_{\vec{k}}$ is related to the time integral of the local expansion parameter, providing the number of e-foldings, from an initial hypersurface (that we take at time of horizon exit for the mode $\vec{k}$) to the final hypersurface of constant energy density. In single field inflation, we have

$$\zeta \ =\ N\left[\varphi + \delta\varphi\right] - \langle N\rangle \qquad , \tag{4.36}$$

where $\langle N\rangle$ is the spatial average of the first term on the right-hand side. The quantity $\varphi+\delta\varphi$ corresponds to the homogeneous value for the scalar field plus its perturbation built, as above, on a space-time geometry that includes the contributions of long-wavelength modes. The previous schematic expression can be expanded in the scalar fluctuations, and gives in momentum space [3]

$$\zeta_{\vec{k}} \ =\ N_\varphi(k')\,\delta_{\vec{k}}\varphi(k', \bar{g}_{ij}) + \ldots \qquad . \tag{4.37}$$

Notice that functions on the right-hand-side are evaluated at time of horizon exit of the mode $\vec{k}$, which is sensitive to the change in the background geometry due to long-wavelength modes. That is, their argument is k' instead of k. As in section 4.2, the function $N_\varphi = dN/d\varphi$ is given by $N_\varphi = V/(dV/d\varphi)$. The remaining terms in the δN expansion, understood in the dots of eq. (4.37), are slow-roll suppressed with respect to

[3] For the purposes of this work, we can truncate the δN expansion to the first, leading order term in slow-roll. Including higher order terms is straightforward, as we discuss in Appendix 4.7.2.

the first one. Using the results obtained earlier, we get for $\zeta_{\vec{k}}$ an expression in terms of Gaussian random variables as follows

$$\zeta_{\vec{k}} = \left[m^{\frac{1}{2}}(\hat{k})\, N_\varphi(k')\, H(k') \right] \frac{\hat{a}_{\vec{k}}}{(2k^3)^{\frac{1}{2}}} \quad . \tag{4.38}$$

The dependence on long-wavelength background quantities is contained in the overall factor between squared parenthesis. Eq. (4.38), possibly including higher order terms in the δN-expansion, is all what we need to straightforwardly compute inflationary observables, associated to n-point functions of curvature perturbations, including the effects of long-wavelength modes. Eq. (4.38) can be regarded as an extension of δN-formalism. It includes the contributions of long-wavelength scalar and tensor modes in the expression for the curvature perturbation ζ.

As an application of eq. (4.38), we rederive the expression for log-enhanced contributions to the power spectrum. We start with the two-point function of the curvature perturbation

$$\begin{aligned} \langle\, \zeta_{\vec{k}}\, \zeta_{\vec{p}}\, \rangle &= \frac{1}{2\,(kp)^{\frac{3}{2}}}\, \langle\, m^{\frac{1}{2}}(\hat{k}) m^{\frac{1}{2}}(\hat{p})\, N_\varphi(k') H(k')\, N_\varphi(p') H(p')\, \hat{a}_{\vec{k}} \hat{a}_{\vec{p}}\, \rangle \\ &= \frac{(2\pi)^3 \delta^{(3)}(\vec{k}+\vec{p})}{2k^3}\, \langle\, m(\hat{k})\, N_\varphi^2(k') H^2(k')\, \rangle \qquad , \end{aligned} \tag{4.39}$$

where for passing from first to second line, we used Wick's theorem and contracted the Gaussian variables $\hat{a}_{\vec{k}}$ and $\hat{a}_{\vec{p}}$. Indeed, $\hat{a}_{\vec{k}}$ is only allowed to contract with $\hat{a}_{\vec{p}}$, since any other quantity depends on modes with momenta much smaller than k. One obtains the following expression for the power spectrum:

$$\mathcal{P}_\zeta(k) \,=\, \frac{1}{(2\pi)^2} \langle m(\hat{k})\, N_\varphi^2(k') H^2(k') \rangle \qquad . \tag{4.40}$$

The argument of the average on the right-hand side depends on long-wavelength scalar and tensor contributions, which, as shown in eq. (4.11), have non-vanishing two-point functions. In absence of contributions of long-wavelength modes, eq. (4.40) provides the following tree-level result

$$\mathcal{P}_\zeta^{(0)}(k) \,=\, \frac{1}{(2\pi)^2}\, N_\varphi^2(k) H^2(k) \qquad , \tag{4.41}$$

which also coincides with the definition of the IR-safe power spectrum provided in section 4.2. Notice that the dependence on the scale k in $\mathcal{P}_\zeta^{(0)}$ occurs only through the dependence on the time of horizon exit of the right-hand side. Using this fact, eq. (4.40) can be rewritten as

$$\mathcal{P}_\zeta(k) \,=\, \langle m(\hat{k}) \mathcal{P}_\zeta^{(0)}(k') \rangle \quad . \tag{4.42}$$

Recall that $\hat{k}$ represents the unit vector along the direction of $\vec{k}$, while k' in the previous expression is associated to k via eq. (4.28). Using these formulae, eq. (4.42) can be rewritten as

$$\mathcal{P}_\zeta(k) = \left\langle \left[\left(e^{-\bar{\gamma}}\right)_{ij} \hat{k}_i \hat{k}_j \right]^{-3/2} \mathcal{P}_\zeta^{(0)} \left(e^{-\bar{\zeta}} e^{-\bar{\gamma}/2} \vec{k} \right) \right\rangle \qquad . \tag{4.43}$$

Not surprisingly, this corresponds exactly to equation (4.7), obtained with the method of section 4.2.

4.4 Two-point function and the power spectrum

In this section, we analyze the log-enhanced corrections due to scalar and tensor long-wavelength modes to the power spectrum of curvature perturbation. Using the results from sec. 4.2 or sec. 4.3, the power spectrum is given by the formula

$$\mathcal{P}_\zeta(k) = \langle m(\hat{k})\mathcal{P}_\zeta^{(0)}(k')\rangle \tag{4.44}$$

$$= \left\langle \left[\left(e^{-\bar{\gamma}}\right)_{ij}\hat{k}_i\hat{k}_j\right]^{-3/2} \mathcal{P}_\zeta^{(0)}\left(e^{-\bar{\zeta}}e^{-\bar{\gamma}/2}\vec{k}\right)\right\rangle \quad . \tag{4.45}$$

As explained in section 4.2, this implies that we can deal with scalar perturbations to all orders, resumming the complete series, in case an exact expression for the tree level power spectrum is known. We will return to this important topic at the end of this section; for the moment we focus on calculating, in full generality, the leading log-enhanced contributions to the power spectrum. In order to do so, it is sufficient to expand eq. (4.45) in $\bar{\zeta}$ and $\bar{\gamma}$. The following equations are useful for this purpose

$$m(\hat{k}) = \left[\left(e^{-\bar{\gamma}}\right)_{ij}\hat{k}_i\hat{k}_j\right]^{-3/2} = 1 + \frac{3}{2}\bar{\gamma}_{ij}\,\hat{k}_i\hat{k}_j - \frac{3}{4}\bar{\gamma}_{il}\bar{\gamma}_{lj}\,\hat{k}_i\hat{k}_j + \frac{15}{8}\left(\bar{\gamma}_{ij}\,\hat{k}_i\hat{k}_j\right)^2 + \mathcal{O}(\bar{\gamma}_{ij}^3) \tag{4.46}$$

$$\ln k' = \ln k - \bar{\zeta} - \Delta \tag{4.47}$$

$$\Delta = \frac{1}{2}\,\bar{\gamma}_{ij}\hat{k}_i\hat{k}_j - \frac{1}{4}\bar{\gamma}_{il}\bar{\gamma}_{lj}\,\hat{k}_i\hat{k}_j + \frac{1}{4}\left(\bar{\gamma}_{ij}\,\hat{k}_i\hat{k}_j\right)^2 + \mathcal{O}(\bar{\gamma}_{ij}^3) \quad . \tag{4.48}$$

Here, k' denotes the Euclidean length of the vector $e^{-\bar{\zeta}}e^{-\bar{\gamma}/2}\vec{k}$. We will also make use of the identity (see also [80]):

$$\langle\, \bar{\gamma}_{ij}\ \bar{\gamma}_{lm}\,\rangle = \frac{1}{30}\,\langle\,\mathrm{tr}\,\bar{\gamma}^2\,\rangle\,\left[\,3\,(\delta_{il}\delta_{jm} + \delta_{im}\delta_{jl}) - 2\,\delta_{ij}\delta_{lm}\right] \quad , \tag{4.49}$$

where $\langle\,\mathrm{tr}\,\bar{\gamma}^2\,\rangle = \sum_{ij}\langle\,\bar{\gamma}_{ij}\ \bar{\gamma}_{ij}\,\rangle$. From this, it is easy to check that a cancellation leads to $\langle m(\hat{k})\rangle = 1 + \mathcal{O}(\bar{\gamma}^4)$. We can then expand eq. (4.44) up to the first non-vanishing contributions. We obtain

$$\begin{aligned}\mathcal{P}_\zeta(k) &= \mathcal{P}_\zeta^{(0)}(k)\left\langle m(\hat{k})\cdot\left[1 - \left(\Delta + \bar{\zeta}\right)\ \frac{1}{\mathcal{P}_\zeta^{(0)}(k)}\,\frac{d\mathcal{P}_\zeta^{(0)}(k)}{d\ln k} + \frac{\bar{\zeta}^2}{2}\,\frac{1}{\mathcal{P}_\zeta^{(0)}(k)}\,\frac{d^2\mathcal{P}_\zeta^{(0)}(k)}{d(\ln k)^2}\right]\right\rangle \\ &= \left\{1 - \left[\langle\,(m(\hat{k}) - 1)\,\Delta\,\rangle + \langle\,\Delta\,\rangle\right]\ \frac{d}{d\ln k} + \frac{\langle\,\bar{\zeta}^2\,\rangle}{2}\frac{d^2}{d(\ln k)^2}\right\}\mathcal{P}_\zeta^{(0)}(k) \\ &= \left(1 - \frac{1}{20}\langle\,\mathrm{tr}\,\bar{\gamma}^2\,\rangle\frac{d}{d\ln k} + \frac{1}{2}\langle\,\bar{\zeta}^2\,\rangle\frac{d^2}{d(\ln k)^2}\right)\mathcal{P}_\zeta^{(0)}(k) \quad .\end{aligned} \tag{4.50}$$

This equation was also found in [80] [4]. Neglecting tensor contributions, this reproduces the results of log-enhanced corrections to the power spectrum due to scalar fluctuations given in [64, 89].

Taking another point of view, we note that eq. (4.50) can be obtained by expanding ζ, the curvature perturbation in uniform-energy-density gauge, in terms of $\delta\varphi$, the scalar field perturbation in flat gauge. Up to quadratic order in $\delta\varphi$, the relevant gauge transformation

[4] Note that in [80] the result for corrections due to tensors is expressed in terms of the quantity $\langle\,\bar{\gamma}^2_{\rm GS}\,\rangle \equiv \frac{1}{4}\sum_{ij}\langle\,\bar{\gamma}_{ij}\ \bar{\gamma}_{ij}\,\rangle = \frac{1}{4}\langle\,\mathrm{tr}\,\bar{\gamma}^2\,\rangle$. Tensor contributions to inflationary observables, using different methods, have been also considered in [124, 127].

is the one between ζ and $\zeta_n = -(H/\dot{\varphi})\delta\varphi$ given in eq. (A.8) of [22]. If we focus on terms that are leading order in slow-roll and neglect terms vanishing at superhorizon scales, all IR divergences arising from the expansion in (A.8) of [22] are captured by our result. However, the complete IR correction requires the inclusion of term $\sim \delta\varphi^3$. This can be realized using the δN-formalism, and it was shown in [64] that an appropriately modified version of this formalism correctly computes the scalar part of eq. (4.50) (see also Sect. 4.3 of the present paper).

For a weakly scale-dependent power spectrum, the explicit values for $\langle\, \bar{\zeta}^2 \,\rangle$ and $\langle\, \mathrm{tr}\, \bar{\gamma}^2 \,\rangle$ were already given in eq. (4.11). Using the definitions of the spectral index of curvature perturbations n_ζ, its running α_ζ and the tensor-to-scalar ratio $r = N_\varphi^{-2} = 2\epsilon$,

$$n_\zeta - 1 = \frac{d \ln \mathcal{P}_\zeta^{(0)}}{d \ln k} \qquad \alpha_\zeta = \frac{d^2 \ln \mathcal{P}_\zeta^{(0)}}{d(\ln k)^2} \qquad r = \frac{\langle\, \mathrm{tr}\, \bar{\gamma}^2 \,\rangle}{8 \langle\, \bar{\zeta}^2 \,\rangle} \quad , \tag{4.51}$$

the leading order correction to the power spectrum can be written as

$$\mathcal{P}_\zeta(k) \;=\; \mathcal{P}_\zeta^{(0)}(k) \left\{ 1 + \frac{1}{2} \left[(n_\zeta - 1)^2 + \alpha_\zeta - \frac{4r}{5} (n_\zeta - 1) \right] \mathcal{P}_\zeta^{(0)}(k)\, \ln(kL) \right\} \tag{4.52}$$

The agreement[5] of eqs. (4.50) and (4.52) with [80] is a non-trivial check for our approach.

We learn that long-wavelength modes provide log-enhanced contributions to the power-spectrum that are suppressed by second order slow-roll parameters, and by a factor of $\mathcal{P}_\zeta^{(0)}$. The latter is determined by WMAP to be $\mathcal{P}_\zeta^{(0)} \simeq 2.3 \times 10^{-9}$ [18].

Let us stress the quite non-trivial fact that scalar and tensor long-wavelength modes contribute at the same (second) order in a slow-roll expansion. This is due to the cancellation leading to $\langle m(\hat{k}) \rangle = 1 + \mathcal{O}(\bar{\gamma}^4)$. In any case, this property is specific of the power spectrum: as we will learn in the next section, corrections to non-Gaussianity parameters do not share this property.

Having calculated the leading order correction to the power spectrum, we turn to evaluating scalar perturbations to all orders as described in section 4.2. We start with a inflationary potential for which the spectral index is constant. This is realized for the famous example of power law inflation [128]. The potential is $V = V_0 \exp\left[-\sqrt{\frac{2}{q}}\,\varphi\right]$, with constant q, and the scale factor evolves as $a(t) = a_0 t^q$. In this set-up, the equations for scalar fluctuations can be solved exactly without having to rely on a slow-roll approximation. For this particular model, we assume that our scale of interest k is much smaller than k_{max}, reflecting the transition to scales that have never left the horizon during inflation. Hence, the integral in eq. (4.18) is well approximated by setting $\bar{\zeta}_{\mathrm{min}}$ to $-\infty$. The power spectrum of curvature perturbations reads [129, 130]

$$\mathcal{P}_\zeta^{(0)}(k) \;=\; \mathcal{P}_\zeta^{(0)}(k_0) \left(\frac{k}{k_0} \right)^{-2/(q-1)} \quad . \tag{4.53}$$

So the spectral index $n_\zeta - 1 = -2/(q-1)$ is constant as desired. We then obtain

$$\mathcal{P}_\zeta^{(0)}(k e^{-\bar{\zeta}}) = \mathcal{P}_\zeta^{(0)}(k)\; e^{-(n_\zeta - 1)\bar{\zeta}} \quad . \tag{4.54}$$

[5]Note that the authors of [80] chose a different parameterization of the power spectrum, namely $\mathcal{P}_\zeta^{(0)} \sim k^{n(k)-1}$. This leads to slightly different numerical factors. For instance, $d^2\mathcal{P}_\zeta^{(0)}/d(\ln k)^2 = [(n-1)^2 + 2\alpha]\mathcal{P}_\zeta^{(0)}$ in their parameterization.

Plugging this expression into eq. (4.18), one finds an integral that can be solved analytically. We get

$$\mathcal{P}_\zeta(k) = \mathcal{P}_\zeta^{(0)}(k) \exp\left(\frac{\sigma_\zeta^2 (n_\zeta - 1)^2}{2}\right) \quad . \tag{4.55}$$

This expression captures *at all orders* the contributions of long-wavelength modes. In a sense, we are providing the function whose series expansion has been found in [80]. Notice that the corrections are not independent of the scale k since σ_ζ^2 is a function of k (e.g. $\sigma_\zeta^2 = \mathcal{P}_\zeta^{(0)} \ln(kL)$ for a weak scale-dependence of $\mathcal{P}_\zeta^{(0)}$).

We expect a similar behavior including other contributions in more general models of inflation, for example associated with the running of the spectral index; however, solving the integral analytically might be more difficult in these models. For instance, the chaotic potential investigated in [80], $V(\varphi) = \lambda\varphi^\alpha$ ($\alpha > 0$), leads to the following tree-level power spectrum:

$$\mathcal{P}_\zeta^{(0)}(k) = \left(\frac{N_\varphi H}{2\pi}\right)^2 = \frac{1}{(2\pi)^2}\frac{\lambda}{3\alpha^2}\varphi^{\alpha+2}(k) \quad . \tag{4.56}$$

The scalar field value in dependence of the horizon-exit time of the mode k is given by the differential equation $d\varphi/(d\ln k) = -\alpha/\varphi$. This can be integrated to yield

$$\varphi(k) = \sqrt{\varphi^2(k_{\rm max}) + 2\alpha \ln\frac{k_{\rm max}}{k}} \quad . \tag{4.57}$$

Note that the condition $\bar\zeta \geq \bar\zeta_{\rm min}$ guarantees $\varphi(e^{-\bar\zeta}k) \geq \varphi(k_{\rm max})$ for all possible values $\bar\zeta$. Hence, the integral in eq. (4.18) is well-defined and finite. As already described in sec. 4.2, the series expansion can be recovered easily from the integral expression in eq. (4.18). For this purpose, one can expand $\mathcal{P}_\zeta^{(0)}(e^{-\bar\zeta}k)$, as given in eq. (4.56), and make use of the moments for the Gaussian probability distribution (see eqs. (4.16) and (4.17)). Derivatives of the power spectrum (4.56) w.r.t. $\ln k$ can be expressed in terms of the spectral index $n_\zeta - 1 = -\alpha(\alpha+2)/\varphi^2$ and the model parameter α :

$$A_l = \frac{1}{\mathcal{P}_\zeta^{(0)}}\frac{d^l\mathcal{P}_\zeta^{(0)}}{d(\ln k)^l} = \left(\frac{n_\zeta - 1}{\frac{\alpha}{2}+1}\right)^l \prod_{i=1}^{l}(\frac{\alpha}{2} + 2 - i) \quad . \tag{4.58}$$

Hence, the series expansion is given by

$$\mathcal{P}_\zeta(k) = \mathcal{P}_\zeta^{(0)}(k)\left[1 + \sum_{n=1}^{\infty}\frac{(2n-1)!!}{(2n)!}\, A_{2n}\, \left(\sigma_\zeta^2\right)^n\right] \quad . \tag{4.59}$$

In the last part of this section, we discuss the question of convergence of the series expansion returning to the general case (see also [80]). The series expansion in eq. (4.16) was

$$\mathcal{P}_\zeta(k) = \mathcal{P}_\zeta^{(0)}(k)\left[1 + \sum_{n=1}^{\infty}\frac{\langle\,\bar\zeta^{2n}\,\rangle}{(2n)!}\,\frac{1}{\mathcal{P}_\zeta^{(0)}(k)}\,\frac{d^{2n}\,\mathcal{P}_\zeta^{(0)}(k)}{d(\ln k)^{2n}}\right] \quad , \tag{4.60}$$

and we have parametrically $\langle\,\bar\zeta^{2n}\,\rangle \sim \langle\,\bar\zeta^2\,\rangle^n$. Since $\ln k' = \ln k - \bar\zeta$, this is similar to a Taylor expansion of the power spectrum in $\ln k$ around the scale k. At every order in the

expansion, corrections consist of two counteracting contributions. On the one hand, there is the factor $\langle\, \bar{\zeta}^2 \,\rangle^n$, with

$$\langle\, \bar{\zeta}^2 \,\rangle = \int_{1/L}^{k} \frac{dq}{q}\, \mathcal{P}_\zeta^{(0)}(q) \quad , \tag{4.61}$$

that involves a log-enhancement (even though it is suppressed by the smallness of the power spectrum). On the other hand, there are derivatives of the power spectrum that consist of slow-suppressed quantities and to which we will refer as late-time suppression. The word 'late-time' indicates that derivatives of the power spectrum in eq. (4.60), i.e. the slow-suppressed quantities, are evaluated at the scale k. By contrast, the quantity $\langle\, \bar{\zeta}^2 \,\rangle$ receives contributions from all modes in the range from $1/L$ to the scale k. Convergence of the series expansion depends on the ability of the late-time suppression to compensate the log-enhancement due to $\langle\, \bar{\zeta}^2 \,\rangle$.

We will perform an order of magnitude analysis and, hence, we do not distinguish between quantities that are of the same order in slow-roll, like the slow-roll parameters ϵ and η. Instead, we generically characterize the slow-roll suppression by an appropriate power of ϵ. A derivative $d/d(\ln k)$ acting on $\mathcal{P}_\zeta^{(0)}$ precisely corresponds to one such power of ϵ. Hence, the late-time suppression is given by

$$\frac{1}{\mathcal{P}_\zeta^{(0)}(k)} \frac{d^{2n}\, \mathcal{P}_\zeta^{(0)}(k)}{d(\ln k)^{2n}} \sim \epsilon^{2n}(k) \quad . \tag{4.62}$$

Therefore, in our order of magnitude analysis, eq. (4.60) can be written as

$$\frac{\mathcal{P}_\zeta(k)}{\mathcal{P}_\zeta^{(0)}(k)} - 1 \sim \sum_{n=1}^{\infty} \left(\epsilon^2(k) \langle\, \bar{\zeta}^2 \,\rangle\right)^n \quad , \tag{4.63}$$

and the convergence of the series expansion requires $\epsilon^2 \langle\, \bar{\zeta}^2 \,\rangle < 1$.

Let us first consider a weakly scale-dependent power spectrum. Here, 'weakly scale-dependent' means that the power spectrum $\mathcal{P}_\zeta^{(0)}$ has only a very mild scale-dependence on the complete range from $1/L$ to k such that eq. (4.61) essentially yields

$$\langle\, \bar{\zeta}^2 \,\rangle = \mathcal{P}_\zeta^{(0)}\ \ln(kL) \sim \frac{H^2}{\epsilon}\ \ln(kL) \quad . \tag{4.64}$$

The logarithm is given by the number of observed e-foldings $N \simeq Ht$. Therefore, it remains to verify the relation

$$\epsilon^2 \langle\, \bar{\zeta}^2 \,\rangle \sim \epsilon\, H^3 t < 1 \quad . \tag{4.65}$$

As shown by [131, 132], the requirement of being in a non-eternally inflating phase constrains the time to obey $t < R\,S \sim H^{-3}$, where R and S are deSitter radius and entropy, respectively. Hence, the criterium for convergence reduces to $\epsilon < 1$, which is fulfilled by construction in slow-roll inflationary models. Therefore, under the assumption of a weakly scale-dependent power spectrum, the series is always converging. However, this is not surprising. The assumption of a 'weakly scale-dependent' power spectrum can be made mathematically more precise by demanding that the scale-dependence of $\mathcal{P}_\zeta^{(0)}$ is negligible in the integral in eq. (4.61) (such that $\langle\, \bar{\zeta}^2 \,\rangle = \mathcal{P}_\zeta^{(0)} \ln(kL)$). This yields

$$\frac{1}{\mathcal{P}_\zeta^{(0)}(k)} \frac{d^n \mathcal{P}_\zeta^{(0)}}{d(\ln k)^n}\bigg|_k [\,\ln(kL)\,]^n \ll 1 \qquad n > 0 \quad , \tag{4.66}$$

from which we could have concluded the convergence of the series in eq. (4.60) directly.

In spite of all that was said above, convergence breaks down for the model of chaotic inflation characterized by the power spectrum (4.56) (see also [80]). The integration in the expression of $\langle\, \bar{\zeta}^2 \,\rangle$ in this model needs to be performed over several orders of magnitude in the scalar background field φ. Therefore the slow-roll parameter $\epsilon \sim 1/\varphi^2$ is changing over several orders of magnitude. This clearly violates the approximation of a weak scale-dependence. Consequently, convergence is not obvious in this model and an investigation of the convergence behavior requires a more precise evaluation of $\langle\, \bar{\zeta}^2 \,\rangle$. Indeed, $\langle\, \bar{\zeta}^2 \,\rangle \sim \int (H^2/\epsilon)\, dq/q$ is completely dominated by contributions at very early times t_i. Hence, the expansion parameter $\langle\, \bar{\zeta}^2 \,\rangle$ is much larger than $\mathcal{P}_\zeta^{(0)}(k) \ln(kL)$. By contrast, the coefficients in eq. (4.60), i.e. the late-time suppression, consist of slow-roll parameters which are large compared to those at early times t_i. Hence, the late-time suppression cannot compensate the enhancement at early times leading to a breakdown of convergence.

In principle, this effect is also present for tensor corrections, though less severe since the power spectrum of tensor modes is not enhanced by $1/\epsilon$. Therefore, in this model the breakdown of convergence due to scalar contributions occurs first. This observation is also in agreement with the findings in [80], showing that the effect of scalars dominates.

We note that a breakdown of convergence implies that one cannot trust conventional perturbation theory. However, this only applies to the conventionally defined power spectrum at sufficiently large L. In our philosophy, one should instead consider higher-order corrections to IR-safe quantities like the power spectrum $\mathcal{P}_\zeta^{(0)}(k)$ defined in eq. (4.6). We know that the leading-order corrections to this object will not be log-enhanced. While we have not shown this in the present paper, we expect that also higher-order corrections will benefit from our IR-safe definition and hence that conventional QFT perturbation theory, based on the smallness of ζ and of slow-roll parameters, will be reliable.

4.5 Three-point function and the bispectrum

The bispectrum accounts for the simplest contribution to non-Gaussianity. Starting from the three-point function in momentum space, one extracts the *bispectrum* from its connected part:

$$\langle \zeta_{\vec{k_1}} \zeta_{\vec{k_2}} \zeta_{\vec{k_3}} \rangle \equiv (2\pi)^3 \delta^{(3)}(\vec{k}_1 + \vec{k}_2 + \vec{k}_3)\ B_\zeta(\vec{k}_1, \vec{k}_2) \qquad . \tag{4.67}$$

In this section, for definiteness we focus on non-Gaussianity of local form (see [46] for a recent review) [6]. The corresponding bispectrum is well-described by

$$B_\zeta(\vec{k}_1, \vec{k}_2) \;=\; \frac{6}{5} f_{\rm NL}(\vec{k}_1, \vec{k}_2)\ [P_\zeta(k_1) P_\zeta(k_2) + perms] \quad , \tag{4.68}$$

where $f_{\rm NL}$ is a slowly-varying function and we have introduced the uncurly power spectrum $P_\zeta(k) = 2\pi^2\, \mathcal{P}_\zeta(k)/k^3$. Here and henceforth, we indicate with *perms* all non-trivial cyclic permutations of $\vec{k}_1, \vec{k}_2$ and $\vec{k}_3 = -(\vec{k}_1 + \vec{k}_2)$. The dependence of $P_\zeta(k)$ on the long-wavelength background modes is characterized

$$P_\zeta(k) \;=\; \left\langle e^{-3\bar{\zeta}}\ P_\zeta^{(0)}\,(k') \right\rangle \quad . \tag{4.69}$$

[6] Other forms of non-Gaussianity can also be described with techniques similar to the ones we are are going to develop.

With the formalism of sec. 4.2 for higher correlation functions, we may immediately write down $f_{\rm NL}$ including long-wavelength corrections:

$$\begin{aligned} f_{\rm NL} &= \frac{5}{6}\frac{B_\zeta(\vec{k}_1,\vec{k}_2)}{[P_\zeta(k_1)P_\zeta(k_2)+perms]} \\ &= \frac{5}{6}\frac{\langle\ e^{-6\bar{\zeta}}\ B_\zeta^{(0)}(\vec{k}_1',\vec{k}_2')\ \rangle}{\langle\ e^{-3\bar{\zeta}}\ P_\zeta^{(0)}(k_1')\,\rangle\langle\ e^{-3\bar{\zeta}}\ P_\zeta^{(0)}(k_2')\,\rangle + perms} \quad . \end{aligned} \tag{4.70}$$

The remaining task is to evaluate (4.70). This requires knowledge on the tree-level bispectrum $B_\zeta^{(0)}$, which is model dependent.

As an illustrative example, we consider the form

$$B_\zeta^{(0)} = \frac{6}{5}\left[P_\zeta^{(0)}(k_1)P_\zeta^{(0)}(k_2)\ f_\zeta(k_3)+perms\right] \quad . \tag{4.71}$$

This tree-level bispectrum is motivated by a curvature perturbation which is given by a Gaussian part, ζ^G, plus $f_\zeta(k)$ times the Gaussian part squared, i.e.

$$\zeta_{\vec{k}} = \zeta^G_{\vec{k}} + f_\zeta(k)\left(\zeta^G\star\zeta^G\right)_{\vec{k}} \quad . \tag{4.72}$$

Here, the operator $\star$ denotes a convolution. In concrete examples, f_ζ depends on the scales k only by means of the dependence on times of horizon exit for each mode [40, 65]. Note that the tree-level bispectrum (4.71) has a slightly different scale-dependence than eq. (4.68). They only match for the popular assumption of f_ζ being scale-invariant or in the squeezed limit, where one scale is much smaller than the others (say $k_1 \ll k_2, k_3$). Indeed, one has $f_{\rm NL}^{(0)} = f_\zeta$ in these cases.

We stress that the bispectrum (4.71) neglects the presence of intrinsic non-Gaussianity in the second order scalar field fluctuations. To include this contribution, one has to apply the bispectrum given by Maldacena [22]. In order to keep equations simple, we will neglect this presence of intrinsic non-Gaussianity and apply eq. (4.71).

Note that the primary field of validity of eq. (4.71) is in multi-field, e.g. curvaton-type, models with observable non-Gaussianity. In addition, it arises in the squeezed limit of single field slow-roll inflation. In that case, our modified δN-formalism, presented in section 4.3, reproduces the correct result for $f_{\rm NL}^{(0)}$, i.e. $f_{\rm NL}^{(0)} = 5/12\ (1-n_\zeta)$ (see appendix 4.7.2). This agreement shows that, contrary to the conventional δN-formalism, our modified version of δN provides correct results also for the 3-point function in the squeezed limit. Consequently, the following calculation is correct in the squeezed limit, even though we made the simplifying assumption of negligible intrinsic non-Gaussianity.

Proceeding as we did for the power spectrum, we perform a slow-roll expansion for the quantities inside the averages in eq. (4.70), focussing on the non-vanishing contributions

at leading order in slow-roll. After some calculation, this yields

$$f_{\rm NL} = f_{\rm NL}^{(0)} \left[1 + \frac{\Omega(\vec{k}_1,\vec{k}_2,\vec{k}_3)\; P_\zeta^{(0)}(k_1)\, P_\zeta^{(0)}(k_2)\, f_\zeta(k_3) + perms}{P_\zeta^{(0)}(k_1)\, P_\zeta^{(0)}(k_2) f_\zeta(k_3) + perms} \right] \tag{4.73}$$

$$= f_{\rm NL}^{(0)} \left[1 + \frac{\Omega(\vec{k}_1,\vec{k}_2,\vec{k}_3)\; k_3^3 + \Omega(\vec{k}_3,\vec{k}_1,\vec{k}_2)\; k_2^3 + \Omega(\vec{k}_2,\vec{k}_3,\vec{k}_1)\; k_1^3}{k_1^3+k_2^3+k_3^3} \right] \tag{4.74}$$

$$f_{\rm NL}^{(0)} = \frac{5}{6} \frac{B_\zeta^{(0)}(\vec{k}_1,\vec{k}_2)}{P_\zeta^{(0)}(k_1) P_\zeta^{(0)}(k_2) + perms} \tag{4.75}$$

$$\begin{aligned}
\Omega(\vec{k}_1,\vec{k}_2,\vec{k}_3) = {} & \frac{3}{20} \langle \,\mathrm{tr}\,\bar{\gamma}^2 \,\rangle \left[3(\hat{k}_1\cdot\hat{k}_2)^2 - 1 \right] \\
& - \frac{1}{20} \langle \,\mathrm{tr}\,\bar{\gamma}^2 \,\rangle \left\{ 2\left[3(\hat{k}_1\cdot\hat{k}_2)^2 - 1 \right] \frac{1}{\mathcal{P}_\zeta^{(0)}} \frac{d\mathcal{P}_\zeta^{(0)}}{d\ln k} + 3\left[(\hat{k}_1\cdot\hat{k}_3)^2 + (\hat{k}_2\cdot\hat{k}_3)^2 - 1 \right] \frac{1}{f_\zeta} \frac{d\, f_\zeta}{d\ln k} \right\} \\
& + \frac{\langle\, \bar{\zeta}^2 \,\rangle}{2} \left\{ \frac{1}{f_\zeta} \frac{d^2 f_\zeta}{d(\ln k)^2} + 2 \left(\frac{1}{\mathcal{P}_\zeta^{(0)}} \frac{d\mathcal{P}_\zeta^{(0)}}{d\ln k} \right)^2 + 4 \frac{1}{f_\zeta\, \mathcal{P}_\zeta^{(0)}} \frac{d\, f_\zeta}{d\ln k} \frac{d\mathcal{P}_\zeta^{(0)}}{d\ln k} \right\} \quad .
\end{aligned} \tag{4.76}$$

Here $\hat{k}_i \cdot \hat{k}_j$ corresponds to the cosine of the angle between the vectors $\vec{k}_i$ and $\vec{k}_j$. $\langle \,\mathrm{tr}\,\bar{\gamma}^2 \,\rangle$ and $\langle\, \bar{\zeta}^2 \,\rangle$ are defined as before. In the previous expression for Ω, the scale at which we evaluate $\mathcal{P}_\zeta^{(0)}$, f_ζ and their derivatives is any one of the k_i: the difference among these quantities evaluated at different scale is slow-roll suppressed with respect to the contributions we are examining. As a result, a cancellation of corrections originating from the numerator and the denominator in eq. (4.73) occurs. This removes terms containing second derivatives of the power spectrum. Moreover, it is sufficient to take into account the naive scaling $P_\zeta^{(0)}(k) \sim k^{-3}$ in eq. (4.73), leading to the simpler form in eq. (4.74). In eq. (4.75), we defined the leading order non-Gaussianity parameter $f_{\rm NL}^{(0)}$.

In some cases, it may be useful to perform an average over directions of the vectors. However, we note that the δ-function sets constraints on this averaging procedure. As an example, we focus on the particular case of squeezed configurations, i.e. $k_1 \ll k_2, k_3$. For these configurations, one of the permutation terms can be dropped and the δ-function requires $(\hat{k}_2\cdot\hat{k}_3)^2 = 1$. The pair of unit-vectors $\hat{k}_1, \hat{k}_2$ or $\hat{k}_1, \hat{k}_3$ is statistically independent. Hence, the directional averaging gives $(\hat{k}_1\cdot\hat{k}_2)^2 = (\hat{k}_1\cdot\hat{k}_3)^2 = 1/3$. Therefore, having performed the directional averaging, the expression for squeezed configurations reads

$$f_{\rm NL} = f_{\rm NL}^{(0)} \left[1 + \Omega(\vec{k}_1,\vec{k}_2,\vec{k}_3) \right] \tag{4.77}$$

$$\begin{aligned}
\Omega(\vec{k}_1,\vec{k}_2,\vec{k}_3) = {} & -\frac{1}{20} \langle \,\mathrm{tr}\,\bar{\gamma}^2 \,\rangle \frac{1}{f_\zeta} \frac{d\, f_\zeta}{d\ln k} \\
& + \frac{\langle\, \bar{\zeta}^2 \,\rangle}{2} \left\{ \frac{1}{f_\zeta} \frac{d^2 f_\zeta}{d(\ln k)^2} + 2 \left(\frac{1}{\mathcal{P}_\zeta^{(0)}} \frac{d\mathcal{P}_\zeta^{(0)}}{d\ln k} \right)^2 + 4 \frac{1}{f_\zeta\, \mathcal{P}_\zeta^{(0)}} \frac{d\, f_\zeta}{d\ln k} \frac{d\mathcal{P}_\zeta^{(0)}}{d\ln k} \right\} \quad .
\end{aligned} \tag{4.78}$$

We stress that under the directional averaging the first term on the right-hand side in eq. (4.76) vanishes. Indeed, we will see below that, keeping the directional information,

precisely this term turns out to be the leading order correction. Therefore, this example illustrates that such procedures have to be handled with care.

Neglecting tensor fluctuations, the special case of corrections to $f_{\rm NL}$ in squeezed configurations was also discussed in [80]. In this case, corrections are solely given by the last line in eq. (4.76), which reads

$$\Omega(\vec{k}_1,\vec{k}_2,\vec{k}_3) = \frac{\langle\,\bar{\zeta}^2\,\rangle}{2}\left\{\frac{1}{f_\zeta}\frac{d^2 f_\zeta}{d(\ln k)^2} + 2\left(\frac{1}{\mathcal{P}_\zeta^{(0)}}\frac{d\mathcal{P}_\zeta^{(0)}}{d\ln k}\right)^2 + 4\frac{1}{f_\zeta\,\mathcal{P}_\zeta^{(0)}}\frac{d\,f_\zeta}{d\ln k}\frac{d\mathcal{P}_\zeta^{(0)}}{d\ln k}\right\} \quad . \tag{4.79}$$

Our result basically agrees with the findings of [80]. In order to have complete agreement, one needs to take into account the runnings of $\mathcal{P}_\zeta^{(0)}$ and f_ζ in the calculation of the bispectrum in [80] (their eqs. (5.9)-(5.11)). Including this effect, their final formula for $f_{\rm NL}$, eq. (5.14), slightly changes. Like in our findings, the running of the power spectra from the denominator disappears since it cancels against corresponding terms from the numerator. The effect of the running of f_ζ appears precisely as the first term on the right-hand side of eq. (4.79). The second and third term on the right-hand side of eq. (4.79) are already present in eq. (5.14) in [80].

We now return to the general form of corrections to $f_{\rm NL}$, i.e. eqs. (4.73)-(4.76). Remarkably, we find that in single-field, slow-roll inflation tensors provide the dominant contribution in slow-roll, i.e. the first term on the RHS in eq. (4.76). This contribution results in a correction proportional to first order slow-roll parameters, while the others are of second order. Indeed, we observe that, at leading order in slow-roll, the dominant contribution is originating from the prefactor

$$\langle m(\hat{k}_1)m(\hat{k}_2)\rangle \;=\; 1 + \frac{3}{20}\,\langle {\rm tr}\bar{\gamma}^2\rangle\,\left[3(\hat{k}_1\cdot\hat{k}_2)^2 - 1\right] \qquad , \tag{4.80}$$

which multiplies the tree-level bispectrum. From this we find that the dominant log-enhanced contribution to $f_{\rm NL}$, in a slow-roll expansion, reads

$$f_{\rm NL} \;=\; f_{\rm NL}^{(0)}\,\left[1 + \frac{6r}{5}\,\mathcal{P}_\zeta^{(0)}\;\ln(kL)\;\frac{(3(\hat{k}_1\cdot\hat{k}_2)^2-1)\;k_3^3 + (3(\hat{k}_3\cdot\hat{k}_1)^2-1)\;k_2^3 + (3(\hat{k}_2\cdot\hat{k}_3)^2-1)\;k_1^3}{k_1^3+k_2^3+k_3^3}\right] \quad . \tag{4.81}$$

Interestingly, these log-enhanced contributions to $f_{\rm NL}$ do not depend on the tilt of the power spectrum, and so are also present for spectral index equal to one.

In conclusion, log-enhanced contributions to $f_{\rm NL}$ can be expressed in terms of observable quantities. Tensor contributions are proportional to first order slow-roll parameters, and are suppressed by the tree-level power spectrum. Very similar results hold for parameters associated to the trispectrum, $g_{\rm NL}$ and $\tau_{\rm NL}$. It is straightforward to obtain them proceeding exactly as done in this section.

Local non-Gaussianity in single field, slow-roll inflation turns out to be small. On the other hand, models, in which a second field takes part in the generation of curvature perturbations as in the curvaton scenario, can lead to large values of $f_{\rm NL}$ (see e.g. [30]). In the approximation in which only the curvaton field is responsible for curvature perturbations, the tree level bispectrum reads

$$B_\zeta^{(0)}(\vec{k}_1,\vec{k}_2) = f_\sigma(\vec{k}_1,\vec{k}_2)\;\left[\frac{2\pi^2}{k_1^3}\mathcal{P}_\sigma(k_1)\;\frac{2\pi^2}{k_2^3}\mathcal{P}_\sigma(k_2) + perms\right] \qquad , \tag{4.82}$$

where σ indicates the curvaton field. Our approach can be applied also to this case, although it requires additional work to calculate the contributions of long-wavelength scalar modes to inflationary observables, since more than one scalar field is present. We outline a method to do this in Appendix 4.7.2, but a more complete discussion of this issue is left for future work. In this case, enhancement effects associated with long-wavelength modes could turn out to be more important than the ones discussed so far.

4.6 Discussion

We have considered IR effects associated with backreaction of long-wavelength scalar and tensor modes in inflationary backgrounds. We proposed an infrared-safe definition of correlation functions involving curvature fluctuations, with no sensitivity on long-wavelength contributions. The essential idea was to make use of the proper invariant distance on the reheating surface where the curvature perturbation is evaluated. By using the invariant distance, one automatically absorbs longer wavelength modes in the background and obtains n-point functions for the curvature perturbation that are free from IR contributions associated with long-wavelength modes. We showed how to re-interpret our results in terms of conventionally defined n-point functions. This allowed us to provide closed expressions for the latter that manifestly exhibit the dependence on long-wavelength modes. In our approach, IR corrections automatically emerge in a resummed, all-orders form. We then applied our approach to the analysis of inflationary observables built from (conventionally defined) two- and three-point functions of the curvature perturbation. We showed how to compute the leading scalar and tensor IR effects on the power spectrum and on the bispectrum, in single field, slow-roll inflation. Our corrections to the power spectrum (both from long-wavelength scalar and tensor modes) and to $f_{\rm NL}$ (from long-wavelength scalar modes) agree (essentially) with Giddings and Sloth [80] (obtained by somewhat different methods). The advantage of our approach is that it directly provides resummed, all-orders expressions. We extend [80] by tensor corrections to $f_{\rm NL}$. This is, in fact, the dominant piece! We also explicitly computed, in a specific inflationary model, the complete, all-orders expression for scalar long-wavelength contributions to inflationary observables. Furthermore, we analyzed the question of convergence of IR corrections. Using entropy bounds given in [131, 132], we found that for a weak scale-dependence the convergence of the series of IR corrections is guaranteed. However, despite the existence of these entropy bounds and the fulfillment of slow-roll conditions, the convergence of the IR-correction series may break down if the scale-dependence is not sufficiently weak.

Summarizing, we have provided a simple formalism to calculate and investigate inflationary IR corrections. Maybe more importantly, we have provided simple definitions of IR-safe correlation functions which make it possible to avoid IR enhancement altogether.

We have also shown that in all cases, where the δN-formalism is applicable, our results can be equivalently obtained in terms of a suitable generalization of the δN-formalism, extending the discussion of chapter 3 (see also [64]). In the present work, we included the effects of graviton long-wavelength modes, and we explained how to calculate IR contributions to arbitrary n-point functions involving curvature perturbations.

A natural question is how to extend our results to the case in which more than one field plays an active role in generating the curvature perturbations. In this case, IR effects might play a role more important than the one for single field inflation. We outlined in an Appendix a method to treat this problem, but we leave a more complete discussion for future work.

4.7 Appendices

4.7.1 Comparison of $\mathcal{P}_\zeta$ and $\mathcal{P}_\zeta^{(0)}$

The definitions of the IR-sensitive power spectrum $\mathcal{P}_\zeta$ and the IR-safe power spectrum $\mathcal{P}_\zeta^{(0)}$ are

$$\mathcal{P}_\zeta(k) = \frac{k^3}{2\pi^2}\int d^3y\; e^{-i\vec{k}\vec{y}}\,\langle\,\zeta(\vec{x})\;\zeta(\vec{x}+\vec{y})\,\rangle \tag{4.83}$$

$$\mathcal{P}_\zeta^{(0)}(k) = \frac{k^3}{2\pi^2}\int d^3z\; e^{-i\vec{k}\vec{z}}\,\langle\,\zeta(\vec{x})\;\zeta(\vec{x}+e^{-\bar{\zeta}}\,e^{-\bar{\gamma}/2}\,\vec{z})\,\rangle \qquad . \tag{4.84}$$

Here, $\vec{z}$ and $\vec{y}$ are related by $z^i = e^{\bar{\zeta}}\left(e^{\bar{\gamma}/2}\right)_{ij}\,y^j$. Comparing the two yields

$$\mathcal{P}_\zeta(k) = \left\langle\; \frac{k^3}{2\pi^2}\int d^3y\; e^{-i\vec{k}\vec{y}}\,\zeta(\vec{x})\;\zeta(\vec{x}+\vec{y})\;\right\rangle \tag{4.85}$$

$$= \left\langle\; \frac{k^3}{2\pi^2}\int d^3y\; e^{-i\vec{k}\vec{y}}\,\zeta(\vec{x})\;\zeta(\vec{x}+e^{-\bar{\zeta}}e^{-\bar{\gamma}/2}(e^{\bar{\zeta}}e^{\bar{\gamma}/2}\vec{y})\;)\;\right\rangle \tag{4.86}$$

$$= \left\langle\; \frac{k^3}{2\pi^2}\,e^{-3\bar{\zeta}}\int d^3z\;\exp\{-i(e^{-\bar{\zeta}}e^{-\bar{\gamma}/2}\vec{k})\vec{z}\}\;\;\zeta(\vec{x})\;\zeta(\vec{x}+e^{-\bar{\zeta}}e^{-\bar{\gamma}/2}\vec{z})\;\right\rangle \tag{4.87}$$

$$= \left\langle\; \left[\left(e^{-\bar{\gamma}}\right)_{ij}\hat{k}_i\hat{k}_j\right]^{-3/2}\;\mathcal{P}_\zeta^{(0)}\left(e^{-\bar{\zeta}}e^{-\bar{\gamma}/2}\vec{k}\right)\right\rangle \qquad . \tag{4.88}$$

In the first line, we included the integral and prefactors in the average. Note that this does not affect the averaging process over pairs of points separated by the coordinate vector $\vec{y}$. From the second to the third line, we performed a coordinate transformation of the integration variable from y to z. Since the determinant of $e^{\bar{\gamma}}$ is one, tensor fluctuations do not effect this transformation. Therefore, only scalar fluctuations appear as a prefactor in the third line. Consequently, we need to add tensor fluctuations by hand in this prefactor, in order to express the third line in terms of the IR-safe power spectrum $\mathcal{P}_\zeta^{(0)}$. This results in the prefactor in the last line, which only consists of tensor fluctuations. In this last line, the vector $\hat{k}$ is a unit vector in $\vec{k}$-direction and the average is performed over the background quantities $\bar{\zeta}(\vec{x})$ and $\bar{\gamma}_{ij}(\vec{x})$.

4.7.2 Extension of δN-formalism

In this appendix, we discuss in more detail how our results can be understood in terms of a δN approach. In a previous paper [64], written in collaboration with Byrnes and Nurmi, we showed how a suitable extension of the δN-formalism allows for the computation of leading-log contributions to the power spectrum, due to scalar long-wavelength fluctuations. Here, we extend our work to include tensor modes and to compute log-enhanced corrections to non-Gaussianity parameters.

Let us start with single field inflation. For this purpose, we will adopt the same gauge as in section 4.3. By means of the δN-formalism, the curvature perturbation ζ can then be expressed in terms of the number of e-foldings evaluated on a background given by the scalar field φ and its perturbation $\delta\varphi$:

$$\zeta \;=\; N\left[\varphi+\delta\varphi\right] - \langle N\rangle \quad . \tag{4.89}$$

The previous expression admits an expansion in terms of scalar fluctuations

$$\zeta_{\vec{k}} \,=\, N_{\varphi}(k')\delta_{\vec{k}}\varphi(k',\bar{g}_{ab}) + \frac{1}{2}N_{\varphi\varphi}(k')\left[(\delta\varphi\star\delta\varphi)_{\vec{k}}\,(k',\bar{g}_{ab}) - \langle\delta\varphi\star\delta\varphi\rangle\right] + ... \quad , \tag{4.90}$$

where we use the notation of the main text, and the Gaussian, first-order scalar fluctuation $\delta_{\vec{k}}\varphi$ is given in eq. (4.34). The effect of long-wavelength modes is encoded in the shift of the time of horizon exit, and in the function m, contained in the expression of $\delta_{\vec{k}}\varphi$. Long-wavelength mode contributions are controlled by the averaged quantities $\bar{\zeta}$ and $\bar{\gamma}_{ij}$.

With the previous expression, we neglect intrinsic non-Gaussianity of $\delta_{\vec{k}}\varphi$. Hence, this formalism is only applicable in situations where this is negligible. However, this condition is fulfilled in several models, e.g. models in which non-Gaussianity of the local form can acquire sizeable values as in multiple field inflation or curvaton-like mechanisms [133]. In light of these models, it is worthwhile to develop formalisms that neglect the presence of second order fluctuations.

Using the previous formula, it is straightforward to compute n-point functions of curvature perturbations, and compute leading log-enhanced corrections to inflationary observables. It is important to stress that, due to the choice of a gauge with $\delta_{\vec{q}}\varphi = 0$ for $q \ll k$, convolutions appearing in the second term of eq. (4.90) do not involve integration over all the modes, but have a lower cut-off slightly below the scale k. This implies that convolutions, when appearing in n-point functions, do not provide further log-enhanced contributions with respect to the ones associated with long-wavelength background modes. All the IR dependence is then contained in the quantities $\bar{\zeta}$ and $\bar{\gamma}$.

As an example, let us work out explicitly the expression for the three-point function in the squeezed limit, including the effects of long-wavelength modes, using eq. (4.90). Our method is similar to [81]. The second term on the right-hand side in eq. (4.90) is irrelevant for squeezed configurations and will be neglected. The contribution to the bispectrum is

$$\begin{aligned}\langle\,\zeta_{\vec{k}_1}\zeta_{\vec{k}_2}\zeta_{\vec{k}_3}\,\rangle = \frac{1}{\sqrt{8k_1^3k_2^3k_3^3}}\;\langle\Big[m^{\frac{1}{2}}(\hat{k}_1)\,(N_{\varphi}H)(k_1')\;\hat{a}_{\vec{k}_1}\Big]\;\Big[m^{\frac{1}{2}}(\hat{k}_2)\,(N_{\varphi}H)(k_2')\;\hat{a}_{\vec{k}_2}\Big]\\ \Big[m^{\frac{1}{2}}(\hat{k}_3)\,(N_{\varphi}H)(k_3')\;\hat{a}_{\vec{k}_3}\Big]\rangle\;\;.\end{aligned} \tag{4.91}$$

In the limit in which $k_1 \ll k_2 \simeq k_3$, the size of the vector k_1 is comparable to the size of the long-wavelength modes relative to the vectors k_2 and k_3. The latter are included in the shift of the time of horizon exit $t_{k_2'}$ and on $m(\hat{k}_2)$, respectively, $t_{k_3'}$ and $m(\hat{k}_3)$. Taking into account this fact, and using Wick's theorem, we can write in this limit the following non-vanishing contribution

$$\langle\,\zeta_{\vec{k}_1}\zeta_{\vec{k}_2}\zeta_{\vec{k}_3}\,\rangle = (2\pi)^3\delta^{(3)}(\vec{k}_2+\vec{k}_3)\;\frac{1}{2k_2^3\sqrt{2k_1^3}}\;\langle\,\Big[m^{\frac{1}{2}}(\hat{k}_1)(N_{\varphi}H)(k_1')\;\hat{a}_{\vec{k}_1}\Big]\;\Big[m(\hat{k}_2)\,(N_{\varphi}H)^2\,(k_2')\Big]\,\rangle\;\;. \tag{4.92}$$

Since $k_1 \ll k_2$, the only possibility to contract $\hat{a}_{\vec{k}_1}$ is the background contribution originating from $(N_{\varphi}H)^2(k_2')$. By expanding the latter and by means of the definition of $\bar{\zeta}$, this contraction yields

$$\langle\,\hat{a}_{\vec{k}_1}\,(N_{\varphi}H)^2(k_2')\,\rangle = -\langle\,\hat{a}_{\vec{k}_1}\,\bar{\zeta}\,\rangle\;\;\frac{d\,(N_{\varphi}H)^2}{d\ln k}\bigg|_{k_2'} = -m^{\frac{1}{2}}(\hat{k}_1)\,\frac{(N_{\varphi}H)(k_1')}{\sqrt{2k_1^3}}\;\;\frac{d\,(N_{\varphi}H)^2}{d\ln k}\bigg|_{k_2'}\;\;. \tag{4.93}$$

Therefore, we find for the bispectrum:

$$B_\zeta(\vec{k}_1,\vec{k}_2) = \frac{-1}{4(k_1k_2)^3}\,\langle\left[m(\hat{k}_1)(N_\varphi H)^2(k_1')\right]\left[m(\hat{k}_2)(N_\varphi H)^2(k_2')\right]\left.\frac{d\ln\mathcal{P}_\zeta^{(0)}}{d\ln k}\right|_{k_2'}\rangle \quad . \tag{4.94}$$

At leading order, we neglect the contribution from the background ($k_i' \to k_i$ and $m(\hat{k}_i) = 1$). This provides the following tree-level result for the non-Gaussianity parameter

$$f_{\rm NL}^{(0)}(k) = -\frac{5}{12}\left.\frac{d\ln\mathcal{P}_\zeta^{(0)}}{d\ln k}\right|_k = \frac{5}{12}(1-n_\zeta(k)) \quad , \tag{4.95}$$

that is Maldacena's consistency relation [22, 123]. Hence, the complete form for $f_{\rm NL}$, obtained from formula (4.94), can be expressed through $f_{\rm NL}^{(0)}$, giving

$$f_{\rm NL} = \frac{\langle\, m(\hat{k}_1)\mathcal{P}_\zeta^{(0)}(k_1')\;\; m(\hat{k}_2)\mathcal{P}_\zeta^{(0)}(k_2')\;\; f_{\rm NL}^{(0)}(k_2')\,\rangle}{\langle\, m(\hat{k}_1)\mathcal{P}_\zeta^{(0)}(k_1')\,\rangle\,\langle\, m(\hat{k}_2)\mathcal{P}_\zeta^{(0)}(k_2')\,\rangle} \quad , \tag{4.96}$$

in agreement with formula (4.70) in the squeezed limit. We can then proceed as done in the main text to extract leading log-enhanced contributions.

Let us briefly discuss the case in which multiple scalar fields affect the curvature perturbation. The δN-formalism is very well suited to study this case, as discussed in the original paper by Sasaki and Stewart [25]. We adopt a gauge with vanishing scalar metric fluctuations, i.e. the long-wavelength modes of the scalar field are not vanishing. The curvature perturbation (that in the case of multiple fields is not generally conserved) can be expressed as an expansion in terms of all the scalar fields involved

$$\zeta_{\vec{k}}(t_f) \;=\; N_I\left[t_f,\{\varphi_0\}\right]\,\delta_{\vec{k}}\varphi^I\left[\{\varphi_0\}\right] + \frac{1}{2}N_{IJ}\left[t_f,\{\varphi_0\}\right]\,\left\{\left(\delta\varphi^I\star\delta\varphi^J\right)_{\vec{k}}\left[\{\varphi_0\}\right] - \langle\delta\varphi^I\star\delta\varphi^J\rangle\right\} + \cdots \quad , \tag{4.97}$$

where the capital latin indices of N denote derivatives w.r.t. the scalar fields and summation over repeated indices is understood. Here, $\{\varphi_0\}$ denotes the dependence on the homogeneous values φ_0^I of the scalar fields. As in Sasaki and Stewart, we have replaced the dependence on the time of horizon exit t_k of the various functions, with the value of homogeneous solutions of the scalar equations at t_k: $\varphi_0^I \equiv \varphi_0^I(t_k)$.

Then, the inclusion of the effects of scalar and tensor long-wavelength modes can be done as in the previous sections, although the procedure is a bit more laborious. We express a given function $\varphi^I(t,\vec{x})$, the solution of the field equations, as

$$\varphi^I(t,\vec{x}) \;=\; \varphi_0^I(t) + \delta\bar{\varphi}^I(t) + \delta\varphi^I(t,\vec{x}) \quad , \tag{4.98}$$

where $\delta\bar{\varphi}^I(t)$ is an average over long-wavelength modes, similar to the ones we performed in the main text. The effect of long-wavelength scalar fluctuations is to shift the values of φ_0^I, that appear in eq. (4.97), to $\varphi_0^I + \delta\bar{\varphi}^I$. In a sense, they play the same role of shifting the time of horizon exit, although with multiple fields there is not a one to one correspondence between time and values of the scalar solution. After passing to momentum space, the inclusion of long-wavelength scalar perturbations implies that the expansion in eq. (4.97) becomes

$$\begin{aligned}\zeta_{\vec{k}}(t_f) = {} & N_I\left[t_f,\{\varphi_0+\delta\bar{\varphi}\}\right]\,\delta_{\vec{k}}\varphi^I\left[\{\varphi_0+\delta\bar{\varphi}\}\right] \\ & + \frac{1}{2}N_{IJ}\left[t_f,\{\varphi_0+\delta\bar{\varphi}\}\right]\,\left\{\left(\delta\varphi^I\star\delta\varphi^J\right)_{\vec{k}}\left[\{\varphi_0+\delta\bar{\varphi}\}\right] - \langle\delta\varphi^I\star\delta\varphi^J\rangle\right\} + \cdots\end{aligned} \tag{4.99}$$

to take into account the shifts of the homogeneous solution of the scalar fields. The inclusion of tensor long-wavelength contribution, on the other hand, is very simple: since correlations between tensor and scalar modes vanish, the effect of tensors is precisely identical to that discussed in the previous sections. It can be taken into account with a proper redefinition of the time of horizon exit of a given mode $t_k \to t_{k'}$. One can then repeat in this case the very same steps that we took in the previous sections, generalizing our results to multiple fields. This will be done in future work, where we will also discuss in this context the possibility of having large non-Gaussianity from loop effects [83], with sizeable scale-dependence [52, 82].

Chapter 5

Scale-dependent non-Gaussianity probes inflationary physics

The content of this chapter is published in [65].

In chapter 5, we calculate the scale dependence of the bispectrum and trispectrum in (quasi) local models of non-Gaussian primordial density perturbations, and characterize this scale dependence in terms of new observable parameters. They can help to discriminate between models of inflation, since they are sensitive to properties of the inflationary physics that are not probed by the standard observables. We find consistency relations between these parameters in certain classes of models. We apply our results to a scenario of modulated reheating, showing that the scale dependence of non-Gaussianity can be significant. We also discuss the scale dependence of the bispectrum and trispectrum, in cases where one varies the shape as well as the overall scale of the figure under consideration. We conclude this chapter providing a formulation of the curvature perturbation in real space, which generalises the standard local form by dropping the assumption that $f_{\rm NL}$ and $g_{\rm NL}$ are constants.

5.1 Introduction

Inflation is the simplest framework which explains the origin of the observed power spectrum of temperature fluctuations in the cosmic microwave background [18]. It is now widely accepted that non-Gaussianity is a powerful probe to discriminate between the many currently viable inflationary models [17,44–49]. It is usually parameterized in terms of a single constant parameter, $f_{\rm NL}$, corresponding to the amplitude of the bispectrum normalized to the square of the power spectrum of primordial curvature fluctuations [21,50]. More recently it has become common to further characterize local non-Gaussianity including the two non-linearity parameters associated to the trispectrum, called $g_{\rm NL}$ and $\tau_{\rm NL}$, again treating them as constants [84]. However, it has been recently pointed out, both from theoretical [40, 51–53] and observational viewpoints [54], that $f_{\rm NL}$ is not necessarily constant. We show the same holds true for $g_{\rm NL}$ and $\tau_{\rm NL}$. As happens with the power spectrum and the spectral index, they are characterized by a scale dependence, that which denote respectively with $n_{f_{\rm NL}}$, $n_{g_{\rm NL}}$ and $n_{\tau_{\rm NL}}$. For example, if $f_{\rm NL}$ is large and positive on large scale structure scales [134–137], but has a smaller value on the largest CMB scales then this would require that $f_{\rm NL}$ is scale dependent. Any scale dependence of the non-linearity parameters provides a new and potentially powerful observational probe

of inflationary physics.

In this chapter, we discuss a new approach to study the scale dependence of the non-linearity parameters, based on the δN-formalism [25, 37, 38]. This allows us to obtain an expression for the curvature perturbation that generalizes the local Ansatz introduced in [21, 50], and that contains the aforementioned scale-dependent parameters. For the single field case, the curvature perturbation can be schematically written as

$$\zeta_{\vec{k}} = \zeta^{\rm G}_{\vec{k}} + \frac{3}{5} f^{\rm p}_{\rm NL} \left(1 + n_{f_{\rm NL}} \ln k\right) \left(\zeta^{\rm G} \star \zeta^{\rm G}\right)_{\vec{k}} + \frac{9}{25} g^{\rm p}_{\rm NL} \left(1 + n_{g_{\rm NL}} \ln k\right) \left(\zeta^{\rm G} \star \zeta^{\rm G} \star \zeta^{\rm G}\right)_{\vec{k}} ,$$

where $\zeta^{\rm G}_{\vec{k}}$ is a Gaussian variable, and $f^{\rm p}_{\rm NL}$ and $g^{\rm p}_{\rm NL}$ are constants. Our approach allows us to directly calculate $n_{f_{\rm NL}}$, $n_{g_{\rm NL}}$ and $n_{\tau_{\rm NL}}$ in models with an arbitrary inflationary potential and an arbitrary number of fields, assuming slow-roll inflation. We also assume the field perturbations are Gaussian at Hubble exit. Our results depend only on the slow-roll parameters evaluated at Hubble exit, and on the derivatives of N, the e-folding number. In particular, we find that $n_{f_{\rm NL}}$ and $n_{g_{\rm NL}}$ are sensitive to third and fourth derivatives of the potential along the directions in field space that are responsible for generating non-Gaussianities. These do not in general coincide with the adiabatic direction (during inflation) and such features cannot therefore be probed by only studying the spectral index and its running [138]. In the case that a single field generates the curvature perturbation there is a consistency relation between $n_{f_{\rm NL}}$ and $n_{\tau_{\rm NL}}$ which is the derivative of the consistency relation between $f_{\rm NL}$ and $\tau_{\rm NL}$. We explicitly show how this consistency relation is violated in multiple field models.

In the framework of slow-roll inflation, there are various ways to generate large non-Gaussianity, in models in which more than one field play a role during the inflationary process. This is the case of multiple field inflation [87, 139–147], in which two or more fields contribute to the curvature perturbations. But there are also approaches in which, although more than one field is light during inflation, only one of them contributes significantly to the curvature perturbations (the most studied examples are the curvaton [148–164] and modulated reheating [165–167] [168] scenarios). In this work, we apply our general findings to this last class of models. We consider set-ups in which an isocurvature field remains subdominant during inflation (as required in order to have an observable level of non-Gaussianity [169]), but represents the main source of curvature fluctuations after inflation ends. In this case, neither the spectral index of the power spectrum of curvature perturbations, nor its running are sensitive to the third and fourth derivative of the potential of the subdominant field. Hence the scale dependence of non-Gaussian parameters provide a unique opportunity to probe self interactions in these scenarios. As an example, in the modulated reheating scenario, it is possible for any of the non-Gaussian parameters to be large. We show that if the modulaton field has self interactions, for example a quartic potential, then all of $f_{\rm NL}$, $n_{f_{\rm NL}}$, $g_{\rm NL}$ and $n_{g_{\rm NL}}$ can be large and provide novel information about the mechanism which generates curvature perturbations. We will also consider mixed scenarios in which the inflaton perturbations are not neglected [170–173]. We note that the scale dependence of equilateral type non-Gaussianity is also of theoretical and observational interest [174–177].

We have previously shown [40] that provided one scales all three sides of the bispectrum at the same rate then $n_{f_{\rm NL}}$ is a constant (and hence it is simplest to focus on an equilateral configuration). We show a similar result for the trispectrum parameters. Since it may be of interest to consider more general variations in which one changes the shape of the figure under consideration, we also consider this case. We find the combination of shape and

scale dependence which maximizes $n_{f_{\rm NL}}$ and show that it is never significantly larger than the standard result, in which one keeps the shape fixed. However we single out interesting limits in which there is no scale dependence, corresponding to squeezed figures.

While in most of the chapter we work in momentum space, in the last part we also discuss how to describe our results in coordinate space. We provide an expression for the curvature perturbations in real space, that generalizes the simplest local Ansatz [50], and that exhibits directly in coordinate space the effect of scale dependence of non-Gaussian parameters.

The plan of this chapter is as follows: In Sec. 5.2 we extend and simplify the results from our previous paper to give general results for the non-linearity parameters, including those which measure the trispectrum. In Sec. 5.3 we reduce the results to general single field models and derive a consistency relation. In Sec. 5.4 we consider simple one or two-field models in which one field, e.g. the curvaton, generates non-Gaussianity but we do not exclude the Gaussian perturbations from the inflaton. Many popular models in the literature fall into this class and the reader may choose to skip straight to this section where the results and notation are significantly simpler. As an explicit example we study modulated reheating. In Sec. 5.5 we consider in detail the scale dependence of the bispectrum and the trispectrum, and how this can be affected by the shape of the triangle or quadrilaterum. In Sec. 5.6 we consider how to generalize the coordinate space expression of the curvature perturbation to include scale dependence. Finally we discuss our results in Sec. 5.7.

5.2 General results

In this section, we discuss a new approach to analyze the scale dependence of quasi-local non-Gaussianity, by means of a suitable implementation of the δN-formalism. Using the δN-formalism [25, 37, 38], the curvature perturbation for a system of n scalar fields φ_a is given by the expression

$$\zeta(t_f,\vec{x}) = \sum_a N_a(t_f,t_i)\delta\varphi^a(t_i,\vec{x}) + \frac{1}{2}\sum_{ab} N_{ab}(t_f,t_i)\delta\varphi^a(t_i,\vec{x})\delta\varphi^b(t_i,\vec{x}) + \cdots \ , \qquad (5.1)$$

where t_f labels a uniform energy density hypersurface and t_i denotes a spatially flat hypersurface. The result is valid on super-horizon scales where spatial gradients can be neglected. In this work, we do not consider secondary effects on curvature perturbations arising from late-time physics (see [178] for a review), nor the effects of possible isocurvature modes during the late universe. The quantities N_a and N_{ab} denote derivatives of the number of e-foldings along the scalar fields. We choose t_i as a time soon after the horizon crossing of all the modes of interest. Written in momentum space, Eq. (5.1) reads

$$\zeta_{\vec{k}}(t_f) = \sum_a N_a(t_f,t_i)\delta\varphi^a_{\vec{k}}(t_i) + \frac{1}{2}\sum_{ab} N_{ab}(t_f,t_i)\left(\delta\varphi^a(t_i)\star\delta\varphi^b(t_i)\right)_{\vec{k}} + \cdots \ . \qquad (5.2)$$

Here $k < a(t_i)H(t_i)$, since we focus on super-horizon scales, and $\star$ denotes a convolution:

$$\left(\delta\varphi^a(t_i)\star\delta\varphi^b(t_i)\right)_{\vec{k}} \equiv \int \frac{d^3q}{(2\pi)^3}\ \delta\varphi^a_{\vec{q}}(t_i)\delta\varphi^b_{\vec{k}-\vec{q}}(t_i) \ . \qquad (5.3)$$

To analyze the statistical properties of the curvature perturbation it is useful to express the results in terms of scalar perturbations evaluated at horizon crossing $\delta\varphi^a_{\vec{k}}(t_k)$.

Assuming the fields φ_a obey slow roll dynamics during inflation and have canonical kinetic terms, $\delta\varphi^a_{\vec{k}}(t_k)$ are Gaussian up to slow roll corrections [22, 179]. These corrections are irrelevant in cases where the non-Gaussianities are large, $|f_{\rm NL}| \gg 1$ or $|g_{\rm NL}| \gg 1$. Therefore, in our analysis we take the fields $\delta\varphi^a_{\vec{k}}(t_k)$ to be Gaussian at horizon crossing, $k = a(t_k)H(t_k)$. In [40] the result (5.2) was expressed in terms of $\delta\varphi^a_{\vec{k}}(t_k)$ by setting $t_i \to t_k(k)$. This makes the coefficients $N_{ab...}$ implicitly dependent on k. In this work, we follow a different approach, choosing a fixed t_i for all observable k modes, and explicitly solving for the perturbations at t_i as a function of $\delta\varphi^a_{\vec{k}}(t_k)$. Besides being more transparent, this method allows us to easily write down explicit results for the scale-dependence of non-linearity parameters. The two approaches are compared in detail in Appendix 5.8.2.

We first note that, assuming slow roll, the evolution of super-horizon scale fluctuations $\delta\varphi^a(t,\vec{x})$ from some initial spatially flat hypersurface at $t_0 < t_i$ to the spatially flat hypersurface at t_i can be expressed in terms of the Taylor expansion

$$\delta\varphi^a(t_i,\vec{x}) = \sum_b \frac{\partial\varphi^a(t_i)}{\partial\varphi^b(t_0)}\delta\varphi^b(t_0,\vec{x}) + \frac{1}{2}\sum_{bc}\frac{\partial^2\varphi^a(t_i)}{\partial\varphi^b(t_0)\partial\varphi^c(t_0)}\delta\varphi^b(t_0,\vec{x})\delta\varphi^c(t_0,\vec{x}) + \cdots \ . \quad (5.4)$$

Here we have also assumed the fields have canonical kinetic terms, i.e. the metric in field space is flat. The result (5.4) follows directly from the application of the δN-formalism where any super-horizon region, labeled by $\vec{x}$, evolves as a separate FRW universe with its own initial conditions. Since we assume that slow roll conditions are satisfied, the initial conditions are set by the field values $\{\varphi^a(t_0)\}$ alone, i.e. any dependence on the field time derivatives can be neglected. Therefore,

$$\delta\varphi^a(t_i,\vec{x}) = \varphi^a(t_i)(\{\varphi^b(t_0) + \delta\varphi^b(t_0,\vec{x})\}) - \varphi^a(t_i)(\{\varphi^b(t_0)\}) \ , \quad (5.5)$$

where $\varphi^a(t_i)(...)$ denote FRW solutions with the initial conditions set at t_0. Eq. (5.4) is obtained by expanding this with respect to $\{\delta\varphi^b(t_0,\vec{x})\}$ while keeping fixed the number of e-foldings between t_0 and t_i. This corresponds to choosing t_0 and t_i as spatially flat hyper-surfaces, since it amounts to comparing different realizations of FRW universes that all undergo the same number of e-foldings between t_0 and t_i.

The coefficients in Eq. (5.4) can easily be computed by solving the slow roll equations of motion, $3H\dot{\varphi}_a = -V_a$. We find

$$\varphi^a(t_i) = \varphi^a(t_0) - \sqrt{2\epsilon_a}\ln(a_i/a_0) + \mathcal{O}\left(\epsilon^{3/2}\ln^2(a_i/a_0)\right) \ , \quad (5.6)$$

where the slow roll parameters are evaluated at t_0 and defined as usual: $\epsilon_a = (V_a/(3H^2))^2/2$ and $\eta_{ab} = V_{ab}/(3H^2)$ (with $M_{\rm P} \equiv 1$). In the following we neglect the slow-roll suppressed corrections $\mathcal{O}(\epsilon^{3/2}\ln^2(a_i/a_0))$, where $\mathcal{O}(\epsilon^{3/2})$ denotes terms involving powers of ϵ_a and η_{ab} up to 3/2. The validity of this approximation is discussed in more detail below and also in Appendix 5.8.1. Differentiating Eq. (5.6) once with respect to the initial field values, and keeping $\ln(a_i/a_0)$ fixed, we find

$$\frac{\partial\varphi^a(t_i)}{\partial\varphi^b(t_0)} = \delta_{ab} + \epsilon_{ab}\ln(a_i/a_0) \ , \quad (5.7)$$

where we have defined

$$\epsilon_{ab} \equiv 2\sqrt{\epsilon_a\epsilon_b} - \eta_{ab} \ . \quad (5.8)$$

The higher order derivatives in Eq. (5.6) can be computed in a similar way and the results are given in Appendix 5.8.1.

By substituting Eq. (5.4) into the coordinate space expression for the curvature perturbation (5.1), taking the Fourier transform and thereafter setting $t_0 = t_k$, we arrive at the result

$$\zeta_{\vec{k}} = \sum_a \zeta^{\mathrm{G},a}_{\vec{k}} + \sum_{ab} f_{ab}(k)(\zeta^{\mathrm{G},a} \star \zeta^{\mathrm{G},b})_{\vec{k}} + \sum_{abc} g_{abc}(k)(\zeta^{\mathrm{G},a} \star \zeta^{\mathrm{G},b} \star \zeta^{\mathrm{G},c})_{\vec{k}} + \cdots \,. \tag{5.9}$$

Here $\zeta^{\mathrm{G},a}_{\vec{k}}$ are Gaussian fields defined as

$$\zeta^{\mathrm{G},a}_{\vec{k}}(t_i, t_k) = \sum_b N_a \, \delta\varphi^b_{\vec{k}}(t_k) \left[\delta_{ab} + \epsilon_{ab} \ln \frac{a_i H_i}{k}\right] \theta(a_i H_i - k) \,. \tag{5.10}$$

The Gaussianity of this quantity follows from our assumption of the perturbations $\delta\varphi^a_{\vec{k}}(t_k)$ being Gaussian at the horizon crossing. For brevity, from now on we suppress the time arguments of the derivatives of N, denoting $N_{ab\ldots} \equiv N_{ab\ldots}(t_f, t_i)$. The theta function in Eq. (5.10) is included to constrain the convolutions to only include super-horizon scales, $k < a_i H_i$. The matrices $f_{ab}(k)$ and $g_{abc}(k)$ are given by

$$f_{ab}(k) = \frac{1}{2}\frac{N_{ab}}{N_a N_b} + \frac{1}{2}\sum_c \frac{N_c F^{(2)}_{cab}}{N_a N_b} \ln \frac{a_i H_i}{k}, \tag{5.11}$$

$$g_{abc}(k) = \frac{1}{6}\frac{N_{abc}}{N_a N_b N_c} + \frac{1}{6 N_a N_b N_c}\sum_d \left(3 N_{da} F^{(2)}_{dbc} + N_d F^{(3)}_{dabc}\right) \ln \frac{a_i H_i}{k} \,, \tag{5.12}$$

where $k < a_i H_i$ and $F^{(m)}_{ab_1\ldots b_m}$ denotes the k-independent part of the m:th order coefficient in Eq. (5.4). They are proportional to combinations of slow roll parameters and their explicit expressions are given in Appendix 5.8.1.

Our results are derived to first order in $\ln a_i H_i/k$. In Eqs. (5.11) and (5.12) the terms proportional to $\ln a_i H_i/k$ represent small corrections to the k-independent parts except in the cases where $f_{ab}(k_i)$ and $g_{abc}(k_i)$ are comparable to slow roll parameters or even smaller. Such components, however, do not generate observable non-Gaussianity and therefore do not play an important role in our discussion. For this reason, we can safely perform the expansion in $\ln a_i H_i/k$. Since the higher order terms arising in this expansion are further slow roll suppressed, and since we can choose t_i such that the logarithms never get larger than $\mathcal{O}(10)$ for the super-horizon modes in our observable universe, we can truncate the expansion at first order.

Instead of expanding in $\ln a_i H_i/k$, we can also choose one of our observable super-horizon modes as a pivot-scale, $k_{\mathrm{p}} < a_i H_i$, and expand Eqs. (5.11) and (5.12) around this point. To first order in $\ln(k/k_{\mathrm{p}})$ the results are given by

$$f_{ab}(k) = f_{ab}(k_{\mathrm{p}}) \left(1 + n_{f,ab} \ln \frac{k}{k_{\mathrm{p}}}\right) \,, \tag{5.13}$$

$$g_{abc}(k) = g_{abc}(k_{\mathrm{p}}) \left(1 + n_{g,abc} \ln \frac{k}{k_{\mathrm{p}}}\right) \,, \tag{5.14}$$

where we have defined[1]

$$n_{f,ab} \equiv \frac{d\ln|f_{ab}|}{d\ln k} = -\sum_c \frac{N_c F^{(2)}_{cab}}{N_{ab}} \,, \quad n_{g,abc} \equiv \frac{d\ln|g_{abc}|}{d\ln k} = -\sum_d \left(3\frac{N_{da}}{N_{abc}} F^{(2)}_{dbc} + \frac{N_d}{N_{abc}} F^{(3)}_{dabc}\right) \,. \tag{5.15}$$

[1]It is important to realise that $n_{f,ab}$ ($n_{g,abc}$) is only defined in the case where $f_{ab} \neq 0$ ($g_{abc} \neq 0$) in the limit $k \to a_i H_i$. If f_{ab} (g_{ab}) vanishes, it is convenient to define the derivative in Eq. (5.15) to be identically zero.

Provided that $n_{f,ab}$ and $n_{g,abc}$ are not much larger than $\mathcal{O}(0.01)$, truncating the above series at first order leads to an error of a few per cents at most. Neglecting slow roll corrections, we can write $f_{ab}(k_{\rm p}) = N_{ab}/(2N_aN_b)$ and $g_{abc}(k_{\rm p}) = N_{abc}/(6N_aN_bN_c)$. This precision suffices when treating the k-independent terms in our expressions, since we are only interested in computing scale-dependencies to leading order in slow roll. In what follows, we will therefore always write the constant terms to leading order precision in slow roll.

Finally, using Eqs. (5.13) and (5.14), we can express Eq. (5.9) as

$$\begin{aligned}\zeta_{\vec{k}} &= \sum_a \zeta^{{\rm G},a}_{\vec{k}} + \sum_{ab} f_{ab}(k_{\rm p})\left(1 + n_{f,ab}\ln\frac{k}{k_{\rm p}}\right)(\zeta^{{\rm G},a} \star \zeta^{{\rm G},b})_{\vec{k}} \\ &\quad + \sum_{abc} g_{abc}(k_{\rm p})\left(1 + n_{g,abc}\ln\frac{k}{k_{\rm p}}\right)(\zeta^{{\rm G},a} \star \zeta^{{\rm G},b} \star \zeta^{{\rm G},c})_{\vec{k}} + \cdots \ .\end{aligned} \tag{5.16}$$

This result is the starting point for our analysis of the scale-dependence of non-linearity parameters. Explicit expressions for $n_{f,ab}$ and $n_{g,abc}$ are given in Appendix 5.8.1 and the scale-dependency arising from the fields $\zeta^{{\rm G},a}_{\vec{k}}$ can be computed using standard methods. Therefore, using Eq. (5.16) we can explicitly compute the scale-dependencies of $f_{\rm NL}$, $g_{\rm NL}$ and $\tau_{\rm NL}$ for any model with slow roll dynamics during inflation.

5.2.1 Two point function and power spectrum

Here we re-derive some well-known results for the scale dependence of the spectrum of curvature perturbations; they will be useful in what follows for analyzing the scale-dependence of bispectrum and trispectrum. The two point function of the scalar field perturbations $\delta\varphi^a_{\vec{k}}(t_k)$ at horizon crossing is given by

$$\langle \delta\varphi^a_{\vec{k}_1}(t_k)\delta\varphi^b_{\vec{k}_2}(t_k)\rangle = (2\pi)^3\delta(\vec{k}_1+\vec{k}_2)\frac{2\pi^2}{k_1^3}\left(\frac{H(t_k(k_1))}{2\pi}\right)^2\left[\delta_{ab} + 2c\,(1-\delta_{ab})\,\epsilon_{ab}\right] \ , \tag{5.17}$$

where $c = 2 - \ln 2 - \gamma \simeq 0.73$ with γ being the Euler-Mascheroni constant. Both the diagonal $a = b$ and off-diagonal $a \neq b$ components are given to leading order in slow roll. Note that although the off-diagonal components are slow roll suppressed compared to the diagonal components, their scale dependence has no further suppression and therefore gives a contribution comparable to the scale-dependence of the diagonal components. Therefore, we need to retain the off-diagonal contributions in our analysis.

Using this together with Eqs. (5.10) and (5.16), we can express the power spectrum of ζ, defined by $\langle\zeta_{\vec{k}_1}\zeta_{\vec{k}_2}\rangle \equiv (2\pi)^3\delta(\vec{k}_1+\vec{k}_2)\,P(k_1)$, in the form

$$P(k) = \frac{2\pi^2}{k^3}\mathcal{P}(k) = \frac{2\pi^2}{k^3}\sum_{ab}\mathcal{P}_{ab}(k) \ . \tag{5.18}$$

Here

$$\mathcal{P}_{ab}(k) \equiv \left(\frac{H(t_i)}{2\pi}\right)^2 N_aN_b\left[\delta_{ab}\left(1 - 2\epsilon_{\rm H}\,\ln\frac{k}{k_p}\right) + 2\epsilon_{ab}\left(\tilde{c} - \ln\frac{k}{k_p}\right)\right] \ , \tag{5.19}$$

and we have defined $\epsilon_{\rm H} = -\dot{H}/H^2$ and $\tilde{c} = c + \ln(a_iH_i/k_{\rm p})$. Subleading slow roll corrections are again neglected in the scale-independent terms.

Defining a quantity

$$n_{ab} - 1 \equiv \frac{d\ln \mathcal{P}_{ab}}{d\ln k} = -\delta_{ab}(2\epsilon_{\rm H} + 2\epsilon_{ab}) - \frac{1}{\tilde{c}}(1-\delta_{ab}) \ , \tag{5.20}$$

we can write the spectral index as

$$n_\zeta - 1 \equiv \frac{d\ln \mathcal{P}}{d\ln k} = \sum_{ab}\left(\frac{\mathcal{P}_{ab}}{\mathcal{P}}\right) n_{ab} - 1 = -2\epsilon_{\rm H} - 2\frac{\sum_{ab}\epsilon_{ab}N_aN_b}{\sum_c N_c^2} \ . \tag{5.21}$$

This agrees with the result given in [25].

5.2.2 Three point function and $f_{\rm NL}$

We now proceed to apply our approach to derive the scale dependence of non-linearity parameters. Using previous definitions we can write $f_{\rm NL}$ in a general multiple field case as

$$\begin{aligned} f_{\rm NL}(k_1,k_2,k_3) &\equiv \frac{5}{6}\frac{B(k_1,k_2,k_3)}{P(k_1)P(k_2) + 2\,\text{perms}} \\ &= \frac{5}{3}\frac{\sum_{abcd}(k_1k_2)^{-3}\mathcal{P}_{ac}(k_1)\mathcal{P}_{bd}(k_2)f_{cd}(k_3) + 2\,\text{perms}}{(k_1k_2)^{-3}\mathcal{P}(k_1)\mathcal{P}(k_2) + 2\,\text{perms}} \ , \end{aligned} \tag{5.22}$$

where the bispectrum is defined by $(2\pi)^3\delta(\vec{k}_1+\vec{k}_2+\vec{k}_3)B(k_1,k_2,k_3) = \langle\zeta_{\vec{k}_1}\zeta_{\vec{k}_2}\zeta_{\vec{k}_3}\rangle$.

In the equilateral case, $k_i = k$ for $i = 1, 2$ and 3, this simplifies to

$$f_{\rm NL}(k) = \frac{5}{3}\frac{\sum_{abcd}\mathcal{P}_{ac}(k)\mathcal{P}_{bd}(k)f_{cd}(k)}{\mathcal{P}(k)^2} \ , \tag{5.23}$$

and using Eqs. (5.13) and (5.19), we find the scale dependence of $f_{\rm NL}(k)$ is given by

$$n_{f_{\rm NL}} \equiv \frac{d\ln|f_{\rm NL}(k)|}{d\ln k} = \frac{1}{f_{\rm NL}(k_{\rm p})}\sum_{ab} f_{\rm NL}^{ab}\left(2n_{{\rm multi},a} + n_{f,ab}\right) \ . \tag{5.24}$$

Here we have defined [37]

$$f_{\rm NL}^{ab} \equiv \frac{5}{6}\frac{N_aN_bN_{ab}}{(\sum_c N_c^2)^2} \ , \qquad f_{\rm NL}(k_{\rm p}) = \sum_{ab} f_{\rm NL}^{ab} \ , \tag{5.25}$$

and

$$\begin{aligned} n_{{\rm multi},a} &\equiv n_{aa} - n_\zeta - 2\sum_c(1-\delta_{ac})\epsilon_{ac}\frac{N_c}{N_a} &(5.26)\\ &= 2\sum_{cd}\epsilon_{cd}\left(\frac{N_cN_d}{\sum_b N_b^2} - \delta_{ad}\frac{N_c}{N_a}\right) \ . &(5.27) \end{aligned}$$

All the quantities in Eq. (5.24) depend on combinations of slow roll parameters and on the constant coefficients N_a, N_{ab} in the δN expansion (recall that the explicit expression for $n_{f,ab}$ is given by Eq. (5.105)). For a given model these can all be regarded as known quantities and the scale-dependence of $f_{\rm NL}$ can therefore be directly read off from the above result without doing any further computations.

In Eq. (5.24) we can clearly identify two sources of scale dependence. The contribution proportional to $n_{f,ab}$ follows from the non-linear evolution of perturbations outside the horizon [40]. The part proportional to $n_{\mathrm{multi},a}$ is associated with the scale dependence of factors of the form $\mathcal{P}_{ac}/\mathcal{P}$ in equation (5.23). It is present only in the multi-field case (indeed for a single field model this factor is equal to unity) and arises due to the presence of multiple unrelated Gaussian fields $\zeta^{\mathrm{G},a}$ in the expansion of ζ in (5.16). This generates deviations from the local form and makes f_{NL} scale-dependent even if the perturbations would evolve linearly outside the horizon. Indeed, by setting $n_{f,ab} = 0$ we recover the results of a multi-local case analyzed separately in [40].

As shown in [40], the scale dependence of f_{NL} is given by the same result (5.24) for the class of variations where the sides are scaled by the same constant factor, $\vec{k}_i \to \alpha\vec{k}_i$. For such shape-preserving variations where only the overall scale of the triangle is varied, the result does not depend on the triangle shape. This holds at leading order in slow roll. Generic variations changing both the scale and the shape of the triangle are considered in Sec. 5.5.

5.2.3 Four point function, g_{NL} and τ_{NL}

The connected part of the four point correlator of ζ can be written in the form

$$\langle\zeta_{\vec{k}_1}\zeta_{\vec{k}_2}\zeta_{\vec{k}_3}\zeta_{\vec{k}_4}\rangle = (2\pi)^3\delta(\sum_{i=1}^{4}\vec{k}_i)\left[\,\tau_{\mathrm{NL}}(k_1,k_2,k_3,k_4,k_{13})\left(\,P(k_1)P(k_2)P(|\vec{k}_1+\vec{k}_3|)+11\,\mathrm{perm}\,\right)\right.$$
$$\left.+\,\frac{54}{25}g_{\mathrm{NL}}(k_1,k_2,k_3,k_4)\left(\,P(k_1)P(k_2)P(k_3)+3\,\mathrm{perm}\,\right)\,\right]\,, \tag{5.28}$$

where we have defined $k_{ij} \equiv |\vec{k}_i + \vec{k}_j|$. The functions τ_{NL} and g_{NL} are given by

$$\tau_{\mathrm{NL}}(k_1,k_2,k_3,k_4,k_{13}) = 4\,\frac{(k_1k_2k_{13})^{-3}\sum_{abcdef}\mathcal{P}_{ac}(k_1)\mathcal{P}_{be}(k_2)\mathcal{P}_{df}(k_{13})f_{cd}(k_3)f_{ef}(k_4)+11\,\mathrm{perm}}{(k_1k_2k_{13})^{-3}\,\mathcal{P}(k_1)\mathcal{P}(k_2)\mathcal{P}(k_{13})+11\,\mathrm{perm}}\,, \tag{5.29}$$

$$g_{\mathrm{NL}}(k_1,k_2,k_3,k_4) = \frac{25}{9}\,\frac{(k_1k_2k_3)^{-3}\sum_{abcdef}P_{ad}(k_1)P_{be}(k_2)P_{cf}(k_3)g_{def}(k_4)+3\,\mathrm{perms}}{(k_1k_2k_3)^{-3}\,\mathcal{P}(k_1)\mathcal{P}(k_2)\mathcal{P}(k_3)+3\,\mathrm{perm}}\,. \tag{5.30}$$

In the case of a square, $k = k_i$ (notice that τ_{NL}, but not g_{NL}, is sensitive to the angles between the vectors and different equilateral figures in general yield different results), the above expressions reduce to

$$\tau_{\mathrm{NL}}(k) = 4\sum_{abcdef}\frac{\mathcal{P}_{ac}(k)\mathcal{P}_{be}(k)\mathcal{P}_{df}(\sqrt{2}k)f_{cd}(k)f_{ef}(k)}{\mathcal{P}(k)^3}\,, \tag{5.31}$$

$$g_{\mathrm{NL}}(k) = \frac{25}{9}\sum_{abcdef}\frac{\mathcal{P}_{ad}(k)\mathcal{P}_{be}(k)\mathcal{P}_{cf}(k)g_{def}(k)}{\mathcal{P}(k)^3}\,. \tag{5.32}$$

The scale-dependence can be computed similarly to the analysis of the bispectrum above.

Using Eqs. (5.13), (5.14) and (5.19), we find

$$n_{\tau_{\rm NL}} \equiv \frac{d\ln|\tau_{\rm NL}(k)|}{d\ln k} = \frac{1}{\tau_{\rm NL}(k_{\rm p})}\sum_{abcd}\tau_{\rm NL}^{abcd}\left[(2n_{\rm multi,a}-(n_\zeta-1)-2\epsilon_{\rm H})\delta_{bc}-2\epsilon_{bc}+2n_{f,ab}\delta_{bc}\right] , \tag{5.33}$$

$$n_{g_{\rm NL}} \equiv \frac{d\ln|g_{\rm NL}(k)|}{d\ln k} = \frac{1}{g_{\rm NL}(k_{\rm p})}\sum_{abc} g_{\rm NL}^{abc}\left(3n_{{\rm multi},a}+n_{g,abc}\right) , \tag{5.34}$$

where $\epsilon_H = -\dot{H}/H^2$, and [84, 142]

$$\tau_{\rm NL}^{abcd} = \frac{N_a N_{ab} N_{cd} N_d}{(\sum_e N_e^2)^3} , \qquad \tau_{\rm NL}(k_{\rm p}) = \sum_{abcd}\tau_{\rm NL}^{abcd}\delta_{bc} , \tag{5.35}$$

$$g_{\rm NL}^{abc} = \frac{25}{54}\frac{N_a N_b N_c N_{abc}}{(\sum_d N_d^2)^3} , \qquad g_{\rm NL}(k_{\rm p}) = \sum_{abc} g_{\rm NL}^{abc} . \tag{5.36}$$

The scale-dependencies are fully determined by the constant coefficients N_a, N_{ab}, N_{abc} in the δN expression and by combinations of slow-roll parameters, which enter the results through Eqs. (5.105) and (5.106). Although the expressions appear lengthy in their general form, considerable simplifications typically occur when considering specific models. We will discuss examples in Sections 5.3 and 5.4.

Similarly to $n_{f_{\rm NL}}$, we can again distinguish two physically different contributions in the expressions for $n_{\tau_{\rm NL}}$ and $n_{g_{\rm NL}}$. The parts proportional to $n_{f,ab}$ and $n_{g,abc}$ in Eqs. (5.33) and (5.34) respectively arise from the non-linear evolution outside the horizon. The other contributions describe deviations from the local form due to the presence of multiple fields, similarly to what we discussed in the previous section.

The results (5.33) and (5.34) hold not only for the special case of a square, but for any variations where all the sides are scaled by the same constant factor, $\vec{k}_i \to \alpha\vec{k}_i$. These variations preserve the shape of the momentum space figure and change only its overall scale. We will prove this result in Sec. 5.5 where we also discuss generic variations that simultaneously change both the scale and the shape.

Having presenting our formalism and the general results, we will discuss in the next two sections applications to specific cases.

5.3 General single field case

We start by discussing models where the primordial curvature perturbation effectively arises from a single scalar field, which does not need to be the inflaton and we call σ. In this case, the functions $f_{\sigma\sigma}(k)$ and $g_{\sigma\sigma\sigma}(k)$ appearing in the expansion of ζ, Eq. (5.16), are up to numerical factors equal to $f_{\rm NL}(k)$ and $g_{\rm NL}(k)$, evaluated for the equilateral configurations. This can be seen directly from Eqs. (5.23) and (5.32). We can therefore rewrite Eq. (5.16) as

$$\zeta_{\vec{k}} = \zeta^{\rm G}_{\vec{k}} + \frac{3}{5}f_{\rm NL}(k)(\zeta^{\rm G}\star\zeta^{\rm G})_{\vec{k}} + \frac{9}{25}g_{\rm NL}(k)(\zeta^{\rm G}\star\zeta^{\rm G}\star\zeta^{\rm G})_{\vec{k}} + \cdots . \tag{5.37}$$

As we will discuss in Sec. 5.4, this result applies for example to the curvaton scenario and modulated reheating in the limit where the inflaton perturbations are negligible. We therefore call all the models where the curvature perturbation can be expressed in the form (5.37) as general single field models.

According to Eqs. (5.13) and (5.14), the non-linearity parameters $f_{\rm NL}(k)$ and $g_{\rm NL}(k)$ are now given by

$$f_{\rm NL}(k) = \frac{5}{6}\frac{N''}{N'^2}\left(1+n_{f_{\rm NL}}\ln\frac{k}{k_{\rm p}}\right) , \tag{5.38}$$

$$g_{\rm NL}(k) = \frac{25}{54}\frac{N'''}{N'^3}\left(1+n_{g_{\rm NL}}\ln\frac{k}{k_{\rm p}}\right) , \tag{5.39}$$

where the primes denote derivatives with respect to σ and $n_{f_{\rm NL}} = n_{f,\sigma\sigma}, n_{g_{\rm NL}} = n_{g,\sigma\sigma\sigma}$. Using the explicit expressions (5.105) and (5.106) in the Appendix 5.8.1, we obtain

$$n_{f_{\rm NL}} = \frac{N'}{N''}\left[\sqrt{2\epsilon_\sigma}(4\epsilon_\sigma - 3\eta_{\sigma\sigma}) + \frac{V'''}{3H^2}\right] , \tag{5.40}$$

$$n_{g_{\rm NL}} = 3\frac{N''^2}{N'''N'}\,n_{f_{\rm NL}} - \frac{N'}{N'''}\left[24\epsilon_\sigma^2 - 24\epsilon_\sigma\eta_{\sigma\sigma} + 3\eta_{\sigma\sigma}^2 + \frac{4\sqrt{2\epsilon_\sigma}\,V'''}{3H^2} - \frac{V''''}{3H^2}\right] . \tag{5.41}$$

The same results can of course be directly obtained from Eqs. (5.24) and (5.34). If σ is an isocurvature field during inflation, $\epsilon_\sigma = 0$ in the above expressions.

For the general single field case Eq. (5.31) further yields

$$\tau_{\rm NL}(k) = \left(\frac{6f_{\rm NL}(k)}{5}\right)^2 , \tag{5.42}$$

up to scale-independent slow roll corrections. Therefore, the scale-dependencies of $\tau_{\rm NL}$ and $f_{\rm NL}$ are related by

$$n_{\tau_{\rm NL}} = 2n_{f_{\rm NL}} . \tag{5.43}$$

This simple consistency relation is characteristic for general single field models. In multiple field models, the relation (5.42) is in general violated and consequently the result (5.43) is no longer true.

5.4 Two field models of inflation

After considering single field models, in this section we discuss some scenarios in which more than one field can play an important role in the inflationary process. We focus on a class of models that contains the most important examples of inflationary set-ups characterized by large non-Gaussianity.

Many models of inflation that generate sizeable non-Gaussianity are characterized by the presence of a field σ, with significant non-Gaussian perturbations, that is isocurvature during inflation. The inflaton field φ also has its own perturbations, which for convenience can be considered as Gaussian. When the inflaton perturbations provide non-negligible contributions to the curvature fluctuation spectrum, the scenario is called a mixed scenario [170–173]. In order to generate large non-Gaussianity by means of the field σ, it is required that $\dot\sigma \ll \dot\varphi$, and hence $\epsilon_\sigma \ll \epsilon_\varphi$ [169]. From this relation, it follows that the trajectory in field space while observable modes exit the horizon is nearly straight. Therefore it is a good approximation to treat the fields as uncorrelated [180]. We also make the common assumption that the potential is separable,

$$W(\sigma,\varphi) = U(\varphi) + V(\sigma) . \tag{5.44}$$

Hence, the only potentially non-negligible slow roll parameters in such a scenario are the following

$$\epsilon_{\rm H} = \epsilon_\varphi = -\frac{\dot{H}}{H^2} \ , \qquad \eta_\varphi = \frac{U''}{3H^2} \ , \qquad \eta_\sigma = \frac{V''}{3H^2} \ , \qquad \xi^2_\varphi = \frac{U'''U'}{9H^4} \ , \qquad \xi^2_\sigma = \frac{V'''U'}{9H^4} \ . \tag{5.45}$$

In this case, the curvature perturbation reads[2]

$$\zeta(\vec{k}) = \zeta^{G,\varphi}_{\vec{k}} + \zeta^{G,\sigma}_{\vec{k}} + f_\sigma(k) \left(\zeta^{G,\sigma} \star \zeta^{G,\sigma}\right)_{\vec{k}} + g_\sigma(k)(\zeta^{G,\sigma} \star \zeta^{G,\sigma} \star \zeta^{G,\sigma})_{\vec{k}} \ . \tag{5.46}$$

Although the assumed form of ζ is simplified, in practice the vast majority of models in the literature, characterized by large quasi-local non-Gaussianity, satisfy the above Ansatz to a good enough accuracy for observational purposes. For this reason we will limit our attention to models with curvature perturbation satisfying Eq. (5.46) in this section.

In the limit that f_σ and g_σ are independent of k, we recover the multivariate local model [40]. In the case that $\zeta^{G,\varphi} = 0$ we have the general single field model we have analyzed in section 5.3, but here we assume this field was an isocurvature mode during horizon crossing. We will consider these two cases in more detail later in this section.

The power spectrum is given by

$$\mathcal{P}_\zeta(k) = \mathcal{P}_\varphi(k) + \mathcal{P}_\sigma(k) = \mathcal{P}_\varphi(k)(1 - w_\sigma(k))^{-1} \ , \tag{5.47}$$

where we have introduced the ratio

$$w_\sigma(k) = \frac{\mathcal{P}_\sigma}{\mathcal{P}_\zeta} \ . \tag{5.48}$$

Note that neglecting all the slow-roll corrections, and hence also the scale dependence, $w_\sigma = N^2_\sigma/(N^2_\varphi + N^2_\sigma)$. To lowest order in slow roll, the spectral index $n_\zeta - 1$ and tensor-to-scalar ratio r_T satisfy the following relations [181]

$$\begin{aligned} n_\zeta - 1 &= (n_\sigma - 1)w_\sigma + (n_\varphi - 1)(1 - w_\sigma) \\ &= -(6 - 4w_\sigma)\epsilon_{\rm H} + 2(1 - w_\sigma)\eta_\varphi + 2w_\sigma\eta_\sigma \ , \qquad (5.49) \\ r_T &\equiv \frac{\mathcal{P}_T}{\mathcal{P}_\zeta} = \frac{8}{N^2_\sigma + N^2_\varphi} \\ &= 8\, N_\varphi^{-2}\,(1 - w_\sigma) \ , \qquad (5.50) \end{aligned}$$

where $\mathcal{P}_T = 8H^2_k/(4\pi^2)$ is the power spectrum of tensor perturbations and we have defined

$$n_\sigma - 1 = \frac{d\ln\mathcal{P}_\sigma}{d\ln k} \ , \qquad n_\varphi - 1 = \frac{d\ln\mathcal{P}_\varphi}{d\ln k} \ , \qquad n_\zeta - 1 = \frac{d\ln\mathcal{P}_\zeta}{d\ln k} \ . \tag{5.51}$$

The non-Gaussianity parameter $f_{\rm NL}$ in the equilateral limit, and the trispectrum non-linearity parameters in the case of a square configuration, are given by

$$\begin{aligned} f_{\rm NL}(k) &= \frac{5}{3} w^2_\sigma(k) f_\sigma(k) \ , \qquad (5.52) \\ \tau_{\rm NL}(k) &= 4 w_\sigma(k)^2 w_\sigma(\sqrt{2}k) f^2_\sigma(k) \ , \qquad (5.53) \\ g_{\rm NL}(k) &= \frac{25}{9} w^3_\sigma(k) g_\sigma(k) \ . \qquad (5.54) \end{aligned}$$

[2]We have used a simplified notation for this section compared to the rest of the paper. Since all cross terms such as $P_{\varphi\sigma}$ are negligibly small in this scenario we use only a single index φ or σ where appropriate, e.g. for $\eta_\sigma \equiv \eta_{\sigma\sigma}$ and $g_\sigma \equiv g_{\sigma\sigma\sigma}$.

Therefore their scale dependence is given by

$$n_{f_{\rm NL}} \equiv \frac{d\ln|f_{\rm NL}|}{d\ln k} = 2(n_\sigma - n_\zeta) + \frac{d\ln|f_\sigma|}{d\ln k} \tag{5.55}$$

$$= 4(1-w_\sigma)(2\epsilon_{\rm H} + \eta_\sigma - \eta_\varphi) + \frac{N_\sigma}{N_{\sigma\sigma}}\left(\frac{V'''}{3H^2} - \sqrt{2\epsilon_{\rm H}}\,\eta_\sigma\left(\frac{1}{\omega_\sigma}-1\right)^{1/2}\right), \tag{5.56}$$

$$n_{\tau_{\rm NL}} = 3(n_\sigma - n_\zeta) + 2\frac{d\ln|f_\sigma|}{d\ln k} \tag{5.57}$$

$$= 6(1-w_\sigma)(2\epsilon_{\rm H} + \eta_\sigma - \eta_\varphi) + \frac{2N_\sigma}{N_{\sigma\sigma}}\left(\frac{V'''}{3H^2} - \sqrt{2\epsilon_{\rm H}}\,\eta_\sigma\left(\frac{1}{\omega_\sigma}-1\right)^{1/2}\right), \tag{5.58}$$

$$n_{g_{\rm NL}} = 3(n_\sigma - n_\zeta) + \frac{d\ln|g_\sigma|}{d\ln k} \tag{5.59}$$

$$= 6(1-w_\sigma)(2\epsilon_{\rm H} + \eta_\sigma - \eta_\varphi) + \frac{3\,N_{\sigma\sigma}}{N_{\sigma\sigma\sigma}}\frac{V'''}{3H^2} \tag{5.60}$$

$$+\frac{N_\sigma}{N_{\sigma\sigma\sigma}}\left(\frac{V''''}{3H^2} - 3\eta_\sigma^2 + \sqrt{2\epsilon_{\rm H}}\,\frac{V'''}{3H^2}\left(\frac{1}{\omega_\sigma}-1\right)^{1/2}\right),$$

where we have used the results derived in Sec. 5.2 and the fact that $N_{\varphi\varphi}$, $N_{\varphi\sigma}$ and their derivatives are negligible in the class of models we are considering, see Eq. (5.46). The quantities on the right hand side of each equation should be evaluated at an initial time t_i shortly after the horizon crossing time of all the modes of observational interest. Observe that our results for $n_{f_{\rm NL}}$ and $n_{g_{\rm NL}}$ depend on the derivatives of the potential, in combinations that do not correspond to traditional slow-roll parameters. This turns out be useful to probe these quantities, that cannot be tested by the power spectrum and its derivatives. We are going to discuss this in detail in what follows.

Observational constraints on the bispectrum are given in [18] while constraints on $g_{\rm NL}$ are given in [182,183] (see also [184]) and for both $g_{\rm NL}$ and $\tau_{\rm NL}$ in [185]. Forecasts for future constraints on all three parameters are given in [186,187] while forecast constraints on $n_{f_{\rm NL}}$ are given in [54]. There are currently no forecasts for how well the scale dependence of the trispectrum parameters could be constrained or measured. Observational constraints on a model with the form (5.46), without considering the scale-dependence of $f_{\rm NL}$ or w_σ, are given in [188].

5.4.1 Limiting cases

After presenting the general formulae for the two-field case, we discuss important examples of general single field inflation, that arise as limiting cases of the previous discussion of two-field inflation.

Isocurvature single field

In the case that a single field σ, which is subdominant to the inflaton during inflation, generates the primordial curvature perturbation, one has $w_\sigma = 1$ which implies $n_\sigma = n$, $r_T \simeq 0$ and $N_\sigma \gg 1$.

In this scenario, it is useful to express the spectral index and its running up to second order, to understand which parameters are currently constrained by observations. From

[180], we have

$$n_\zeta - 1 = -2\epsilon_{\rm H} + 2\eta_\sigma + \left(-\frac{22}{3} + 8c\right)\epsilon_{\rm H}^2 + \frac{2}{3}\eta_\sigma^2 + \left(\frac{8}{3} - 4c\right)\epsilon_{\rm H}\eta_\varphi + \left(\frac{2}{3} - 4c\right)\epsilon_{\rm H}\eta_\sigma \ , \tag{5.61}$$

$$\alpha_\zeta = -8\epsilon_{\rm H}^2 + 4\epsilon_{\rm H}\eta_\varphi + 4\epsilon_{\rm H}\eta_\sigma \ , \tag{5.62}$$

where $c = 2 - \ln 2 - \gamma \simeq 0.73$. Notice that, in the previous formulae, the slow-roll parameters ξ_σ and ξ_φ do not appear in the running of the spectral index, because they are weighted by negligible quantities. This implies that third and higher derivatives of the potential do not enter in the previous quantities.

The non-Gaussianity observables (which follow as special cases of the formulae discussed in the first part of this section, when taking the limit $\omega_\sigma \to 1$) are

$$f_{\rm NL} = \frac{5}{3}f_\sigma = \frac{5}{6}\frac{N_{\sigma\sigma}}{N_\sigma^2} \ , \qquad g_{\rm NL} = \frac{25}{9}g_\sigma = \frac{25}{54}\frac{N_{\sigma\sigma\sigma}}{N_\sigma^3} \ , \tag{5.63}$$

$$n_{f_{\rm NL}} = \frac{n_{\tau_{\rm NL}}}{2} \simeq \frac{N_\sigma}{N_{\sigma\sigma}}\frac{V'''}{3H^2} \simeq \frac{5}{6}\frac{{\rm sgn}(N_\sigma)}{f_{\rm NL}}\sqrt{\frac{r_{\rm T}}{8}}\frac{V'''}{3H^2} \ , \tag{5.64}$$

$$n_{g_{\rm NL}} \simeq 3\,\frac{N_{\sigma\sigma}}{N_{\sigma\sigma\sigma}}\frac{V'''}{3H^2} + \frac{N_\sigma}{N_{\sigma\sigma\sigma}}\left(\frac{V''''}{3H^2} - 3\eta_\sigma^2\right) \tag{5.65}$$

$$\simeq \frac{5}{3}\frac{{\rm sgn}(N_\sigma)\,f_{\rm NL}}{g_{\rm NL}}\sqrt{\frac{r_{\rm T}}{8}}\frac{V'''}{3H^2} + \frac{25}{54}\frac{1}{g_{\rm NL}}\frac{r_{\rm T}}{8}\frac{V''''}{3H^2} \simeq 2\frac{f_{\rm NL}^2}{g_{\rm NL}}n_{f_{\rm NL}} + \frac{25}{54}\frac{1}{g_{\rm NL}}\frac{\mathcal{P}_\zeta^{-1}}{6\pi^2}V'''' \ . \tag{5.66}$$

Here $f_{\rm NL}$ and $g_{\rm NL}$ denote the non-linearity parameters evaluated for equilateral configurations at some pivot scale, $k = k_{\rm p}$. As discussed in Sec. 5.2, $k_{\rm p}$ can be chosen as any of the super-horizon modes in our observable universe and the results are independent on this choice, up to subleading slow-roll corrections.

In the previous formulae, we have presented several different ways of expressing $n_{f_{\rm NL}}$ and $n_{g_{\rm NL}}$ (in Eq. (5.66) we have dropped the negligible contribution $\eta_\sigma^2 r_{\rm T} \lesssim 10^{-6}$). This is in order to make it easier to estimate their magnitude in different ways, depending on the available quantities. We also note that in some cases the previous formulae might include terms at different orders in slow roll, in which case one should neglect the subleading terms (since additional terms at the same order might also have been neglected). In general, they are suppressed by some combination of the tensor-to-scalar ratio, divided by non-linearity parameters. But their size could be significant, if σ has either a large cubic or quartic self interaction. As we mentioned earlier, the power spectrum does not contain information on these parameters, even if the running of the spectral index can be measured. Hence $n_{f_{\rm NL}}$ appears to be the best way of probing the cubic self interaction, while in principle $n_{g_{\rm NL}}$ could probe the quartic derivative of the isocurvaton field.

Although we have written $n_{f_{\rm NL}} \sim 1/f_{\rm NL}$, the prefactor to $1/f_{\rm NL}$ will in general depend on some of the same model parameters as $f_{\rm NL}$ so one should not view the two parameters as being inversely proportional (an explicit example is given in [51]). In the case that $f_{\rm NL}$ follows an exact power law behavior, $f_{\rm NL} \propto k^{n_{f_{\rm NL}}}$ then $f_{\rm NL}$ and $n_{f_{\rm NL}}$ are of course independent. However if $f_{\rm NL} = A\ln(k) + B$ where A and B are constants, then $n_{f_{\rm NL}} = A/(A\ln(k) + B) = A/f_{\rm NL}$. In this case $n_{f_{\rm NL}}$ and $f_{\rm NL}$ are not independent. Nonetheless one can easily check that the running of $n_{f_{\rm NL}}$ satisfies $\alpha_{f_{\rm NL}} = -n_{f_{\rm NL}}^2$ so it is a good approximation to treat $n_{f_{\rm NL}}$ as constant provided that $|n_{f_{\rm NL}}| \ll 1$.

Consider, as a first example, the curvaton scenario [148–164] in the pure curvaton limit. In this case all of the non-Gaussianity parameters will have some scale dependence unless the curvaton has exactly a quadratic potential, in which case it can be treated as a free test field during inflation. This is manifest from eqs. (5.64) and (5.65)[3]. In [40] we computed $n_{f_{\rm NL}}$ for curvaton models with a quartic self-interaction term, $V = m^2\sigma^2/2 + \lambda\sigma^4$, finding a scale dependence proportional to η_σ, which tends to be too small to be of observable interest. The result might be different for other type of interactions and it would be interesting to compute $n_{f_{\rm NL}}$ and $n_{g_{\rm NL}}$ for generic interacting curvaton models. This, however, requires a numerical study and is beyond the scope of the current work [189]. Here we will instead consider the modulated reheating scenario as an example of isocurvature single field models. In this case there is little constraint on the form of the modulaton potential and we can use results derived in the literature to compute the scale dependencies.

Modulated reheating

In this scenario, an isocurvature field σ during inflation modulates the decay rate of the inflaton field into radiation. Because the expansion rate of the universe changes after the decay, this process can convert the initial isocurvature perturbations of the modulaton field into the primordial curvature perturbation [165–168]. This is closely related to the model of modulated preheating [165–167] and modulated trapping [190] (see also [191]). This process leads to some level of non-Gaussianity, which depends on the efficiency of the transfer, on the functional form of the decay rate $\Gamma(\sigma)$ and on the potential of the modulaton field $V(\sigma)$. The form of the inflaton potential during horizon crossing is unconstrained, assuming the inflaton perturbations can be neglected, but its shape around the minimum does influence reheating and we assume it has a quadratic potential while it is oscillating.

For simplicity we will consider the case that $\Gamma \ll H_e$, where H_e is the Hubble parameter measured at the end of inflation t_e. Hence we are assuming that the inflaton decays long after the end of inflation. In this case, the curvature perturbation in real space can be written as [168, 173]

$$\zeta(t_f,\vec{x}) \simeq -\frac{1}{6}\frac{\Gamma_{\sigma_i}}{\Gamma}\,\delta\sigma(t_i,\vec{x}) + \frac{1}{2}\left(-\frac{1}{6}\frac{\Gamma_{\sigma_i}}{\Gamma}\right)_{\sigma_i}\times\delta\sigma(t_i,\vec{x})^2 + \frac{1}{6}\left(-\frac{1}{6}\frac{\Gamma_{\sigma_i}}{\Gamma}\right)_{\sigma_i\sigma_i}\times\delta\sigma(t_i,\vec{x})^3 + \cdots\,, \tag{5.67}$$

where t_i is a time soon after the horizon crossing of modes of interest. Using Eq. (5.63) we find the constant parts of $f_{\rm NL}$ and $g_{\rm NL}$ are given by

$$f_{\rm NL} = 5\left(1 - \frac{\Gamma\Gamma_{\sigma_i\sigma_i}}{\Gamma_{\sigma_i}^2}\right)\,, \tag{5.68}$$

$$g_{\rm NL} = \frac{50}{3}\left(2 - 3\frac{\Gamma\Gamma_{\sigma_i\sigma_i}}{\Gamma_{\sigma_i}^2} + \frac{\Gamma^2\Gamma_{\sigma_i\sigma_i\sigma_i}}{\Gamma_{\sigma_i}^3}\right)\,. \tag{5.69}$$

The scale dependencies of $f_{\rm NL}$ and $g_{\rm NL}$ can be computed using Eqs. (5.64) and (5.65). From these equations it is obvious that a potentially large scale dependence, accompanied

[3]For a quadratic model $N_{\sigma\sigma\sigma} = 0$ (when working to first order in $r = \rho_\sigma/(3H^2)$, i.e. considering the curvaton as a test field) and hence $g_{\rm NL} = 0$. As explained in Sec. (5.2), in this case we define $n_{g_{\rm NL}} = 0$ instead of using the formally divergent result (5.65).

with large values for $f_{\rm NL}$ and $g_{\rm NL}$, can arise only if the modulaton field σ has large self interactions. For the rest of this section we will consider the case of a quartic potential

$$V(\sigma) = \frac{\lambda}{4!}\sigma^4 \ , \qquad \lambda > 0 \ . \tag{5.70}$$

In keeping with the previous literature, we neglect the energy density of the σ field after the end of reheating, as studying this goes beyond the realms of this project.

Using Eqs. (5.64) and (5.65) we find

$$n_{f_{\rm NL}} \simeq -\frac{5}{f_{\rm NL}}\frac{\Gamma}{\Gamma_{\sigma_i}}\frac{\lambda\sigma_i}{3H_i^2} \sim 0.1\frac{\sqrt{\lambda\eta_\sigma}}{f_{\rm NL}\,\mathcal{P}_\zeta^{1/2}} \ , \tag{5.71}$$

$$n_{g_{\rm NL}} \simeq 2\frac{f_{\rm NL}^2}{g_{\rm NL}}n_{f_{\rm NL}} + \frac{50}{3g_{\rm NL}}\frac{\Gamma^2}{\Gamma_{\sigma_i}^2}\frac{\lambda}{3H_i^2} \sim 2\frac{f_{\rm NL}^2}{g_{\rm NL}}n_{f_{\rm NL}} + 4\times 10^{-3}\frac{\lambda}{g_{\rm NL}\,\mathcal{P}_\zeta} \ , \tag{5.72}$$

where $\eta_\sigma = \lambda\sigma_i^2/(6H_i^2)$. In the expression for $n_{g_{\rm NL}}$ we have neglected the contribution proportional to η_σ^2 in Eq. (5.65) which is negligible compared to $\lambda/(3H_i^2)$ because $\lambda\sigma_i^4 \ll H_i^2$ by construction.

The quantities $n_{f_{\rm NL}}$ and $n_{g_{\rm NL}}$ could be large, by making a suitable choice of the parameters. At first sight, it seems easy to obtain values for these parameters of order 10^{-1}, large enough to be detectable, and at the same time compatible with the assumptions that underlie our analysis of Section 5.2. This is correct, but we have to ensure that the parameters satisfy stringent constraints in order to obtain acceptable values for the tilt of the spectral index. Indeed, assuming inflation lasted considerably longer than 60 efoldings, a natural initial value for the field σ is [91]

$$\sigma_i \sim \left(\frac{3}{\pi^2}\right)^{\frac{1}{4}}\frac{H_i}{\lambda^{1/4}} \ , \tag{5.73}$$

(a different argument changes the power of λ from 1/4 to 1/3 and the numerical factors [192], but the difference is not very important here). Plugging the previous estimate in the expression for $\eta_\sigma = \lambda\sigma_i^2/(6H_i^2)$, and requiring that this parameter is less than 10^{-2}, we find the following bound for the coupling λ:

$$\eta_\sigma \simeq \left(\frac{\lambda}{12\pi^2}\right)^{1/2} \lesssim 10^{-2} \ \Rightarrow \ \lambda \lesssim 10^{-2} \ . \tag{5.74}$$

The condition $\Gamma \ll H_e$ can place further bounds on η_σ since the modulaton is assumed to remain nearly frozen until the inflaton decay. We will not further address this issue here.

Plugging the previous results in (5.71) and (5.72), and using $\mathcal{P}_\zeta = 2.5\times 10^{-9}$ for the normalization of the power spectrum, we find

$$|n_{f_{\rm NL}}| \sim \lambda^{3/4}\,\frac{600}{|f_{\rm NL}|} \lesssim \frac{20}{|f_{\rm NL}|} \ , \tag{5.75}$$

$$|n_{g_{\rm NL}}| \sim \lambda\,\frac{2\times 10^6}{|g_{\rm NL}|} \lesssim \frac{2\times 10^4}{|g_{\rm NL}|} \ . \tag{5.76}$$

where the inequalities are saturated for $\lambda \sim 10^{-2}$. In the estimate for $n_{g_{\rm NL}}$, we have neglected the first term in Eq. (5.72),

$$2\frac{f_{\rm NL}^2}{|g_{\rm NL}|}\,|n_{f_{\rm NL}}| \sim \lambda^{3/4}\,\frac{10^3\,|f_{\rm NL}|}{|g_{\rm NL}|} \ , \tag{5.77}$$

which is subdominant compared to the second term if $\lambda^{1/4} \gtrsim 5 \times 10^{-4}|f_{\rm NL}|$. For $|f_{\rm NL}| \sim 100$, this corresponds to $\lambda \gtrsim 6 \times 10^{-6}$. In the opposite case, $\lambda^{1/4} \lesssim 5 \times 10^{-4}|f_{\rm NL}|$, the estimate for $n_{g_{\rm NL}}$ is given by Eq. (5.77) instead of Eq. (5.76).

We conclude that both $n_{f_{\rm NL}}$ and $n_{g_{\rm NL}}$ could acquire relatively large values, even if the values of $f_{\rm NL}$ and $g_{\rm NL}$ saturate their current observational bounds. It is however important to emphasize that $|n_{f_{\rm NL}}|$ or $|n_{g_{\rm NL}}| \gg 0.01$ is outside the regime of validity of our formulae, since the accuracy of the expansions performed in Sec. 5.2 starts to become inadequate.

5.4.2 Two-field local case

As a last example, we briefly discuss the so called two field local case, for which f_σ and g_σ are independent of k. This demonstrates an explicit violation of the relation (5.43). In this scenario, the formulae at the beginning of this section provide

$$\tau_{\rm NL} = \left(\frac{6}{5} f_{\rm NL}\right)^2 \frac{1}{w_\sigma} \,, \tag{5.78}$$

which shows that, in principle, the parameter w_σ is an observable. The scale dependences of the non-linearity parameters satisfy the following relation

$$n_{\tau_{\rm NL}} = n_{g_{\rm NL}} = \frac{3}{2} n_{f_{\rm NL}} \,. \tag{5.79}$$

So, as previously stated, we have a different consistency relation between $n_{f_{\rm NL}}$ and $n_{\tau_{\rm NL}}$ in this case compared to the single field case, Eq. (5.43). Furthermore there is an additional consistency relation from $n_{g_{\rm NL}}$. However two-field local models are likely to arise from a test field with a quadratic potential [40], in which case the amplitude of $g_{\rm NL}$ tends to be too small to be observable.

As an explicit example we consider the mixed inflaton-curvaton scenario, assuming the curvaton field has a quadratic potential. We discussed this model previously at the level of the bispectrum in [40], and found that in a natural limit $n_{f_{\rm NL}} = -2(n_\zeta - 1)$. It therefore follows that for this model $n_{\tau_{\rm NL}}$ is even larger,

$$n_{\tau_{\rm NL}} = -3(n_\zeta - 1) \,. \tag{5.80}$$

In this model $g_{\rm NL} \sim f_{\rm NL}$ [156] which is too small to be of observational interest [187].

5.5 Shape dependence

In the previous sections, we concentrated our analysis on the scale dependence of equilateral figures (triangles and quadrilatera). Moreover, we only considered the possibility of varying simultaneously all of the sides of the figure by the same proportion. In this section, we study more general situations in which scale dependence can arise in parameters characterizing local non-Gaussianity. In particular, we consider the case in which the figure under consideration is not equilateral, and the case in which we vary the size of only one side, keeping the lengths of the other sides fixed.

We start by studying these issues for the parameter $f_{\rm NL}$, generalizing the arguments developed in Sec. 5.2.2, and using the same quantities introduced there. Expanding Eq. (5.22), around a pivot scale $k_{\rm p}$ using Eq. (5.13), we obtain

$$f_{\rm NL}(k_1,k_2,k_3) = \sum_{ab} f_{\rm NL}^{ab} \left(1 + \frac{k_3^3 \left(n_{{\rm multi},a} \ln \frac{k_1 k_2}{k_{\rm p}^2} + n_{f,ab} \ln \frac{k_3}{k_{\rm p}} \right) + 2\,{\rm perms}}{k_1^3 + k_2^3 + k_3^3} \right) \,. \tag{5.81}$$

As in the previous sections, the result is given to first order in $\ln(k_i/k_{\rm p})$ and both the scale-dependent and scale-independent parts are given to leading order in slow roll.

In this approximation, setting for simplicity $k_{\rm p} = 1$, equation (5.81) can be re-expressed in a more elegant way as

$$f_{\rm NL}(k_1, k_2, k_3) \;=\; \sum_{ab} f_{\rm NL}^{ab} \frac{(k_1 k_2)^{n_{{\rm multi},a}}\, k_3^{3+n_{f,ab}} + 2\,\text{perms}}{k_1^3 + k_2^3 + k_3^3} \;. \tag{5.82}$$

Indeed, since both $n_{{\rm multi},a}$ and $n_{f,ab}$, for each a, b, are proportional to slow-roll parameters, an expansion of Eq. (5.82) at first order in slow-roll provides Eq. (5.81). For general single field models, it reduces to

$$f_{\rm NL}(k_1, k_2, k_3) \;=\; f_{\rm NL}^{\rm p} \frac{k_1^{3+n_{f_{\rm NL}}} + k_2^{3+n_{f_{\rm NL}}} + k_3^{3+n_{f_{\rm NL}}}}{k_1^3 + k_2^3 + k_3^3} \;, \tag{5.83}$$

where $f_{\rm NL}^{\rm p}$ denotes $5f_{\sigma\sigma}/3$ evaluated at the pivot scale and $n_{f_{\rm NL}} = n_{f,\sigma\sigma}$. These simple ways of expressing the parameter $f_{\rm NL}$ are particularly suitable to analyze how the triangle shape affects the scale dependence. The single field expression (5.83) is equivalent to the analogous result given in Section 3.3 of [40], as one can easily check using Appendix 5.8.2. Eq. (5.83) however takes a much simpler form than the result in [40] as a consequence of cancellations that occur when explicitly writing out the results in terms of slow roll parameters.

We note that, although (5.83) is not of the form $f_{\rm NL} \propto (k_1 k_2 k_3)^{n_{f_{\rm NL}}/3}$ which [54] used in order to make observational forecasts for $n_{f_{\rm NL}}$, the bispectrum is a sum of three simple, product separable terms

$$B_\zeta(k_1, k_2, k_3) \propto (k_1 k_2)^{n_\zeta - 4} k_3^{n_{f_{\rm NL}}} + 2 \text{ perms} \;, \tag{5.84}$$

and that it only depends on one new parameter $n_{f_{\rm NL}}$. In the multiple field case the bispectrum will typically depend on more parameters than just $n_{f_{\rm NL}}$, see (5.82). An exception is the two-field local model discussed in Sec. 5.4.2, in which case (we also use Eq. (5.55))

$$B_\zeta(k_1, k_2, k_3) \propto (k_1 k_2)^{n_\zeta + (n_{f_{\rm NL}}/2) - 4} + 2 \text{ perms} \;. \tag{5.85}$$

Notice that it therefore follows from (5.84) and (5.85) that models with the same $f_{\rm NL}$ and $n_{f_{\rm NL}}$ can have different bispectral shapes which generalise in different ways the local shape. It is possible that observations may distinguish between these shapes and that we could therefore learn whether $n_{f_{\rm NL}}$ arises due to single or multi-field effects (or a combination of the two)[4].

In Sec. 5.2, we limited our considerations to the scale dependence of $f_{\rm NL}$ for equilateral triangles. On the other hand, by means of Eq. (5.82) one can observe that, considering a common rescaling for all the three vectors, say $\vec{k}_i \to \alpha \vec{k}_i$, our previous results remains valid *regardless* of the triangle shape. Namely,

$$\frac{\partial \ln f_{\rm NL}(\alpha k_1, \alpha k_2, \alpha k_3)}{\partial \ln \alpha}\Big|_{\alpha=1} = \sum_{ab} f_{\rm NL}^{ab} \left(2 n_{{\rm multi},a} + n_{f,ab}\right) \;. \tag{5.86}$$

which is exactly our previous result.

[4] CB thanks Sarah Shandera for pointing this out.

While the scale dependence of $f_{\rm NL}$, when simultaneously varying the triangle sides, does not depend on the triangle shape, there are other situations in which it does. We might indeed be interested on the scale dependence of $f_{\rm NL}$, when varying the size of only one of the triangle sides, keeping the other two fixed (and the triangle closed). In this case, the result does depend on the triangle shape. We focus for simplicity on the single-field case, for which the analysis is particularly simple, we do not expect our results to change much when considering multiple fields. When varying $\vec{k}_1 \to \alpha\vec{k}_1$, equation (5.82) becomes

$$f_{\rm NL}(\alpha k_1, k_2, k_3) \,=\, f_{\rm NL}^{\rm p} \frac{\alpha^{3+n_{f_{\rm NL}}}\, k_1^{3+n_{f_{\rm NL}}} + k_2^{3+n_{f_{\rm NL}}} + k_3^{3+n_{f_{\rm NL}}}}{\alpha^3\, k_1^3 + k_2^3 + k_3^3} \,. \tag{5.87}$$

It is clear that the dependence on α, in this expression, goes to zero in the limit in which k_1 vanishes. This is because the coefficients of the terms depending on α, in equation (5.82), become very suppressed with respect to the remaining terms. This situation corresponds to a squeezed triangle: for this shape, we then learn that the value of $f_{\rm NL}$ does not change when varying the length of the triangles shortest side.

In order to determine the triangle shape that leads to maximal scale dependence, one is then lead to focus on the opposite limit. That is, on configurations for which k_1^3 is as large as possible, with respect to $k_2^3 + k_3^3$. In this case, indeed, the coefficients of the terms depending on α, in equation (5.82), become dominant with respect to the other terms.

This expectation is correct, as shown by the following more detailed analysis. Taking the logarithmic derivative of $f_{\rm NL}$ along α, we find, at leading order in slow-roll:

$$\left.\frac{\partial \ln f_{\rm NL}(\alpha k_1, k_2, k_3)}{\partial \ln \alpha}\right|_{\alpha=1} \,=\, \frac{n_{f_{\rm NL}}}{1+x^3+y^3}\left(1 - \frac{3x^3 \ln x + 3y^3 \ln y}{1+x^3+y^3}\right) \,, \tag{5.88}$$

where we have defined $x = k_2/k_1$, $y = k_3/k_1$. We have checked that the terms inside the parenthesis are not important for determining the location of the maxima of the previous expression. The maxima of Eq. (5.88) are therefore determined by the prefactor $(1+x^3+y^3)^{-1}$, which is maximized for triangles that minimize the combination x^3+y^3. This corresponds, as anticipated from our previous expectation, to the shape for which k_1^3 is as large as possible, with respect to the combination $k_2^3 + k_3^3$. Calling θ the angle between k_1 and k_2, we have $y^2 \,=\, (1-x)^2 + 2x\,(1-\cos\theta)$. So we can write

$$x^3 + y^3 \,=\, x^3 + \left[(1-x)^2 + 2x\,(1-\cos\theta)\right]^{\frac{3}{2}} \,. \tag{5.89}$$

It is easy to see that the previous expression is minimized for $\theta = 0$ and $x = 1/2$, that is for a folded triangle for which $k_2 = k_3 = k_1/2$. Plugging these values in (5.88), we find

$$\left.\frac{\partial \ln f_{\rm NL}}{\partial \ln \alpha}\right|_{\alpha=1} \,\simeq\, 1.1\, n_{f_{\rm NL}} \,, \tag{5.90}$$

so we learn that, for the shape that maximizes the scale dependence, we gain around ten per cent with respect to the case in which we vary simultaneously all the sides of the triangle. Plots in Fig. 5.1 represent the logarithmic derivative of $f_{\rm NL}$ along α, and graphically show the results discussed so far. Notice that the shape which maximizes the scale dependence is indeed given by folded triangles.

A similar procedure, that generalizes what we have done in Sec. 5.2.3, can be applied to analyze $g_{\rm NL}$ and $\tau_{\rm NL}$. Expanding Eqs. (5.29) and (5.30) around a pivot scale $k_{\rm p}$ using

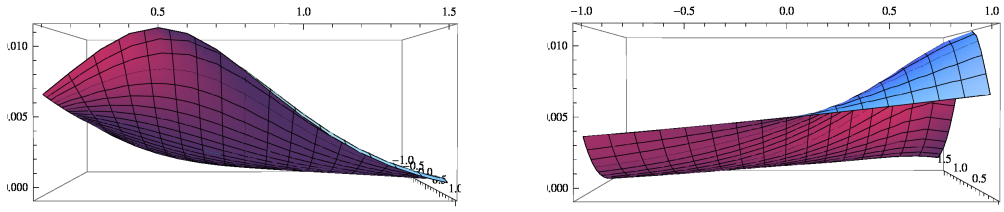

Figure 5.1: Behavior of the quantity $\partial \ln f_{\rm NL}/\partial \ln \alpha$, as a simultaneous function of x (taken between 0 and 1.5) and of $\cos\theta$. The two plots represent the same figure from two different points of view, that emphasize respectively the dependence on x and on $\cos\theta$. We have chosen $n_{f_{\rm NL}} = 0.01$.

Eqs. (5.13), (5.14) and (5.19), we obtain the results

$$g_{\rm NL}(k_1,k_2,k_3,k_4) = \sum_{abc} g_{\rm NL}^{abc}\left(1 + \frac{k_4^3\left(n_{{\rm multi},a}\ln\frac{k_1k_2k_3}{k_{\rm p}^3} + n_{g,abc}\ln\frac{k_4}{k_{\rm p}}\right) + 4\,{\rm perms}}{k_1^3+k_2^3+k_3^3+k_4^3}\right)\,, \tag{5.91}$$

$$\begin{aligned}\tau_{\rm NL}(k_1,k_2,k_3,k_4,k_{13}) = \sum_{abcd}\tau_{\rm NL}^{abcd}\Bigg(\delta_{bc} + \Bigg(&\frac{\delta_{bc}\left(n_{{\rm multi},a}\ln\frac{k_1k_2}{k_{\rm p}^2} + (n_{bb}-n_\zeta)\ln\frac{k_{13}}{k_{\rm p}}\right)}{k_1^3k_2^3k_{13}^3}\\ &+ \frac{\delta_{bc}\left(n_{f,ab}\ln\frac{k_3k_4}{k_{\rm p}^2}\right) - (1-\delta_{bc})(4\sqrt{\epsilon_b\epsilon_c}-2\eta_{bc})\ln\frac{k_{13}}{k_{\rm p}}}{k_1^3k_2^3k_{13}^3} + 11\,{\rm perms}\Bigg)\\ &\times\left(\frac{1}{k_1^3k_2^3k_{13}^3} + 11\,{\rm perms}\right)^{-1}\Bigg)\,.\end{aligned} \tag{5.92}$$

We can then proceed with arguments very similar to the ones developed for $f_{\rm NL}$. Writing $\vec{k}_i \to \alpha\vec{k}_i$ in Eqs. (5.91) and (5.92), taking a logarithmic derivative with respect to α and finally setting $\alpha = 1$, we immediately recover the results (5.33) and (5.34), derived in Sec. 5.2 for $n_{\tau_{\rm NL}}$ and $n_{g_{\rm NL}}$ for equilateral configurations. This shows that for the class of shape preserving variations, $\vec{k}_i \to \alpha\vec{k}_i$, the results are independent of the figure shape.

In the single field case, if we vary only one of the sides, say the one labeled by k_1, then the scale dependence vanishes when $k_1 \to 0$. We numerically analyzed for which shapes the scale dependence is maximal. For the case of $g_{\rm NL}$, the analysis is a straightforward generalization of what we did for $f_{\rm NL}$. The shape associated with maximal scale dependence corresponds to a folded polygon, in which three of the sides lie over the side whose length is varied. That is,

$$k_1 = 3k_2 = 3k_3 = 3k_4\,. \tag{5.93}$$

Again, for maximal scale dependence we gain order ten per cent with respect to the case in which we vary all the sides simultaneously.

We also performed a numerical analysis to study $\tau_{\rm NL}$, finding again maximal scale dependence for the folded shape of Eq. (5.93). For this parameter, we gain around $20-25$

percent with respect to the case in which we vary all the sides by the same amount (this result resonates with the consistency relation (5.43)).

5.6 Curvature perturbation in coordinate space

An additional important feature of our approach to the scale dependence of local non-Gaussianity, is that it allows one to express the results in coordinate space. In this section, we show how the scale dependent coefficients appearing in the momentum space expansion of curvature perturbation (5.16) manifest themselves in coordinate space. It is clear that scale dependence will cause deviations from the local form, for which $\zeta(\vec{x})$ can be expressed as a power series of a Gaussian variable $\zeta^{\rm G}(\vec{x})$ with constant coefficients. Using the general single field case as an example, we work out the expression for $\zeta(\vec{x})$ in the scale-dependent case and quantify how it deviates from the local form.

In the general single field case, Eq. (5.9) can be written as

$$\begin{aligned}\zeta_{\vec{k}} &= \zeta^{\rm G}_{\vec{k}} + \frac{3}{5} f_{\rm NL}(k_{\rm p}) \left(1 + n_{f_{\rm NL}}\, \theta(k_i - k) \ln\frac{k}{k_i}\right) (\zeta^{\rm G} \star \zeta^{\rm G})_{\vec{k}} \\ &\quad + \frac{9}{25} g_{\rm NL}(k_{\rm p}) \left(1 + n_{g_{\rm NL}}\, \theta(k_i - k) \ln\frac{k}{k_i}\right) (\zeta^{\rm G} \star \zeta^{\rm G} \star \zeta^{\rm G})_{\vec{k}} + \cdots \,,\end{aligned} \tag{5.94}$$

which coincides with Eq. (5.37) up to slow roll corrections for constant terms. This form is useful for our analysis since the horizon scale $k_i = a_i H_i$ appears explicitly. We have inserted the theta functions $\theta(k_i - k)$ to explicitly indicate that the result holds only for super-horizon modes $k < k_i$. $k_i > k_p$ should correspond to a physically smaller scale than any of the modes of interest. Recall that similar theta functions are included in our definition of $\zeta^{\rm G}_{\vec{k}}$, Eq. (5.10). Therefore $\zeta^{\rm G}_{\vec{k}}$ can be viewed as a smoothed quantity; in Fourier space the window function is simply a top hat with the cutoff set at the horizon scale k_i.

Taking the inverse Fourier transform of (5.94) we find

$$\begin{aligned}\zeta(\vec{x}) &= \zeta^{\rm G}(\vec{x}) + \frac{3}{5} f_{\rm NL}(k_{\rm p}) \zeta^{\rm G}(\vec{x})^2 + \frac{9}{25} g_{\rm NL}(k_{\rm p}) \zeta^{\rm G}(\vec{x})^3 \\ &\quad + \frac{3}{5} f_{\rm NL}(k_{\rm p}) n_{f_{\rm NL}} \int \frac{d^3k}{(2\pi)^3}\, e^{i\vec{k}\cdot\vec{x}} \theta(k_i - k) (\zeta^{\rm G} \star \zeta^{\rm G})_{\vec{k}} \ln\frac{k}{k_i} \\ &\quad + \frac{9}{25} g_{\rm NL}(k_{\rm p}) n_{g_{\rm NL}} \int \frac{d^3k}{(2\pi)^3}\, e^{i\vec{k}\cdot\vec{x}} \theta(k_i - k) (\zeta^{\rm G} \star \zeta^{\rm G} \star \zeta^{\rm G})_{\vec{k}} \ln\frac{k}{k_i} + \cdots \,.\end{aligned} \tag{5.95}$$

The two integrals describe deviations from the local form. They can be written more explicitly by performing the following manipulations

$$\begin{aligned}\int \frac{d^3k}{(2\pi)^3}\, e^{i\vec{k}\cdot\vec{x}} \theta(k_i - k) (\zeta^{\rm G} \star \zeta^{\rm G})_{\vec{k}} \ln\frac{k}{k_i} &= \int d^3y \int \frac{d^3k}{(2\pi)^3}\, e^{i\vec{k}\cdot(\vec{x}-\vec{y})} \theta(k_i - k)\, \zeta^{\rm G}(\vec{y})^2 \ln\frac{k}{k_i} \\ &= \int d^3y\, \zeta^{\rm G}(\vec{y})^2 \frac{1}{2\pi^2} \frac{\sin(k_i|\vec{x}-\vec{y}|) - {\rm Si}(k_i|\vec{x}-\vec{y}|)}{|\vec{x}-\vec{y}|^3} \\ &\equiv \int d^3y\, \zeta^{\rm G}(\vec{y})^2\, I(|\vec{x}-\vec{y}|) \,,\end{aligned} \tag{5.96}$$

and similarly for the second integral. Using this we can rewrite Eq. (5.95) as

$$\zeta(\vec{x}) = \zeta^{\rm G}(\vec{x}) + \frac{3}{5} f_{\rm NL}(k_{\rm p}) \left(\zeta^{\rm G}(\vec{x})^2 + n_{f_{\rm NL}} \int d^3y \, I(|\vec{x}-\vec{y}|) \, \zeta^{\rm G}(\vec{y})^2 \right) \qquad (5.97)$$
$$+ \frac{9}{25} g_{\rm NL}(k_{\rm p}) \left(\zeta^{\rm G}(\vec{x})^3 + n_{g_{\rm NL}} \int d^3y \, I(|\vec{x}-\vec{y}|) \, \zeta^{\rm G}(\vec{y})^3 \right) + \cdots \, .$$

This result clearly shows how the scale dependence of $f_{\sigma\sigma}$ and $g_{\sigma\sigma\sigma}$ in Eq. (5.16) renders $\zeta(\vec{x})$ a nonlocal function of $\zeta^{\rm G}(\vec{x})$. Because of the integrals in Eq. (5.97), the curvature perturbation $\zeta(\vec{x})$ can not be expressed in terms of $\zeta^{\rm G}(\vec{x})$ evaluated at the same point $\vec{x}$ but one needs to know $\zeta^{\rm G}(\vec{y})$ in the entire region where $I(|\vec{x}-\vec{y}|)$ is non-vanishing. The behavior of $I(|\vec{x}-\vec{y}|)$ is depicted in Fig. 5.2 which also displays the inverse Fourier transform,

$$W(|\vec{x}-\vec{y}|) = \frac{\sin(k_i\,|\vec{x}-\vec{y}|) - k_i\,|\vec{x}-\vec{y}|\cos(k_i\,|\vec{x}-\vec{y}|)}{2\pi^2|\vec{x}-\vec{y}|^3}, \qquad (5.98)$$

of the top hat window function $\theta(k_i - k)$ included in the definition of $\zeta^{\rm G}_{\vec{k}}$, Eq. (5.10). Both $W(x)$ and $I(x)$ are approximatively constant at scales $x \lesssim (k_i)^{-1}$. They both fall

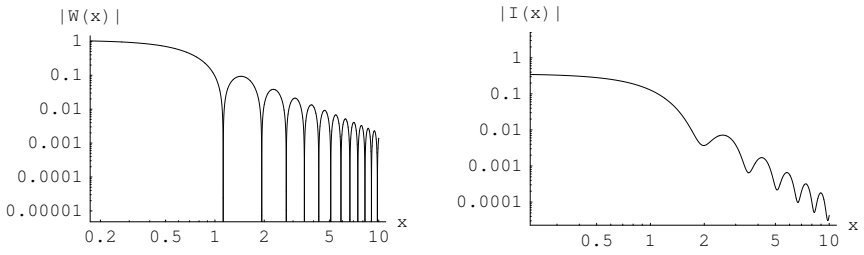

Figure 5.2: Absolute values of the functions W and I plotted on logarithmic scales for the choice $k_i = 4$ (in arbitrary units).

off for $x \gtrsim (k_i)^{-1}$ but $I(x)$ remains negative definite unlike $W(x)$ which starts to oscillate rapidly. Keeping in mind that a smoothing over $W(x)$ is implicit in the definition of $\zeta^{\rm G}(\vec{x})$, we therefore see that the convolutions of $\zeta^{\rm G}(\vec{x})$ with $I(x)$ in Eq. (5.97) pick up a non-trivial contribution from the superhorizon modes $x \gtrsim (k_i)^{-1}$ where $W(x)$ effectively falls off faster than $I(x)$. This contribution makes Eq. (5.97) deviate from the local form.

The analysis can in principle be straightforwardly generalized to the multi-field case. The difference compared to the general single field case is the appearance of several unrelated Gaussian fields $\zeta^{{\rm G},a}_{\vec{k}}$ in Eq. (5.16). This in general makes it impossible to write $\zeta(\vec{x})$ as a series of a single Gaussian field even if the coefficients in Eq. (5.16) would be constants.

5.7 Discussion

We have discussed a new approach, based on the δN-formalism, for studying the scale dependence of non-Gaussianity parameters. We have obtained explicit expressions for the scale dependence of the quantities $f_{\rm NL}$, $\tau_{\rm NL}$ and $g_{\rm NL}$ associated with the bispectrum and trispectrum of primordial curvature perturbations. Our results depend on the slow-roll parameters evaluated at horizon exit, and on the derivatives of the number of e-foldings and the inflationary potential. The parameters controlling the scale dependence

of non-Gaussianity depend on properties of the inflationary potential, namely its third and fourth derivatives, which in all observationally interesting cases cannot be probed by only studying the spectral index of the power spectrum and its running.

As a consequence, the scale dependence of non-Gaussianity provides additional powerful observables, able to offer novel information about the mechanism which generates the curvature perturbations. We demonstrated these features in the concrete example of modulated reheating. In models with a quartic potential for the modulating field, we have shown that the associated non-linearity parameters, and their scale dependence, can be large enough to be observable.

While in most of the discussion we worked in momentum space, in the last part we also discussed how to describe our results in coordinate space. We provided an expression for curvature perturbations in coordinate space, that generalizes the frequently used local Ansatz, and that exhibits directly in real space the effects of scale dependence of non-Gaussian parameters.

Our results allow us to put onto a firm basis the phenomenological parameterizations of the scale dependence of non-Gaussian observables. In many models of observational interest, our formulae are relatively simple and depend on a single new parameter, the scale dependence of the non-linearity parameter. It would be interesting to use these results for analysing or simulating non-Gaussian data. At the same time, our investigation allows us to identify which properties inflationary models have to satisfy, in order to obtain large non-Gaussianity with sizeable scale dependence. It would be interesting to apply it to analyse further models, for example those in which multiple fields interact during inflation or where the non-Gaussianity is generated by an inhomogeneous end of inflation.

5.8 Appendices

5.8.1 Explicit expressions for $n_{f,ab}$ and $n_{g,ab}$

For a system of slowly rolling scalar fields φ_a, the equations of motion are given by $3H\dot{\varphi}_a = -V_a$ and $3H^2 = V$, to leading order in slow roll. Here we are interested in the evolution during a short time interval from t_0 to t_i. The slow roll equations can easily be solved for φ_a as

$$\varphi^a(t_i) = \varphi^a(t_0) - \sqrt{2\epsilon_a}\ln(a_i/a_0) + \mathcal{O}\left(\epsilon^{3/2}\ln^2(a_i/a_0)\right) \ , \tag{5.99}$$

where we have used the identity $H\mathrm{d}t = \mathrm{d}\ln a$, which holds to leading order in slow roll. In the following we use the notation $\mathcal{O}(\epsilon^n)$ to denote the combinations of the slow roll parameters ϵ_a, η_{ab} of order ϵ^n.

Differentiating Eq. (5.99) with respect to $\varphi^a(t_0)$ and keeping the number of e-foldings $\ln(a_i/a_0)$ fixed, we can compute the coefficients appearing in Eq. (5.4). We choose the initial time t_0 as the time t_k of horizon crossing of a mode k, defined by $a_k H_k = k$. Using $\ln(a_i/a_k) = \ln(a_i H_i/k)$, which is valid at leading order in slow roll, the three first

coefficients in Eq. (5.4) can be written as

$$\frac{\partial\varphi^a(t_i)}{\partial\varphi^b(t_k)} = \delta_{ab} + \epsilon_{ab}\ln\,\frac{a_iH_i}{k} + \mathcal{O}\left(\left\{\epsilon^2, \frac{\epsilon^{1/2}V'''}{3H^2}\right\}\left(\ln\frac{a_iH_i}{k}\right)^2\right)\,, \tag{5.100}$$

$$\frac{\partial^2\varphi^a(t_i)}{\partial\varphi^b(t_k)\partial\varphi^c(t_k)} = F^{(2)}_{abc}\ln\,\frac{a_iH_i}{k} + \mathcal{O}\left(\left\{\epsilon^{5/2}, \frac{\epsilon V'''}{3H^2}, \frac{\epsilon^{1/2}V''''}{3H^2}\right\}\left(\ln\frac{a_iH_i}{k}\right)^2\right)\,, \tag{5.101}$$

$$\frac{\partial^3\varphi^a(t_i)}{\partial\varphi^b(t_k)\partial\varphi^c(t_k)\partial\varphi^d(t_k)} = F^{(3)}_{abcd}\ln\,\frac{a_iH_i}{k} + \mathcal{O}\left(\left\{\epsilon^3, \frac{\epsilon^{3/2}V'''}{3H^2}, \frac{\epsilon V''''}{3H^2}, \frac{\epsilon^{1/2}V'''''}{3H^2}\right\}\left(\ln\frac{a_iH_i}{k}\right)^2\right)\,, \tag{5.102}$$

where the primes in $\mathcal{O}(V''')$ etc. denote derivatives with respect any of the fields φ_a, and

$$F^{(2)}_{abc} = \sqrt{2}\left(-4\sqrt{\epsilon_a\epsilon_b\epsilon_c} + \eta_{ab}\sqrt{\epsilon_c} + \eta_{bc}\sqrt{\epsilon_a} + \eta_{ca}\sqrt{\epsilon_b} - \frac{1}{\sqrt{2}}\frac{V_{abc}}{3H^2}\right)\,, \tag{5.103}$$

$$\begin{aligned} F^{(3)}_{abcd} &= -4(\eta_{ad}\sqrt{\epsilon_b\epsilon_c} + \eta_{bd}\sqrt{\epsilon_c\epsilon_a} + \eta_{cd}\sqrt{\epsilon_a\epsilon_b}) \\ &\quad + \sqrt{\epsilon_d}\left(24\sqrt{\epsilon_a\epsilon_b\epsilon_c} - 4\eta_{ab}\sqrt{\epsilon_c} - 4\eta_{bc}\sqrt{\epsilon_a} - 4\eta_{ca}\sqrt{\epsilon_b} + \sqrt{2}\frac{V_{abc}}{3H^2}\right) \\ &\quad + \sqrt{2\epsilon_c}\frac{V_{abd}}{3H^2} + \sqrt{2\epsilon_a}\frac{V_{bcd}}{3H^2} + \sqrt{2\epsilon_b}\frac{V_{cad}}{3H^2} + \eta_{ab}\eta_{cd} + \eta_{bc}\eta_{ad} + \eta_{ca}\eta_{bd} - \frac{V_{abcd}}{3H^2}\,. \end{aligned} \tag{5.104}$$

Substituting these into Eq. (5.15),

$$n_{f,ab} = -\sum_c \frac{N_cF^{(2)}_{cab}}{N_{ab}}\,, \tag{5.105}$$

$$n_{g,abc} = -\sum_d\left(3\frac{N_{da}}{N_{abc}}F^{(2)}_{dbc} + \frac{N_d}{N_{abc}}F^{(3)}_{dabc}\right)\,, \tag{5.106}$$

we obtain fully explicit results for the parameters $n_{f,ab}$ and $n_{g,abc}$. The results are derived retaining only terms up to first order in $\ln(a_iH_i/k)$ in Eqs. (5.100) - (5.102). Higher order terms are suppressed by slow-roll parameters and their combinations with the derivatives of the potential. The former are small by construction and the latter also naturally remain small, provided that the flatness of the scalar field potential during inflation is not a result of extreme fine-tuning. Furthermore, since the logarithms never grow very large for the observable super-horizon modes, $\ln(a_iH_i/k) \lesssim \mathcal{O}(10)$, we conclude that the higher order contributions can indeed be neglected at first order.

5.8.2 On the different formulations of the δN approach

The δN expression for the super-horizon-scale curvature perturbation

$$\zeta_{\vec{k}}(t_f) = \sum_a N_a(t_f,t_i)\delta\varphi^a_{\vec{k}}(t_i) + \frac{1}{2}\sum_{ab}N_{ab}(t_f,t_i)\int\frac{d^3q}{(2\pi)^3}\,\delta\varphi^a_{\vec{q}}(t_i)\delta\varphi^b_{\vec{k}-\vec{q}}(t_i) + \cdots\,, \tag{5.107}$$

is by construction independent of the choice of the initial spatially flat hypersurface $t_i \geq t_k$. This property follows from the definition of the curvature perturbation [23] as demonstrated in [40]. A commonly used choice is to set t_i equal to the time t_k of horizon

crossing of the mode k. The analysis in [40] was performed using this choice. In our current work, we have instead chosen t_i as a time soon after t_k following e.g. [25]. Here we explicitly compare the two choices. For simplicity, we consider only terms up to second order in Eq. (5.107). Generalization to higher orders is straightforward.

Using the chain rule it is easy to switch between the coefficients $N_{ab..}(t_f, t_i)$ and $N_{ab..}(t_f, t_k)$ in the two different formulations. For the first and second order terms shown in Eq. (5.107) we obtain

$$N_a(t_f, t_i) \equiv \frac{\partial N(t_f, t_i)}{\partial \varphi^a(t_i)} = \sum_b \frac{\partial N(t_f, t_k)}{\partial \varphi^b(t_k)} \frac{\partial \varphi^b(t_k)}{\partial \varphi^a(t_i)} \,, \tag{5.108}$$

$$\begin{aligned} N_{ab}(t_f, t_i) \equiv & \frac{\partial^2 N(t_f, t_i)}{\partial \varphi^a(t_i) \partial \varphi^b(t_i)} = \sum_c \frac{\partial N(t_f, t_k)}{\partial \varphi^c(t_k)} \frac{\partial^2 \varphi^c(t_k)}{\partial \varphi^a(t_i) \partial \varphi^b(t_i)} \\ & + \sum_{cd} \frac{\partial \varphi^c(t_k)}{\partial \varphi^a(t_i)} \frac{\partial \varphi^d(t_k)}{\partial \varphi^b(t_i)} \frac{\partial^2 N(t_f, t_k)}{\partial \varphi^c(t_k) \partial \varphi^d(t_k)} \,. \end{aligned} \tag{5.109}$$

In the second equality of both equations we have replaced the time argument t_i in $N(t_f, t_i)$ by t_k making use of the fact that t_i and t_k both label spatially flat hypersurfaces. This implies that $N(t_i, t_k)$, the number of e-foldings from t_k to t_i, is a constant under differentiation with respect to the fields. Writing $N(t_f, t_i) = N(t_f, t_k) - N(t_i, t_k)$, we thus immediately see that $N(t_f, t_i)$ can be replaced by $N(t_f, t_k)$ in Eqs. (5.108) and (5.109).

Substituting Eqs. (5.108) and (5.109) into Eq. (5.107), we obtain

$$\begin{aligned} \zeta_{\vec{k}}(t_f) = & \sum_a N_a(t_f, t_k) \left(\frac{\partial \varphi^a(t_k)}{\partial \varphi^b(t_i)} \delta\varphi^b_{\vec{k}}(t_i) + \frac{1}{2} \frac{\partial^2 \varphi^a(t_k)}{\partial \varphi^b(t_i) \partial \varphi^c(t_i)} \int \frac{d^3q}{(2\pi)^3} \, \delta\varphi^b_{\vec{q}}(t_i) \delta\varphi^c_{\vec{k}-\vec{q}}(t_i) \right) \\ & + \frac{1}{2} \sum_{ab} N_{ab}(t_f, t_k) \left(\frac{\partial \varphi^a(t_k)}{\partial \varphi^c(t_i)} \frac{\partial \varphi^b(t_k)}{\partial \varphi^d(t_i)} \int \frac{d^3q}{(2\pi)^3} \, \delta\varphi^c_{\vec{q}}(t_i) \delta\varphi^d_{\vec{k}-\vec{q}}(t_i) \right) + \cdots \,. \end{aligned} \tag{5.110}$$

On the other hand, according to Eq. (5.4) we have

$$\delta\varphi^a_{\vec{k}}(t_k) = \frac{\partial \varphi^a(t_k)}{\partial \varphi^b(t_i)} \delta\varphi^b_{\vec{k}}(t_i) + \frac{1}{2} \frac{\partial^2 \varphi^a(t_k)}{\partial \varphi^b(t_i) \partial \varphi^c(t_i)} \int \frac{d^3q}{(2\pi)^3} \, \delta\varphi^b_{\vec{q}}(t_i) \delta\varphi^c_{\vec{k}-\vec{q}}(t_i) + \cdots \,. \tag{5.111}$$

In arriving at this result we have first taken the Fourier transform of Eq. (5.4) and only thereafter set one of the time arguments equal to t_k. Using Eq. (5.111) we can rewrite Eq. (5.110) as

$$\zeta_{\vec{k}}(t_f) = \sum_a N_a(t_f, t_k) \delta\varphi^a_{\vec{k}}(t_k) + \frac{1}{2} \sum_{ab} N_{ab}(t_f, t_k) \int \frac{d^3q}{(2\pi)^3} \, \delta\varphi^a_{\vec{q}}(t_k) \delta\varphi^b_{\vec{k}-\vec{q}}(t_k) + \cdots \,. \tag{5.112}$$

This way of writing $\zeta_{\vec{k}}(t_f)$ is equivalent to Eq. (5.107) and the two expressions differ formally only by the choice of the initial time t_i, as expected. The relation between the coefficients in the two formulations is given by Eqs. (5.108) and (5.109), and the field perturbations are related by Eq. (5.111). These results explicitly show how to switch from one formulation to another.

In [40], the result for $n_{f_{\rm NL}}$, measuring the scale dependence of $f_{\rm NL}$, was expressed in terms of the parameters $n_I = \mathrm{d} \ln N_I(t_f, t_k)/\mathrm{d} \ln k$ and $n_{IJ} = \mathrm{d} \ln N_{IJ}(t_f, t_k)/\mathrm{d} \ln k$, see e.g. Eq. (69) in that paper. (Here we follow the notation of [40] and label the scalar field species φ_I by capital letters. This also serves to distinguish the parameters n_I and n_{IJ}

from the quantities defined in the current work.) Using Eqs. (5.108) and (5.109) together with the results derived in Appendix 5.8.1, we readily obtain explicit expressions for these parameters

$$n_I = \frac{\mathrm{d}\ln N_I(t_f,t_k)}{\mathrm{d}\ln k} = -\sum_J \frac{N_J}{N_I}\,\epsilon_{IJ}\ , \tag{5.113}$$

$$n_{IJ} = \frac{\mathrm{d}\ln N_{IJ}(t_f,t_k)}{\mathrm{d}\ln k} = n_{f,IJ} - \sum_K \left(\frac{N_{IK}\,\epsilon_{KJ}}{N_{IJ}} + \frac{N_{JK}\,\epsilon_{KI}}{N_{IJ}}\right)\ . \tag{5.114}$$

In the rightmost expressions we have suppressed the time arguments t_i for brevity, e.g. $N_I \equiv N_I(t_f,t_i)$. Using these results, it is straightforward to check that the general expression given for $n_{f_{\rm NL}}$ in Eq. (69) of [40] agrees with our Eq. (5.24).

Chapter 6

A weak lensing view on primordial non-Gaussianities

The content of this chapter is published in [66].

We investigate the signature of primordial non-Gaussianities in the weak lensing bispectrum, in particular the signals generated by local, orthogonal and equilateral non-Gaussianities. The questions we address include the signal-to-noise ratio generated in the Euclid weak lensing survey (we find the 1σ-errors for $f_{\rm NL}$ are 200, 575 and 1628 for local, orthogonal and equilateral non-Gaussianities, respectively), misestimations of $f_{\rm NL}$ if one chooses the wrong non-Gaussianity model (misestimations by up to a factor of ± 3 in $f_{\rm NL}$ are possible, depending on the choice of the model), the probability of noticing such a mistake (improbably large values for the χ^2-functional occur from $f_{\rm NL} \sim 200$ on), degeneracies of the primordial bispectrum with other cosmological parameters (only the matter density Ω_m plays a significant role), and the subtraction of the much larger, structure-formation generated bispectrum. If a prior on a standard wCDM-parameter set is available from Euclid and Planck, the structure formation bispectrum can be predicted accurately enough for subtraction, and any residual structure formation bispectrum would influence the estimation of $f_{\rm NL}$ to a minor degree. Configuration-space integrations which appear in the evaluation of χ^2-functionals and related quantities can be carried out very efficiently with Monte-Carlo techniques, which reduce the complexity by a factor of $\mathcal{O}(10^4)$ while delivering sub-percent accuracies. Weak lensing probes smaller scales than the CMB and hence provide an additional constraint on non-Gaussianities, even though they are not as sensitive to primordial non-Gaussianities as the CMB.

6.1 Introduction

As cosmological data improves, it is becoming increasingly feasible to probe models of the early universe. In particular, primordial non-Gaussianity has emerged as a leading window onto the physics of inflation and the early universe (for reviews, see [45, 193, 194]). Although non-Gaussian perturbations could in principle take any form, in practice searching for just a few shapes of the bispectrum (3-point correlation function) allows one to discriminate between entire classes of models [18, 88, 195]. Many alternative models to inflation produce the same non-Gaussian shapes, and therefore can also be constrained at the same time.

The theory of primordial non-Gaussianities is very evolved, and predictions for non-Gaussianities in different observational channels have been made: number counts and large-scale structure statistics [49, 196–198], the cosmic microwave background even outside the Sachs-Wolfe regime [199, 200] and gravitational lensing [201–204].

Most constraints on non-Gaussianities are reported using CMB-observations, either by measuring the bispectrum of the temperature perturbation directly [183, 205–211], by measuring the skewness of weighted averaged CMB-patches [212] or by quantifying the corresponding Minkowski functionals [213–215]. The tightest bounds on the amplitude $f_{\rm NL}$ of the bispectrum, $-10 \leq f_{\rm NL} \leq 74$ has been obtained by [18].

So far, observational constraints on the weak lensing bispectrum [216, 217] mainly concerned the non-Gaussianities generated by structure formation and their breaking of the Ω_m-σ_8 degeneracy [218], and first results have been obtained using the skewness of the aperture-mass statistic [219, 220].

In this chapter we forecast the constraints which the weak lensing bispectrum will be able to make on primordial non-Gaussianity, especially with a view to Euclid. Although the constraints are not competitive with the CMB if the non-Gaussianities are scale independent, they are complementary since they probe smaller scales compared to the CMB and provide constraints on a possible scale-dependence [175]. A scale dependence of $f_{\rm NL}$ at the same order as the spectral index of the power spectrum is natural [65] and it may be much stronger, e.g. a "step–function" which is zero on large scales and large on small scales [221]. Weak lensing also has lower systematic errors than other large scale structure probes such as the galaxy bispectrum, scale dependent bias and cluster counts. Because the weak shear provides a linear mapping of the cosmic matter distribution, the statistical properties of the source field are conserved in the observable.

After a brief recapitulation of cosmology and structure formation in Sect. 6.2 we introduce primordial and structure formation non-Gaussianities in Sect. 6.3, in particular the bispectral shapes and the motivation for studying them. The mapping of non-Gaussianities by weak gravitational lensing is treated in Sect. 6.4, where we investigate the properties of the weak lensing bispectrum in its scale- and configuration dependence, and how it builds up as a function of survey depth. Statistical questions concerning the signal strength and misestimations of the non-Gaussianity parameter are addressed in Sect. 6.5, before we focus on systematic errors in the non-Gaussianity parameter due to incompletely removed structure formation non-Gaussianities in Sect. 6.6. We summarise our main results in Sect. 6.7 and provide visualisations of the weak lensing bispectrum sourced by different non-Gaussianity shapes in Appendix 6.8.1.

The reference cosmological model used is a spatially flat wCDM cosmology with Gaussian adiabatic initial perturbations for the cold dark matter density. The specific parameter choices are $\Omega_m = 0.25$, $n_s = 1$, $\sigma_8 = 0.8$, $\Omega_b = 0.04$ and $H_0 = 100\,h\,\mathrm{km/s/Mpc}$, with $h = 0.72$. The dark energy equation of state is constant in time with a value of $w = -0.9$.

6.2 Cosmology and structure formation

In spatially flat dark energy cosmologies with the matter density parameter Ω_m, the Hubble function $H(a) = \mathrm{d}\ln a/\mathrm{d}t$ is given by

$$\frac{H^2(a)}{H_0^2} = \frac{\Omega_m}{a^3} + \frac{1-\Omega_m}{a^{3(1+w)}} \quad , \tag{6.1}$$

for a constant dark energy equation of state-parameter w. Comoving distance χ and scale factor a are related by

$$\chi = c \int_a^1 \frac{\mathrm{d}a}{a^2 H(a)} \quad , \tag{6.2}$$

such that the comoving distance is given in units of the Hubble distance $\chi_H = c/H_0$. For the linear matter power spectrum $P(k)$ which describes the Gaussian fluctuation properties of the linearly evolving density field δ,

$$\langle \delta(\vec{k}) \delta(\vec{k}') \rangle = (2\pi)^3 \, \delta^{(3)}(\vec{k} + \vec{k}') \; P(k) \tag{6.3}$$

the ansatz $P(k) \propto k^{n_s} T^2(k)$ is chosen with the transfer function $T(k)$, which is well approximated by the fitting formula

$$T(q) = \frac{\ln(1 + 2.34q)}{2.34q} \times p(q)^{-1/4} \quad , \tag{6.4}$$

for low-matter density cosmologies [222]. The polynomial $p(q)$ is given by $p(q) = 1 + 3.89q + (16.1q)^2 + (5.46q)^3 + (6.71q)^4$. The wave vector $k = q\Gamma$ enters rescaled by the shape parameter Γ [223],

$$\Gamma = \Omega_m \, h \, \exp\left[-\Omega_b \left(1 + \frac{\sqrt{2h}}{\Omega_m} \right) \right] \quad . \tag{6.5}$$

The fluctuation amplitude is normalised to the value σ_8 on the scale $R = 8$ Mpc$/h$,

$$\sigma_R^2 = \frac{1}{2\pi^2} \int \mathrm{d}k \, k^2 \, W_R^2(k) \; P(k) \quad , \tag{6.6}$$

with a Fourier-transformed spherical top-hat $W_R(k) = 3j_1(kR)/(kR)$ as the filter function. $j_\ell(x)$ denotes the spherical Bessel function of the first kind of order ℓ [224]. The linear growth of the density field, $\delta(\vec{x}, a) = D_+(a)\delta(\vec{x}, a = 1)$, is described by the growth function $D_+(a)$, which is the solution to the growth equation [225–227],

$$\frac{\mathrm{d}^2}{\mathrm{d}a^2} D_+(a) + \frac{1}{a} \left(3 + \frac{\mathrm{d} \ln H}{\mathrm{d} \ln a} \right) \frac{\mathrm{d}}{\mathrm{d}a} D_+(a) = \frac{3}{2a^2} \, \Omega_m(a) \; D_+(a) \quad . \tag{6.7}$$

6.3 Non-Gaussianities

6.3.1 Primordial non-Gaussianities

We write the primordial bispectra in terms of the Bardeen curvature perturbation Φ [12, 20], which may be related to the primordial curvature perturbation $\zeta = 5\Phi/3$ (see e.g. chapter 8 in [14]) and the CMB temperature anisotropy in the Sachs-Wolfe limit $\Delta T/T = -\Phi/3$ [33]. The bispectrum of Φ is defined by

$$\langle \Phi(\vec{k}_1) \Phi(\vec{k}_2) \Phi(\vec{k}_3) \rangle = (2\pi)^3 \, \delta^{(3)}(\vec{k}_1 + \vec{k}_2 + \vec{k}_3) \; B_\Phi(k_1, k_2, k_3) \quad . \tag{6.8}$$

We will be particularly interested in three bispectral shapes, which cover the expected shape from a wide range of inflationary models [45]. They are defined as:

1. **Local shape.** This is defined by

$$B_\Phi^{local}(k_1,k_2,k_3) = 2A^2\, f_{\rm NL}^{local}\, \left(k_1^{n_s-4}k_2^{n_s-4} + (2\ perm)\right) \quad , \tag{6.9}$$

where the amplitude A is defined by $P_\Phi(k) = Ak^{n_s-1}$. It may arise through a simple Taylor expansion about the Gaussian (linearised) perturbation $\Phi(x) = \Phi_G(x) + f_{\rm NL}\Phi_G^2$, although this is not the most general ansatz for Φ which gives rise to the local bispectrum. The local shape typically arises from super-horizon evolution of the curvature perturbation ($k \ll aH$), which occurs for example in some multifield inflation models [146,228], during modulated reheating [166], in the curvaton scenario [30] (the last three models are closely connected [229]), as well as the ekpyrotic scenario [230] and non-local inflation [231].

2. The **equilateral shape** is given by

$$\begin{aligned} B_\Phi^{equil}(k_1,k_2,k_3) = 6A^2 f_{\rm NL}^{equil} \Big(&-2\,(k_1k_2k_3)^{2(n_s-4)/3} \\ &- \left[(k_1k_2)^{(n_s-4)} + (2\ perm)\right] \\ &+ \left[k_1^{(n_s-4)/3}k_2^{2(n_s-4)/3}k_3^{n_s-4} + (5\ perm)\right]\Big) \quad . \end{aligned} \tag{6.10}$$

This shape typically arises in models with non-canonical kinetic terms, the most studied example being Dirac-Born-Infeld inflation [232, 233]. Also various other models can produce this shape [234–238].

3. The **orthogonal shape** is given by [239]

$$\begin{aligned} B_\Phi^{ortho}(k_1,k_2,k_3) = 6A^2 f_{\rm NL}^{ortho} \Big(&-8\,(k_1k_2k_3)^{2(n_s-4)/3} \\ &- 3\left[(k_1k_2)^{(n_s-4)} + (2\ perm)\right] \\ &+ 3\left[k_1^{(n_s-4)/3}k_2^{2(n_s-4)/3}k_3^{n_s-4} + (5\ perm)\right]\Big) \quad , \end{aligned} \tag{6.11}$$

and it was constructed in order to be orthogonal to both the equilateral shape and to a lesser extent the local shape.

The local model is maximised for squeezed triangles $k_1 \ll k_2 \simeq k_3$, the equilateral model is maximised for equilateral triangles $k_1 \simeq k_2 \simeq k_3$ while the orthogonal model receives contributions from a broader range of triangles. Another frequently considered shape is the enfolded one, which is maximised for "flattened" isosceles triangles $k_1 \simeq k_2 \simeq k_3/2$, but this can be written as a linear combination of the three shapes above. We note that although the above three shapes cover many classes of non-Gaussian models, there do exist other shapes which cannot be written as a combination of the above three shapes including localised or oscillating bispectra, which may be caused by a feature in the inflatons potential [240,241], particle production while observable modes are crossing the horizon [242] (but a burst of particle production later in inflation generates local non-Gaussianity, [243]), or an inflaton potential with superimposed oscillations [244, 245].

Because $f_{\rm NL}$ for all three shapes is normalised to an equilateral triangle, but the signal-to-noise is maximised for different triangle shapes depending on the configuration it is not surprising that the error bars on the three shapes are significantly different [246]. In line with this expectation, we find that weak lensing can constrain the local model most tightly

and the equilateral model least well. When investigating relative magnitudes between structure formation bispectra and primordial ones, we restrict ourselves to the equilateral case, as all primordial bispectra have equal values for this configuration. An alternative normalisation was proposed by [246].

A mild scale dependence of $f_{\rm NL}$ is natural, for both the local model [65, 189, 247], and the equilateral and orthogonal models [174, 248–250], and it may be much stronger, e.g. a "step–function" which is zero on large scales and large on small scales [221]. Although we treat $f_{\rm NL}$ as constant in this chapter, the motivation for considering scale-dependence is important because weak lensing probes smaller scales than the CMB and hence the CMB bounds may not apply here, see Sec. 6.4. Observational probes have been considered in [54, 175, 251, 252].

For converting the bispectrum of the potential fluctuations to those of the density field we use the Newtonian Poisson equation for each occurence of the potential in the bispectrum [253],

$$\Delta\Phi = \frac{3}{2}\frac{\Omega_m}{\chi_H^2}\delta \;\longrightarrow\; \delta(k,a) = \frac{2}{3\Omega_m}\,D_+(a)\,(\chi_H k)^2\,T(k)\,\Phi(k) \quad . \tag{6.12}$$

The horizon entry of each mode is governed by the transfer function $T(k)$ and it grows $\propto D_+(a)$ in the linear regime, such that

$$B_\delta(k_1,k_2,k_3,a) = \prod_{i=1}^{3}\left(\frac{2}{3\Omega_m}\,D_+(a)\,(\chi_H k_i)^2\,T(k_i)\right)\,B_\Phi(k_1,k_2,k_3) \quad . \tag{6.13}$$

We choose the normalisation factor A to be consistent for each linearly evolving mode of the density field with our definition of σ_8.

6.3.2 Non-Gaussianities from structure formation

Nonlinear processes in structure formation break the homogeneity of the growth equation and generate non-Gaussian features in the initially close to Gaussian density field. From Eulerian perturbation theory (see [254–257]), the first order contribution to the bispectrum $B_\delta(\vec{k}_1,\vec{k}_2,\vec{k}_3)$ (for an introduction, see [258, 259]) of the density field from nonlinear structure formation is given by:

$$B_\delta(\vec{k}_1,\vec{k}_2,\vec{k}_3,a) = \sum_{\substack{i,j=1,2,3\\ i\neq j}} D_+^4(a)\,M(\vec{k}_i,\vec{k}_j)\,P(k_i)\,P(k_j) \quad , \tag{6.14}$$

where the classical mode coupling function is $M(\vec{k}_i,\vec{k}_j)$

$$M(\vec{k}_i,\vec{k}_j) = \frac{10}{7} + \left(\frac{k_i}{k_j}+\frac{k_j}{k_i}\right)x + \frac{4}{7}x^2 \quad . \tag{6.15}$$

$x = \vec{k}_i\vec{k}_j/(k_ik_j)$ denotes the cosine between the wave vectors $\vec{k}_i$ and $\vec{k}_j$. Due to the fact that $P(k,a)$ grows $\propto D_+^2(a)$ in linear structure formation, the bispectrum scales with $D_+^4(a)$ in lowest order perturbation theory. In terms of non-Gaussianity parameters and configuration dependences, structure formation non-Gaussianities are strongest for the squeezed configuration because the mode coupling function $M(\vec{k}_i,\vec{k}_j)$ assumes the largest values for parallel wave vectors (with the cosine being one, $x=1$), and therefore resembles non-Gaussianities of the local type. Their strength in the weak shear bispectrum corresponds to an $f_{\rm NL}$-parameter of $\mathcal{O}(10^4)$, i.e. two orders of magnitude larger than the primordial non-Gaussianities weak lensing can probe.

6.4 Weak gravitational lensing

6.4.1 Convergence spectrum

The weak lensing convergence κ follows from a line-of-sight integration weighted with the lensing efficiency $W_\kappa(\chi)$ (for reviews, see [260, 261]),

$$\kappa = \int_0^{\chi_H} \mathrm{d}\chi \, W_\kappa(\chi) \, \delta \tag{6.16}$$

and reflects, because of its linearity, all statistical properties of the density field δ. The weak lensing efficiency is given by

$$W_\kappa(\chi) = \frac{3\Omega_m}{2a} \, \frac{1}{\chi_H^2} \, G(\chi) \, \chi \quad , \tag{6.17}$$

with the weighted distance distribution $G(\chi)$ of the lensed galaxies,

$$G(\chi) = \int_\chi^{\chi_H} \mathrm{d}\chi' \, q(z) \frac{\mathrm{d}z}{\mathrm{d}\chi'} \frac{\chi' - \chi}{\chi'} \quad . \tag{6.18}$$

The spectrum $C_\kappa(\ell)$ then results from applying Limber's equation [262],

$$C_\kappa(\ell) = \int_0^{\chi_H} \frac{\mathrm{d}\chi}{\chi^2} \, W_\kappa^2(\chi) P(k = \ell/\chi, a) \quad . \tag{6.19}$$

For the galaxy redshift distribution $q(z)$ we assume a standard shape,

$$q(z) = q_0 \left(\frac{z}{z_0}\right)^2 \exp\left(-\left(\frac{z}{z_0}\right)^\beta\right) \mathrm{d}z \qquad \text{with} \qquad \frac{1}{q_0} = \frac{z_0}{\beta} \, \Gamma\left(\frac{3}{\beta}\right), \tag{6.20}$$

with the median redshift set to 0.9, as projected for Euclid.

6.4.2 Convergence bispectrum

Similarly as in the case of the weak shear spectrum $C_\kappa(\ell)$ we use the Limber-equation in the flat-sky approximation,

$$B_\kappa(\vec{\ell}_1, \vec{\ell}_2, \vec{\ell}_3) = \int_0^{\chi_H} \frac{\mathrm{d}\chi}{\chi^4} \, W^3(\chi) \, B_\delta(\vec{k}_1, \vec{k}_2, \vec{k}_3, a) \quad , \tag{6.21}$$

with $\vec{k}_p = \vec{\ell}_p/\chi$, $p = 1, 2, 3$, for projection of the flat-sky convergence bispectrum B_κ [219,263–267]. The spherical bispectrum $B_\kappa(\ell_1, \ell_2, \ell_3)$ is related to the flat-sky bispectrum $B_\kappa(\vec{\ell}_1, \vec{\ell}_2, \vec{\ell}_3)$ by [268, 269]

$$B_\kappa(\ell_1, \ell_2, \ell_3) \simeq \begin{pmatrix} \ell_1 & \ell_2 & \ell_3 \\ 0 & 0 & 0 \end{pmatrix} \sqrt{\frac{\prod_{p=1}^3 (2\ell_p + 1)}{4\pi}} B_\kappa(\vec{\ell}_1, \vec{\ell}_2, \vec{\ell}_3) \quad , \tag{6.22}$$

where

$$\begin{pmatrix} \ell_1 & \ell_2 & \ell_3 \\ 0 & 0 & 0 \end{pmatrix}^2 = \frac{1}{2} \int_{-1}^{+1} \mathrm{d}x \, P_{\ell_1}(x) \, P_{\ell_2}(x) \, P_{\ell_3}(x) \tag{6.23}$$

denotes the Wigner-3j symbol, which results from integrating over three Legendre polynomials $P_\ell(x)$ $(x = \cos\theta)$. The Wigner-3j symbol nulls configurations which would violate the triangle inequality, $|\ell_i - \ell_j| \leq \ell_k \leq |\ell_i + \ell_j|$ [224]. The factorials in the Wigner-3j symbol are evaluated using the Stirling approximation for the Γ-function,

$$\Gamma(n+1) = n! \quad \text{with} \quad \Gamma(x) \simeq \sqrt{2\pi}\,\exp(-x)\,x^{x-\frac{1}{2}} \quad , \tag{6.24}$$

for $x \gg 1$ [224]. At this point, it is appropriate to recall two important issues related to the weak shear bispectrum as a line of sight-integrated quantity: The line-of-sight integration causes the non-Gaussianities in the convergence to be weaker than that of the source field, as a consequence of the central limit theorem, because many uncorrelated lensing effects (if the Born approximation is invoked and lens-lens coupling is neglected, see [270–273]) add up to the signal [204]. Secondly, the evaluation of the wave vector $k = \ell/\chi$ in the source field bispectrum B_δ generates a mixing of scales when the distance χ runs over the integration range such that the observed weak lensing bispectrum is a superposition of density field bispectra of varying scale and fixed projected configuration.

6.4.3 Properties of the weak lensing bispectrum

Fig. 6.9 in Appendix 6.8.1 gives a 3-dimensional visual impression of the three different bispectra as observed by weak shear. The weak shear bispectra are given as dimensionless bispectra, by multiplication with the prefactor $(\ell_1\ell_2\ell_3)^{4/3} \sim \ell^4$. There are clear differences in the configuration dependence: Local non-Gaussianities provide large amplitudes for squeezed configurations, i.e. in the corners of the domain admissible by the triangle inequality, orthogonal non-Gaussianities are largest for folded configurations and the equilateral bispectra assume large values if the three multipole orders are equal.

Fig. 6.1 illustrates the contribution $\mathrm{d}C_\kappa(\ell)/\mathrm{d}\chi$ to the spectrum and the contribution $\mathrm{d}B_\kappa(\ell,\ell,\ell)/\mathrm{d}\chi$ to the equilateral bispectrum as a function of comoving distance. For the relevant range of multipoles, modes with wave numbers in the range $0.1 \ldots 1$ Mpc$/h$ are being probed by weak shear, which are larger than those wave numbers measurable in the primary CMB bispectrum and emphasises the necessity of measuring $f_{\rm NL}$ in its scale dependence, in a similar way as advocated by [175] for number counts.

The skewness parameters $S_\kappa(\ell)$ are defined as the ratio between the squared equilateral bispectrum and the cubed spectrum,

$$S_\kappa(\ell) = \sqrt{\frac{B_\kappa^2(\ell,\ell,\ell)}{C_\kappa^3(\ell)}} \quad . \tag{6.25}$$

$S_\kappa(\ell)$ is proportional to $f_{\rm NL}$ (and to σ_8 to lowest order) and is independent of Ω_m. It will become relevant for the signal-to-noise ratio $\Sigma(\ell)$ (see eqn. 6.26 in Sect. 6.5.1). These skewness-parameters are depicted in Fig. 6.2 as a function of median redshift $z_{\rm med}$ of the lensing survey for both the primordial and the structure formation induced weak lensing bispectrum. The skewness parameters increase with increasing survey depth and in case of primordial non-Gaussianities saturate at redshifts of unity, which is an effect of the time evolution of the gravitational potential being mapped out by weak lensing, as perturbations in the potentials decay in the dark energy-dominated phase and are constant in the matter-dominated phase. Structure formation non-Gaussianities decrease slightly for deeper reaching surveys, which is caused by the fact that the structure formation skewness's are building up during Ω_m-domination, as they scale $\propto D_+^4/a^3 \sim a$ in contrast

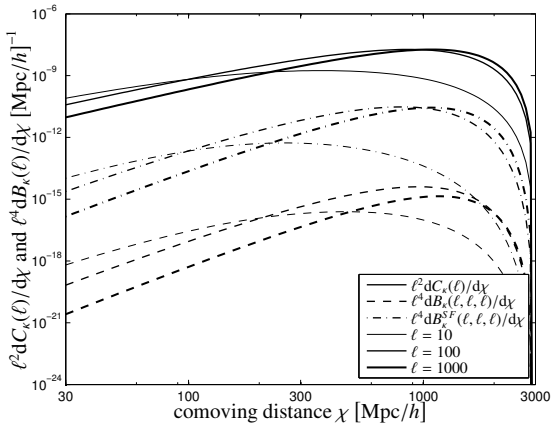

Figure 6.1: Contributions $\ell^2 \mathrm{d}C_\kappa(\ell)/\mathrm{d}\chi$ to the lensing spectrum (solid line), and $\ell^4 \mathrm{d}B_\kappa(\ell,\ell,\ell)/\mathrm{d}\chi$ to the lensing bispectra for both primordial non-Gaussianities (dashed line, $f_{\rm NL} = 1$) and structure formation non-Gaussianities (dash-dotted line), for $\ell = 10$ (thin lines), $\ell = 100$ (medium lines) and $\ell = 1000$ (thick lines). The bispectra are plotted for the equilateral configuration.

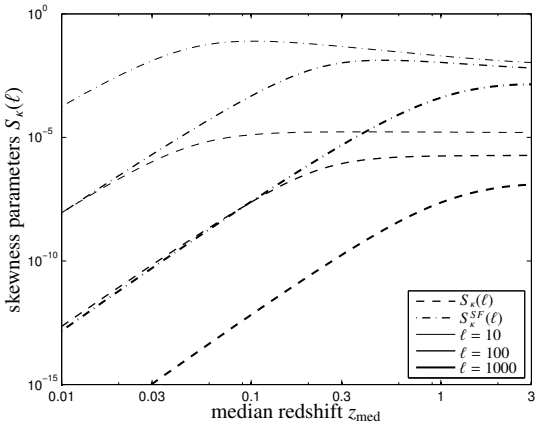

Figure 6.2: Skewness parameter $S_\kappa(\ell)$ for both primordial non-Gaussianities (dashed line, $f_{\rm NL} = 1$) and structure formation non-Gaussianities (dash-dotted line) as a function of the survey depth, for $\ell = 10$ (thin lines), $\ell = 100$ (medium lines) and $\ell = 1000$ (thick lines).

to primordial non-Gaussianities in the potential, which are constant with their scaling $\propto (D_+(a)/a)^3 \sim$ const. The plot suggests that with the redshift range probed by Euclid the largest-possible skewness's are being observed.

6.5 Statistics

6.5.1 What signal-to-noise ratio can one expect?

The cumulative signal-to-noise ratio $\Sigma(\ell)$ for the weak lensing bispectrum $B_\kappa(\ell_1, \ell_2, \ell_3)$ up to multipole order ℓ is given by [263]

$$\Sigma^2(\ell) = \sum_{\ell_1=\ell_{\rm min}}^{\ell} \sum_{\ell_2=\ell_{\rm min}}^{\ell} \sum_{\ell_3=\ell_{\rm min}}^{\ell} \frac{B_\kappa^2(\ell_1,\ell_2,\ell_3)}{\mathrm{cov}(\ell_1,\ell_2,\ell_3)} \quad . \tag{6.26}$$

The summation is carried out with the condition $\ell_1 \leq \ell_2 \leq \ell_3$ [266], such that the covariance becomes

$$\mathrm{cov}(\ell_1,\ell_2,\ell_3) = \frac{\Delta(\ell_1,\ell_2,\ell_3)}{f_{\rm sky}}\, \tilde{C}(\ell_1)\, \tilde{C}(\ell_2)\, \tilde{C}(\ell_3) \quad , \tag{6.27}$$

where the function $\Delta(\ell_1, \ell_2, \ell_3)$ counts the multiplicity of triangle configurations and is defined as

$$\Delta(\ell_1,\ell_2,\ell_3) = \begin{cases} 6, & \ell_1 = \ell_2 = \ell_3 \\ 2, & \ell_i = \ell_j \text{ for } i \neq j \\ 1, & \ell_1 \neq \ell_2 \neq \ell_3 \neq \ell_1 \end{cases} \quad . \tag{6.28}$$

$f_{\rm sky}$ denotes the fraction of the observed sky and is set to $f_{\rm sky} = 1/2$ for Euclid. The observed spectra

$$\tilde{C}(\ell) = C(\ell) + \frac{\sigma_\epsilon^2}{n} \quad , \tag{6.29}$$

with the number density of ellipticity measurements per steradian n, which is set to 40 galaxies per squared arcminute, corresponding to the projected Euclid performance. Instead of a direct summation over ℓ_1, ℓ_2, ℓ_3 we use a Monte-Carlo integration technique and consider the evaluation of eqn. (6.26) as a three-dimensional integration, for which we use publicly available CUBA-library [274].

The cumulative signal-to-noise ratio $\Sigma(\ell)$ for a measurement of the weak shear bispectrum is depicted in Fig. 6.3 as a function of ℓ and for all three non-Gaussianity types. As the signal strength Σ is proportional to the non-Gaussianity parameter $f_{\rm NL}$, it is convenient to plot the ratio $\Sigma(\ell)/f_{\rm NL}$. The plot suggests that weak lensing bispectra sourced by primordial non-Gaussianities could only be measured with Euclid for $f_{\rm NL}$ significantly larger than 100. Orthogonal bispectra are weaker by a factor of 3 compared to local bispectra, and equilateral bispectra generate the weakest signal, being a factor of 8 weaker than local non-Gaussianities. The four different MC-integration algorithms agree well in their results for $\Sigma(\ell)$, and when the number of sampling points is chosen to be $\propto \ell$, the algorithms retain accuracies, indicating that the adaptive algorithms take account of the symmetry properties of the integrand. At $\ell = 1000$, is is sufficient to compute $\mathcal{O}(10^5)$ samples, which reduces the number of evaluations of the integrand by a factor of 10^4 compared to the exact evaluation, which would require $\mathcal{O}(10^9)$ evaluations, for precisions on the sub-percent level. We will restrict ℓ-space integrations to multipoles $\lesssim 1000$, because the increase in signal when extending the ℓ-range is marginal for primordial non-Gaussianities and additionally, it helps to avoid scales influenced by baryonic physics and intrinsic alignments [275, 276].

The configuration dependence of the contribution to the integrated signal is given in Fig. 6.9 (Appendix 6.8.1) for the three bispectrum types considered here. The panels show the weak shear bispectrum in units of the noise, $B_\kappa(\ell_1,\ell_2,\ell_3)/\sqrt{\mathrm{cov}(\ell_1,\ell_2,\ell_3)}$ as a function of ℓ_1, ℓ_2 and ℓ_3. While the local non-Gaussianity provides the largest contributions for squeezed configurations, the orthogonal non-Gaussianity shows a much uniformer contribution throughout ℓ-space, and the equilateral non-Gaussianity is only providing significant amplitudes for very small values of ℓ. This behavior is reflected in in the cumulative signal-to-noise ratio, as shown in Fig. 6.3. From the signal-to-noise ratios one can already estimate the accuracy for a measurement of $f_{\rm NL}$. The conditional Cramér-Rao bounds $\sigma_{f_{\rm NL}} = 1/\sqrt{F_{f_{\rm NL}f_{\rm NL}}}$ on the non-Gaussianity parameter (which are at the same time the non-Gaussianities required to generate a signal of unity) are $\sigma_{f_{\rm NL}} = 200$ (local), $\sigma_{f_{\rm NL}} = 575$ (orthogonal) and $\sigma_{f_{\rm NL}} = 1628$ (equilateral) which is significantly weaker than other probes such as the primary CMB, due to the Gaussianising effect of the line-of-sight integrations [204].

6.5.2 Would one misestimate $f_{\rm NL}$ using the wrong bispectrum?

The χ^2-functional constructed for measuring the noise-weighted mismatch between the true bispectrum B_κ^t and the wrongly assumed bispectrum B_κ^w for interpreting the data reads:

$$\chi^2 = \sum_{\ell_1=\ell_{\rm min}}^{\ell} \sum_{\ell_2=\ell_{\rm min}}^{\ell} \sum_{\ell_3=\ell_{\rm min}}^{\ell} \frac{\left[\alpha B_\kappa^w(\ell_1,\ell_2,\ell_3) - B_\kappa^t(\ell_1,\ell_2,\ell_3)\right]^2}{\mathrm{cov}(\ell_1,\ell_2,\ell_3)} \tag{6.30}$$

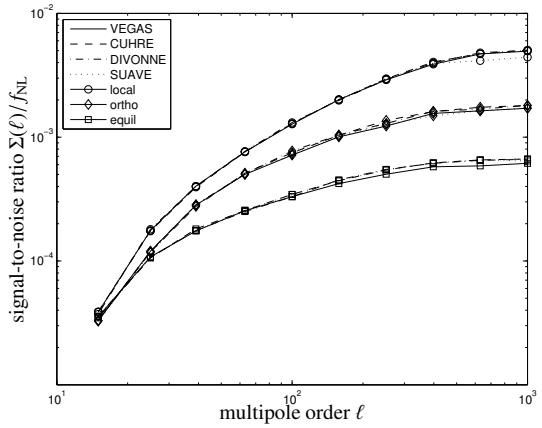

Figure 6.3: Cumulative signal-to-noise ratio $\Sigma(\ell)/f_{\rm NL}$ as a function of maximum multipole order ℓ, for local (circles), orthogonal (lozenges) and equilateral (squares) non-Gaussianities. The figure compares the result from different Monte-Carlo integration routines.

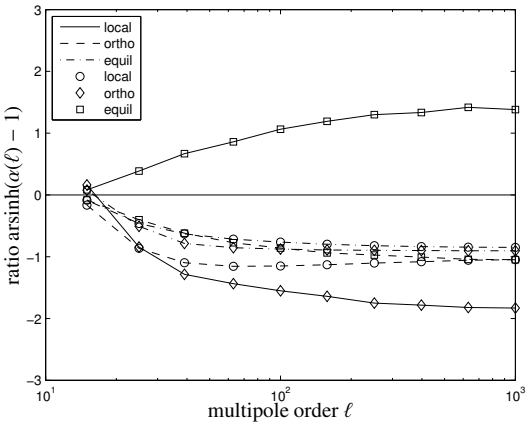

Figure 6.4: The ratio $\alpha(\ell)$ of inferred $f_{\rm NL}$-value to the true $f_{\rm NL}$-value as a function of maximum multipole order ℓ. The true non-Gaussianity model is indicated by the line style, whereas the wrongly chosen non-Gaussianity model is given by the marker style: local (circles, solid lines), orthogonal (lozenges, dashed lines) and equilateral (squares, dash-dotted lines) non-Gaussianities.

and yields the best fitting α from the minimisation $\partial\chi^2/\partial\alpha = 0$.

The variable α measures the ratio between the wrongly inferred non-Gaussianity parameter $f_{\rm NL}$ and the true value, and is given by Fig. 6.4 as a function of maximum multipole order considered in the integration of the χ^2-functional. For weak signals this ratio is very close to unity, and differences emerge when the integration is carried out to larger multipoles, and the signal becomes stronger. Misestimations in $f_{\rm NL}$ up to half an order of magnitude appear possible, including wrong signs for $f_{\rm NL}$-estimates. Most combinations of B_κ^t and B_κ^w yield very small values for the estimated $f_{\rm NL}$-parameter (equivalently, $\alpha \simeq -1$) when choosing the wrong non-Gaussianity. Again, the evaluations necessary for determining α are carried out as an MC-integration with the CUBA-library [274].

6.5.3 Would one notice fitting the wrong bispectrum?

Now, the question appears if one would notice the assumption of a wrong primordial bispectrum when fitting for the non-Gaussianity parameter $f_{\rm NL}$. This can be quantified by the probability q of obtaining data more extreme than the one at hand. This probability q (Fisher's p-value) is given as a function of the true $f_{\rm NL}$ under the assumption of a Gaussian likelihood, which is well justified given the very large number of degrees of freedom (although doubts have been raised about how accurate this is, see [277]). As shown in Fig. 6.5 for all combinations between true non-Gaussianity types and wrongly fitted non-Gaussianity models, this probability drops very rapidly towards very small numbers for $f_{\rm NL}$-values of a few hundred, indicating that it would be very difficult to reconcile non-Gaussianities of that strength with observations if the wrong non-Gaussianity model had been chosen. For $f_{\rm NL}$-values smaller than 100 the signal is so weak that no significant discrepancies between data and model appear, for any type of non-Gaussianity.

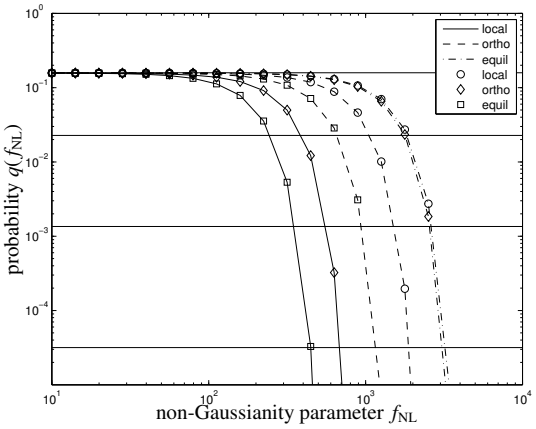

Figure 6.5: Probability $q(f_{\rm NL})$ of obtaining data as extreme as a wrong fit to the weak lensing bispectrum by choosing the wrong non-Gaussianity model (indicated by the line style) to data (indicated by the marker style): local (circles, solid lines), orthogonal (lozenges, dashed lines) and equilateral (squares, dash-dotted lines) non-Gaussianities. The horizontal lines indicate $1, 2, 3, 4\sigma$ confidence intervals and ℓ has been set to 1000.

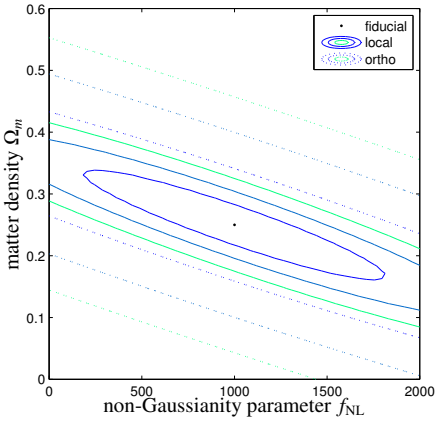

Figure 6.6: 1σ, 2σ and 3σ-constraints on the non-Gaussianity parameter $f_{\rm NL}$ and the matter density Ω_m, for the local non-Gaussianity (solid lines) and the orthogonal non-Gaussianity (dotted lines) at $\ell = 1000$, from a numerical MC-integration of the Fisher-matrix.

6.5.4 Do parameter constraints depend on non-Gaussianity?

The Fisher-matrix formalism [278] is widely used in cosmology for deriving parameter forecasts, and requires in the case of the bispectrum as the signal-to-noise ratio the summation over all triangle configurations:

$$F_{\mu\nu} = \sum_{\ell_1=\ell_{\rm min}}^{\ell} \sum_{\ell_2=\ell_{\rm min}}^{\ell} \sum_{\ell_3=\ell_{\rm min}}^{\ell} \frac{\partial B_\kappa}{\partial x_\mu} \frac{1}{{\rm cov}(\ell_1,\ell_2,\ell_3)} \frac{\partial B_\kappa}{\partial x_\nu} \quad . \tag{6.31}$$

The explicit summation can be replaced by a $\mathrm{d}^3\ell$-integration, which can be carried out using the MC-technique outlined in Sect. 6.5.1. Resulting simultaneous constraints on Ω_m and $f_{\rm NL}$ from the weak shear bispectrum sourced only by primordial non-Gaussianities with no other priors are given in Fig. 6.6 for local and orthogonal models at a reference $f_{\rm NL} = 1000$. The equilateral bispectrum does not constrain the parameter pair in a meaningful way due to the weak signal.

6.6 Systematics due to structure formation

6.6.1 Can one subtract the structure formation bispectrum?

Naturally, the small primordial non-Gaussianities are superseded by much stronger non-Gaussianities due to nonlinearities in the cosmic structure formation processes, which affects the measurability of $f_{\rm NL}$. There exists an accurate description of the structure formation bispectrum provided by Eulerian perturbation theory on the scales of interest (compare Sect. 6.3.2, and [255]), if the cosmology is known – but there are always

uncertainties in the cosmological parameter set, which would result in an uncertainty in predicting the structure formation bispectrum. If the structure formation bispectrum is not properly subtracted from the observed bispectrum, there will be errors in the estimation of the non-Gaussianity parameter $f_{\rm NL}$ for the primordial bispectrum, which can be quantified with the χ^2-functional,

$$\chi^2 = \sum_{\ell_1=\ell_{\rm min}}^{\ell} \sum_{\ell_2=\ell_{\rm min}}^{\ell} \sum_{\ell_3=\ell_{\rm min}}^{\ell} \frac{\left[\alpha B_\kappa^t(\ell_1,\ell_2,\ell_3) - \Delta B_\kappa(\ell_1,\ell_2,\ell_3)\right]^2}{{\rm cov}(\ell_1,\ell_2,\ell_3)} \quad , \tag{6.32}$$

describing the fit of a primordial bispectrum B_κ^t to data ΔB_κ,

$$\Delta B_\kappa(\ell_1,\ell_2,\ell_3) = B_\kappa^t(\ell_1,\ell_2,\ell_3) + B_\kappa^{t,{\rm SF}}(\ell_1,\ell_2,\ell_3) - B_\kappa^{w,{\rm SF}}(\ell_1,\ell_2,\ell_3) \tag{6.33}$$

which contain the true primordial bispectrum B_κ^t itself, the very large structure formation bispectrum $B^{t,{\rm SF}}$ for the true cosmology, from which the structure formation bispectrum $B^{w,{\rm SF}}$ has been subtracted, possibly incompletely, by assuming the wrong cosmology. Derivation $\partial\chi^2/\partial\alpha = 0$ yields the best fitting α, which is related to the misestimated $f_{\rm NL}^w = \alpha f_{\rm NL}$ and the deviation from the true non-Gaussianity $\delta = \alpha - 1$.

Distributions $p(\delta){\rm d}\delta$ have been derived for all bispectrum types by drawing 10^3 samples from a Gaussian likelihood for the parameters Ω_m, σ_8, h, n_s and w of a standard spatially flat dark energy model. The covariance matrix has been constructed using the icosmo resource for the Euclid weak lensing and BAO data [279], and provides an excellent prior on the cosmological parameters. By this sampling process of δ it is possible to propagate the entire uncertainty in the cosmological parameter set onto the estimate of $f_{\rm NL}$. As shown by Fig. 6.7, the resulting distribution is very close to Gaussian, with zero mean and standard deviations of $\sigma_{f_{\rm NL}} = 119$ (local), $\sigma_{f_{\rm NL}} = 372$ (orthogonal) and $\sigma_{f_{\rm NL}} = 511$ (equilateral), which is similar to the statistical uncertainty of measuring $f_{\rm NL}$ and thus constitutes a serious error. The width of the distributions are independent of the true value $f_{\rm NL}$, and the relative error $\delta/f_{\rm NL}$ scales $\propto 1/f_{\rm NL}$. Misestimates of that magnitude make it very difficult to assign a primordial origin to a non-zero residual bispectrum, given the current bounds on $f_{\rm NL}$. All integrations were computed up to $\ell = 1000$.

6.6.2 What happens if a better prior is available?

The uncertainty in predicting the weak shear bispectrum generated by nonlinear structure formation can be reduced if a stronger prior on the cosmological parameter set is available or if the complexity of the model is reduced, e.g. if the wCDM dark energy cosmology would be replaced by the simpler ΛCDM cosmology. Fig. 6.8 illustrates the distributions $p(\delta){\rm d}\delta$ of the difference δ between the inferred non-Gaussianity parameter and the true parameter, if the contamination of the bispectrum is computed by drawing 10^3 sample wCDM cosmologies from a Gaussian likelihood whose covariance matrix incorporates constraints from Euclid weak shear spectra, Euclid baryon acoustic oscillations and in addition Planck's constraints from the observation of primary CMB temperature and polarisation spectra. In comparison to the distributions shown in Fig. 6.7, the width is now much reduced, by about a factor of 4, allowing measurements down to smaller values for $f_{\rm NL}$. The specific uncertainties are $\sigma_{f_{\rm NL}} = 29$ (local), $\sigma_{f_{\rm NL}} = 98$ (orthogonal) and $\sigma_{f_{\rm NL}} = 149$ (equilateral), all stated as standard deviations of the distribution $p(\delta){\rm d}\delta$. These uncertainties are below current bounds on $f_{\rm NL}$ and are small enough for studies of primordial non-Gaussianities. Again, all integrations were carried out up to $\ell = 1000$.

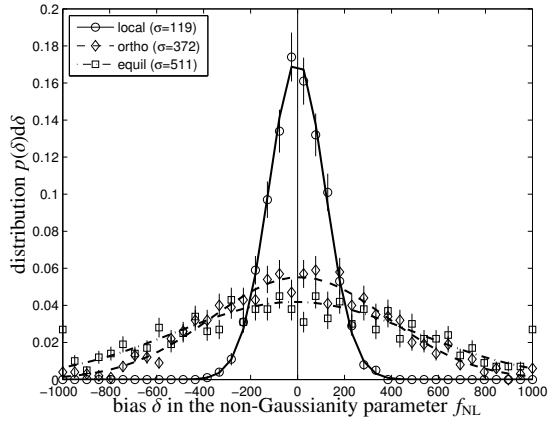

Figure 6.7: Distributions $p(\delta)\mathrm{d}\delta$ of the bias δ between the inferred non-Gaussianity parameter and the true parameter f_{NL} if the structure formation bispectrum is not completely removed, due to uncertainties in the cosmological model, for local (circles, solid line), orthogonal (lozenges, dashed line) and equilateral (squares, dash-dotted line) non-Gaussianities. As priors, Euclid weak lensing and baryon acoustic oscillations were used.

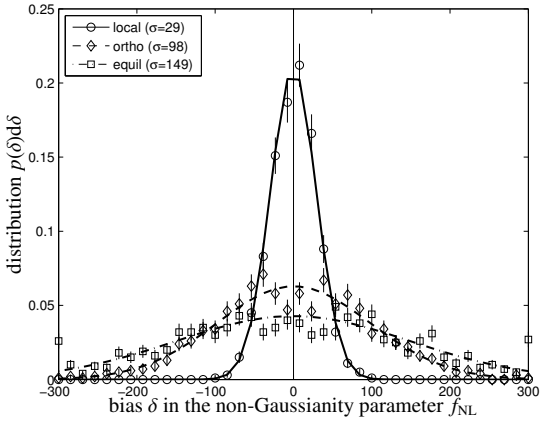

Figure 6.8: Distributions $p(\delta)\mathrm{d}\delta$ of the bias δ with an enhanced prior for the cosmological model with constraints from weak lensing, baryon acoustic oscillations (both Euclid) and CMB temperature and polarisation spectra (Planck), for local (circles, solid line), orthogonal (lozenges, dashed line) and equilateral (squares, dash-dotted line) non-Gaussianities.

6.7 Summary

The topic of this chapter are measurements of primordial bispectra in weak shear data from Euclid, comparisons between different types of non-Gaussianity configuration dependences, statistical questions concerning the inference of the non-Gaussianity parameter f_{NL} and the removal of the much stronger structure formation induced bispectrum. Although not as sensitive as observations of the CMB-bispectrum or the galaxy bispectrum for scale-free non-Gaussianities, weak lensing can place useful independent constraints on non-Gaussianities, in particular on smaller scales where CMB bounds might not apply. It is less prone to systematics than other large-scale structure probes and provides a direct linear mapping of the density field, which conserves its statistical properties.

1. Primordial non-Gaussianities provide a rather weak signal in the weak shear bispectrum (because of the Gaussianising effect of the line-of-sight integration, [204]), and signal-to-noise ratios of order unity can only be expected for $f_{\mathrm{NL}} = 200, 575, 1628$ for local, orthogonal and equilateral non-Gaussianities, respectively, where this measurement is most sensitive to scales $0.1 \ldots 1\ (\mathrm{Mpc}/h)^{-1}$. These bounds are weaker than those from e.g. observations of the CMB bispectrum, but will serve nevertheless for cross validation, in particular given the absence of strong systematics in weak shear data, or as bounds on scale-dependent non-Gaussianity, because weak lensing maps out scales which are not constrained by the CMB and is sensitive to scales probed by number counts.

2. Configuration space integrations can be very efficiently carried out by Monte-Carlo integration schemes, at a fraction of the computational cost. Computations of the

signal-to-noise ratio, of χ^2-functionals or of the Fisher-matrix $F_{\mu\nu}$ can be done with accuracies below a percent with $\mathcal{O}(10^5)$ evaluations instead of $\mathcal{O}(10^9)$ evaluations for the direct sum over ℓ_1, ℓ_2 and ℓ_3. Very good results were obtained with the CUBA library [274].

3. Fitting the wrong bispectrum type to data yields serious misestimates in the non-Gaussianity parameter $f_{\rm NL}$. Depending on the combination of true and false model there are two cases: either the estimated $f_{\rm NL}$ becomes very small, or the estimate for $f_{\rm NL}$ is a factor of $\sim \pm 3$ too large. When looking at numerical values for the χ^2-functional, one would notice strong discrepancies between data and model when fitting the wrong non-Gaussianity type from values of $f_{\rm NL}$ of a few hundred on.

4. The much stronger structure formation bispectrum can be subtracted with a prediction of its bispectrum from perturbation theory if the cosmology is known precisely enough. Propagating the uncertainty in the cosmological parameter set onto the misestimation of $f_{\rm NL}$ if the structure formation bispectrum is not correctly subtracted yielded typical uncertainties of 29, 98 and 149 for local, orthogonal and equilateral non-Gaussianities, much less than the statistical accuracy. As a prior on the cosmological parameters we assumed a Gaussian likelihood for a wCDM model combining Euclid's weak shear with baryon acoustic oscillations and Planck's observations of primary CMB anisotropies. Similar ratios between the numerical value of $f_{\rm NL}$ and the standard cosmological parameters were found by [202].

Many of our investigations can be straightforwardly generalised to other probes of large-scale structure statistics. We intend to generalise our investigations to higher polyspectra and to apply ideas from Bayesian model selection [280, 281] for assigning probabilities to the problem of choosing the correct non-Gaussianity type.

6.8 Appendix

6.8.1 Configuration dependence

Fig. 6.9 compares the configuration dependence of the bispectrum and of the signal strength in a weak lensing experiment. As a representation, we chose to plot the dimensionless weak convergence bispectrum $(\ell_1\ell_2\ell_3)^{4/3}B_\kappa(\ell_1,\ell_2,\ell_3)$ and the convergence bispectrum in units of the noise, $B_\kappa(\ell_1,\ell_2,\ell_3)/\sqrt{\mathrm{cov}(\ell_1,\ell_2,\ell_3)}$, which when added in quadrature yields the signal-to-noise ratio. The factor $(\ell_1\ell_2\ell_3)^{4/3} \sim \ell^4$ makes the angular bispectra dimensionless.

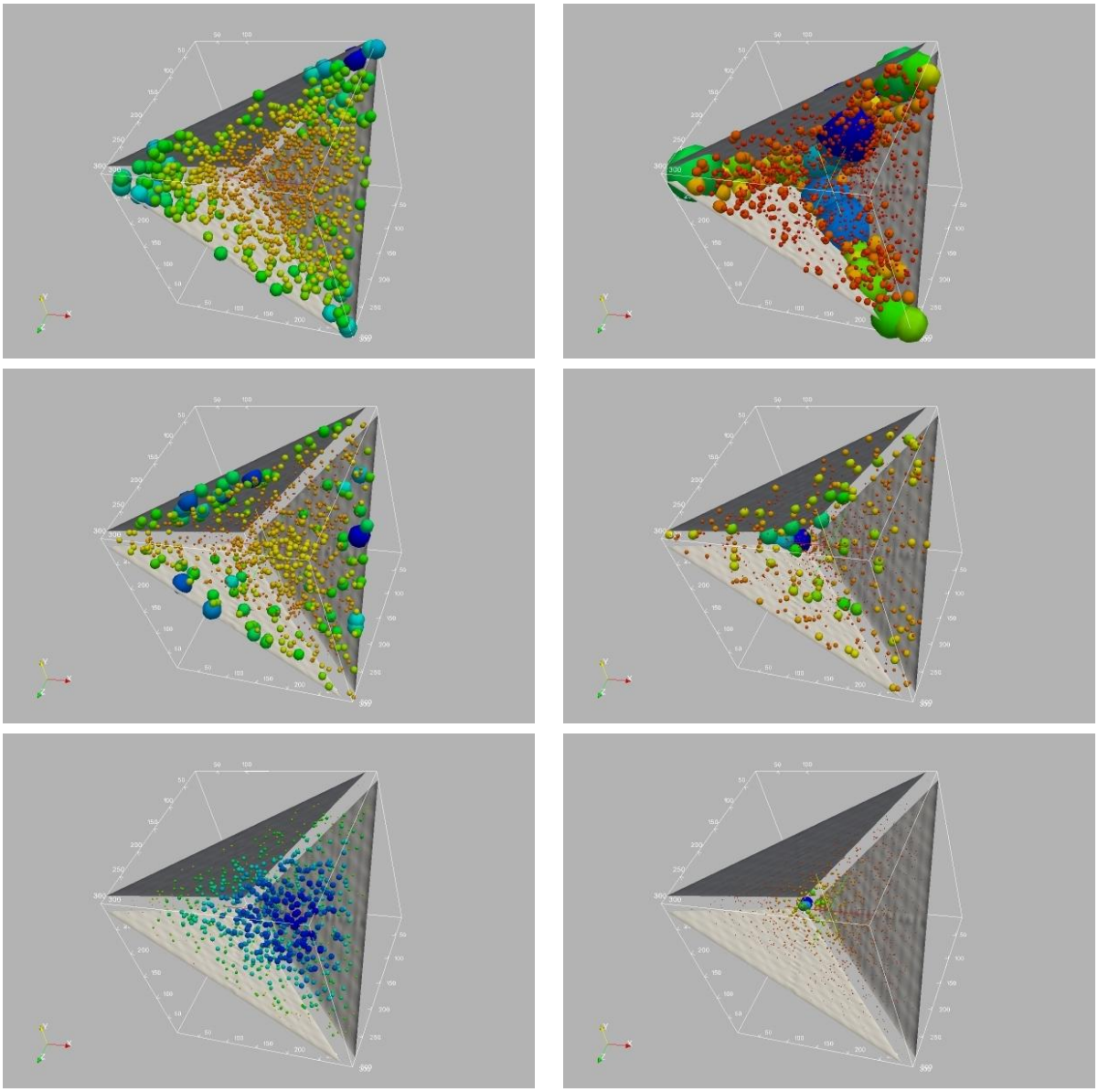

Figure 6.9: Configuration dependence $(\ell_1\ell_2\ell_3)^{4/3}B_\kappa(\ell_1,\ell_2,\ell_3)$ (first column) and signal-to-noise ratio $B_\kappa(\ell_1,\ell_2,\ell_3)/\sqrt{\mathrm{cov}(\ell_1,\ell_2,\ell_3)}$ (second column) of the weak lensing bispectrum, for local (first row), orthogonal (second row) and equilateral (third row) non-Gaussianities. The size of the blobs and their colour is proportional to the bispectrum, where a correct relative normalisation in the columns is maintained. Configurations outside the grey bounding planes violate the triangle inequality.

Chapter 7

Conclusions

We started this thesis with an introduction in chapter 2, where we discussed the underlying concepts of the main part of this theses. These were: the theory of inflation, the theory of cosmological perturbations, the δN-formalism, non-Gaussianity and IR effects in inflationary correlation functions. Furthermore, we gave an overview over the main part of this thesis in sec. 2.5.

The main part of this thesis has started in chapter 3 where we have studied IR divergences during inflation using both the δN-formalism and a simple, phenomenological approach based just on the geometry of the reheating surface. By implementing a simple modification of the δN-formalism, we took into account the effect of modes that left the horizon long before the scales we are observing on the Hubble scale. Including this effect provides new log-enhanced contributions to the power spectrum, at the same order in H and slow-roll parmeters as the standard classical loop corrections. We found that the combination of all contributions can be assembled in an elegant formula, in which the log-enhanced contributions are weighted by the second derivative of the tree level power spectrum, with respect to the inflaton field.

This result can be understood intuitively by considering two power spectra: One is defined locally on the surface of reheating, using invariant distances to define the correlator. The other is based on the coordinate distance on this surface and depends on global features of this surface, in particular on long-wavelength modes. When expressed in terms of the local spectrum, this latter, global spectrum exhibits an IR divergence associated to the size of the region on which it is measured. It is, in fact, this latter spectrum that is calculated in the δN-formalism and the log-divergence found in both approaches is precisely the same. This provides strong support for the modification of the δN-formalism we propose. In the case of an exactly scale invariant spectrum, the IR logarithms are absent. For an observer dealing with a scale-dependent spectrum and having a very large region available for his measurement, the use of the local spectrum, which is not affected by our IR effects, appears to be clearly favoured.

In chapter 4, we continued our considerations of IR effects and generalised our analysis to the backreaction of long-wavelength scalar and tensor modes in inflationary backgrounds. Furthermore, we proposed an infrared-safe definition of correlation functions involving curvature fluctuations, with no sensitivity on long-wavelength contributions. The essential idea was to make use of the proper invariant distance on the reheating surface where the curvature perturbation is evaluated. By using the invariant distance, one automatically absorbs longer wavelength modes in the background and obtains n-point functions for the curvature perturbation that are free from IR contributions associated

with long-wavelength modes. We showed how to re-interpret our results in terms of conventionally defined n-point functions. This allowed us to provide closed expressions for the latter that manifestly exhibit the dependence on long-wavelength modes. In our approach, IR corrections automatically emerge in a resummed, all-orders form. We then applied our approach to the analysis of inflationary observables built from (conventionally defined) two- and three-point functions of the curvature perturbation. We showed how to compute the leading scalar and tensor IR effects on the power spectrum and on the bispectrum, in single field, slow-roll inflation. Our corrections to the power spectrum (both from long-wavelength scalar and tensor modes) and to $f_{\rm NL}$ (from long-wavelength scalar modes) agree (essentially) with Giddings and Sloth [80] (obtained by somewhat different methods). The advantage of our approach is that it directly provides resummed, all-orders expressions. We extend [80] by tensor corrections to $f_{\rm NL}$. This is, in fact, the dominant piece! We also explicitly computed, in a specific inflationary model, the complete, all-orders expression for scalar long-wavelength contributions to inflationary observables. Furthermore, we analysed the question of convergence of IR corrections. Using entropy bounds given in [131, 132], we found that for a weak scale-dependence the convergence of the series of IR corrections is guaranteed. However, despite the existence of these entropy bounds and the fulfilment of slow-roll conditions, the convergence of the IR-correction series may break down if the scale-dependence is not sufficiently weak.

Summarising, we have provided a simple formalism to calculate and investigate inflationary IR corrections. Maybe more importantly, we have provided simple definitions of IR-safe correlation functions which make it possible to avoid IR enhancement altogether.

We have also shown that in all cases, where the δN-formalism is applicable, our results can be equivalently obtained in terms of a suitable generalisation of the δN-formalism. In the present work, we included the effects of graviton long-wavelength modes, and we explained how to calculate IR contributions to arbitrary n-point functions involving curvature perturbations.

A natural question is how to extend our results on IR effects of inflationary correlation functions to the case in which more than one field plays an active role in generating the curvature perturbations. In this case, IR effects might play a role more important than the ones for single field inflation where corrections always appear suppressed by the smallness of the (scalar and tensor) power spectrum. In Appendix 4.7.2 of chapter 4, we outlined a method to treat this problem. One major complication, arising when considering multi-field inflation, is that local patches do not necessarily take the same trajectory in field space. In single-field inflation, the scalar field rolls down its potential on the given, 1-dimensional field trajectory. Fluctuations occur exclusively along the trajectory and its precisely these fluctuations which appear in our resummed, all-orders expression. In multi-field inflation, there are certainly fluctuations transverse to the (background) trajectory. In order to generalise our definition of an infrared-safe correlation function and to find a corresponding resummed, all-orders relation to conventional spectra, it is essential to clarify the impact of these effects. Note that the presence of transverse fluctuations and the locally different trajectories, even though clearly related, may enter the averaging process in different ways. In addition, it is unclear how the mismatch of number of scalar field perturbations and number of scalar metric perturbations affects the averaging process. In single-field inflation, there is one curvature perturbation ζ and one scalar field perturbation $\delta\varphi$, among which one can switch by a change of gauge. By contrast, in the multi-field case there are several scalar field perturbations but still only one curvature perturbation. At a particular time during inflation, ζ is probably related to only one

direction in field space. It may even be for some models (sometimes denoted as "single-source" models) that this is true for the entire time of inflation relevant to us. However, particularly in view of turns of the inflationary trajectory the direction in field space sourcing ζ may change over time. Consequently, originally transverse fluctuations may become fluctuations along the inflationary trajectory, possibly effecting the curvature perturbation ζ. As a last point, we want to mention that additional fields typically yield an inhomogeneous end of inflation. Contrary to the single-field case, multi-field inflation does not necessarily end at a specific, model-dependent field value of the inflaton. Instead, additional fields can locally shift this field value denoting the end of inflation. This is likely to cause further complications in the search for infrared-safe correlation functions in multi-field inflation.

Furthermore, it would be desirable to adapt our results to CMB measurements. So far, our findings are all expressed in quantities defined on a spatial hypersurface, e.g. the reheating surface. Thus, they are applicable to observables directly measured on these hypersurfaces. By contrast, CMB measurements observe quantities projected on a two-sphere and evolved to the present day. The corresponding calculation of this projection and the evolution process can be split into three parts: the evolution of these quantities from reheating to decoupling, the transformation of these quantities into CMB temperature fluctuations at the time of decoupling and the evolution of temperature fluctuations in the CMB from decoupling till the time of observation. Each of these three processes is affected by non-linearities. Therefore, even though possibly simple at leading order, e.g. on the Sachs-Wolfe plateau, this projection process is highly non-trivial for higher order effects and also left for future work.

As a last continuation of our work on infrared effects, we would like to mention the generalisation to correlation functions of tensor perturbations γ. So far, we have considered only n-point functions of the comoving curvature perturbation ζ (however including tensor corrections to these n-point functions). Correlators of tensor perturbations are suppressed by the tensor-to-scalar ratio and have not been observed yet. Still this generalisation may be worthwile, particularly in light of stability questions in (quasi) deSitter spacetime. Most likely a generalisation to n-point functions of tensor perturbations γ would require to apply a complete quantum mechanical treatment like the In-In formalism. Nevertheless, due to the conservation of γ on superhorizon scales it is not inconceivable that an analogous split into a quantum mechanical sub- and semiclassical superhorizon regime may yield similar simplification to the ones for the curvature perturbation ζ.

In chapter 5 we discussed a new approach, based on the δN-formalism, for studying the scale dependence of non-Gaussianity parameters. We have obtained explicit expressions for the scale dependence of the quantities $f_{\rm NL}$, $\tau_{\rm NL}$ and $g_{\rm NL}$ associated with the bispectrum and trispectrum of primordial curvature perturbations. Our results depend on the slow-roll parameters evaluated at horizon exit, and on the derivatives of the number of e-foldings and the inflationary potential. The parameters controlling the scale dependence of non-Gaussianity depend on properties of the inflationary potential, namely its third and fourth derivatives, which in all observationally interesting cases cannot be probed by only studying the spectral index of the power spectrum and its running.

As a consequence, the scale dependence of non-Gaussianity provides additional powerful observables, able to offer novel information about the mechanism which generates the curvature perturbations. We demonstrated these features in the concrete example of modulated reheating. In models with a quartic potential for the modulating field, we have shown that the associated non-linearity parameters, and their scale dependence, can

be large enough to be observable.

While in most of the discussion we worked in momentum space, in the last part we also discussed how to describe our results in coordinate space. We provided an expression for curvature perturbations in coordinate space, that generalises the frequently used local ansatz, and that exhibits directly in real space the effects of scale dependence of non-Gaussian parameters.

Our results allow us to put onto a firm basis the phenomenological parametrisation of the scale dependence of non-Gaussian observables. In many models of observational interest, our formulae are relatively simple and depend on a single new parameter, the scale dependence of the non-linearity parameter. It would be interesting to use these results for analysing or simulating non-Gaussian data. At the same time, our investigation allows us to identify which properties inflationary models have to satisfy in order to obtain large non-Gaussianity with sizable scale dependence. It would be interesting to apply it to analyse further models, for example those in which multiple fields interact during inflation or where the non-Gaussianity is generated by an inhomogeneous end of inflation.

Finally, in chapter 6 we investigated the possibility to constrain primordial non-Gaussianity, especially with a view on Euclid. We analysed comparisons between different types of non-Gaussianity configuration dependencies, statistical questions concerning the inference of the non-Gaussianity parameter $f_{\rm NL}$ and the removal of the much stronger structure formation induced bispectrum. Although not as sensitive as observations of the CMB-bispectrum or the galaxy bispectrum for scale-free non-Gaussianities, weak lensing can place useful independent constraints on non-Gaussianities, in particular on smaller scales where CMB bounds might not apply. It is less prone to systematics than other large-scale structure probes and provides a direct linear mapping of the density field, which conserves its statistical properties.

We found that a signal-to-noise ratio of order unity can only be expected for $f_{\rm NL} = 200, 575, 1628$ for local, orthogonal and equilateral non-Gaussianities, respectively, where this measurement is most sensitive to scales $0.1 \ldots 1\ (\mathrm{Mpc}/h)^{-1}$. These bounds are weaker than those from e.g. observations of the CMB bispectrum, but will serve nevertheless for cross validation or as bounds on scale-dependent non-Gaussianity, because weak lensing maps out scales which are not constrained by the CMB and is sensitive to scales probed by number counts.

Configuration space integrations can be very efficiently carried out by Monte-Carlo integration schemes, at a fraction of the computational cost. Computations of the signal-to-noise ratio, of χ^2-functionals or of the Fisher-matrix can be done with accuracies below a percent with $\mathcal{O}(10^5)$ evaluations instead of $\mathcal{O}(10^9)$ evaluations for the direct summation.

In addition we analysed the question if one would notice fitting the wrong bispectrum type to data, yielding serious misestimates in the non-Gaussianity parameter $f_{\rm NL}$. Depending on the combination of true and false model there are two cases: either the estimated $f_{\rm NL}$ becomes very small or the estimate for $f_{\rm NL}$ is a factor of $\sim \pm 3$ too large. When looking at numerical values for the χ^2-functional, one would notice strong discrepancies between data and model from values of $f_{\rm NL}$ of a few hundred on.

The much stronger structure formation bispectrum can be subtracted with a prediction of its bispectrum from perturbation theory if the cosmology is known precisely enough. Propagating the uncertainty in the cosmological parameter set onto the misestimation of $f_{\rm NL}$ if the structure formation bispectrum is not correctly subtracted yielded uncertainties much less than the statistical accuracy. As a prior on the cosmological parameters we

assumed a Gaussian likelihood for a wCDM model combining Euclid's weak shear with baryon acoustic oscillations and Planck's observations of primary CMB anisotropies. Similar ratios between the numerical value of $f_{\rm NL}$ and the standard cosmological parameters were found by [202].

Many of the investigations in chapter 6 can be straightforwardly generalised to other probes of large-scale structure statistics. Furthermore, it is desirable to generalise our analysis of the bispectrum to higher polyspectra and to apply ideas from Bayesian model selection [280, 281] for assigning probabilities to the problem of choosing the correct non-Gaussianity type.

Acknowledgements

With the last sentences of this thesis I want to mention and thank the people who gave me support and advice during my time as a doctoral student and who made this time so wonderful and exceptional for me.

I owe my deepest gratitude to my supervisor Arthur Hebecker for his outstanding supervision, encouragement, guidance and support. There are certainly not many supervisors who care so much about their students. I am deeply grateful to you for this great time, for the possibilty to work on this exciting project, for all I have learned from you and for all what you have done for me during this past two and a half years.

I am also indebted to my co-supervisors Christof Wetterich, who also agreed to co-referee this thesis, and Matthias Bartelmann, who also agreed to be a member of my thesis defense committee, for their valuable advices and help.

I am grateful to my collaborators Gianmassimo Tasinato, Christian Byrnes, Sami Nurmi and Björn Malte Schäfer (in addition to Arthur Hebecker). I enjoyed so much working with you guys and I learned a lot from each of you.

During my doctoral studies I have been supported by the doctorate scholarship of the *Studienstiftung des Deutschen Volkes*. I am truely thankful to this great institution for their support.

During the past two and a half years, I had the luck to have terrific colleagues and friends around me here at the Institute for Theoretical Physics in Heidelberg. I would like to thank Sonja, Melanie, Cornelia, Ghazal, Miriam, Johanna, Benoît, Sebastian, Philipp, Timo, Eduard, Christoph, Alexander, Heinrich, Henning, Johannes, Gabriell, Max, Ivan, Sven, Konrad, Chahan and everyone else I forgot to mention here. Thanks a lot for the great time with you! Furthermore, I want to thank my friends Ana, Laure, Emanuel, Christian, Gero, Francesco, Misha, Matteo, Jens and Julian for awesome times in Heidelberg and at the rocks.

I am deeply grateful to my brother Sascha and my parents Irmgard and Klaus. You have always given me support and advice wherever you can. There are no words how grateful I am to have you.

Bibliography

[1] S. Weinberg, "Dreams of a final theory: The Search for the fundamental laws of nature",.

[2] A. H. Guth, "The Inflationary Universe: A Possible Solution to the Horizon and Flatness Problems", *Phys.Rev.* **D23** (1981) 347–356.

[3] A. A. Starobinsky, "Relict Gravitation Radiation Spectrum and Initial State of the Universe. (In Russian)", *JETP Lett.* **30** (1979) 682–685.

[4] A. A. Starobinsky, "A New Type of Isotropic Cosmological Models Without Singularity", *Phys.Lett.* **B91** (1980) 99–102.

[5] A. D. Linde, "A New Inflationary Universe Scenario: A Possible Solution of the Horizon, Flatness, Homogeneity, Isotropy and Primordial Monopole Problems", *Phys. Lett.* **B108** (1982) 389–393.

[6] A. Albrecht and P. J. Steinhardt, "Cosmology for Grand Unified Theories with Radiatively Induced Symmetry Breaking", *Phys. Rev. Lett.* **48** (1982) 1220–1223.

[7] V. F. Mukhanov and G. Chibisov, "Quantum Fluctuation and Nonsingular Universe. (In Russian)", *JETP Lett.* **33** (1981) 532–535.

[8] V. F. Mukhanov and G. V. Chibisov, "The Vacuum energy and large scale structure of the universe", *Sov. Phys. JETP* **56** (1982) 258–265.

[9] A. A. Starobinsky, "Dynamics of Phase Transition in the New Inflationary Universe Scenario and Generation of Perturbations", *Phys. Lett.* **B117** (1982) 175–178.

[10] S. W. Hawking, "The Development of Irregularities in a Single Bubble Inflationary Universe", *Phys. Lett.* **B115** (1982) 295.

[11] A. H. Guth and S. Y. Pi, "Fluctuations in the New Inflationary Universe", *Phys. Rev. Lett.* **49** (1982) 1110–1113.

[12] J. M. Bardeen, P. J. Steinhardt, and M. S. Turner, "Spontaneous Creation of Almost Scale - Free Density Perturbations in an Inflationary Universe", *Phys. Rev.* **D28** (1983) 679.

[13] V. F. Mukhanov, H. Feldman, and R. H. Brandenberger, "Theory of cosmological perturbations. Part 1. Classical perturbations. Part 2. Quantum theory of perturbations. Part 3. Extensions", *Phys.Rept.* **215** (1992) 203–333.

[14] A. Riotto, "Inflation and the theory of cosmological perturbations", arXiv:hep-ph/0210162.

[15] K. A. Malik and D. Wands, "Cosmological perturbations", *Phys.Rept.* **475** (2009) 1–51, arXiv:0809.4944 [astro-ph]. * Brief entry *.

[16] D. Baumann, "TASI Lectures on Inflation", arXiv:0907.5424 [hep-th].

[17] X. Chen, "Primordial Non-Gaussianities from Inflation Models", *Adv. Astron.* **2010** (2010) 638979, arXiv:1002.1416 [astro-ph.CO].

[18] **WMAP** Collaboration, E. Komatsu *et al.*, "Seven-Year Wilkinson Microwave Anisotropy Probe (WMAP) Observations: Cosmological Interpretation", *Astrophys. J. Suppl.* **192** (2011) 18, arXiv:1001.4538 [astro-ph.CO].

[19] R. Durrer, M. Kunz, and A. Melchiorri, "Cosmic structure formation with topological defects", *Phys.Rept.* **364** (2002) 1–81, arXiv:astro-ph/0110348 [astro-ph].

[20] J. M. Bardeen, "Gauge Invariant Cosmological Perturbations", *Phys.Rev.* **D22** (1980) 1882–1905.

[21] D. S. Salopek and J. R. Bond, "Nonlinear evolution of long wavelength metric fluctuations in inflationary models", *Phys. Rev.* **D42** (1990) 3936–3962.

[22] J. M. Maldacena, "Non-Gaussian features of primordial fluctuations in single field inflationary models", *JHEP* **05** (2003) 013, arXiv:astro-ph/0210603.

[23] D. H. Lyth, K. A. Malik, and M. Sasaki, "A general proof of the conservation of the curvature perturbation", *JCAP* **0505** (2005) 004, arXiv:astro-ph/0411220.

[24] S. Weinberg, "Quantum contributions to cosmological correlations", *Phys. Rev.* **D72** (2005) 043514, arXiv:hep-th/0506236.

[25] M. Sasaki and E. D. Stewart, "A General analytic formula for the spectral index of the density perturbations produced during inflation", *Prog. Theor. Phys.* **95** (1996) 71–78, arXiv:astro-ph/9507001.

[26] J. chan Hwang, "Cosmological perturbations with multiple scalar fields", arXiv:gr-qc/9608018 [gr-qc].

[27] Y. Nambu and A. Taruya, "Evolution of cosmological perturbation in reheating phase of the universe", *Prog.Theor.Phys.* **97** (1997) 83–89, arXiv:gr-qc/9609029 [gr-qc].

[28] A. Taruya and Y. Nambu, "Cosmological perturbation with two scalar fields in reheating after inflation", *Phys.Lett.* **B428** (1998) 37–43, arXiv:gr-qc/9709035 [gr-qc].

[29] K. A. Malik, "A not so short note on the Klein-Gordon equation at second order", *JCAP* **0703** (2007) 004, arXiv:astro-ph/0610864 [astro-ph].

[30] D. H. Lyth, C. Ungarelli, and D. Wands, "The primordial density perturbation in the curvaton scenario", *Phys. Rev.* **D67** (2003) 023503, arXiv:astro-ph/0208055.

[31] K. Enqvist, J. Hogdahl, S. Nurmi, and F. Vernizzi, "A Covariant generalization of cosmological perturbation theory", *Phys.Rev.* **D75** (2007) 023515, arXiv:gr-qc/0611020 [gr-qc].

[32] D. H. Lyth and Y. Rodriguez, "Non-Gaussianity from the second-order cosmological perturbation", *Phys.Rev.* **D71** (2005) 123508, arXiv:astro-ph/0502578 [astro-ph].

[33] R. Sachs and A. Wolfe, "Perturbations of a cosmological model and angular variations of the microwave background", *Astrophys.J.* **147** (1967) 73–90.

[34] L. H. Ford, "Quantum field theory in curved spacetime", arXiv:gr-qc/9707062.

[35] M. Spradlin, A. Strominger, and A. Volovich, "Les Houches lectures on de Sitter space", arXiv:hep-th/0110007.

[36] C. Kiefer and D. Polarski, "Why do cosmological perturbations look classical to us?", *Adv.Sci.Lett.* **2** (2009) 164–173, arXiv:0810.0087 [astro-ph]. * Brief entry *.

[37] D. H. Lyth and Y. Rodriguez, "The inflationary prediction for primordial non-gaussianity", *Phys. Rev. Lett.* **95** (2005) 121302, arXiv:astro-ph/0504045.

[38] A. A. Starobinsky, "Multicomponent de Sitter (Inflationary) Stages and the Generation of Perturbations", *JETP Lett.* **42** (1985) 152–155.

[39] D. Wands, K. A. Malik, D. H. Lyth, and A. R. Liddle, "A new approach to the evolution of cosmological perturbations on large scales", *Phys. Rev.* **D62** (2000) 043527, arXiv:astro-ph/0003278.

[40] C. T. Byrnes, S. Nurmi, G. Tasinato, and D. Wands, "Scale dependence of local $f_{\rm NL}$", *JCAP* **1002** (2010) 034, arXiv:0911.2780 [astro-ph.CO].

[41] G. I. Rigopoulos and E. P. S. Shellard, "The Separate Universe Approach and the Evolution of Nonlinear Superhorizon Cosmological Perturbations", *Phys. Rev.* **D68** (2003) 123518, arXiv:astro-ph/0306620.

[42] D. Langlois and F. Vernizzi, "A geometrical approach to nonlinear perturbations in relativistic cosmology", *Class.Quant.Grav.* **27** (2010) 124007, arXiv:1003.3270 [astro-ph.CO]. * Temporary entry *.

[43] D. Wands, "Multiple field inflation", *Lect.Notes Phys.* **738** (2008) 275–304, arXiv:astro-ph/0702187 [ASTRO-PH].

[44] C. T. Byrnes and K.-Y. Choi, "Review of local non-Gaussianity from multi-field inflation", *Adv. Astron.* **2010** (2010) 724525, arXiv:1002.3110 [astro-ph.CO].

[45] E. Komatsu, "Hunting for Primordial Non-Gaussianity in the Cosmic Microwave Background", *Class. Quant. Grav.* **27** (2010) 124010, arXiv:1003.6097 [astro-ph.CO].

[46] D. Wands, "Local non-Gaussianity from inflation", *Class. Quant. Grav.* **27** (2010) 124002, arXiv:1004.0818 [astro-ph.CO].

[47] A. P. S. Yadav and B. D. Wandelt, "Primordial Non-Gaussianity in the Cosmic Microwave Background", arXiv:1006.0275 [astro-ph.CO].

[48] J. R. Fergusson, M. Liguori, and E. P. S. Shellard, "The CMB Bispectrum", arXiv:1006.1642 [astro-ph.CO].

[49] V. Desjacques and U. Seljak, "Primordial non-Gaussianity in the large scale structure of the Universe", *Advances in Astronomy* (2010) , arXiv:1006.4763 [astro-ph.CO]. * Temporary entry *.

[50] E. Komatsu and D. N. Spergel, "Acoustic signatures in the primary microwave background bispectrum", *Phys. Rev.* **D63** (2001) 063002, arXiv:astro-ph/0005036.

[51] C. T. Byrnes, K.-Y. Choi, and L. M. H. Hall, "Large non-Gaussianity from two-component hybrid inflation", *JCAP* **0902** (2009) 017, arXiv:0812.0807 [astro-ph].

[52] J. Kumar, L. Leblond, and A. Rajaraman, "Scale Dependent Local Non-Gaussianity from Loops", *JCAP* **1004** (2010) 024, arXiv:0909.2040 [astro-ph.CO].

[53] F. Bernardeau, "Mode coupling evolution in arbitrary inflationary backgrounds", *JCAP* **1102** (2011) 017, arXiv:1003.3575 [astro-ph.CO].

[54] E. Sefusatti, M. Liguori, A. P. S. Yadav, M. G. Jackson, and E. Pajer, "Constraining Running Non-Gaussianity", *JCAP* **0912** (2009) 022, arXiv:0906.0232 [astro-ph.CO].

[55] A. Vilenkin and L. H. Ford, "Gravitational Effects upon Cosmological Phase Transitions", *Phys. Rev.* **D26** (1982) 1231.

[56] A. D. Linde, "Scalar Field Fluctuations in Expanding Universe and the New Inflationary Universe Scenario", *Phys. Lett.* **B116** (1982) 335.

[57] A. Vilenkin, "QUANTUM FLUCTUATIONS IN THE NEW INFLATIONARY UNIVERSE", *Nucl. Phys.* **B226** (1983) 527.

[58] A. D. Linde and R. (ed.) Brandenberger, "Inflation and quantum cosmology",.

[59] S. Weinberg, "Quantum contributions to cosmological correlations. II: Can these corrections become large?", *Phys. Rev.* **D74** (2006) 023508, arXiv:hep-th/0605244.

[60] D. H. Lyth, "The curvature perturbation in a box", *JCAP* **0712** (2007) 016, arXiv:0707.0361 [astro-ph].

[61] M. Gerstenlauer, A. Hebecker, and G. Tasinato, "Inflationary Correlation Functions without Infrared Divergences", *JCAP* **1106** (2011) 021, arXiv:1102.0560 [astro-ph.CO].

[62] B. Allen and A. Folacci, "THE MASSLESS MINIMALLY COUPLED SCALAR FIELD IN DE SITTER SPACE", *Phys. Rev.* **D35** (1987) 3771.

[63] K. Kirsten and J. Garriga, "Massless minimally coupled fields in de Sitter space: O(4) symmetric states versus de Sitter invariant vacuum", *Phys. Rev.* **D48** (1993) 567–577, arXiv:gr-qc/9305013.

[64] C. T. Byrnes, M. Gerstenlauer, A. Hebecker, S. Nurmi, and G. Tasinato, "Inflationary Infrared Divergences: Geometry of the Reheating Surface vs. δN Formalism", *JCAP* **1008** (2010) 006, arXiv:1005.3307 [hep-th].

[65] C. T. Byrnes, M. Gerstenlauer, S. Nurmi, G. Tasinato, and D. Wands, "Scale-dependent non-Gaussianity probes inflationary physics", *JCAP* **1010** (2010) 004, arXiv:1007.4277 [astro-ph.CO].

[66] B. M. Schäfer, A. Grassi, M. Gerstenlauer, and C. T. Byrnes, "A weak lensing view on primordial non-Gaussianities", arXiv:1107.1656 [astro-ph.CO]. * Temporary entry *.

[67] A. A. Starobinsky, "STOCHASTIC DE SITTER (INFLATIONARY) STAGE IN THE EARLY UNIVERSE",.

[68] N. Bartolo, S. Matarrese, M. Pietroni, A. Riotto, and D. Seery, "On the Physical Significance of Infra-red Corrections to Inflationary Observables", *JCAP* **0801** (2008) 015, arXiv:0711.4263 [astro-ph].

[69] K. Enqvist, S. Nurmi, D. Podolsky, and G. I. Rigopoulos, "On the divergences of inflationary superhorizon perturbations", *JCAP* **0804** (2008) 025, arXiv:0802.0395 [astro-ph].

[70] D. Seery, "Magnetogenesis and the primordial non-gaussianity", *JCAP* **0908** (2009) 018, arXiv:0810.1617 [astro-ph].

[71] Y. Urakawa and T. Tanaka, "Influence on Observation from IR Divergence during Inflation. I", *Prog. Theor. Phys.* **122** (2009) 779–803, arXiv:0902.3209 [hep-th].

[72] Y. Urakawa and T. Tanaka, "Influence on observation from IR divergence during inflation – Multi field inflation –", *Prog. Theor. Phys.* **122** (2010) 1207–1238, arXiv:0904.4415 [hep-th].

[73] D. Seery, "A parton picture of de Sitter space during slow-roll inflation", *JCAP* **0905** (2009) 021, arXiv:0903.2788 [astro-ph.CO].

[74] R. Durrer, G. Marozzi, and M. Rinaldi, "On Adiabatic Renormalization of Inflationary Perturbations", *Phys. Rev.* **D80** (2009) 065024, arXiv:0906.4772 [astro-ph.CO].

[75] L. Senatore and M. Zaldarriaga, "On Loops in Inflation", *JHEP* **12** (2010) 008, arXiv:0912.2734 [hep-th].

[76] F. Finelli, G. Marozzi, A. A. Starobinsky, G. P. Vacca, and G. Venturi, "Stochastic growth of quantum fluctuations during slow-roll inflation", *Phys. Rev.* **D82** (2010) 064020, arXiv:1003.1327 [hep-th].

[77] T. Prokopec and G. Rigopoulos, "Path Integral for Inflationary Perturbations", *Phys. Rev.* **D82** (2010) 023529, arXiv:1004.0882 [gr-qc].

[78] D. Seery, "Infrared effects in inflationary correlation functions", *Class. Quant Grav.* **27** (2010) 124005, arXiv:1005.1649 [astro-ph.CO].

[79] F. Kuhnel and D. J. Schwarz, "Large-Scale Suppression from Stochastic Inflation", *Phys. Rev. Lett.* **105** (2010) 211302, arXiv:1003.3014 [hep-ph].

[80] S. B. Giddings and M. S. Sloth, "Semiclassical relations and IR effects in de Sitter and slow-roll space-times", *JCAP* **1101** (2011) 023, arXiv:1005.1056 [hep-th].

[81] L. E. Allen, S. Gupta, and D. Wands, "Non-Gaussian perturbations from multi-field inflation", *JCAP* **0601** (2006) 006, arXiv:astro-ph/0509719.

[82] T. Suyama and F. Takahashi, "Non-Gaussianity from Symmetry", *JCAP* **0809** (2008) 007, arXiv:0804.0425 [astro-ph].

[83] L. Boubekeur and D. H. Lyth, "Detecting a small perturbation through its non-Gaussianity", *Phys. Rev.* **D73** (2006) 021301, arXiv:astro-ph/0504046.

[84] C. T. Byrnes, M. Sasaki, and D. Wands, "The primordial trispectrum from inflation", *Phys. Rev.* **D74** (2006) 123519, arXiv:astro-ph/0611075.

[85] C. T. Byrnes, K. Koyama, M. Sasaki, and D. Wands, "Diagrammatic approach to non-Gaussianity from inflation", *JCAP* **0711** (2007) 027, arXiv:0705.4096 [hep-th].

[86] D. Seery, J. E. Lidsey, and M. S. Sloth, "The inflationary trispectrum", *JCAP* **0701** (2007) 027, arXiv:astro-ph/0610210.

[87] C. T. Byrnes and G. Tasinato, "Non-Gaussianity beyond slow roll in multi-field inflation", *JCAP* **0908** (2009) 016, arXiv:0906.0767 [astro-ph.CO].

[88] E. Komatsu *et al.*, "Non-Gaussianity as a Probe of the Physics of the Primordial Universe and the Astrophysics of the Low Redshift Universe", arXiv:0902.4759 [astro-ph.CO].

[89] L. Senatore, "Talk at perimeter institute",.

[90] Y. Urakawa and T. Tanaka, "IR divergence does not affect the gauge-invariant curvature perturbation", *Phys. Rev.* **D82** (2010) 121301, arXiv:1007.0468 [hep-th].

[91] A. A. Starobinsky and J. Yokoyama, "Equilibrium state of a selfinteracting scalar field in the De Sitter background", *Phys. Rev.* **D50** (1994) 6357–6368, arXiv:astro-ph/9407016.

[92] M. Sasaki, H. Suzuki, K. Yamamoto, and J. Yokoyama, "Superexpansionary divergence: Breakdown of perturbative quantum field theory in space-time with accelerated expansion", *Class. Quant. Grav.* **10** (1993) L55–L60.

[93] H. Suzuki, M. Sasaki, K. Yamamoto, and J. Yokoyama, "Probability distribution functional for equal time correlation functions in curved space", *Int. J. Mod. Phys.* **A9** (1994) 221–238.

[94] J.-O. Gong and E. D. Stewart, "The density perturbation power spectrum to second-order corrections in the slow-roll expansion", *Phys. Lett.* **B510** (2001) 1–9, arXiv:astro-ph/0101225.

[95] Y. Urakawa and T. Tanaka, "Natural selection of inflationary vacuum required by infra-red regularity and gauge-invariance", arXiv:1009.2947 [hep-th].

[96] C. P. Burgess, L. Leblond, R. Holman, and S. Shandera, "Super-Hubble de Sitter Fluctuations and the Dynamical RG", *JCAP* **1003** (2010) 033, arXiv:0912.1608 [hep-th].

[97] A. Rajaraman, J. Kumar, and L. Leblond, "Constructing Infrared Finite Propagators in Inflating Space-time", *Phys. Rev.* **D82** (2010) 023525, arXiv:1002.4214 [hep-th].

[98] C. P. Burgess, R. Holman, L. Leblond, and S. Shandera, "Breakdown of Semiclassical Methods in de Sitter Space", *JCAP* **1010** (2010) 017, arXiv:1005.3551 [hep-th].

[99] E. Kahya, V. Onemli, and R. Woodard, "The ζ-ζ Correlator Is Time Dependent", *Phys.Lett.* **B694** (2010) 101–107, arXiv:1006.3999 [astro-ph.CO].

[100] H. R. S. Cogollo, Y. Rodriguez, and C. A. Valenzuela-Toledo, "On the Issue of the ζ Series Convergence and Loop Corrections in the Generation of Observable Primordial Non- Gaussianity in Slow-Roll Inflation. Part I: the Bispectrum", *JCAP* **0808** (2008) 029, arXiv:0806.1546 [astro-ph].

[101] A. Riotto and M. S. Sloth, "On Resumming Inflationary Perturbations beyond One-loop", *JCAP* **0804** (2008) 030, arXiv:0801.1845 [hep-ph].

[102] A. M. Polyakov, "De Sitter Space and Eternity", *Nucl. Phys.* **B797** (2008) 199–217, arXiv:0709.2899 [hep-th].

[103] M. van der Meulen and J. Smit, "Classical approximation to quantum cosmological correlations", *JCAP* **0711** (2007) 023, arXiv:0707.0842 [hep-th].

[104] M. S. Sloth, "On the one loop corrections to inflation and the CMB anisotropies", *Nucl. Phys.* **B748** (2006) 149–169, arXiv:astro-ph/0604488.

[105] A. D. Linde, "Particle Physics and Inflationary Cosmology", arXiv:hep-th/0503203.

[106] J.-O. Gong, H. Noh, and J. chan Hwang, "Non-linear corrections to inflationary power spectrum", *JCAP* **1104** (2011) 004, arXiv:1011.2572 [astro-ph.CO].

[107] D. H. Lyth, "Non-gaussianity and cosmic uncertainty in curvaton-type models", *JCAP* **0606** (2006) 015, arXiv:astro-ph/0602285.

[108] W. Unruh, "Cosmological long wavelength perturbations", arXiv:astro-ph/9802323.

[109] G. Geshnizjani, "Back reaction of long wavelength perturbations during inflation",. Ph.D. Thesis (Advisor: Robert Brandenberger).

[110] G. Geshnizjani and R. Brandenberger, "Back reaction and local cosmological expansion rate", *Phys. Rev.* **D66** (2002) 123507, arXiv:gr-qc/0204074.

[111] G. Geshnizjani and R. Brandenberger, "Back reaction of perturbations in two scalar field inflationary models", *JCAP* **0504** (2005) 006, arXiv:hep-th/0310265.

[112] L. A. Kofman and A. D. Linde, "Generation of Density Perturbations in the Inflationary Cosmology", *Nucl. Phys.* **B282** (1987) 555.

[113] A. D. Linde, "Lectures on inflationary cosmology", arXiv:hep-th/9410082.

[114] V. F. Mukhanov, L. R. W. Abramo, and R. H. Brandenberger, "On the back reaction problem for gravitational perturbations", *Phys. Rev. Lett.* **78** (1997) 1624–1627, arXiv:gr-qc/9609026.

[115] L. R. W. Abramo, R. H. Brandenberger, and V. F. Mukhanov, "The energy-momentum tensor for cosmological perturbations", *Phys. Rev.* **D56** (1997) 3248–3257, arXiv:gr-qc/9704037.

[116] N. C. Tsamis and R. P. Woodard, "Relaxing the cosmological constant", *Phys. Lett.* **B301** (1993) 351–357.

[117] S. P. Miao, N. C. Tsamis, and R. P. Woodard, "De Sitter Breaking through Infrared Divergences", *J. Math. Phys.* **51** (2010) 072503, arXiv:1002.4037 [gr-qc].

[118] T. S. Koivisto and T. Prokopec, "Quantum backreaction in evolving FLRW spacetimes", *Phys. Rev.* **D83** (2011) 044015, arXiv:1009.5510 [gr-qc].

[119] N. P. Myhrvold, "THE EXISTENCE AND STABILITY OF SEMICLASSICAL DE SITTER AND ANTI-DE SITTER SPACE-TIMES", *Phys. Lett.* **B132** (1983) 308.

[120] L. H. Ford, "QUANTUM INSTABILITY OF DE SITTER SPACE-TIME", *Phys. Rev.* **D31** (1985) 710.

[121] I. Antoniadis, J. Iliopoulos, and T. N. Tomaras, "QUANTUM INSTABILITY OF DE SITTER SPACE", *Phys. Rev. Lett.* **56** (1986) 1319.

[122] I. Antoniadis and E. Mottola, "GRAVITON FLUCTUATIONS IN DE SITTER SPACE", *J. Math. Phys.* **32** (1991) 1037–1044.

[123] P. Creminelli and M. Zaldarriaga, "Single field consistency relation for the 3-point function", *JCAP* **0410** (2004) 006, arXiv:astro-ph/0407059.

[124] D. Seery, M. S. Sloth, and F. Vernizzi, "Inflationary trispectrum from graviton exchange", *JCAP* **0903** (2009) 018, arXiv:0811.3934 [astro-ph].

[125] I. Zaballa, Y. Rodriguez, and D. H. Lyth, "Higher order contributions to the primordial non- gaussianity", *JCAP* **0606** (2006) 013, arXiv:astro-ph/0603534.

[126] D. Seery, "One-loop corrections to the curvature perturbation from inflation", *JCAP* **0802** (2008) 006, arXiv:0707.3378 [astro-ph].

[127] E. Dimastrogiovanni and N. Bartolo, "One-loop graviton corrections to the curvature perturbation from inflation", *JCAP* **0811** (2008) 016, arXiv:0807.2790 [astro-ph].

[128] F. Lucchin and S. Matarrese, "Power Law Inflation", *Phys. Rev.* **D32** (1985) 1316.

[129] D. H. Lyth and E. D. Stewart, "The Curvature perturbation in power law (e.g. extended) inflation", *Phys. Lett.* **B274** (1992) 168–172.

[130] E. D. Stewart and D. H. Lyth, "A more accurate analytic calculation of the spectrum of cosmological perturbations produced during inflation", *Phys. Lett.* **B302** (1993) 171–175, arXiv:gr-qc/9302019.

[131] N. Arkani-Hamed, S. Dubovsky, A. Nicolis, E. Trincherini, and G. Villadoro, "A Measure of de Sitter Entropy and Eternal Inflation", *JHEP* **05** (2007) 055, arXiv:0704.1814 [hep-th].

[132] S. Dubovsky, L. Senatore, and G. Villadoro, "The Volume of the Universe after Inflation and de Sitter Entropy", *JHEP* **04** (2009) 118, arXiv:0812.2246 [hep-th].

[133] T. Suyama, T. Takahashi, M. Yamaguchi, and S. Yokoyama, "On Classification of Models of Large Local-Type Non- Gaussianity", *JCAP* **1012** (2010) 030, arXiv:1009.1979 [astro-ph.CO].

[134] R. Jimenez and L. Verde, "Implications for Primordial Non-Gaussianity (f_{NL}) from weak lensing masses of high-z galaxy clusters", *Phys. Rev.* **D80** (2009) 127302, arXiv:0909.0403 [astro-ph.CO].

[135] D. E. Holz and S. Perlmutter, "The most massive objects in the Universe", arXiv:1004.5349 [astro-ph.CO].

[136] L. Cayon, C. Gordon, and J. Silk, "Probability of the most massive cluster under non-Gaussian initial conditions", arXiv:1006.1950 [astro-ph.CO].

[137] M. Baldi and V. Pettorino, "High-z massive clusters as a test for dynamical coupled dark energy", arXiv:1006.3761 [astro-ph.CO].

[138] D. Wands, "Inflationary parameters and primordial perturbation spectra", *New Astron. Rev.* **47** (2003) 781–786, arXiv:astro-ph/0306523.

[139] G. I. Rigopoulos, E. P. S. Shellard, and B. J. W. van Tent, "Quantitative bispectra from multifield inflation", *Phys. Rev.* **D76** (2007) 083512, arXiv:astro-ph/0511041.

[140] F. Vernizzi and D. Wands, "Non-Gaussianities in two-field inflation", *JCAP* **0605** (2006) 019, arXiv:astro-ph/0603799.

[141] T. Battefeld and R. Easther, "Non-gaussianities in multi-field inflation", *JCAP* **0703** (2007) 020, arXiv:astro-ph/0610296.

[142] D. Seery and J. E. Lidsey, "Non-gaussianity from the inflationary trispectrum", *JCAP* **0701** (2007) 008, arXiv:astro-ph/0611034.

[143] N. Barnaby and J. M. Cline, "Nongaussianity from Tachyonic Preheating in Hybrid Inflation", *Phys. Rev.* **D75** (2007) 086004, arXiv:astro-ph/0611750.

[144] K.-Y. Choi, L. M. H. Hall, and C. van de Bruck, "Spectral running and non-Gaussianity from slow-roll inflation in generalised two-field models", *JCAP* **0702** (2007) 029, arXiv:astro-ph/0701247.

[145] S. Yokoyama, T. Suyama, and T. Tanaka, "Primordial Non-Gaussianity in Multi-Scalar Slow-Roll Inflation", *JCAP* **0707** (2007) 013, arXiv:0705.3178 [astro-ph].

[146] C. T. Byrnes, K.-Y. Choi, and L. M. H. Hall, "Conditions for large non-Gaussianity in two-field slow- roll inflation", *JCAP* **0810** (2008) 008, arXiv:0807.1101 [astro-ph].

[147] D. Battefeld and T. Battefeld, "On Non-Gaussianities in Multi-Field Inflation (N fields): Bi- and Tri-spectra beyond Slow-Roll", *JCAP* **0911** (2009) 010, arXiv:0908.4269 [hep-th].

[148] S. Mollerach, "ISOCURVATURE BARYON PERTURBATIONS AND INFLATION", *Phys. Rev.* **D42** (1990) 313–325.

[149] A. D. Linde and V. F. Mukhanov, "Nongaussian isocurvature perturbations from inflation", *Phys. Rev.* **D56** (1997) 535–539, arXiv:astro-ph/9610219.

[150] K. Enqvist and M. S. Sloth, "Adiabatic CMB perturbations in pre big bang string cosmology", *Nucl. Phys.* **B626** (2002) 395–409, arXiv:hep-ph/0109214.

[151] D. H. Lyth and D. Wands, "Generating the curvature perturbation without an inflaton", *Phys. Lett.* **B524** (2002) 5–14, arXiv:hep-ph/0110002.

[152] T. Moroi and T. Takahashi, "Effects of cosmological moduli fields on cosmic microwave background", *Phys. Lett.* **B522** (2001) 215–221, arXiv:hep-ph/0110096.

[153] K. Enqvist and S. Nurmi, "Non-gaussianity in curvaton models with nearly quadratic potential", *JCAP* **0510** (2005) 013, arXiv:astro-ph/0508573.

[154] A. D. Linde and V. Mukhanov, "The Curvaton Web", *JCAP* **0604** (2006) 009, arXiv:astro-ph/0511736.

[155] K. A. Malik and D. H. Lyth, "A numerical study of non-gaussianity in the curvaton scenario", *JCAP* **0609** (2006) 008, arXiv:astro-ph/0604387.

[156] M. Sasaki, J. Valiviita, and D. Wands, "Non-gaussianity of the primordial perturbation in the curvaton model", *Phys. Rev.* **D74** (2006) 103003, arXiv:astro-ph/0607627.

[157] K. Enqvist, S. Nurmi, and G. I. Rigopoulos, "Parametric Decay of the Curvaton", *JCAP* **0810** (2008) 013, arXiv:0807.0382 [astro-ph].

[158] Q.-G. Huang, "Curvaton with Polynomial Potential", *JCAP* **0811** (2008) 005, arXiv:0808.1793 [hep-th].

[159] P. Chingangbam and Q.-G. Huang, "The Curvature Perturbation in the Axion-type Curvaton Model", *JCAP* **0904** (2009) 031, arXiv:0902.2619 [astro-ph.CO].

[160] K. Enqvist, S. Nurmi, G. Rigopoulos, O. Taanila, and T. Takahashi, "The Subdominant Curvaton", *JCAP* **0911** (2009) 003, arXiv:0906.3126 [astro-ph.CO].

[161] A. Chambers, S. Nurmi, and A. Rajantie, "Non-Gaussianity from resonant curvaton decay", *JCAP* **1001** (2010) 012, arXiv:0909.4535 [astro-ph.CO].

[162] K. Enqvist, S. Nurmi, O. Taanila, and T. Takahashi, "Non-Gaussian Fingerprints of Self-Interacting Curvaton", *JCAP* **1004** (2010) 009, arXiv:0912.4657 [astro-ph.CO].

[163] P. Chingangbam and Q.-G. Huang, "New features in curvaton model", *Phys. Rev.* **D83** (2011) 023527, arXiv:1006.4006 [astro-ph.CO].

[164] C. P. Burgess *et al.*, "Non-standard primordial fluctuations and nongaussianity in string inflation", *JHEP* **08** (2010) 045, arXiv:1005.4840 [hep-th].

[165] L. Kofman, "Probing string theory with modulated cosmological fluctuations", arXiv:astro-ph/0303614.

[166] G. Dvali, A. Gruzinov, and M. Zaldarriaga, "A new mechanism for generating density perturbations from inflation", *Phys. Rev.* **D69** (2004) 023505, arXiv:astro-ph/0303591.

[167] M. Zaldarriaga, "Non-Gaussianities in models with a varying inflaton decay rate", *Phys. Rev.* **D69** (2004) 043508, arXiv:astro-ph/0306006.

[168] T. Suyama and M. Yamaguchi, "Non-Gaussianity in the modulated reheating scenario", *Phys. Rev.* **D77** (2008) 023505, arXiv:0709.2545 [astro-ph].

[169] D. Langlois, F. Vernizzi, and D. Wands, "Non-linear isocurvature perturbations and non- Gaussianities", *JCAP* **0812** (2008) 004, arXiv:0809.4646 [astro-ph].

[170] D. Langlois and F. Vernizzi, "Mixed inflaton and curvaton perturbations", *Phys. Rev.* **D70** (2004) 063522, arXiv:astro-ph/0403258.

[171] G. Lazarides, R. R. de Austri, and R. Trotta, "Constraints on a mixed inflaton and curvaton scenario for the generation of the curvature perturbation", *Phys. Rev.* **D70** (2004) 123527, arXiv:hep-ph/0409335.

[172] K. Ichikawa, T. Suyama, T. Takahashi, and M. Yamaguchi, "Non-Gaussianity, Spectral Index and Tensor Modes in Mixed Inflaton and Curvaton Models", *Phys. Rev.* **D78** (2008) 023513, arXiv:0802.4138 [astro-ph].

[173] K. Ichikawa, T. Suyama, T. Takahashi, and M. Yamaguchi, "Primordial Curvature Fluctuation and Its Non-Gaussianity in Models with Modulated Reheating", *Phys. Rev.* **D78** (2008) 063545, arXiv:0807.3988 [astro-ph].

[174] X. Chen, "Running Non-Gaussianities in DBI Inflation", *Phys. Rev.* **D72** (2005) 123518, arXiv:astro-ph/0507053.

[175] M. LoVerde, A. Miller, S. Shandera, and L. Verde, "Effects of Scale-Dependent Non-Gaussianity on Cosmological Structures", *JCAP* **0804** (2008) 014, arXiv:0711.4126 [astro-ph].

[176] J. Khoury and F. Piazza, "Rapidly-Varying Speed of Sound, Scale Invariance and Non- Gaussian Signatures", *JCAP* **0907** (2009) 026, arXiv:0811.3633 [hep-th].

[177] S. Renaux-Petel, "Combined local and equilateral non-Gaussianities from multifield DBI inflation", *JCAP* **0910** (2009) 012, arXiv:0907.2476 [hep-th].

[178] N. Bartolo, S. Matarrese, and A. Riotto, "Non-Gaussianity and the Cosmic Microwave Background Anisotropies", arXiv:1001.3957 [astro-ph.CO].

[179] D. Seery and J. E. Lidsey, "Primordial non-gaussianities from multiple-field inflation", *JCAP* **0509** (2005) 011, arXiv:astro-ph/0506056.

[180] C. T. Byrnes and D. Wands, "Curvature and isocurvature perturbations from two-field inflation in a slow-roll expansion", *Phys. Rev.* **D74** (2006) 043529, arXiv:astro-ph/0605679.

[181] D. Wands, N. Bartolo, S. Matarrese, and A. Riotto, "An observational test of two-field inflation", *Phys. Rev.* **D66** (2002) 043520, arXiv:astro-ph/0205253.

[182] V. Desjacques and U. Seljak, "Signature of primordial non-Gaussianity of φ^3-type in the mass function and bias of dark matter haloes", *Phys. Rev.* **D81** (2010) 023006, arXiv:0907.2257 [astro-ph.CO].

[183] P. Vielva and J. L. Sanz, "Constraints on $f_{\rm NL}$ and $g_{\rm NL}$ from the analysis of the N-pdf of the CMB large scale anisotropies", arXiv:0910.3196 [astro-ph.CO].

[184] S. Chongchitnan and J. Silk, "A Study of High-Order Non-Gaussianity with Applications to Massive Clusters and Large Voids", *Astrophys. J.* **724** (2010) 285–295, arXiv:1007.1230 [astro-ph.CO].

[185] J. Smidt *et al.*, "A Measurement of Cubic-Order Primordial Non-Gaussianity (g_{NL} and τ_{NL}) With WMAP 5-Year Data", arXiv:1001.5026 [astro-ph.CO].

[186] N. Kogo and E. Komatsu, "Angular Trispectrum of CMB Temperature Anisotropy from Primordial Non-Gaussianity with the Full Radiation Transfer Function", *Phys. Rev.* **D73** (2006) 083007, arXiv:astro-ph/0602099.

[187] J. Smidt *et al.*, "CMB Constraints on Primordial non-Gaussianity from the Bispectrum (f_{NL}) and Trispectrum (g_{NL} and τ_{NL}) and a New Consistency Test of Single-Field Inflation", *Phys. Rev.* **D81** (2010) 123007, arXiv:1004.1409 [astro-ph.CO].

[188] D. Tseliakhovich, C. Hirata, and A. Slosar, "Non-Gaussianity and large-scale structure in a two-field inflationary model", *Phys. Rev.* **D82** (2010) 043531, arXiv:1004.3302 [astro-ph.CO].

[189] C. T. Byrnes, K. Enqvist, and T. Takahashi, "Scale-dependence of Non-Gaussianity in the Curvaton Model", *JCAP* **1009** (2010) 026, arXiv:1007.5148 [astro-ph.CO].

[190] D. Langlois and L. Sorbo, "Primordial perturbations and non-Gaussianities from modulated trapping", *JCAP* **0908** (2009) 014, arXiv:0906.1813 [astro-ph.CO].

[191] N. Barnaby, "On Features and Nongaussianity from Inflationary Particle Production", *Phys. Rev.* **D82** (2010) 106009, arXiv:1006.4615 [astro-ph.CO].

[192] K. Dimopoulos, G. Lazarides, D. Lyth, and R. Ruiz de Austri, "Curvaton dynamics", *Phys. Rev.* **D68** (2003) 123515, arXiv:hep-ph/0308015.

[193] N. Bartolo, E. Komatsu, S. Matarrese, and A. Riotto, "Non-Gaussianity from inflation: Theory and observations", *Phys.Rept.* **402** (2004) 103–266, arXiv:astro-ph/0406398 [astro-ph].

[194] D. Langlois, "Primordial non-Gaussianities", arXiv:1102.5052 [astro-ph.CO]. * Temporary entry *.

[195] F. Bernardeau and J.-P. Uzan, "Inflationary models inducing non-Gaussian metric fluctuations", *Phys.Rev.* **D67** (2003) 121301, arXiv:astro-ph/0209330 [astro-ph].

[196] L. Verde, "Non-Gaussianity from Large-Scale Structure Surveys", *Advances in Astronomy* **2010** (2010) , arXiv:1001.5217 [astro-ph.CO].

[197] V. Desjacques and U. Seljak, "Primordial non-Gaussianity from the large-scale structure", *Classical and Quantum Gravity* **27** no. 12, (June, 2010) 124011–+, arXiv:1003.5020 [astro-ph.CO].

[198] C. Fedeli, C. Carbone, L. Moscardini, and A. Cimatti, "The clustering of galaxies and galaxy clusters: constraints on primordial non-Gaussianity from future wide-field surveys", *MNRAS* **414** (June, 2011) 1545–1559, arXiv:1012.2305 [astro-ph.CO].

[199] J. R. Fergusson and E. P. S. Shellard, "Primordial non-Gaussianity and the CMB bispectrum", *Phys. Rev. D* **76** no. 8, (Oct., 2007) 083523–+, arXiv:astro-ph/0612713.

[200] J. R. Fergusson, M. Liguori, and E. P. S. Shellard, "General CMB and primordial bispectrum estimation: Mode expansion, map making, and measures of $F_{\rm NL}$", *Phys. Rev. D* **82** no. 2, (July, 2010) 023502–+, arXiv:0912.5516 [astro-ph.CO].

[201] C. Fedeli, F. Pace, L. Moscardini, M. Grossi, and K. Dolag, "The effect of primordial non-Gaussianity on the skeleton of cosmic shear maps", *ArXiv e-prints 1103.5396* (Mar., 2011) , arXiv:1103.5396 [astro-ph.CO].

[202] F. Pace, L. Moscardini, M. Bartelmann, E. Branchini, K. Dolag, M. Grossi, and S. Matarrese, "A numerical study of the effects of primordial non-Gaussianities on weak lensing statistics", *MNRAS* **411** (Feb., 2011) 595–606, arXiv:1005.0242 [astro-ph.CO].

[203] L. Marian, S. Hilbert, R. E. Smith, P. Schneider, and V. Desjacques, "Measuring Primordial Non-gaussianity Through Weak-lensing Peak Counts", *ApJL* **728** (Feb., 2011) L13+, arXiv:1010.5242 [astro-ph.CO].

[204] D. Jeong, F. Schmidt, and E. Sefusatti, "Primordial Non-Gaussianity and the Statistics of Weak Lensing and other Projected Density Fields", *ArXiv e-prints 1104.0926* (Apr., 2011) , arXiv:1104.0926 [astro-ph.CO].

[205] E. Komatsu, "Wilkinson Microwave Anisotropy Probe constraints on non-Gaussianity", *New Astronomy* **47** (Nov., 2003) 797–803.

[206] P. Creminelli, A. Nicolis, L. Senatore, M. Tegmark, and M. Zaldarriaga, "Limits on non-Gaussianities from WMAP data", *JCAP* **5** (May, 2006) 4–+, arXiv:astro-ph/0509029.

[207] A. P. S. Yadav and B. D. Wandelt, "Evidence of Primordial Non-Gaussianity ($f_{\rm NL}$) in the Wilkinson Microwave Anisotropy Probe 3-Year Data at 2.8σ", *Physical Review Letters* **100** no. 18, (May, 2008) 181301–+, arXiv:0712.1148.

[208] A. Curto, E. Martínez-González, and R. B. Barreiro, "Improved Constraints on Primordial Non-Gaussianity for the Wilkinson Microwave Anisotropy Probe 5-Year Data", *ApJ* **706** (Nov., 2009) 399–403, arXiv:0902.1523 [astro-ph.CO].

[209] E. Komatsu, J. Dunkley, M. R. Nolta, C. L. Bennett, B. Gold, G. Hinshaw, N. Jarosik, D. Larson, M. Limon, L. Page, D. N. Spergel, M. Halpern, R. S. Hill, A. Kogut, S. S. Meyer, G. S. Tucker, J. L. Weiland, E. Wollack, and E. L. Wright, "Five-Year Wilkinson Microwave Anisotropy Probe Observations: Cosmological Interpretation", *ApJS* **180** (Feb., 2009) 330–376, arXiv:0803.0547.

[210] P. Vielva and J. L. Sanz, "Analysis of non-Gaussian cosmic microwave background maps based on the N-pdf. Application to Wilkinson Microwave Anisotropy Probe data", *MNRAS* **397** (Aug., 2009) 837–848, arXiv:0812.1756.

[211] B. Casaponsa, R. B. Barreiro, A. Curto, E. Martínez-González, and P. Vielva, "Wilkinson Microwave Anisotropy Probe 7-yr constraints on $f_{\rm NL}$ with a fast wavelet estimator", *MNRAS* **411** (Mar., 2011) 2019–2025, arXiv:1009.0632 [astro-ph.CO].

[212] P. Mukherjee and Y. Wang, "Wavelets and Wilkinson Microwave Anisotropy Probe Non-Gaussianity", *ApJ* **613** (Sept., 2004) 51–60, arXiv:astro-ph/0402602.

[213] P. Cabella, M. Liguori, F. K. Hansen, D. Marinucci, S. Matarrese, L. Moscardini, and N. Vittorio, "Primordial non-Gaussianity: local curvature method and statistical significance of constraints on $f_{\rm NL}$ from WMAP data", *MNRAS* **358** (Apr., 2005) 684–692, arXiv:astro-ph/0406026.

[214] J. R. Gott, W. N. Colley, C.-G. Park, C. Park, and C. Mugnolo, "Genus topology of the cosmic microwave background from the WMAP 3-year data", *MNRAS* **377** (June, 2007) 1668–1678, arXiv:astro-ph/0610764.

[215] C. Hikage, T. Matsubara, P. Coles, M. Liguori, F. K. Hansen, and S. Matarrese, "Limits on primordial non-Gaussianity from Minkowski Functionals of the WMAP

temperature anisotropies", *MNRAS* **389** (Sept., 2008) 1439–1446, arXiv:0802.3677.

[216] F. Bernardeau, L. van Waerbeke, and Y. Mellier, "Patterns in the weak shear 3-point correlation function", *A&A* **397** (Jan., 2003) 405–414, arXiv:astro-ph/0201029.

[217] X. Shi, P. Schneider, and B. Joachimi, "Relations between three-point configuration space shear and convergence statistics", *ArXiv e-prints* (May, 2011) , arXiv:1105.2309 [astro-ph.CO].

[218] B. Ménard, M. Bartelmann, and Y. Mellier, "Measuring Ω_0 with higher-order quasar-galaxy correlations induced by weak lensing", *A&A* **409** (Oct., 2003) 411–421.

[219] P. Schneider, L. van Waerbeke, B. Jain, and G. Kruse, "A new measure for cosmic shear", *MNRAS* **296** (June, 1998) 873–892, arXiv:astro-ph/9708143.

[220] E. Semboloni, T. Schrabback, L. van Waerbeke, S. Vafaei, J. Hartlap, and S. Hilbert, "Weak lensing from space: first cosmological constraints from three-point shear statistics", *MNRAS* **410** (Jan., 2011) 143–160, arXiv:1005.4941 [astro-ph.CO].

[221] A. Riotto and M. S. Sloth, "Strongly Scale-dependent Non-Gaussianity", *Phys.Rev.* **D83** (2011) 041301, arXiv:1009.3020 [astro-ph.CO].

[222] J. M. Bardeen, J. R. Bond, N. Kaiser, and A. S. Szalay, "The statistics of peaks of Gaussian random fields", *ApJ* **304** (May, 1986) 15–61.

[223] N. Sugiyama, "Cosmic Background Anisotropies in Cold Dark Matter Cosmology", *ApJS* **100** (Oct., 1995) 281.

[224] M. Abramowitz and I. A. Stegun, *Handbook of Mathematical Functions*. Handbook of Mathematical Functions, New York: Dover, 1972, 1972.

[225] M. S. Turner and M. White, "CDM models with a smooth component", *Phys. Rev. D* **56** (Oct., 1997) 4439–+, arXiv:astro-ph/9701138.

[226] L. Wang and P. J. Steinhardt, "Cluster Abundance Constraints for Cosmological Models with a Time-varying, Spatially Inhomogeneous Energy Component with Negative Pressure", *ApJ* **508** (Dec., 1998) 483–490, arXiv:astro-ph/9804015.

[227] E. V. Linder and A. Jenkins, "Cosmic structure growth and dark energy", *MNRAS* **346** (Dec., 2003) 573–583, arXiv:astro-ph/0305286.

[228] J. Elliston, D. J. Mulryne, D. Seery, and R. Tavakol, "Evolution of $f_{\rm NL}$ to the adiabatic limit", arXiv:1106.2153 [astro-ph.CO]. * Temporary entry *.

[229] L. Alabidi, K. Malik, C. T. Byrnes, and K.-Y. Choi, "How the curvaton scenario, modulated reheating and an inhomogeneous end of inflation are related", *JCAP* **1011** (2010) 037, arXiv:1002.1700 [astro-ph.CO].

[230] J.-L. Lehners, "Ekpyrotic Non-Gaussianity: A Review", *Adv.Astron.* **2010** (2010) 903907, arXiv:1001.3125 [hep-th]. * Temporary entry *.

[231] N. Barnaby and J. M. Cline, "Predictions for Nongaussianity from Nonlocal Inflation", *JCAP* **0806** (2008) 030, arXiv:0802.3218 [hep-th].

[232] E. Silverstein and D. Tong, "Scalar speed limits and cosmology: Acceleration from D-cceleration", *Phys.Rev.* **D70** (2004) 103505, arXiv:hep-th/0310221 [hep-th].

[233] M. Alishahiha, E. Silverstein, and D. Tong, "DBI in the sky", *Phys.Rev.* **D70** (2004) 123505, arXiv:hep-th/0404084 [hep-th].

[234] N. Arkani-Hamed, P. Creminelli, S. Mukohyama, and M. Zaldarriaga, "Ghost inflation", *JCAP* **0404** (2004) 001, arXiv:hep-th/0312100 [hep-th].

[235] D. Seery and J. E. Lidsey, "Primordial non-gaussianities in single field inflation", *JCAP* **0506** (2005) 003, arXiv:astro-ph/0503692.

[236] X. Chen, M. xin Huang, S. Kachru, and G. Shiu, "Observational signatures and non-Gaussianities of general single field inflation", *JCAP* **0701** (2007) 002, arXiv:hep-th/0605045 [hep-th].

[237] C. Cheung, P. Creminelli, A. Fitzpatrick, J. Kaplan, and L. Senatore, "The Effective Field Theory of Inflation", *JHEP* **0803** (2008) 014, arXiv:0709.0293 [hep-th].

[238] M. Li, T. Wang, and Y. Wang, "General Single Field Inflation with Large Positive Non-Gaussianity", *JCAP* **0803** (2008) 028, arXiv:0801.0040 [astro-ph]. * Brief entry *.

[239] L. Senatore, K. M. Smith, and M. Zaldarriaga, "Non-Gaussianities in Single Field Inflation and their Optimal Limits from the WMAP 5-year Data", *JCAP* **1001** (2010) 028, arXiv:0905.3746 [astro-ph.CO]. * Brief entry *.

[240] X. Chen, R. Easther, and E. A. Lim, "Large Non-Gaussianities in Single Field Inflation", *JCAP* **0706** (2007) 023, arXiv:astro-ph/0611645 [astro-ph].

[241] F. Arroja, A. E. Romano, and M. Sasaki, "Large and strong scale dependent bispectrum in single field inflation from a sharp feature in the mass", arXiv:1106.5384 [astro-ph.CO]. * Temporary entry *.

[242] N. Barnaby, "Nongaussianity from Particle Production During Inflation", *Adv.Astron.* **2010** (2010) 156180, arXiv:1010.5507 [astro-ph.CO]. * Temporary entry *.

[243] D. Battefeld, T. Battefeld, C. Byrnes, and D. Langlois, "Beauty is Distractive: Particle production during multifield inflation", *JCAP* **1108** (2011) 025, arXiv:1106.1891 [astro-ph.CO]. * Temporary entry *.

[244] X. Chen, R. Easther, and E. A. Lim, "Generation and Characterization of Large Non-Gaussianities in Single Field Inflation", *JCAP* **0804** (2008) 010, arXiv:0801.3295 [astro-ph]. * Brief entry *.

[245] X. Chen, "Primordial Features as Evidence for Inflation", arXiv:1104.1323 [hep-th].

[246] J. Fergusson and E. Shellard, "The shape of primordial non-Gaussianity and the CMB bispectrum", *Phys.Rev.* **D80** (2009) 043510, arXiv:0812.3413 [astro-ph].

[247] Q.-G. Huang, "Negative spectral index of f_{NL} in the axion-type curvaton model", *JCAP* **1011** (2010) 026, arXiv:1008.2641 [astro-ph.CO].

[248] N. Bartolo, M. Fasiello, S. Matarrese, and A. Riotto, "Tilt and Running of Cosmological Observables in Generalized Single-Field Inflation", *JCAP* **1012** (2010) 026, arXiv:1010.3993 [astro-ph.CO].

[249] J. Noller and J. Magueijo, "Non-Gaussianity in single field models without slow-roll", *Phys.Rev.* **D83** (2011) 103511, arXiv:1102.0275 [astro-ph.CO].

[250] C. Burrage, R. H. Ribeiro, and D. Seery, "Large slow-roll corrections to the bispectrum of noncanonical inflation", *JCAP* **1107** (2011) 032, arXiv:1103.4126 [astro-ph.CO]. * Temporary entry *.

[251] S. Shandera, N. Dalal, and D. Huterer, "A generalized local ansatz and its effect on halo bias", *JCAP* **1103** (2011) 017, arXiv:1010.3722 [astro-ph.CO].

[252] A. Becker, D. Huterer, and K. Kadota, "Scale-Dependent Non-Gaussianity as a Generalization of the Local Model", *JCAP* **1101** (2011) 006, arXiv:1009.4189 [astro-ph.CO]. * Temporary entry *.

[253] D. Munshi, L. van Waerbeke, J. Smidt, and P. Coles, "From Weak Lensing to non-Gaussianity via Minkowski Functionals", arXiv:1103.1876 [astro-ph.CO]. * Temporary entry *.

[254] V. Sahni and P. Coles, "Approximation methods for non-linear gravitational clustering", *Physics Reports* **262** (Nov., 1995) 1–135, arXiv:astro-ph/9505005.

[255] F. Bernardeau, S. Colombi, E. Gaztañaga, and R. Scoccimarro, "Large-scale structure of the Universe and cosmological perturbation theory", *Physics Reports* **367** (Sept., 2002) 1–248, arXiv:astro-ph/0112551.

[256] T. Matsubara, "Nonlinear perturbation theory integrated with nonlocal bias, redshift-space distortions, and primordial non-Gaussianity", *Phys. Rev. D* **83** no. 8, (Apr., 2011) 083518–+, arXiv:1102.4619 [astro-ph.CO].

[257] R. Scoccimarro and H. M. P. Couchman, "A fitting formula for the non-linear evolution of the bispectrum", *MNRAS* **325** (Aug., 2001) 1312–1316, arXiv:astro-ph/0009427.

[258] J. N. Fry, "Galaxy N-point correlation functions - Theoretical amplitudes for arbitrary N", *ApJL* **277** (Feb., 1984) L5–L8.

[259] J. N. Fry, "The Galaxy correlation hierarchy in perturbation theory", *ApJ* **279** (Apr., 1984) 499–510.

[260] M. Bartelmann and P. Schneider, "Weak gravitational lensing", *Physics Reports* **340** (Jan., 2001) 291–472.

[261] M. Bartelmann, "TOPICAL REVIEW Gravitational lensing", *Classical and Quantum Gravity* **27** no. 23, (Dec., 2010) 233001–+.

[262] D. N. Limber, "The Analysis of Counts of the Extragalactic Nebulae in Terms of a Fluctuating Density Field. II.", *ApJ* **119** (May, 1954) 655–+.

[263] W. Hu, "Power Spectrum Tomography with Weak Lensing", *ApJL* **522** (Sept., 1999) L21–L24, arXiv:astro-ph/9904153.

[264] M. Takada and B. Jain, "The three-point correlation function in cosmology", *MNRAS* **340** (Apr., 2003) 580–608, arXiv:astro-ph/0209167.

[265] M. Takada and B. Jain, "Three-point correlations in weak lensing surveys: model predictions and applications", *MNRAS* **344** (Sept., 2003) 857–886, arXiv:astro-ph/0304034.

[266] M. Takada and B. Jain, "Cosmological parameters from lensing power spectrum and bispectrum tomography", *MNRAS* **348** (Mar., 2004) 897–915, arXiv:astro-ph/0310125.

[267] S. Dodelson and P. Zhang, "Weak lensing bispectrum", *Phys. Rev. D* **72** no. 8, (Oct., 2005) 083001–+, arXiv:astro-ph/0501063.

[268] J. Miralda-Escude, "The correlation function of galaxy ellipticities produced by gravitational lensing", *ApJ* **380** (Oct., 1991) 1–8.

[269] N. Kaiser, "Weak gravitational lensing of distant galaxies", *ApJ* **388** (Apr., 1992) 272–286.

[270] A. Cooray and W. Hu, "Second-Order Corrections to Weak Lensing by Large-Scale Structure", *ApJ* **574** (July, 2002) 19–23, arXiv:astro-ph/0202411.

[271] C. Shapiro and A. Cooray, "The Born and lens lens corrections to weak gravitational lensing angular power spectra", *Journal of Cosmology and Astro-Particle Physics* **3** (Mar., 2006) 7–+, arXiv:astro-ph/0601226.

[272] E. Krause and C. M. Hirata, "Weak lensing power spectra for precision cosmology. Multiple-deflection, reduced shear, and lensing bias corrections", *A&A* **523** (Nov., 2010) A28+, arXiv:0910.3786 [astro-ph.CO].

[273] B. M. Schäfer, L. Heisenberg, A. F. Kalovidouris, and D. J. Bacon, "On the validity of the Born approximation for weak cosmic flexions", arXiv:1101.4769 [astro-ph.CO]. * Temporary entry *.

[274] T. Hahn, "CUBA - a library for multidimensional numerical integration", *Computer Physics Communications* **168** (June, 2005) 78–95, arXiv:hep-ph/0404043.

[275] E. Semboloni, C. Heymans, L. van Waerbeke, and P. Schneider, "Sources of contamination to weak lensing three-point statistics: constraints from N-body simulations", *MNRAS* **388** (Aug., 2008) 991–1000, arXiv:0802.3978.

[276] E. Semboloni, H. Hoekstra, J. Schaye, M. P. van Daalen, and I. J. McCarthy, "Quantifying the effect of baryon physics on weak lensing tomography", arXiv:1105.1075 [astro-ph.CO].

[277] T. L. Smith, M. Kamionkowski, and B. D. Wandelt, "The Probability Distribution for Non-Gaussianity Estimators", *ArXiv e-prints* (Apr., 2011) , arXiv:1104.0930 [astro-ph.CO].

[278] M. Tegmark, A. N. Taylor, and A. F. Heavens, "Karhunen-Loeve Eigenvalue Problems in Cosmology: How Should We Tackle Large Data Sets?", *ApJ* **480** (May, 1997) 22–+, arXiv:astro-ph/9603021.

[279] A. Refregier, A. Amara, T. D. Kitching, and A. Rassat, "iCosmo: an interactive cosmology package", *A&A* **528** (Apr., 2011) A33+, arXiv:0810.1285.

[280] R. Trotta, "Applications of Bayesian model selection to cosmological parameters", *MNRAS* **378** (June, 2007) 72–82, arXiv:astro-ph/0504022.

[281] R. Trotta, "Bayes in the sky: Bayesian inference and model selection in cosmology", *Contemporary Physics* **49** (Mar., 2008) 71–104, arXiv:0803.4089.